

FOR REFERENCE ONLY

40 0790249 1



ProQuest Number: 10183202

All rights reserved

INFORMATION TO ALL USERS

The quality of this reproduction is dependent upon the quality of the copy submitted.

In the unlikely event that the author did not send a complete manuscript and there are missing pages, these will be noted. Also, if material had to be removed, a note will indicate the deletion.



ProQuest 10183202

Published by ProQuest LLC (2017). Copyright of the Dissertation is held by the Author.

All rights reserved.

This work is protected against unauthorized copying under Title 17, United States Code  
Microform Edition © ProQuest LLC.

ProQuest LLC.  
789 East Eisenhower Parkway  
P.O. Box 1346  
Ann Arbor, MI 48106 – 1346

# **Modelling the Collapse of Metastable Loess Soils**

---

Harriet Miller

A thesis submitted in partial fulfilment  
of the requirements of  
The Nottingham Trent University  
For the degree of  
Doctor of Philosophy

April 2002

Supervised by: Dr. Ian F. Jefferson, Prof. Ian J. Smalley  
and Dr. Youcef Djerbib

Loess is a geologically young deposit, found all over the world. Large volume reductions can occur in the deposit due to loading and/or wetting. The collapse of a soil due to wetting is often referred to as hydrocollapse. Hydrocollapse of loess soil is a significant hazard for the built environment. This thesis discusses some of the modelling techniques that can be used for collapsible loess soils.

Estimation of the likely magnitude of hydrocollapse can be made by conducting a series of one-dimensional oedometer tests on specimens of the soil. The percentage hydrocollapse calculated in these tests can be used to compare loess samples from different regions. The amount of hydrocollapse observed will depend on the factors such as the density of the deposit and the amount of pore water present in the soil. The influence of each of these properties on the magnitude of hydrocollapse is difficult to determine from natural samples because the properties will be different from one region to another.

An artificial material has been developed to model the behaviour of collapsible loess soils. The properties of the artificial material can be varied and so the relative roles of the constituents can be determined. Another advantage of the artificial material is that it can be formed in the testing rig and therefore is not subjected to any sampling effects before testing. The artificial material has been tested in the oedometer and triaxial equipment. The behaviour of the artificial soil compared well with natural loess soil from the UK. The artificial material also shows similar strength and stiffness to the natural loess soil.

The artificial material was used in a small-scale test of a strip footing. Rising ground water was simulated in the test and the settlement of the footing was monitored. The strip footing test was modelled using finite element techniques and compared with the laboratory results. A simple but effective method of estimating collapse below a strip footing on a collapsible loess soil was determined.

## List of Contents

---

1	Introduction	1
1.1.	Collapsing Soils	1
1.2.	Loess – A Typical Collapsible Soil	2
2	Collapsible Soils	4
2.1	Key papers	4
2.2	Examples of Collapsible Soils	6
2.2.1	Loess	6
2.2.2	Residual soils	6
2.2.3	Man-made fills	7
2.2.4	Quick clay	8
2.3	Why concentrate on loess?	8
2.4	Origin of loess	9
2.5	Composition of Loess	11
2.6	Bonding Mechanisms	13
2.7	Collapse Mechanisms	14
2.8	Suctions	14
2.8.1	Measuring Suctions	15
2.9	Collapse Prediction	16

2.9.1 Laboratory Tests	17
2.9.2 Field Tests	19
2.9.3 Particle Packing	19
2.9.4 Constitutive Modelling	23
2.9.5 Modelling Collapse	27
2.10 The scope of this research	29
3 Element Test Methods	31
3.1 Introduction	31
3.2 Classification	32
3.2.1 Geometrical Characteristics	32
3.2.2 Index Testing	32
3.2.3 Particle Size Analysis	33
3.3 Production Of Artificial Loess Specimens	34
3.3.1 Previous Methods	34
3.3.2 A new approach	36
3.4 Production Methods Used	37
3.5 Mixing Methods	38
3.5.1 Method 1 - The airfall method	38
3.5.2 Method 2a - The wet paste method	38
3.5.3 Method 2b - The spray method	39
3.6 Oedometer Testing	39
3.6.1 Apparatus	39
3.6.2 Samples	40
3.6.3 Testing for hydrocollapse: Single oedometer test	41
3.6.4 Testing for potential hydrocollapse: Double oedometer test	41
3.6.5 Procedure	42
3.6.6 Testing the oedometer for creep	42
3.7 Triaxial Testing	43
3.7.1 Samples	44
3.7.2 Method for Undrained Triaxial Tests	44

3.7.3 Elastic Parameters	45
3.8 Summary	46
4 Element Test Results	47
4.1 Shape of the Particles	49
4.2 Index Testing	52
4.3 Oedometer Test Results	57
4.3.1 Production Method 1 - The air fall method, after Dibben and Assallay	58
4.3.1.1 Particle Shape	61
4.3.1.2 Hydrocollapse and Void Ratio	62
4.3.2 Production Method 2a - The wet method	63
4.3.2.1 Preparation water content	63
4.3.2.2 Water content causing collapse	66
4.3.3 Preparation Method 2b - Spraying Method	67
4.3.4 General Observations for both methods 2a and 2b	68
4.3.5 Clay Content and Void Ratio	70
4.3.6 Effect of Clay Content on hydrocollapse	75
4.3.7 Effect of compressive effort	77
4.3.8 Effect of water content	78
4.3.9 The constrained modulus, D	79
4.4 Triaxial compression Tests	82
4.4.1 Effect of confining pressure	84
4.4.2 Effect of water content	86
4.4.3 Conclusions from Oedometer Tests	89
4.4.4 Conclusions from the Triaxial tests	91
4.5 General Conclusions	91
5 Computer Models to Simulate Collapsible Soils	95
5.1 Summary of Laboratory results	95
5.2 Particle Packing	98
5.3 The Structural Model	99
5.3.1 Introduction	99

5.3.2 Assumptions	99
5.3.3 Methodology	100
5.3.4 Proportion of silt and clay particles	101
5.3.5 Unstable, Metastable and Stable Structures	104
5.3.6 Using the Program	106
5.4 Results	107
5.5 Discussion	112
6 Footing Model Tests - Methods and Results	115
6.1 Introduction	115
6.2 Scale modelling	116
6.3 Dimensions	117
6.4 Test Procedure	119
6.4.1 Setting up the test	119
6.4.2 Fill Placement	122
6.4.3 Running the test	123
6.4.4 Feasibility tests	125
6.5 Results	126
6.5.1 Water content profile	126
6.5.2 Mechanism for wetting the soil	127
6.5.3 Case study 1: Increasing ground water level	128
6.5.4 Observation of the wetting front	135
6.5.5 Case study 2: Initially saturated and then loaded	137
6.5.6 Case study 3: Ponding at the surface	140
6.5.7 Relating the physical footing model to full scale	141
6.5.8 Inaccuracies	143
6.6 Discussion	145
7 Finite Element Models	149
7.1 Introduction	149
7.2 Finite Element Modelling	150

7.2.1 Background	150
7.2.2 Unsaturated Soil Modelling	150
7.3 Simple approach to model collapse	154
7.4 Method of modelling for this study	156
7.5 Modelling the oedometer tests	157
7.6 Modelling the triaxial tests	163
7.7 Finding parameters from the triaxial tests	165
7.7.1 Linear Elastic	165
7.7.2 Other models	167
7.8 Prediction of collapse beneath a strip footing	167
7.8.1 Methods	167
7.8.2 Case 1: Loaded then saturated	169
7.8.3 Case 2. Saturated and then loaded	169
7.8.4 Case 3. Loaded and then saturated from above	170
7.9 Results and Comparison with footing model data	170
7.9.1 Case Study 1: Loaded then saturated from bottom	170
7.9.2 Case Study 2: Saturated and then Loaded	172
7.9.3 Case Study 3: Loaded then saturated from top and bottom	174
7.10 Parametric studies	175
7.11 Scaling effects	177
7.12 Development of computer models	179
7.13 Discussion	180
7.14 Applications	181
8 Artificial Loess and its Correlation with World-wide Loess Deposits	182
8.1 Behaviour of artificial loess	183
8.2 Comparison of artificial loess with world deposits	184
8.2.1 Properties of the Artificial Material	184
8.2.2 The Void Ratio Approach	186
8.2.3 Hydrocollapse Approach	189
8.2.4 Properties of Loess	190
8.2.5 Conclusions from the predictive equations	191

8.3	Parameters affecting collapse	191
8.4	Suggested Method for Assessing the Collapse of a Deposit under load	192
9	Conclusions and Recommendations for Further Research	194
9.1	Development of Artificial Loess	195
9.1.1	Conclusions	195
9.1.2	Further research	197
9.2	Computer Simulations	198
9.2.1	Conclusions	198
9.2.2	Further Research	198
9.3	Laboratory Footing Model	199
9.3.1	Conclusions	199
9.3.2	Further Research	200
9.4	Finite Element Analysis of the Footing	200
9.4.1	Conclusions	200
9.4.2	Further Research	201
9.5	Overall Conclusions	202

Figure 2 1 Bonding mechanisms in loess soil, after Barden et al. (1973)	13
Figure 2 2 (a) Cubic Packing (600) and (b) Orthohombic packing (402) as discussed in Rogers et al. (1994)	20
Figure 2 3 Random Loose Packing (RLP-Left) and Random close packing (RCP-Right) for spheres and loess particles, (after Dijkstra et al., 1995)	21
Figure 2 4 The boundaries of random packing, after Nolan and Kavanagh, (1992).	22
Figure 2 5 Void ratio constitutive surface for a mixture of flint and kaolin under Ko loading, after Fredlund and Rahardjo (1993).	24
Figure 2 6 Loading collapse (LC) yield curve and Suction Increase (SI) yield curve, after Alonso et al, (1987).	26
Figure 2 7 Three-dimensional view of the yield surfaces in (p,q,s) stress space, after Alonso et al., (1987).	26
Figure 2 8 Collapse modelling using one set of parameters for the dry soil and one set of parameters for the saturated soil, after Farias et al. (1998)	28
Figure 2 9 Stress and strain paths, after Farias et al. (1998)	28
Figure 3 1 SEM equipment	33
Figure 3 2 The equipment used for the air fall method of creating a dry sample. Dry mixed clay and silt particles are sieved into the oedometer ring prior to steaming.	35
Figure 3 3 Schematic representation of the tripod sampler	40
Figure 4 1 Oedometer results for two similar artificial samples, showing the repeatability	48
Figure 4 2 Particle size analysis results for kaolinite and silica	55
Figure 4 3 Comparison of particle size distribution for natural and artificial samples	56
Figure 4 4 Typical oedometer results for loess samples from Essex, Star Lane site.	58
Figure 4 5 Oedometer results for artificial samples made with Ballotini balls/kaolinite 80/20 method 1, compared to natural loess from the Star Lane site, Essex.	60
Figure 4 6 Oedometer results for artificial samples made with crushed sand/kaolinite 80/20 Method 1, compared to natural loess from the Star Lane site, Essex.	60
Figure 4 7 Oedometer results for artificial samples made with ground silica/kaolinite 80/20 Method 1, compared to natural loess from the Star Lane site, Essex.	61

Figure 4 8 Percentage hydrocollapse for varying kaolinite content for samples prepared using method 1. Crushed sand and Kaolinite specimens.	62
Figure 4 9 Void ratio at the four stages in an oedometer test. (Method 1 - constant mass, Crushed sand and Kaolinite)	63
Figure 4 10 Comparison of initial voids ratio of samples made with different preparation water contents with ground silica and 10, 30 and 50% kaolinite content.	64
Figure 4 11 Oedometer results for samples made using method 2a. Ground silica/kaolinite content 80/20. Preparation water content 27%. Initial voids ratio, $e=0.72$	65
Figure 4 12 Oedometer results for samples made using method 2a. Ground silica/kaolinite 70/30. Preparation water content 25%. Initial voids ratio, $e=0.81$	65
Figure 4 13 Oedometer results for samples prepared using method 2a. Ground silica/kaolinite 70/30. Preparation water content = 17.5%. Initial voids ratio, $e=1.0$	66
Figure 4 14 Graph to show the relationship between saturation ratio at the time of collapse and amount of hydrocollapse, for specimens prepared with 30% clay content.	67
Figure 4 15 Oedometer results for samples prepared using method 2b. Initial voids ratio, $e = 1.17$ . Preparation water content = 13.5%.	70
Figure 4 16 Loading and unloading of oedometer samples prepared using method 2a. Preparation water content = 25%, initial void ratio 0.6.	71
Figure 4 17 Initial void ratio of the oedometer specimens before loading shown for different preparation methods	71
Figure 4 18 Void ratio of specimens at 200kPa before wetting shown for different preparation methods	72
Figure 4 19 Void ratio of specimens at an applied stress of 200kPa before wetting shown for different initial water contents	72
Figure 4 20 Void ratio of the oedometer samples at 200kPa after wetting	73
Figure 4 21 Void ratios at 200kPa after flooding of the specimens shown against flooding water content	74
Figure 4 22 Illustration of optimum clay content	74
Figure 4 23 Comparison of hydrocollapse for samples prepared using method 2a with 17.5% water content and 30% initial water content for different clay contents.	76
Figure 4 24 Effect of difference between sand and clay on collapse potential at various wetting pressures (Basma and Tuncer, 1992).	77
Figure 4 25 Effect of clay content and preconsolidation pressure on initial void ratio of the artificial samples compacted with the same compressive effort	78
Figure 4 26 Collapsibility versus saturation ratio for test material (Ishihara and Harada, 1994)	79

Figure 4 27 Constrained modulus, $D$ , for the Essex samples, 4300kPa for the unsaturated sample and 2400kPa for the saturated sample	80
Figure 4 28 Constrained modulus, $D$ , found for unsaturated artificial specimens (method 2a) with different initial void ratios and 30% clay content. Equations are given in order of their gradient.	81
Figure 4 29 Constrained modulus, $D$ , for saturated artificial specimens (method 2a) with different initial void ratios and 30% clay content. . Equations are given in order of their gradient.	81
Figure 4 30 Relationship of constrained modulus with initial void ratio for saturated and unsaturated samples, for the results presented in Figures 4.27 and 4.28.	82
Figure 4 31 Deviator stress-strain curves for triaxial tests performed on loess from Pegwell Bay, Kent.	83
Figure 4 32 Typical triaxial tests for artificial loess prepared using method 2a and tests at different initial water contents (%).	84
Figure 4 33 A comparison of typical triaxial test results on artificial samples at different confining pressures. Where $w$ = water content %.	86
Figure 4 34 Young's modulus found using lines of best fit for the artificial specimens tested in undrained, unconsolidated triaxial tests.	88
Figure 4 35 Young's modulus, $E$ , values compared to water content of the sample	88
Figure 4 36 Young's Modulus ( $E$ , kPa) found for the artificial samples against estimated saturation ratio during the test	89
Figure 5 1 Void ratio vs. kaolinite content for artificial loess specimens prepared using method 1.	96
Figure 5 2 Peak hydrocollapse observed for specimens prepared using method 1	96
Figure 5 3 Natural void ratios formed in the samples for different clay contents	97
Figure 5 4 Defining the particle shape.	101
Figure 5 5. Two and three dimensional representations of the space around a silt particle.	103
Figure 5 6 Rules used for the falling particles is the computer simulation	106
Figure 5 7 Screen shot of program interface	107
Figure 5 8 Typical arrangement found from the Air Fall method in the computer program, for a silt diameter six times larger than clay diameter with thirty percent clay.	108
Figure 5 9 Metastable arrangement, void ratio = 0.95, for a silt diameter six times larger than clay diameter with thirty percent clay.	108

Figure 5 10 Stable arrangement (2/5), void ratio = 0.56, for a silt diameter six times larger than clay diameter with thirty percent clay.	109
Figure 5 11 Stable arrangement (1/5), void ratio = 0.367, for a silt diameter six times larger than clay diameter with thirty percent clay.	109
Figure 5 12 Variation of void ratio for Stokes situation with the percentage of smaller particles (fines)	110
Figure 5 13 Variation of void ratio with 10 percent small particles, with maximum and minimum values also shown.	111
Figure 5 14 Variation of standard deviation of void ratio with small particle percentage (fines) for three different silt /clay diameter ratios for Stokes situation.	112
Figure 6 1 Mode of deflection for the footing. The soil acts as a uniformly distributed load.	119
Figure 6 2 Footing test tank dimensions. The gravel layer was used to spread the water over the base of the model and the filter layer was used to stop the silty material mixing with the gravel layer but allowed water through.	120
Figure 6 3 Location of load gauges and transducers on the footing and the soil surface.	121
Figure 6 4 . Equipment for the model footing tests.	121
Figure 6 5 Calibration of the load cell, based on 3 calibration runs.	124
Figure 6 6 Water content profile for the unsaturated condition	126
Figure 6 7 Observed water level in the inlet pipe	127
Figure 6 8 Settlement of the footing on the unsaturated artificial soil for Case Study 1	129
Figure 6 9 Deflection of the footing during wetting Case 1 test1.	131
Figure 6 10 Deflection of footing and two points on the soil with time for Case 1, test 2. Water added at W1, W2, W3	132
Figure 6 11 Vertical displacement of footing. Case 1, test 3	133
Figure 6 12 Final water content profiles for Case 1: tests 2 and 3 and Case 2.	135
Figure 6 13 Deflection of footing with quantity of water for tests 1, 2 and 3.	136
Figure 6 14 Deflection of footing with estimated water depth for tests 1, 2 and 3. Also compared with results for Case 2.	136
Figure 6 15 Deflection of footing with time for Case 2	138
Figure 6 16 Settlement of the footing versus load for various water contents of the artificial material	139
Figure 6 17 Water content profiles for three distances away from the centre of the footing, shown in key.	140
Figure 6 18 Settlements observed for the footing and the soil surface for Case 3: Saturated at the top and bottom	141

Figure 6 19 Water content profile at the end of Case 3.	142
Figure 6 20 Summary of $N_c$ (bearing capacity factor) values from the 1g and centrifuge tests and corresponding FEM simulation, on sand Siddiquee et al (1999)	142
Figure 6 21 Tank movements for Case 1. Loaded then saturated.	144
Figure 6 22 Tank movements for Case 2. Saturated then loaded.	145
Figure 7 1 Yield surface (Wheeler and Sivakumar, 1995) where, $p$ = normal stress, $q$ = shear stress and $s$ = suction.	151
Figure 7 2 LC Yield Surface, after Gens and Alonso (1992)	152
Figure 7 3 Collapse tests on loess under different confining conditions, Alonso et al. (1987). a) Stress path in $p,s$ space. b) Evolution of yield surfaces. c) $(e,p)$ relationship d) Typical oedometer test results. (Erol and El-Ruwaih,1982).	153
Figure 7 4 The principle of the new method to move from one state to another	156
Figure 7 5 Loading arrangement for the simulation of an oedometer test	158
Figure 7 6 Determination of the constrained modulus for the unsaturated and saturated artificial samples with 30% kaolinite content for loads 0-100kPa.	159
Figure 7 7 Comparison of results for linear elastic model in finite element program with artificial samples 30% kaolinite, over the stress range 0-100kPa	159
Figure 7 8 . Comparison of finite element results with those from testing undisturbed specimens from the Star Lane, Essex. 0-100kPa. Where, $E$ = Young's modulus and $D$ = Constrained modulus. Values in kPa.	161
Figure 7 9 Effect of $D$ and $E$ on the vertical deflection of the oedometer sample for 100kPa load. Where, $E$ = Young's modulus and $D$ = Constrained modulus.	161
Figure 7 10 Determination of the constrained modulus for the natural samples for loads 0-50kPa.	162
Figure 7 11 Comparison of results for non-linear elastic model in finite element program with samples from the Start Lane, Essex site, over the range 0-1600kPa	163
Figure 7 12 Layout of grid and boundary conditions for simulating the triaxial test.	164
Figure 7 13 Finding Young's Modulus values from the undrained triaxial tests on two artificial specimens using best fit lines through the data for the results up to 200kPa.	165
Figure 7 14 Triaxial Test Results for artificial specimens with 30% clay content and different initial water contents for lower deviator stress, 0-400kPa	166
Figure 7 15 Finite element results for various values of $E$ (in the range 400 – 20,000kPa) for the triaxial tests, plotted with three of the triaxial test results for specimens with 15.8, 18.8 and 21.0 water content percentages.	167
Figure 7 16 Finite element model grid used to predict the deformations of the footing model	168

Figure 7 17 Applied Stress against deflection for the Finite Element model and the laboratory footing model. Finite element results are shown for values of Young's modulus of 20,000kPa, 13,00kPa, 8,000kPa and 4,000kPa.	171
Figure 7 18 Case 1 comparison of Finite Element results and laboratory footing models. Laboratory footing was loaded to 86kPa. $E = 400\text{kPa}$ for saturated and 13000kPa for unsaturated material.	172
Figure 7 19 Case 2 - Loading against displacement. A comparison between the laboratory footing model and the finite element model, for $E = 400, 600$ and $1000\text{kPa}$ .	173
Figure 7 20 Case 3: deflections of footing due to wetting from the top	174
Figure 7 21 Effect of footing width. NB 31mm was chosen for the laboratory footing model	175
Figure 7 22 Effect of the footing width on the deflection of the footing for a load of 100kPa and an Elastic modulus of 1000kPa.	176
Figure 7 23 Effect of the Elastic Modulus ( $E$ ) on the deflection of the footing, for loads of 86kPa and 100kPa.	176
Figure 7 24 The effect of Poisson's ratio on the deflection of the footing	177
Figure 7 25 Effect of the size of the grid in the finite element analysis.	178
Figure 7 26 The effect of the division methods in the finite element analysis. Where the grid was divided into equal segments (linear) or into smaller segments nearer the footing (non-linear).	178
Figure 7 27 Stress-strain route to model collapse	179
Figure 8 1 Relationship between void ratio and applied stress for two samples with the same constituents but different initial void ratios	186
Figure 8 2 Proposed relationship between moisture content and void ratio for different powers of $m$ , -0.5 and 0.24.	187
Figure 8 3 Proposed relationship between Clay content and void ratio	187
Figure 8 4 Void ratios of specimens and the predicted void ratios given by Equation 1	188
Figure 8 5 Hydrocollapse as observed in the artificial soil specimens tested in the oedometer and estimated hydrocollapse calculated from equation 1.	189
Figure 8 6 Hydrocollapse values for oedometer specimens made with artificial soil compared to the estimated values of hydrocollapse given by equation 2.	190
Figure 8 7 Change of void ratio with vertical loading for various water contents	193

## List of Tables

Table 2 1 Examples of Index properties of some natural loess deposits.	12
Table 2 2 Summary of the methods of measuring suctions	15
Table 3 1 Summary of the oedometer tests undertaken during this project	43
Table 4 1 Summary table of the element tests carried out	47
Table 4 2 Artificial loess index properties	54
Table 4 3 Mineralogical analysis of Kaolinite (Grade 50)	56
Table 4 4 Mineralogical Analysis of Natural Loess found in Essex, Star Lane site.	57
Table 4 5 Summary table of results for the one-dimensional compression tests for methods 2a and 2b.	69
Table 4 6 Young's Modulus $E_{50}$ (in kPa) related to saturation, temperature and confining pressure (Weibe et al, 1998).	86
Table 6 1 The expected deflection of various footing widths and depths	118
Table 6 2 Summary of tests carried out using the model footing.	125
Table 8 1 Properties and collapse coefficient, $i_c$ , at 200kPa for the artificial loess	185
Table 8 2 Estimated hydrocollapse for specimens reported in the literature in Kie (1988). Where $e_i$ = initial void ratio, $m_i$ = initial water content, $m_w$ = flooding water content, $c$ = clay content, $i_c$ = collapse coefficient, $e $ = void ratio before wetting, $e  $ = void ratio after wetting.	191

## List of Plates

---

Plate 4-1 Natural loess from Kazakstan -----	50
Plate 4-2 Clayey Natural loess from Kazakstan -----	50
Plate 4-3 Artificial loess made with ballotini balls and kaolinite -----	51
Plate 4-4 Artificial loess made with crushed sand and kaolinite -----	51
Plate 4-5 Artificial loess prepared using HPF4 silica flour and kaolinite -----	53
Plate 4-6 The shape of the HPF4 silica flour particles -----	53
Plate 6-1 Loading arrangement for the footing test -----	147
Plate 6-2 Failure of the deposit after saturation has occurred through rising ground water	147
Plate 6-3 Failure of the footing test in Case 1 Test 2. Failure mode was punching shear --	148

---

# Notation and Abbreviations

---

## CHAPTER 1

CRISP	CRItical State Program	3
FEM	Finite Element Modelling	3

## CHAPTER 2

402	orthohombic packing	20
600	cubic packing	20
BRE	British Research Establishment	7
CN	co-ordination number	19
$e'$	void ratio before wetting	12
$e''$	void ratio after wetting	18
$e_i$	initial void ratio	12
$e_L$	void ratio at the liquid limit	17
$e_o$	natural void ratio	17
$\Delta e$	change in void ratio due to saturation	12
$\varepsilon_p$	strain due to normal stress	28
$\varepsilon_q$	strain due to deviatoric stress	28

Gs	specific gravity	12
$i_c$	coefficient of collapse	18
LC	Load collapse curve	25
LL	Liquid Limit	12
p	mean normal stress	23
PI	Plastic Index	12
PL	Plastic Limit	12
q	deviatoric stress	25
RCP	random close packing	21
RLP	random loose packing	21
S	Matrix suction ( $u_a - u_w$ )	14
$\sigma^A - \sigma^B$	unbalanced stresses	28
$\sigma^B$	clamped stress	28
$u_a$	pore air pressure	14
$u_w$	pore water pressure	14

### CHAPTER 3

BGS	British Geological Survey	33
D	constrained modulus	46
$E'$	Young's modulus - drained conditions	45
E	Young's Modulus of elasticity	45
$E_u$	undrained Young's modulus	45
$\epsilon_v$	vertical strain	45
HPF4	industrially ground silica flour	37
$h'$	height before wetting	41
$h''$	height after wetting	41
$\Delta h$	change in height ( $h' - h''$ )	41
L	original length	45
LVDT	vertical dial gauge and transducer	41
SEM	Scanning Electron Microscope	32
$\sigma_v$	vertical stress	45
v	Poisson's ratio	45
x	deflection	45

## CHAPTER 4

BSI	British Standards Institute	55
$E_{50}$	stiffness of the soil at 50% of max. deviator stress	85
$e_i$	initial void ratio	63
$e_{\text{pre-c}}$	voids ratio before wetting	63
$e_{\text{post-c}}$	void ratio after wetting	63
$e_f$	final void ratio after loading	63
$q_f$	maximum deviator stress	84

## CHAPTER 5

$A_{12}$	area left in 2-dimensions	103
$A_{13}$	volume left in 3-dimensions	103
$A_C$	area of a clay particle	103
$N_C$	number of clay particles	102
$N_{C2}$	number of clay particles in an equivalent 2D slice	103
$N_{C3}$	number of clay particles in 3-dimensions	103
$P_C$	percentage clay	102
$P_S$	percentage silt	102
$R_C$	radius of a clay particle	102
$R_S$	radius of a silt particle	102
$V_C$	volume of a clay particle	102
$V_S$	volume of a silt particle	102

## CHAPTER 6

$b$	width of the footing	118
$d$	depth of the footing	118
$df$	deflection of the footing in mm	118
$I$	second moment of area	118
$N_\gamma$	bearing capacity factor	143
$w$	Load per unit area on the footing	118
W1 – W4	Wetting stages 1 – 4	129

## CHAPTER 7

CuST	Cubic Strain	165
$D_i$	initial value of stiffness	161
$D_n$	new value of stiffness	161
P	stress applied	161
x	modifying factor	161

## CHAPTER 8

c	clay content	187
$e^l$	void ratio before wetting	192
$e^d$	void ratio after wetting.	192
$e_{200}$	void ratio at an applied stress of 200kPa	187
$e_i$	initial void ratio	192
$i_c$	collapse coefficient	192
m	water content	187
$m_i$	initial water content	192
$m_w$	flooding water content	192

### **1.1. COLLAPSING SOILS**

Collapsing soils present a major problem for geotechnical engineers. There are many types of collapsible soil, such as loess, sensitive clays, volcanic ash, residual soils, man-made fills and colliery spoil. The properties and mineralogical composition of the different types of soils can vary considerably. However, they generally have an open, metastable packing and are geologically young. Loess is one of the most widespread collapsing soils. The aim of this thesis was to model collapse, both physically and numerically. The testing and modelling techniques used in this thesis were concentrated around loess. However, most of the techniques used would be equally valid for other types of collapsible soils.

## **1.2. LOESS – A TYPICAL COLLAPSIBLE SOIL**

Loess covers around 10% of the Earth's land-mass. Most loess is of aeolian origin and has accumulated over large areas of North America, Europe, Russia and China during the last two to three million years. Although, it is claimed that some deposits are of alluvial origin, Bell (2000). Loess particles are mainly of silt size. These particles are sub-angular and sub-rounded and separate from each other, being connected by bonds and bridges with uniformly distributed pores. The bridges are formed of clay-sized materials of clay minerals, fine quartz, feldspar or calcite. This clay-sized material also forms coatings around the grains. As the sand and silt particles are not in contact, the mechanical behaviour of loess is governed by the structure and quality of the bonds, Barden et al. (1973).

Disasters, failures and collapse caused by loess soils are well documented. Hydrocollapse of loess occurs under load and/or wetting and, as such, loess can be considered a major geohazard to the built environment. For example, in 1976, the collapse of the Teton Dam in Idaho occurred while the dam was still being filled for the first time. The catastrophic collapse happened due to lack of understanding of the properties of loess (Smalley, 1992). Smaller subsidence and landslide problems are virtually an everyday occurrence for communities founded on collapsing loess soils (Klukanova and Frankovska, 1995).

The genesis and properties of collapsing loess soils have been researched since the mid 19<sup>th</sup> Century. Much of this research covers a wide range of disciplines, including soil science, geology and engineering. The importance of these soils has meant that a vast body of research has been carried out and reported on. These papers generally report on a particular local loess soil, and give some typical properties and results. Most of the work does not give a global picture of loess, although there are a few notable exceptions that bring some of the key papers together and these will be discussed in Chapter 2.

Due to the fragmented research, different properties can be reported for each location. For example, some papers give clay and carbonate content, others may leave this information out but give liquid limit and plastic limit, making it hard to compare loess from region to region. This comparison is made harder due to the fact that there is more than one way to calculate the amount of collapse observed in the sample (Northmore et al. 1996). Also, 'typical' results are often given for collapse tests, and ranges of properties are given for the

region as a whole, rather than specific properties being related to specific collapse tests. This makes it hard to evaluate the relative influences of the different properties on magnitude of collapse. This project is an attempt to bring loess research together.

The properties of natural loess can be tested but cannot be altered. An artificial loess has been developed in which the properties can be controlled. The artificial loess allows the systematic variation of the constituents, so that their influence on the behaviour of loess can be identified. The exact water, clay and silt contents are known for each specimen of artificial loess. Tests for collapse and strength can be carried out on each specimen and correlated with its properties. Analysis of the test results on the artificial loess has helped to fill in gaps in the knowledge from the literature. This has allowed an evaluation of the key contributors to the magnitude of hydrocollapse.

The artificial loess has been tested in oedometer and triaxial tests and compared with natural loess. Void ratios, strength and magnitude of hydrocollapse all compare well with the natural loess. The artificial loess was then used in a model of a footing on collapsible soil. The behaviour of the footing was monitored during a period of simulated rising ground water level. The deflections of the footing were recorded and compared with a prediction of the amount of footing movement given by a Finite Element Modelling (FEM) analysis, using the CRITICAL State Program (CRISP) developed by Cambridge University. The parameters for the FEM analysis were estimated from the triaxial tests carried out in the laboratory. The project has succeeded firstly, in producing an artificial soil that can be favourably compared to a natural loess soil. Secondly, it has succeeded in predicting the deformations of a footing founded on collapsible material using finite element analysis.

## 2

## Collapsible Soils

---

An extensive literature review has been carried out to give a broad understanding of collapsible soils and in particular loess. The literature has revealed areas that would benefit from further research and explanation, and has helped to clarify the aims and objectives of the project. Loess is the archetypal naturally occurring collapsing soil and has been investigated by numerous authors since the middle of the nineteenth century. Recent review papers have thoroughly discussed collapsible soil composition and behaviour. Papers by Dudley (1970) and Rogers et al. (1994a) together with the work of Assallay (1998) and Dibben (1998) have brought together previous research and are briefly summarised in this chapter. Nevertheless, there are many questions and contentious issues that have not been answered in the literature. This review outlines the areas of research that still need to be addressed and defines the scope of the project. The objective was to provide a consistent and reliable approach to the analysis of collapsible soil behaviour for application in assessment of potential movements of footings supported by collapsible soils.

### 2.1 KEY PAPERS

Dudley (1970) wrote an extensive review of collapsible soils detailing the collapse phenomenon, mechanisms of collapse and the types of soils involved. The paper is now over 30 years old but remains a valuable reference. The paper discusses residual soils and

alluvial sands but not sensitive clays. Schwartz (1985) gave a review of the collapsing soils in South Africa. Many collapsible soils exist in this area such as residual granite sands and aeolian sands, but literature in this area is limited. Procedures to identify and quantify collapse were discussed and some engineering solutions to collapse problems were also given. Mackechnie (1993) produced a review paper of the 18 submissions to the session on collapsible and swelling soils for the 1993 International Soil Mechanics and Foundation Engineering (ISMFE) conference in Rio de Janeiro. The need for a general definition of collapsible soils was raised in this paper. Following this, the NATO Advanced Workshop on the Genesis and properties of collapsible Soils (1994) gave an opportunity to discuss this definition. Rogers (1995) produced a review paper for this conference. This paper discussed the definition of collapsing soils and produced a systematic classification for both natural and man-made materials. A large amount of the literature reviewed was on loess but papers also covered sensitive clays and sands. One of the definitions for collapsible soil from the conference was given as follows:

*“ A collapsible soil is one in which the major structural units are arranged in an open packing, which may become a more stable, closer packing with important geotechnical consequences. In most cases, the structural collapse is caused by loading and/or wetting in unsaturated materials, but higher moisture content and saturated systems such as quick clays and submarine sands may also be considered collapsing soils”.*

This definition was an attempt to include all soils with collapsing characteristics including quick clays, which can sometimes be neglected by these definitions. A global review on collapsible loess soils was written by Rogers et al. (1994a). The wide range of topics under discussion included rheology, thermodynamics, phase movements, particle packing, interparticle bonding, pore structure and distribution, catastrophe theory, topology and simple structural frameworks. Literature from China, North America and Europe were discussed, as well as introducing the literature from Russia. The literature shows an interesting divide of research. The Chinese, North American and European literature is mainly focused on the mechanisms of collapse, whereas the Russian literature also retains interest in the origin (or genesis) of the hydrocollapse properties. What the literature does agree on is that loess is a typical and extensive collapsing deposit.

## 2.2 EXAMPLES OF COLLAPSIBLE SOILS

All soils can exhibit collapse given the required stress history, as shown by Alonso et al. (1987). However, some soils are more prone to collapse behaviour and typically exhibit significant and consistent collapse strain under load and/or wetting. These soils have become known as collapsible and are considered below.

### 2.2.1 Loess

Loess is typically around 60-90% quartz and feldspar particles, 5-30% clay minerals with some carbonates, sulphates and salts. The presence of macro-pores enables the collapse of loess soils to take place. The void ratio expressing the quantity of macro-pores therefore has a determining effect on the degree of collapse, Rogers et al. (1994a). Loess is considered to be unstable as a foundation material because of the potential for large settlement. Problems result because loess undergoes structural collapse when wetted. The problems can be even more severe if differential settlement occurs. An example is a three storey building in Xining, Qinghai, destroyed beyond repair due to subsidence of the foundation soils upon wetting (Qian and Lin, 1988).

Collapse occurs if the initial dry density is low and initial water content is low (Dijkstra et al., 1995). There is still some argument as to why loess collapses. Collapse may occur due to the reduction of suction between the particles or it could be due to the break down of the clay and carbonate bonds between the silt particles, or quite possibly a combination of the two. To elucidate this problem it is necessary to examine both macroscopic and microscopic aspects of loess collapse (Fedá, 1995), (Dibben 1998), (Dibben et al, 1998).

Large areas of the earth's crust are covered with loess. China, America, Eastern Europe and Russia all have deposits ranging in depths from 1m to 100's of metres. For example, around 14 % of the total territory of the old USSR is covered by loess where the deposits are around 20m and deeper (Abelev, 1988). Consequently, many residential buildings in cities and towns and big industrial enterprises have been erected on loess around the world.

### 2.2.2 Residual soils

Residual soils represent a large proportion of collapsible soils. In general, residual soils can be found in plateau regions (Fookes and Best, 1969). They are produced by the in situ weathering of the underlying rock. They are relatively weak materials and usually quite

permeable. A dominant feature of residual soils is the bonding together of the particles by the chemical process of weathering. Bonding may be broken by loading or strain and once broken is irrecoverable. Two other features of residual soils are that they are usually unsaturated and they also inherit discontinuities from the parent rock. Both of these features have a major influence on the engineering behaviour. Two yield points are often observed, the explanation for this is postulated by Vaughan et al. (1988). The bonds during initial loading carry an increasing stress, as the bonded soil is stiffer than a similar soil without bonds. At some point some of the bonds start to yield, and a first yield point is observed. Thereafter, the average contribution of the bonds to the strength of the soil (the bond strength) decreases with increasing strain. However, the soil is still stiffer than it would be in the unbonded state, and the stress on the bonds (the bond stress) continues to increase. The decreasing bond strength will eventually become equal to the increasing bond stress and a second yield occurs. Typically this is followed by large strains, the progressive loss of remaining bond strength and a matching reduction in bond stress, until the soil loses its bonding entirely and becomes de-structured.

### 2.2.3 Man-made fills

Compacted soils are interesting for engineers as they are increasingly being used as new areas for construction. Their behaviour is only just being fully understood. A block of eight two-storey houses in Ilkeston, UK, was built on a stiff clay opencast backfill with a maximum depth of 12m. Soon after the brickwork was completed in 1973, damage was observed at one gable end. The BRE carried out inundation tests in 1975, which indicated that the fill was susceptible to collapse compression. The block was never occupied and was demolished in 1982, at which time the total settlement was estimated at 0.3m, Charles and Watts (1996).

An open, collapsible fabric made up of clay aggregates, and/or sand and silt particles, is the accepted explanation for the high collapse strains, Alonso et al. (1987). A substantial collapse is observed in specimens compacted dry of optimum. Volume reduction occurs when a partly saturated fill becomes saturated, Naylor et al. (1989). Inundation by rising ground water can cause significant settlements in opencast coal mine backfill, Blanchfield and Anderson, (2000). The collapse can occur without any increase in applied stress. This behaviour is being researched by the Building Research Establishment (BRE) and has been discussed in papers by Charles and Watts (1996), Skinner et al (1999) and Skinner (2001).

Non-engineered fill may have been inadequately compacted or placed excessively dry and can undergo a reduction in volume when the moisture content is raised. The moisture content may increase due to downward infiltration from the surface or from rising ground water levels. A methodology for measuring collapse potential in fills is proposed by Charles and Watts (1996).

#### 2.2.4 Quick clay

Quick clays are marine deposits, formed at the end or after the last ice age when melt water from the glaciers carried large quantities of fine grained sediments into the sea, Bell and de Bruyn (1997). They have restricted geographical distribution, occurring in certain parts of the northern hemisphere. However, quick-clay can produce possibly the largest scale collapses. Quick clays are characterised by high sensitivity and they may liquefy when disturbed which can lead to the notable landsliding. Spontaneously, or as a result of an abrupt shock, fluid flow expands in a cumulative manner over large distances, at times on an almost flat surface (Kerr and Drew, 1968). The 1971 St. Vianney landslide was responsible for considerable damage to the town of St. Jean Vianney. The constituent materials were primary minerals of quartz and feldspar, 2-6 microns in size with short-range bonds. The clay-sized primary mineral system accounts for the unusual flow behaviour of the soil. Many destructive landslides have occurred due to the properties of quick clay (Smalley et al, 1975). Inundation can also lead to the failure of foundations beneath a structure.

### 2.3 WHY CONCENTRATE ON LOESS?

Loess is a typical collapsible soil and is found all around the world. It has caused major disasters and understanding its behaviour is important so that foundation designs can be made safer. It is a classic collapsing soil, it has an open packing, is unsaturated (or partially saturated) and collapses upon loading and/or wetting. As loess is unsaturated it therefore has three phases (water, air and soil); this is a growing field of research at the present time. Techniques have been developed to model unsaturated soils which are uncemented, these soils are bonded by suctions only. In loess the bonding is more complex as the larger particles are joined by clay bridges and bonds and carbonate cementation as well as suctions. It is therefore necessary to take into account suctions along with other types of bonding when trying to model the behaviour of such soils. However, a simple model is needed so that modelling is not made over complicated.

## 2.4 ORIGIN OF LOESS

To make a physical model of the soil it is important to look at the processes that the soil has been through to make the structure it has today. Understanding the formation processes of natural deposits of loess should allow a more realistic artificial soil to be produced. The generally accepted western view is that collapse properties in loess are formed due to aeolian deposition. Russian literature supports two theories for the formation of collapsibility in a deposit. The 'syngenetic' theory proposes that the collapse properties are formed in the course of accumulation and early diagenesis of silty sediments in arid conditions, in line with the western view. However, the 'epigenetic' approach is also supported; this proposes that collapsibility can develop in-situ in an originally non-collapsible material. L.S. Berg was the major proponent of the in-situ formation hypothesis and his influence is still felt in geotechnical investigations of loess properties (see Smalley, 1971 and 1991 for a recent history). Denisov and Abelev are two of many researchers who have also discussed the genesis of collapsibility.

Outside Russia the idea of 'epigenetic' formation of collapsibility in loess materials is not recognised. The generally held view is that the silty material is transported and subsequently deposited and held in an open structure by various bonding mechanisms. Smalley and Smalley (1983) and later Tye (2000) reported four main stages in the formation of loess deposits,

- Formation of loess size particles (20-60 $\mu$ m).
- Transportation of the loess material
- Deposition of this material
- Post-depositional modification

In the UK, these stages may have been repeated a number of times to get to its current state. The formation of the basic particles of loess are due to its geological development and the palaeogeographic conditions of the time (Sajgalik and Klukanova, 1994). The source of the silt size particles is also still disputed. Smalley suggests that during periglacial climatic conditions a considerable quantity of particles were weathered with dimensions ranging from 0.1-0.01mm. This is the size of the basic unit in loess. What is not clear from the literature is if some of the clay particles were deposited at the same time as the silt particles

or if only the silt particles were deposited. Other theories show the silt particles can come from mountain and desert sources, see Pye (1995), Wright et al. (1998).

From the UK perspective, once formed, the particles were transported and deposited. Disintegration of the quartz particles and feldspars took place by freezing and thawing of water in the dislocation channels, either during transport or following deposition. First the particles were moved by glacial action, then by fluvial action and then by the wind. The loess may have been picked up and deposited several times by the wind before coming to its present location. Reworked loess such as this is known as a loess-like deposit. A combination of geochemical processes during formation, transportation and deposition affect the amount of carbonate cementation and clay mineral content. Modifications to the cementing agents can take place within the deposit after it has been deposited.

Gourui (1988) identified five stages in the development of loess:

1. The *loessization* stage – Aggregate grains and larger fragment grains in dust (10-50 micrometers in size) form the skeleton grains of loess structure. The loess in the northwest border region of the Loess Plateau in China is at this stage.
2. The *formation* stage - where the silt grains are loosely cemented together under climatic conditions. Rain can initially penetrate the structure and cementation strength is not sufficient to resist the weight of the overlying soil mass. The soil on the top of the deposit will collapse under its own self-weight, creating a layer of soil that will not be penetrated by the rain. The soil beneath this layer is uninfluenced by the rain and forms a self-weight collapsing loess stratum. This self-weight collapsing layer can become 10-15m thick if there is no variation in the climatic conditions. This was also described as the unstable stage by Dibben (1998). Such loess will possess very high collapsibility, low initial pressure of collapse (0.5 kPa) and rapid response to collapse. Loess in the northwest region of the Loess Plateau in China is an example of loess at this stage.
3. The *development* stage - As hydrogeological conditions vary, water will penetrate into the structure and cementation is reduced or even destroyed. The grains rearrange to form a new metastable structure to become a non-self-weight collapsing loess. Cementation between the rearranged grains is gradually developed. The new structure will possess less collapsibility and higher initial pressure of collapse (1 kPa) and

response to collapse will be slower. The loess in the middle region of the loess plate is at this stage of development, for example in Bulgaria.

4. The *degeneration* stage - The soil mass continually extends to non-self-weight collapsing loess stratum, with considerable thickness. The initial collapse pressure is higher (1.5 kPa) and the response to collapse is slower. The loess in the Eastern region of the loess plateau in China corresponds to this stage.
5. The *clayization* stage - If the climate is more humid, weathering and leaching effects will be greater and calcium will be leached out. Some aggregate grains will flow and others will soften and deform under their own weight. The softened grains coagulate with each other. The pore spaces in the soil mass collapse one after another and the inter-grain pores are filled which makes collapsibility gradually disappear. The loess will eventually not possess collapsibility. Loess in partial regions near the Southeast border of the loess plateau in China is at this stage, also loess in the UK, to some extent.

Guorui, (1988) suggests that climatic conditions explain regional differences in loess. Generally, as the climate becomes more humid collapsibility gradually disappears. As is seen in the regions of the Loess Plateau in China, where the Northwest is arid (more collapse) and the Southeast part is humid (less collapse). The more humid atmosphere of the Southeast of China has created a less collapsible deposit, possibly due to the increased bonding during the clayization phase or more self weight collapse as discussed above.

## 2.5 COMPOSITION OF LOESS

The structure of loess is dominated by silt (20-60 $\mu$ m) quartz particles of 8:5:2 aspect ratio, Rogers and Smalley (1993), known as blade-shape particles (Rogers et al., 1994a). The most widespread minerals are quartz, feldspar, carbonates, micas and gypsum which are found in dusty and sandy fractions. In clay fractions, illite, montmorillonite and mixed-layered kaolinite dominate (Osipov and Sokolov, 1995). Most loesses are characterised by carbonate content varying from a fraction of 1 to 25%, medium soluble mineral (gypsum) content – from 4 to 10%, readily soluble salt (chlorides) content – under 2%, half soluble oxides and hydroxides – under 2.4% and humus – 1-2%. Silica and iron oxide may be concentrated as cement at grain contacts and overgrowths of silica occur on the grains of quartz and feldspar.

Collapsible loess soils are characterised by high porosity, usually between 40–48% (Osipov and Sokolov, 1995). Typical void ratios ( $e$ ) are 1.5 for unstable (wind blown deposits) and 1.0 for metastable (pre-collapse) deposits. A denser more uniform structure is formed following collapse, with void ratios reducing to 0.4 - 0.6 in most cases, Dibben (1998).

Authors, Location,	LL %	PL %	PI %	Gs	Natural void ratio, $e_i$	Natural water content %	Void ratio after collapse	Coeff. Subsidence <sup>1</sup> $\Delta e/(1+e')$
Kane (1973) Oakdale, Iowa, US	27	23	4	2.72	0.8-0.94	21-23	0.45	19
El-Ruwaih and Touma (1986) Saudi Arabia,	33- 38	11-24	10- 13	2.55 2.74	1.00	4-23	0.68	16
N. Phein-wej et al. (1992) Thailand, Khon Kaen City,	18	13	5	2.63	0.84	5	0.58	14
Fookes and Best (1969) Kent, England	29- 31	19-21	10	2.72	0.75- 0.63	2-10	0.42	13
Yu Chi-Ying China (1982) Lanzhou, yellow river	30.1	16.3	13.8	2.7	1.08	14.3	0.83	12
Feda (1966) Prague, Czech Republic	26- 38	16-21	12- 19	2.7	0.61	14-17	0.50	7
Tan Tjong Kie (1988) north western China, Lanzhou, Lansu	27	15	12	2.72	1.05	8-11	0.94	5
Qian and Lin (1988) China, northern areas,	27.6	18.2	9.4	2.7	1.03	9	0.93	5
Klukanova and Frankovska (1995) Slovakia,	30	24	6	2.71	0.97	15	-	-
Dibben (1998). Bulgaria.	29	25	4	2.71	1.14	20.1	0.52	29
Dibben (1998). Star Lane, Essex, UK	34	20	14	2.67	0.80	18.4	0.45	20

**Table 2-1 Examples of Index properties of some natural loess deposits.**<sup>2</sup>

<sup>1</sup> After Abelev (1948).

<sup>2</sup> LL = Liquid limit, PL = plastic limit, PI = plastic index, Gs = Specific gravity.

$e_i$  = initial void ratio  $\Delta e$  = change in void ratio at a specific load.  $e'$  = void ratio before collapse

Typical index properties have been collected from the literature and are given in Table 2-1. The collapse coefficient (discussed in Section 2.9.1) at 200kPa is often 10-20%, which presents an enormous risk for buildings built on such material. The low plasticity index, PI, (5-15%) shows loess's sensitivity to changes in water content. It is clear that although the samples have been taken from a wide variety of sites all over the world, the index properties are consistent.

The 'dirt map' is being produced as an INQUA project run by the loess commission. This project has been organised to collect data on loess from around the world. This will form a valuable reference and may make climatic and geographical influences on loess collapsibility more clear.

## 2.6 BONDING MECHANISMS

Metastable structures formed in loess are dependent on a number of factors such as clay bonding and suctions. The main types of bonding are capillary tension (or matrix suction), clay buttresses, bridges and skins which are shown in Figure 2-1. Chemical cementing may also be present.

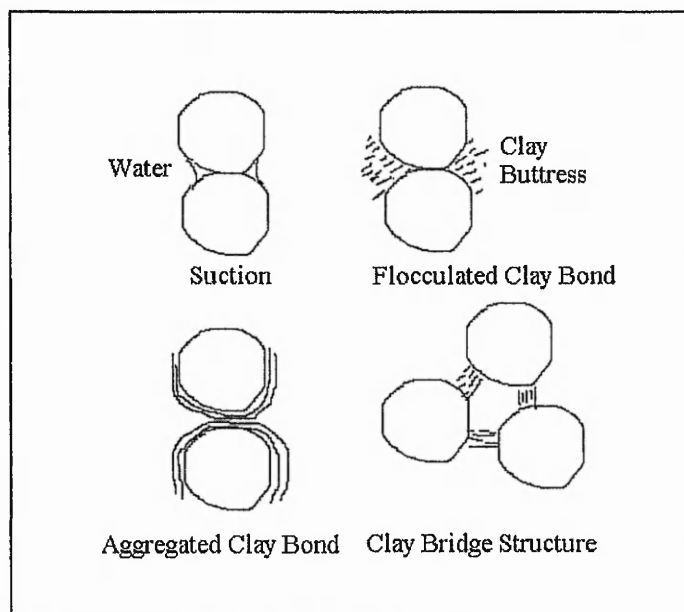


Figure 2-1 Bonding mechanisms in loess soil, after Barden et al. (1973)

Bonding and suctions have been studied in detail by various authors to help explain the collapse mechanism e.g. Barden et al., (1973), (bonding) and Alonso et al., (1987), (suctions). As yet, the role of suctions are still to be fully understood in soils such as loess. The relative contributions of suctions and other forms of bonding are also not well understood, and yet to model these soils successfully it seems vital that the contribution that each bonding mechanism has on the strength of the soil is known.

## 2.7 COLLAPSE MECHANISMS

Hydrocollapse to a new equilibrium occurs when water is introduced to a system. Importantly, both suctions and clay bonding, common in loess soils, are weakened with the addition of water (Bally, 1988), although the degradation process develops at different rates in both systems. Suctions are reduced immediately, clay bridges and buttresses will reduce in strength at a much slower rate and in the case of chemical cementing the reduction in strength may be even slower (Barden et al., 1973). Clay dominated systems may therefore have a slower response than pure suction systems such as non-engineered fill. The original open structure is reduced to a closely packed structure, which is much more stable. Once collapsed (due to increased moisture content and/or load) the deposit will not collapse to the same degree again, as the open macro-pores will never be formed again, unless the deposit is reformed or transported (e.g. by the wind). Soil improvement techniques often use this process to enhance the properties of the ground, see for example Evstatiev (1995).

## 2.8 SUCTIONS

In some structures such as fills and granular material, the bonding between grains is formed entirely from suctions. Suctions are developed due to the menisci within the soil skeleton. If the saturation is low then the air will be continuous and the water will be held at intergranular contacts by surface tension. If the saturation is high, the water will be continuous through the soil and air bubbles will appear as discrete bubbles in the pore water. At intermediate saturations both the water and air phases may be continuous, Anderson et al. (1993). Due to surface tension effects, the pore air pressure,  $u_a$ , will be higher than the pore water pressure,  $u_w$ . Matrix suction,  $S$ , is defined as the difference between the pore air pressure and the pore water pressure ( $u_a - u_w$ ).

## 2.8.1 Measuring suctions

There are a number of techniques to measure suctions described by Fredlund and Rahardjo, (1993). The main techniques are shown in Table 2-2. These methods are explained in detail in Fredlund and Rahardjo (1993). Other techniques have been developed at Imperial College where the use of a suction probe and suction controlled oedometers, Dineen and Burland (1995), and triaxial equipment have been used for a number of years and are still being developed.

However, it is unclear what suction measurements would indicate in a soil such as loess. The capillary tension between two small clay particles will be considerably greater than the capillary tension between two, relatively larger, silt particles. It could be assumed that the suction measurements would give an average suction throughout the sample. The average suction may not indicate the true collapsible nature of the soil.

Name of device	Suction Component Measured	Range (kPa)	Time	Comments
Psychrometers	Total	100-~800	minutes	Constant temperature environment required
Filter paper (in contact)	Matrix	Entire range	7 days	
Filter Paper (no contact)	Total	Entire range	7-14 days	May measure matrix suction when in good contact with moist soil
Tensiometers	Negative pore-water pressures or matrix suction when pore-air pressure is atmospheric	0-90	Minutes	Difficulties with cavitation and air diffusion through ceramic cup
Null-type pressure plate (axis translation)	Matrix	0-1500	Hours	Range of measurement is a function of the air entry value of the ceramic disk
Thermal conductivity	Matrix	0-~400+	Weeks	Indirect measurement using a variable pore size ceramic sensor
Pore fluid squeezer	Osmotic	Entire range	Hours	Used in conjunction with a psychrometer or electrical conductivity measurement
IC tensiometer	Matrix	0- 1800	Minutes	

**Table 2-2 Summary of the methods of measuring suctions**

Total suction is the sum of the matrix suction and osmotic suctions which are the components of free energy of the soil water. Phein-wej et al, (1992)—refers to Udomchoke (1991) who measured the suction pressure of undisturbed loess samples treated for the whole range of degree of saturation and established their correlation. He found that the capillary suction corresponding to the natural water content (10-12%) of Red Loess was around 10-30kPa. This capillary tension is several times smaller than the threshold pressure (100-200kPa) required for the start of collapse found for Red Loess. In addition, it was observed that the full collapse settlement in both the double consolidation tests and plate bearing tests did not develop instantaneously following wetting. In fact, it requires a considerable lapse of time 1-2hr in the plate bearing tests. Therefore any significant role for capillary tension was ruled out by Udomchoke.

To predict the collapse settlement in a period of time, it is necessary to know the characterisitic stress-strain relationships of the soil. The stress-strain behaviour is greatly influenced by its water content. The effect of water content was addressed by Redolfi and Mazo (1994). With the objective of determining the stress-strain relationships for loess specimens from Argentina at different water contents, a number of oedometric tests were conducted under constant suction conditions. Variation of water content was very small when loading under constant suction. Suctions in the range of 100-500 kPa were investigated. The suctions in these samples were significantly higher than the natural suctions reported by Udomchoke (1991). The suctions in these tests will therefore have more influence on the samples.

## 2.9 COLLAPSE PREDICTION

In the following sections some of the methods that are currently used to predict the behaviour of soil are discussed. Particle packing, finite element methods and more simple predictive equations have been used to describe collapse by some authors. Recently a debate at imperial college discussed the motion "this house believes continuum models are past their sell-by-date", Dr. Colin Thornton of Aston University was the speaker for the motion and John Atkinson spoke against the motion. Dr. Thornton's view was to "throw out the garbage and get back to physics". He discussed that particle physics could be applied to soils and would take away the "black box" approach to geotechnical analysis. Against the

motion the view was that "other techniques such as the particle packing approach would have a role to play in improving the constitutive equations".

The debate shows the range of approaches available to geotechnical engineers in order to solve problems. The issue here is which is the most relevant for the current problem. Obviously the majority of people still see continuum models as the future for soil mechanics. However, it is important not to rely solely on the "black box" solutions and think about the physics behind the problem.

### 2.9.1 Laboratory Tests

The main feature of this type of soil is that it is prone to collapse due to its open packing arrangement. After collapse it will form a more closely packed structure. Upon saturation, the bonding disintegrates and a denser structure is achieved by sudden collapse of the soil particles - often known as **hydrocollapse**. Saturation of the soil can occur through infiltration due to pooling of water from above, leakage from pipes and guttering or through rising ground water levels, Schwartz (1985). The collapse of the internal structure occurs when the stresses between particles exceed the bond strength provided by the bridging bonds (Holtz and Gibbs, 1951).

Some authors have discussed collapsibility in terms of fundamental properties of the soil. For example, Denisov (1951), states that collapse is probable when,

$$e_L/e_o < 1 \quad (2.1)$$

where,  $e_L$  = void ratio at the liquid limit  
 $e_o$  = natural void ratio

Criterion based on void ratio, moisture content, Atterberg limits and dry density (e.g. Gibbs and Bara, 1962), have all been developed. These relationships tend to predict the probability of collapse, but not the magnitude of collapse.

The best known technique for testing collapsible soils is to perform one-dimensional compression tests using the oedometer (or consolidometer). Oedometers can be used in two ways to predict collapse. The first is known as a single oedometer test because only one

specimen is required. The oedometer is loaded in increments to apply a certain stress on the specimen, for example, 200kPa, and then the specimen is saturated. The oedometer is subsequently loaded in increments until the applied stress on the specimen is 1600kPa. The second test is the double oedometer test. This test requires two identical specimens, something very difficult to guarantee in natural samples due to sampling effects (Culshaw et al., 1992). One of the specimens is tested unsaturated and the other is saturated before any stress is applied. The oedometers are loaded to apply stresses up to 1600kPa to each of the specimens in the same increments as for the single oedometer test. The difference between the settlements observed in the two samples at a given stress, is assumed to represent the amount of collapse that would be observed in a single oedometer test at the same stress. The coefficient of collapse ( $i_c$ ) is defined by Abelev (1948) and presented by Lutenegger and Hallberg (1988) and is often determined for applied vertical stresses of 200 or 300kPa.

$$i_c = \frac{\Delta e}{1+e'} = \frac{e'-e''}{1+e'} \quad (2.2)$$

where,  $\Delta e$  = decrease in void ratio  
 $e'$  = void ratio before wetting  
 $e''$  = void ratio after wetting

Generally, if  $i_c > 0.02$ , the soil is considered to be collapsible. Oedometer tests are discussed further in chapter 3, on geotechnical testing. Northmore et al. (1996) gives a discussion on other ways to calculate collapse coefficients.

To elucidate the problems associated with collapsible loess soils, a 'model' loess soil has been developed building on the work of Assallay (1998) and Dibben (1998). The model soil behaves in a similar way to natural loess under load and exhibits the same hydrocollapse behaviour when wetted. The material constituents can be directly controlled, thus providing a good method of assessing the effect of varying the contents on the overall collapse behaviour. The artificial material also allows 2 samples to be made 'identically' for use in the double oedometer test. Oedometer tests using the artificial loess have been carried out to examine the effect of varying clay content, initial compaction and initial saturation on the collapse process.

The artificial specimens were produced from silt sized particles mixed with clay. Samples were produced using the same mass (Dibben, 1998) or same void ratio (Assallay, 1998) for each clay content, see chapter 3 for methods. The samples were given an open structure by first sieving the material, were then steamed to produce a low water content and then placed in the oven to develop the clay bonds, see method by Dibben (1998). The limitations of this approach are discussed in chapter 3. Dibben (1998) discussed three important stages in the formation of the artificial loess. Firstly, the unstable stage (after the sample has been sieved into the container) representing an air-fall deposit. Secondly, the metastable stage (pre-collapse) when the sample may be loaded and exhibit relatively stiff behaviour for low loads. Finally, the stable stage (post-collapse) where the sample has been wetted and collapsed due to the load and moisture content of the sample.

### 2.9.2 Field Tests

Field tests have been developed to identify potentially collapsible soils, Houston et al. (2001). The tests normally involve comparing samples in their natural condition with saturated samples. Often, limitations are imposed on the relationships. For example, the saturation must be less than unity and the porosity above 40% (Fookes and Best, 1969). Again, most prediction criteria are qualitative methods, they do not provide details on magnitude or rate of collapse.

### 2.9.3 Particle Packing

Collapse can be defined as the transformation from an open, metastable packing to a closer packed more stable structure of significantly reduced volume (Rogers, 1995). Particle packing was developed to look at individual particles and can be used to understand the transitions from metastable to stable structures. Rogers et al. (1994b) discuss how packing influences a wide range of geotechnical properties including:

- the amount of pore fluid which can be held in a sediment,
- the ease of movement of fluids through a deposit,
- the extent to which dissolved or dispersed materials can be introduced and
- the strength of the aggregate under shearing or vertical stress.

Particle packings can be characterised by their packing density and co-ordination number (CN). The packing density is the fraction of the packing volume occupied by its particles and the co-ordination number is the number of particles that contact a particular particle.

$$\text{Packing Density} = \text{Volume of solids} / (\text{Volume of Solids} + \text{Volume of Voids}) \quad (2.3)$$

The closest packing of a layer of spheres occurs where the spheres are arranged in a rhombus with angles of  $60^\circ$  and  $120^\circ$ . Graton and Fraser (1935) describe six packing arrangements for regular spheres, ranging in density from a relatively open cubic packing to a dense rhombohedral packing. This was extended by Smalley (1970) to give nine possible cells representing simple packings. Uniform packing has been described using unit cells, which is the repeating pattern of particles within the packing. The cubic cell, for example, has 6 square faces and is described by the symbol 600, see Figure 2-2. The first number refers to the number of square faces of the unit cell, the second to the number of faces with acute angles between  $60^\circ$  and  $90^\circ$  and the third with acute angles of less than  $60^\circ$ . A packing of 402 would therefore have 4 square faces and 2 faces with angles of less than  $60^\circ$ , see Figure 2-2.

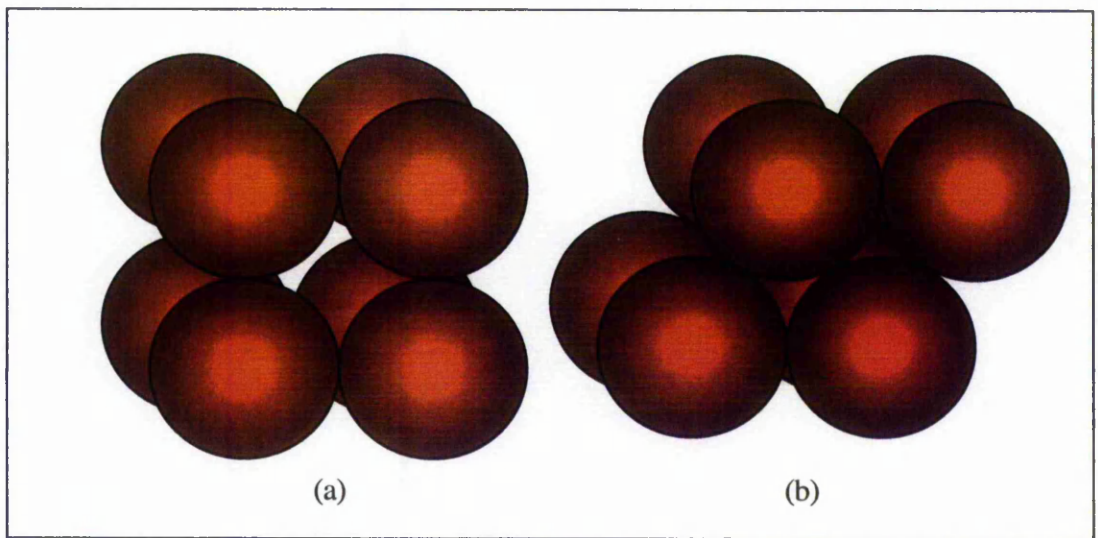


**Figure 2-2 (a) Cubic Packing (600) and (b) Orthohombic packing (402) as discussed in Rogers et al. (1994)**

A key paper, written by Dijkstra et al. (1995), describes the nine different packings in detail. The transformation from state to state is central to the packing problem as applied to loess structure collapse, in which packings transform from loose packing to denser packing. The transition from 600 to 402 might have much in common with the collapse of the loess structure. For loess there is the transition between dust cloud and to initial open structure, the transition from rigid open structure via hydrocollapse to a much more tightly packed

structure. The slow transition from an open Malan loess to a somewhat more tightly packed relatively rigid Wucheng loess could be described in this way (Derbyshire et al., 2000).

Morrow and Graves (1969), pointed to a possible way to assess the transitions and transformations of packing structures. They suggest that one way forward in the study of packings is to concentrate on transitions rather than the basic packings. The transition from one relatively unrealistic model packing to another might in fact model well the transition from one real packing to another. In this way it might be better to model the process than to model the basic structures. They also considered that, although random packings exist, they would contain a high percentage of structures that will be associated with certain unit cells of the regular packings.

Nolan and Kavanagh (1992) have shown some random structures that are directly involved in random packing transitions. These are random loose packing (RLP) and random close packing (RCP) see Figure 2-3. In addition, they have offered a transformation chart that may be applied to the loess collapse situation. They propose four types of random packing. Figure 2-4 indicates the boundaries of the random packing system. They have demarcated regions of CN and packing density in which transitions occur. Their model simulations showed that packing densities lie between 0.509 (RLP) and 0.638 (RCP) see Figure 2-4. The dynamic activities shown on their diagram can be related to loess collapse, if the collapse process is seen as a transition from random loose packing to random close packing. The proposed transition for loess particles shown in Figure 2-4 was added by Dijkstra et al. (1995).

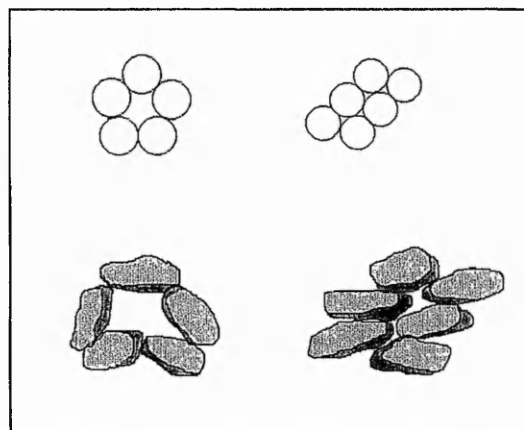


**Figure 2-3 Random Loose Packing (RLP-Left) and Random close packing (RCP-Right) for spheres and loess particles, (after Dijkstra et al., 1995)**

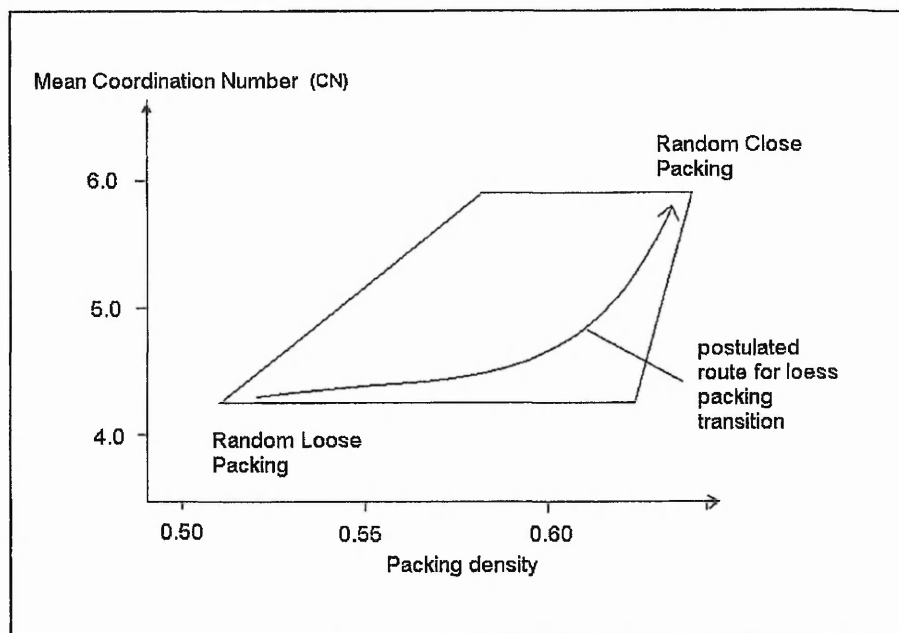


**Figure 2-4** The boundaries of random packing, after Nolan and Kavanagh, (1992).

Tests on contemporary loess show that the voids ratio is usually about 1.0 (i.e. the packing density is about 0.5, half solids and half voids). This structure is metastable and tends to deform relatively easily. The densities theoretically proposed by the computational study by Nolan and Kavanagh (1992), fit in very well with data on pre-and post-collapsed densities of loess. The RLP has a density of 0.5 ( $e=1.0$ ), as seen in natural loess (see Figure 2-4). When collapsed the density is increased, the void ratio expected in a natural collapsed loess would be around 0.5 - 0.6 which equates to a density of 0.66 - 0.625, close to the RCP value of 0.638, (also shown on Figure 2-4). The highest density packing found empirically has been 0.740 which corresponds to void ratios of 0.351, Nolan and Kavanagh (1992). None of the loess investigated within the literature has a void ratio less than this value, as expected. The packing literature helps to elucidate the current understanding of collapse, for it is ultimately the way the particles pack that controls collapsibility.

There are large differences between sphere packings and those composed of simulated loess particles (including differences in packing density, CN, potential surface area for cementation, clay bonding of the structure, sensitivity). Two loess particles may be

sufficient to keep the structure stable due to the blade shape particles. However the model is useful to study particle packing theory, which has been developed using spheres.

#### 2.9.4 Constitutive Modelling

The measurement and description of volume change of unsaturated soils under a variety of stress and suction paths has received considerable attention e.g. Fredlund and Rahardjo (1993). Collapse and swelling behaviour has been frequently reported in the literature. Oedometer tests and suction controlled cells have provided information on volume change and suction changes in loess. Smaller amounts of data are available for isotropic stress conditions for loess.

An increase of suction increases the stiffness of the soil against externally applied pressure (Dudley, 1970). Soils with an open structure experience collapse for a wide range of applied stress,  $p$  (mean normal stress). In fact, the amount of collapse increases with an increase of applied normal stress. Most low plasticity silty clays can either swell or collapse upon saturation depending on the confining stress. If  $p$  is sufficiently low, swelling occurs, or if sufficiently high, collapse occurs (Alonso et al, 1987).

The mechanical behaviour of unbonded, unsaturated soils can be interpreted in terms of changes of two stress variables: net total stress and soil suction, see Matyas and Radhakrishna (1968), and Fredlund and Morgenstern (1977). When the measured volume change of an unsaturated soil subjected to changes in net total stress and soil suction is plotted in a three-dimensional plot ( $e$ -void ratio,  $p$ -applied stress and  $S$ -suction) space, collapse and swelling conditions are readily interpreted and modelled. This was given the term 'state surface' and was proposed as a constitutive relation for unsaturated soils, see Figure 2-5.

This approach, however, has important limitations and was discussed and criticised by Alonso et al. (1987) and Alonso and Gens (1993) as follows:

- a) It is useful to represent volume change under certain isotropic stress paths but this representation can hardly be extended to take account of deviatoric stresses and deformations.

- b) Unsaturated soils exhibit strong irreversible behaviour just as saturated soils do. A consequence of irreversible behaviour is that collapse is stress path dependent if loading and unloading sequences are considered.
- c) An additional strong path dependence is observed in soils that experience suction changes. This feature manifests itself in collapsing soils and, more strongly, in swelling soils. In general, alternate applications of suction and net total stress changes, which lead to a common final value of the effective stresses, rarely result in the same deformation.

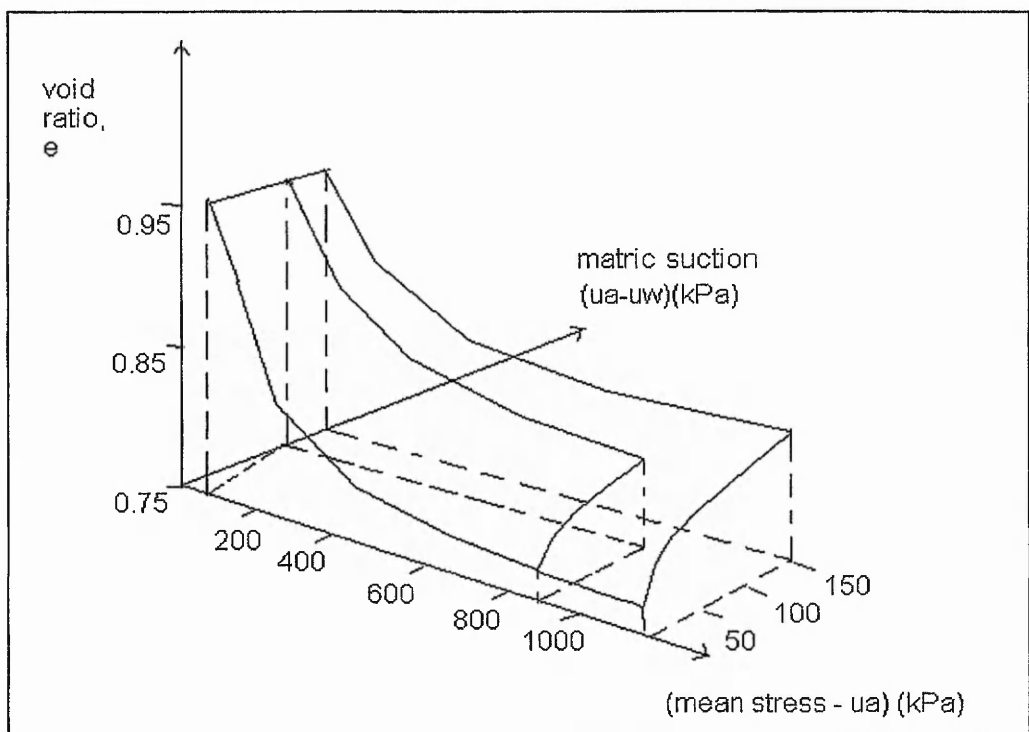


**Figure 2-5 Void ratio constitutive surface for a mixture of flint and kaolin under  $K_0$  loading, after Fredlund and Rahardjo (1993).**

Evidence supporting a non-unique state surface has been reported by many authors in the literature, Lloret and Alonso (1985). The state surfaces tend to be unique only for isotropic and oedometric conditions if the imposed paths always involve a non-decreasing degree of saturation (Matyas and Radhakrishna, 1968), i.e. no drying stages which increase the suction. Barden et al. (1973) came to the same conclusions. Lloret and Alonso (1985) found a unique state surface provided that there was no increase in suction or decrease in load. Also, state surfaces only reflect the response in terms of volume change of the soil to a

given imposed stress path, which does not provide a good framework to integrate volume change behaviour of unsaturated soils into a more general stress-strain relationship.

#### 2.9.4.1 Finite Element Models

Elasto-plastic models such as Cam-Clay and modified Cam-Clay have been used for many years to model saturated soils using critical state parameters, Alonso et al. (1987). These models enabled soil displacements up to failure to be determined for saturated soils. New frameworks have been developed to extend these models to include the effect of suctions for unsaturated soils. These ideas were introduced by Alonso et al. (1987), Wheeler and Sivakumar (1995) and implemented in CRISP84 by Nesnas (1995). The model produced by Alonso et al. (1987) is often referred to as the Barcelona model and is intended to describe unsaturated behaviour, using the knowledge of irreversible strains which occur as a consequence of changes in external stresses and suction for non-cemented, non-expansive soils. The Barcelona model has subsequently incorporated increasing numbers of new features (expansion, chemical and thermal coupling, etc.) and is becoming very comprehensive. Additional parameters need to be included in these models, which increases with the complexity and makes them more difficult to use. A great deal of expertise and effort is needed to generate these parameters and renders the problem even more difficult.

The model uses the ideas of hardening plasticity. The yield surface or locus of points, in relevant stress space, describes the boundary between elastic and plastic deformations. Irreversible deformations occur when the boundary surface is reached, which causes the yield surface to move to a new position. Either loading or decreasing suction may force the yield surface to move if the elastic limits of the yield curve are exceeded. The Load-collapse curve (LC) is shown in Figure 2-6 with axes  $S$ , soil suction and  $p$ , net mean stress. A three dimensional view of the yield surface is presented in Figure 2-7 in  $p, q, s$  space. Where  $p$  (net mean stress) and  $q$  (deviatoric stress) are stress invariants and  $S$  is matrix suction. As load or suction is increased, the yield surface becomes larger and plastic deformations occur.

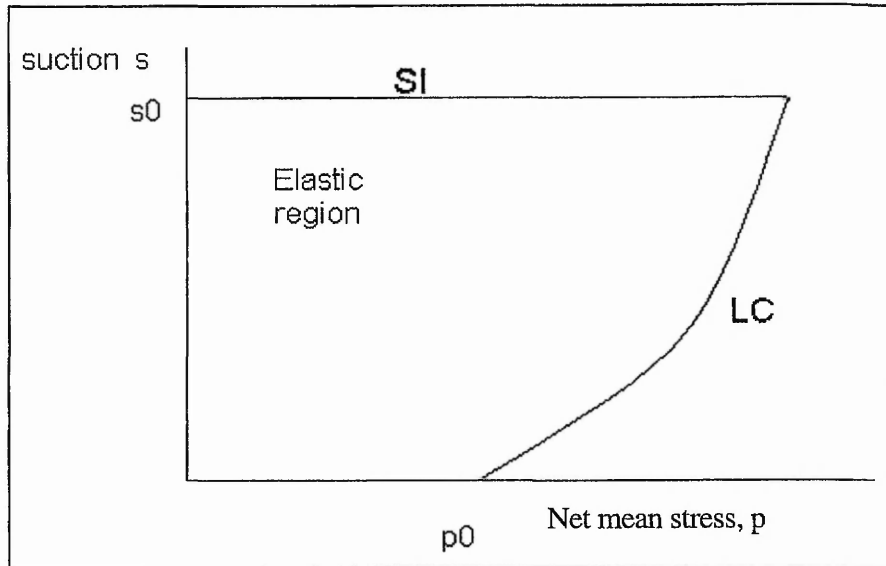


**Figure 2-6 Loading collapse (LC) yield curve and Suction Increase (SI) yield curve, after Alonso et al, (1987).**

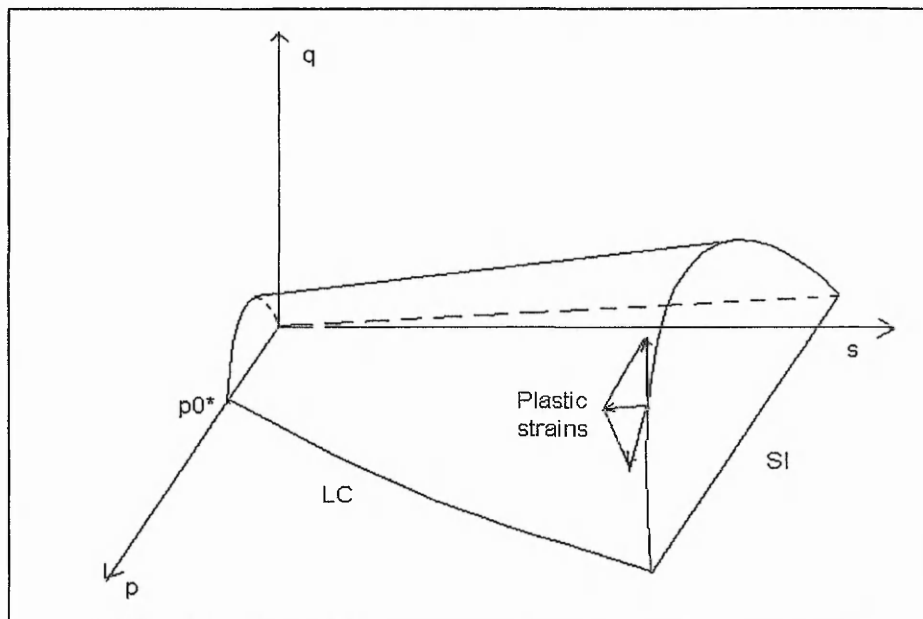


**Figure 2-7 Three-dimensional view of the yield surfaces in (p,q,s) stress space, after Alonso et al., (1987). p=net mean stress, q = deviatoric stress and S = suction**

Nesnas (1995) successfully incorporated an elasto-plastic constitutive model to predict the behaviour of unsaturated soils including collapse into the CRISP program. The model he used was the Barcelona model developed by Alonso et al. (1987). His study showed that the model successfully modelled theoretical results. However this model only predicts the

behaviour of uncemented unsaturated soils whose only bonding is provided by suctions between the particles. There is a wide range of soils that have cementation and other forms of bonding. These soils may not be modelled so successfully, especially given the difficulties in measuring suctions in such soils.

#### 2.9.4.2 Including bonding/cementation in unsaturated frameworks

An addition that has been discussed is the inclusion of bonding terms to include the effects of structure. Leroueil and Vaughan (1990), discuss the influence of structure on engineering behaviour. The concept of yielding developed to describe the effects of stress history in sedimentary clays is used to discuss the effects of structure. The shape of the yield curve due to structure is similar to that due to overconsolidation. They state that the effects of structure are as important in determining engineering behaviour as are the effects of initial porosity and stress-history, which are the basic concepts of soil mechanics. It is concluded that structure and its effects should be treated as a further basic concept of equal importance for natural sedimentary and residual soils.

Gens and Nova (1993) use these concepts to tentatively discuss the inclusion of a bonding term within the Barcelona model. This is a possibility for future work, although this complicates the models further with more parameters, which cost both time and money to derive. These models are becoming increasingly complicated with further additions of new parameters to include new concepts. They rely on the modeller undertaking a large amount of tests to find out the relevant parameters and coefficients to use these equations.

#### 2.9.5 Modelling Collapse

One of the oldest approaches to collapse problems is that presented by Nobari and Duncan (1972). Two property sets are defined, one for dry (d) conditions and one for saturated (s) conditions. Dry conditions are assumed initially up to point A (see Figure 2-8) and then collapse is simulated in two stages. In the first stage, a switch to the saturated curve is performed without strain changes, this is represented by point B. The corresponding stress is known as the clamped stress ( $\sigma^B$ ). In the second stage, equilibrium is restored by the application of the unbalanced stresses,  $\sigma^A - \sigma^B$ , to reach point C.

In order to find the clamped stress,  $\sigma^B$ , (Figure 2-8) for the saturated soil, Nobari and Duncan (1972) proposed that the dry soil is loaded with dry properties ( $w(d)$ ) along the

stress path OPA (Figure 2-9a) and the corresponding strain path OP'A' is recorded (Figure 2-9b). The saturated soil is loaded along the same strain path as the dry soil to find the stress point  $\sigma^B$  for the saturated soil, along the stress path OQB (Figure 2-9c). In Figure 2-9,  $q$  and  $p$  are deviatoric and normal stress invariants respectively and  $\epsilon_q$  and  $\epsilon_p$  are their associated strains.

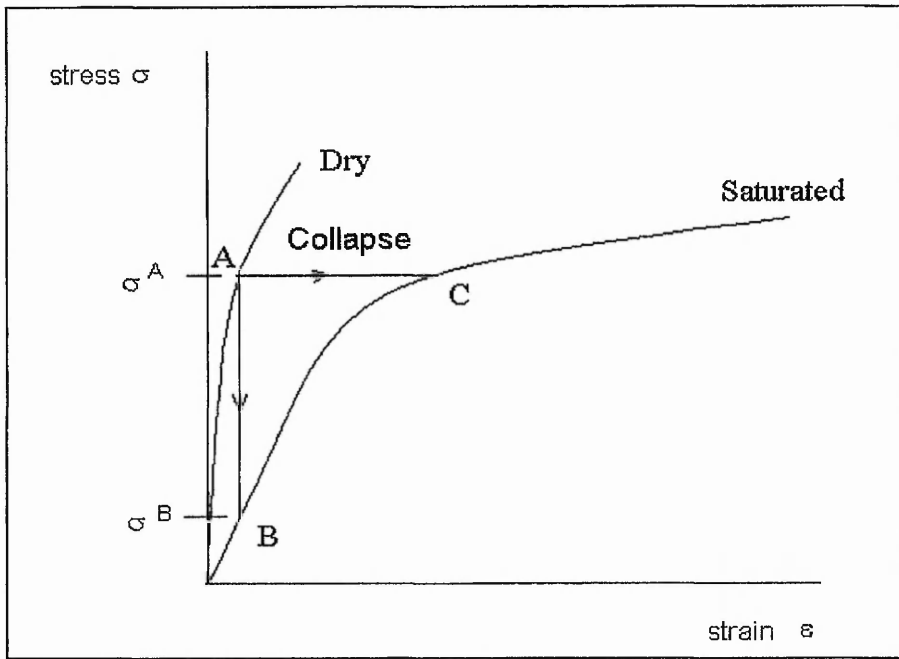


Figure 2-8 Collapse modelling using one set of parameters for the dry soil and one set of parameters for the saturated soil, after Farias et al. (1998)

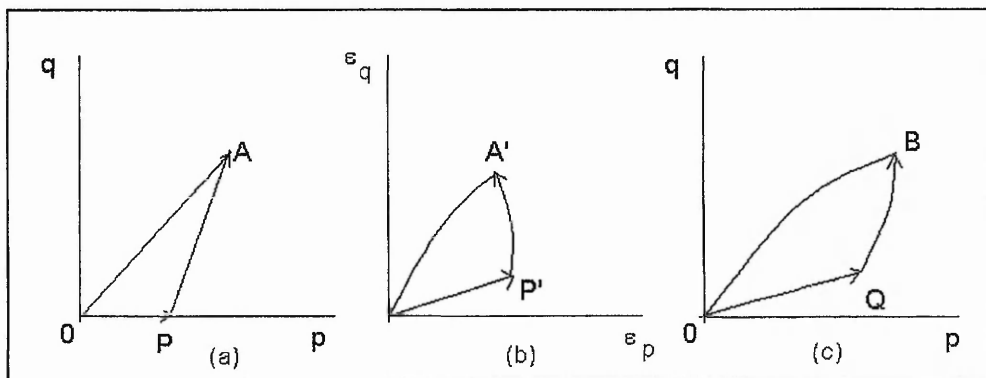


Figure 2-9 Stress and strain paths, after Farias et al. (1998) where  $q$  and  $p$  are deviatoric and normal stress invariants respectively

Nobari and Duncan's method of producing collapse overcomes the difficulties presented by the complexities of the elasto-plastic models described earlier in this section. It is a simple and effective way of evaluating the collapse potential of a deposit. The method uses the same assumption that is used for double oedometer tests. That is that difference in strain (AC) between a dry sample and a saturated sample would also be observed if a sample was loaded initially dry to  $\sigma^A$  and *then* saturated, see Figure 2-8.

Farias et al. (1998) have extended Nobari & Duncan's procedure so that any constitutive model may be used. The method was implemented in finite element routines using non-linear elastic models and critical state models, but still require development to model some behaviours such as the effect of horizontal expansion during collapse.

## 2.10 THE SCOPE OF THIS RESEARCH

From the literature survey it can be seen that many results have been reported on the physical modelling of collapsible soils using oedometer techniques. These techniques have been used to estimate the likely magnitudes of collapse in loess soils. Particle packing ideas can help to explain the phenomena observed in the oedometer tests. Assallay (1998) and Dibben (1998) started to develop an artificial material, which can be used to examine the effect of changing the constituents of the collapsible sample in a controlled way. These models have serious limitations but can be improved upon. There is a lack of comparable data in the literature. The artificial loess will help to broaden the understanding of the effect of the properties of loess on collapse behaviour.

Various approaches have been used to predict the behaviour of collapsible soils the main techniques employed have been discussed in this chapter. The broad aim of this research is to model the collapse both physically and numerically.

From the numerical modelling work presented above it is easy to see that a lot of work has been carried out on unsaturated soil behaviour. However, most of this work has concentrated on uncemented soils, which gain their strength from suctions. Cementation is an important factor for controlling collapsibility in loess and other natural soils.

Elasto-plastic models such as Cam-Clay and modified Cam-Clay have been used for many years to model saturated soils. New frameworks have been developed to extend these models to include the effect of suctions for unsaturated soils. These ideas were introduced by Alonso et al. (1987), Wheeler and Sivakumar (1995) and implemented in CRISP84 by Nesnas (1995). These models were intended for unsaturated, unbonded soils. Additional parameters need to be included in these models for bonding, which increases with the complexity and makes them more difficult to use. A great deal of expertise and effort is needed to generate these parameters and renders the problem even more difficult.

The inclusion of bonding terms allows the effects of structure to be examined. Leroueil and Vaughan (1990), discuss the influence of structure on engineering behaviour. Gens and Nova (1993) use these concepts to discuss the inclusion of a bonding term within the Barcelona model. This is a possibility for future work, although this complicates the models further with more parameters, which cost both time and money to derive. These models are becoming increasingly complicated with further additions of new parameters to include new concepts. The literature review allowed a reassessment of the aims and objectives at the beginning of the project. The aims of the project were to:

1. Determine the factors that influence the saturation collapse of loess soils by using and developing physical and numerical models of the soil.
2. Use the knowledge of unsaturated soil behaviour to produce a numerical model that can take account of cementation effects, to assess the effect of collapse under load/wetting.
3. Implement the model using finite element methods based on this model to compare the predictions of the model against a laboratory model of a footing supported by loess.
4. Compare the artificial and natural loess in terms of collapse.

## **3**

# **Element Test Methods**

---

### **3.1 INTRODUCTION**

The first aim of the project, as stated in Chapter 2, was to determine the factors that influence the saturation collapse of loess soils using a physical model. This chapter describes the methods used to develop the physical (or artificial) model soil. The artificial soil has helped to answer questions about the relative importance of the constituents and properties of the soil on the magnitude of collapse and has provided improved understanding of loess formation and collapse mechanisms. It has also proved to be a good method of producing a large uniform sample for modelling foundations built on loess.

The artificial loess deposits were produced in the laboratory, adapted from methods previously discussed by Dibben (1998) and Assallay (1998) to behave in the same way as a typical natural loess deposit. The silt and clay particles of the natural loess were represented by crushed sand and kaolinite, which were mixed together to form an open structured deposit. The artificial loess was further developed to produce a material with controllable, uniform collapse properties.

This chapter discusses the formation of the model loess and the main testing methods used to examine the geotechnical properties and collapse behaviour of the artificial loess. Index testing and the scanning electron microscope (SEM) were used to study the model soil. Hydrocollapse testing in the oedometers was carried out to assess collapsibility and triaxial tests were used to find values for Young's modulus. Laboratory testing provided plastic and liquid limits, particle shape and hydrocollapse results that were used for comparison with natural loess, hence, linking the artificial model with the behaviour of natural collapsible loess soils.

## **3.2 CLASSIFICATION**

### **3.2.1 Geometrical Characteristics**

Scanning electron microscopy (SEM) is widely used as an analytical tool. SEM testing was carried out at the Department of Geology at The University of Leicester using an SEM of type Leo 435. SEM analysis has the benefits of ease of preparation, good resolution and high magnification range. The technique was used in this project to look at grain shape, soil fabric and clay bonding in the artificial soils. The SEM consists of an electron optics column and an electronics console. Samples were oven dried and carefully fractured to expose an unaltered face to analyse. A small piece of material was glued to the SEM plug. The free soil particles on the surface of each sample were removed using a jet of compressed air. The small samples are coated with gold and then placed in a vacuum. The gold coating helps to avoid the specimen from charging under contact with the electrons. A schematic diagram of this equipment is shown in Figure 3-1. Results of the analysis are shown in chapter 4.

### **3.2.2 Index testing**

Index tests provide a basic classification of the soil that can be used to compare samples. Liquid and plastic limit testing was carried out on all the samples using the method detailed in BS 1377:1990 - Part 2 (BSI, 1990). Specific gravity testing was carried out on all the materials used for making the samples. The gas jar method was employed according to the methods described in BS:1990-Part 2 (BSI, 1990). The moisture content of the artificial samples was controlled using the methods described later, in Chapter 4, Section 4.3.

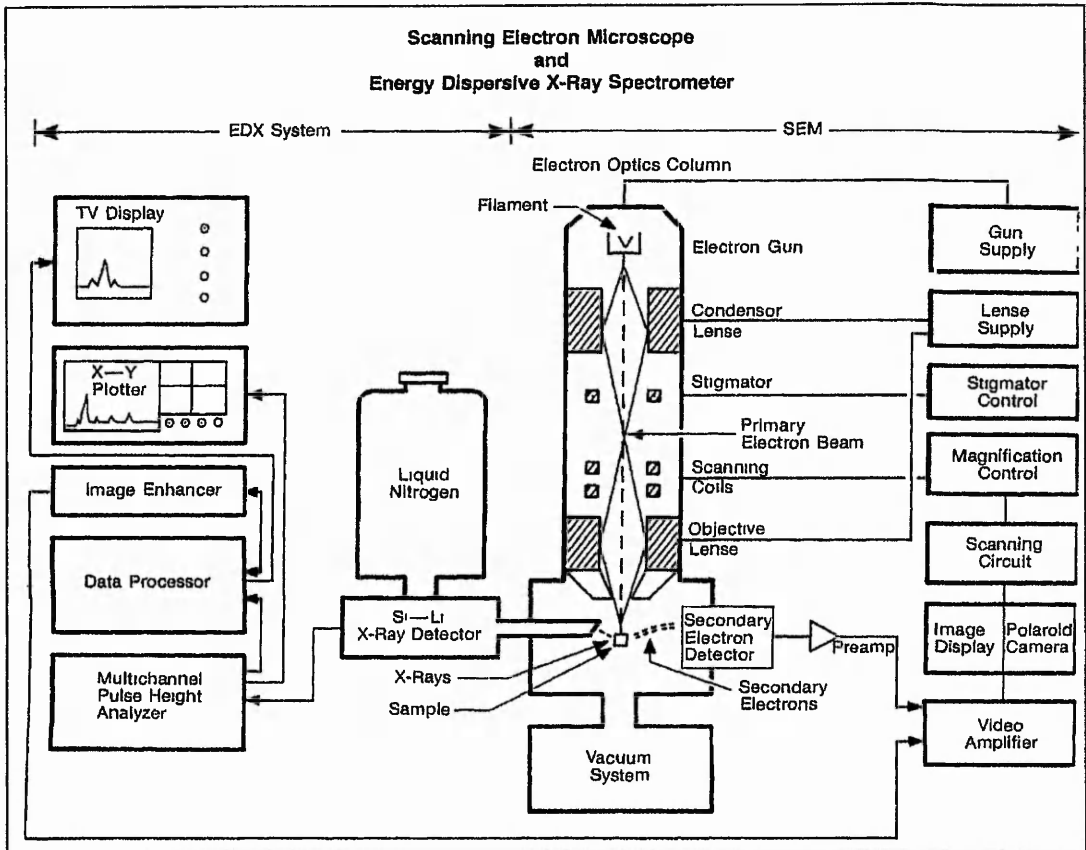


Figure 3-1 SEM equipment

### 3.2.3 Particle Size Analysis

A particle size distribution for each of the three materials used to simulate the silt-sized particles was carried out using the SediGraph, S5100, at the British Geological Survey (BGS) in Keyworth, Nottingham. The SediGraph determines particle sizes by using a sedimentation technique that measures the gravity induced settling rates of different size particles in a liquid of known properties. The largest particles fall fastest while the smallest particles remain in suspension for longer and therefore fall slowest, as described by Stokes' Law. The samples were prepared using Calgon (0.5 Molar Solution of Sodium Hexametaphosphate) which is a de-flocculent and, as such, separated the particles.

As particle shapes are never uniform, the size of the each particle is described using an 'equivalent spherical diameter'. A fine beam of x-rays pass through the sample cell to a detector. The percentage of x-ray beam that reaches the detector is used to calculate the particle size distribution.

### 3.3 PRODUCTION OF ARTIFICIAL LOESS SPECIMENS

To produce the model loess it was necessary to simulate the silt particles and clay bonds that form the basis of loess material. The primary silt particles were simulated using Ballotini balls, Leighton Buzzard sand, crushed to produce silt size particles or HPF4 silica particles. The Ballotini balls are spherical glass particles, purchased in the size range of 4 $\mu$ m to 90  $\mu$ m. The characteristic mode size of loess (Rogers and Smalley, 1993) is 20-60 $\mu$ m. Large ballotini particles were removed using a 63 $\mu$ m sieve. A sedimentation technique was used to reduce the amount of fines using a BS 1377: (BSI, 1990 – Part 2) standard dispersant solution of 33g sodium hexametaphosphate and 7g of sodium carbonate to 1 litre of distilled water. The solution was mixed and shaken well and left to stand for 10 minutes. Ten minutes was calculated using Stokes Law and corresponds to the time taken for particles greater than 20 $\mu$ m to settle, leaving the smaller particles in suspension. The smaller fines can then be decanted off.

Crushed sand was prepared using the mechanised grinder and then the same method as above was used to reduce the resultant silt to the required size range. 'HPF4 Silica Flour' was also purchased (from Hepworth Minerals and Chemicals Ltd) to reduce the amount of time spent grinding the particles to the required size. These particles were purchased in the size range 2 $\mu$ m to 100 $\mu$ m. The same techniques were applied to produce particles within the required size range for artificial loess production.

The clay used was Kaolinite which was found in previous studies to give the best results due to its non-swelling properties (Assallay, 1998).

#### 3.3.1 Previous methods

An air fall specimen was built up using a sieving technique, Dibben (1998). The sieve is held 400mm above the oedometer ring in which the sample is prepared. This is sufficient height to ensure a random deposition within the ring. The initial unstable structure is very sensitive and will collapse almost immediately under its own weight. For the artificial samples a constant mass of 120g of material was used for the crushed sand and 140g of material was used for the ballotini balls. This is in contrast to the work of Assallay (1998) who used a quantity of material capable of producing samples with a constant void ratio of around 0.9.

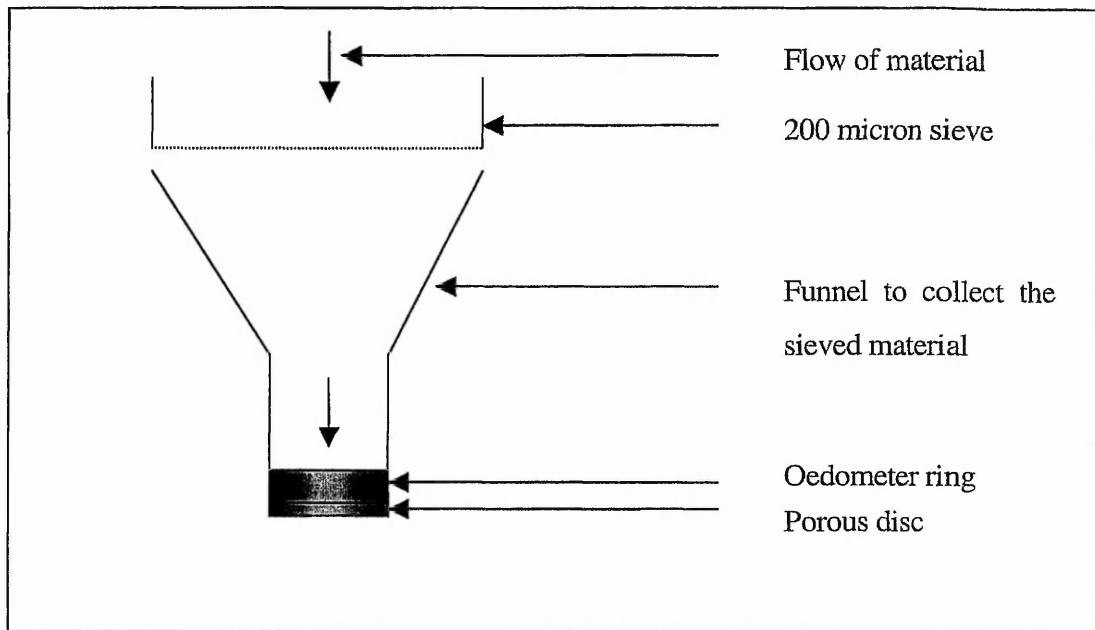


**Figure 3-2 The equipment used for the air fall method of creating a dry sample. Dry mixed clay and silt particles are sieved into the oedometer ring prior to steaming.**

Once the dry sample was formed, it was necessary to add a small amount of moisture to the sample to form the bonds. Distilled water was used for this. Dibben (1998) used a steaming method. The sample was placed over a boiling container of water. The steam from the container was forced through the specimen until the whole sample was wetted. This is determined when the sample became wet and therefore darker in colour at the top of the sample. A period of 1 hour gave a moisture content of around 12-13%.

Assallay (1998) investigated two methods of forming the samples; dry mixing and wet mixing. In the dry mixing method the silt and clay are mixed using a pestle and mortar and sieved through a  $63\mu\text{m}$  sieve to form unstable specimens. In the wet mixing method the particles were again mixed together in the pestle and mortar. Water was added to form a slurry at approximately the Liquid Limit and the slurry was mixed using the pestle and mortar. The wet soil was placed on a glass plate and partial evaporation of water was permitted. The soil lumps were oven-dried and sieved through a  $63\mu\text{m}$  sieve. The oven-dried material was used to form the samples in the oedometer ring and no extra moisture was added, unlike the method employed by Dibben (1998), who used the steaming method.

The steaming method provided better bonding between the particles as the bonds were not broken once the specimen had been formed.

Advantages of these methods:

1. Samples formed using the methods above produced a model soil that behaved in a similar way to natural loess under load and exhibited similar hydrocollapse behaviour when wetted.
2. The material constituents could be directly controlled, thus providing a way of assessing the effect of varying them on overall collapse behaviour

However, key limitations exist in these methods. The disadvantages are as follows:

1. The steaming method employed by Dibben (1998) could only be used on small samples. If larger samples are steamed the lower layers of the sample collapse under the weight of the higher material due to the high water contents produced lower down in the sample.
2. Moisture contents cannot be controlled using the steaming method.
3. Previous methods compared samples with either the same mass (Dibben, 1998) or the same void ratio (Assallay, 1998). The effect of clay content on the initial void ratio is therefore neglected. Initial void ratio will affect the magnitude of hydrocollapse it is therefore important that initial void ratios are not 'forced' but instead are formed 'naturally' so that the effect of the clay content on initial void ratio and quantity of hydrocollapse can be analysed.
4. Since either the mass or void ratio is kept constant, the samples do not relate to natural conditions in the ground. The effort needed to form the sample was greater for specimens with higher clay contents, using the methods employed by Dibben (1998) and Assallay (1998). Initial void ratios were therefore being forced to be unnaturally high for high clay contents, in the previous methods. A new approach is needed to produce samples with more natural void ratios.

### 3.3.2 A new approach

To eliminate effects 3 and 4 a new method was developed to produce more comparable samples. It was decided that instead of forcing the samples to the same void ratio, the samples would be left to form naturally. This was done by using the same energy to compress each of the samples. Each specimen is subjected to a known stress, using the

oedometer apparatus. The stress represents an equivalent overburden pressure and therefore allows the specimen to form at its 'natural' void ratio and mass. This simulates a sample at a given depth, therefore making the samples more comparable to natural samples. In addition, this allows different depths to be simulated by using different formation pressures.

Oedometer tests, triaxial tests and larger scale footing experiments were to be undertaken during this project. Steaming would not be possible in larger samples because the base would become completely saturated while the top would remain dry. The oedometer tests and footing tests must be comparable and therefore made using the same methods. New methods for wetting the samples were investigated. These new methods were developed in the oedometers and assessed for their potential for use in the footing test.

### **3.4 PRODUCTION METHODS USED**

The silt fraction and clay fraction of the loess need to be modelled. To simulate the silt sized fraction of loess, three materials were compared for performance. These were:

1. Ballotini balls
2. Crushed sand
3. HPF4 Silica flour – High purity quartz sand, dry ground, from Hepworth Minerals and Chemicals Ltd.

These materials were all prepared as explained in Section 3.3 to produce silt particles of the required size range. The clay binder used, continuing from the work of Assallay (1998) and Dibben (1998), was kaolin. Assallay reported that this was the only practical clay mineral to use, as the grains do not swell on contact with water. Hydrocollapse results are therefore not masked by swelling behaviour of the clay, as would be the case for a clay such as montmorillonite. Using this clay also means that results from the project can be directly compared to the work of the two previous authors.

### 3.5 MIXING METHODS

#### 3.5.1 Method 1 - The airfall method

Following the method used by Dibben (1998), a number of samples were produced. The samples were made from ballotini, crushed sand or HPF4 to compare the influence of particle shape on the characteristics of the artificial soil. The required amounts of silt and clay fractions were mixed together dry and sieved into the oedometer ring. The sample was tapped down to fill the ring using the same mass of the mixed particles. A pallet knife was used to smooth the surface and the sample was placed on steam bath. The steam was allowed to rise through the sample until the surface of the sample was damp. The sample was then weighed and dried in the oven to enable bond formation. The specimen was finally weighed again before testing in the oedometer.

#### 3.5.2 Method 2a - The wet paste method

Method 2a was developed to eliminate the need for steaming which could not be used in the future for larger samples as it provides no control over water content. As before, the required amounts of silt and clay were mixed together dry. The required amount of water (later referred to as the preparation water content) to form a paste was added and mixed well on a glass plate using a palette knife. The mixture was lightly compacted into the oedometer ring using a 20mm diameter wooden pole. Twenty light taps were used on the surface of the material to ensure that any large air pockets were removed. Care was taken to use the same effort each time a sample was made. A static compressive stress was used to further compress the samples to produce natural initial void ratios, as explained in section 3.3.4. The oedometer ring was placed in the oedometer case and screwed down. This was placed in the oedometer rig and the loading arm and disc were lowered onto the sample. Different overburden pressures were simulated by adding weights to the oedometer, calculated to apply the required stress on the specimen. This approach was used instead of forcing the void ratios to be the same for all clay contents (as in method 1). The sample was then weighed, dried and weighed again before testing. Some samples were oven dried to provide very low moisture contents, others were allowed to dry in air to be tested with higher moisture contents (this is the initial water content of the specimen).

### 3.5.3 Method 2b - The spray method

In this method, spraying the samples instead of steaming was carried out. The sample was formed in the oedometer ring and as in method 2a. The required percentage of silt and clay particles were mixed together. Water was added to form a paste, which was left to dry on a glass plate, as in the Assallay (1998) method. The dry porous disc and ring were weighed and a shallow layer of the dry mixture was crumbled and sieved into the oedometer ring. The dry layer was weighed, sprayed with distilled water and then weighed again. This step was repeated 6 more times to fill the oedometer ring in layers. The specimen was then placed in the oedometer and loaded to achieve the required preconsolidation pressure, as above in Section 3.5.2.

## 3.6 OEDOMETER TESTING

The amount and rate of collapse can be estimated from oedometer tests. The oedometer consolidation test is a well established technique and is described in BS 1372: 1990. The standard technique has been modified to investigate collapse behaviour of metastable soils by Kane, (1969), Jennings and Knight (1975), Handy (1973), Mellors (1978) and Lutteneger and Saber (1988) and many others. This technique is widely used to provide information on collapsibility of soils. The oedometer collapse test has become known as the hydro-collapse test due to the collapse response of the soil upon wetting. The two tests that have been consistently used in the literature are the single oedometer test and the double oedometer test. These methods have been shown to provide similar estimates of the magnitude of hydrocollapse (Lawton et al. 1989).

### 3.6.1 Apparatus

Front lever loading, fixed ring oedometers manufactured by Wykeham Farrance Engineering Limited were used for the oedometer tests. Vertical stresses are applied using dead weights. A counterbalance lever arm can be adjusted to maintain the lever arm in a level position. The applied stress is transferred to the specimen via the load shaft on to the loading yoke to ensure the loading is non-eccentric.

Vertical displacements are measured using a strain gauge with 0.001mm per division. The strain gauges are attached to transducers, which enables the data logger to record the displacements every minute. These two methods of measuring the strain were calibrated in

the laboratory using a micrometer before commencing the experiments. Smooth polished stainless steel rings of 76mm diameter and 19mm height are used to hold the specimens. The rings are held in place using an outer confining ring which slots onto the oedometer rig.

### 3.6.2 Samples

Artificial samples were made using methods 1, 2a and 2b. Method 1 was carried out to compare with the work of Dibben and Assallay. Methods 2a and 2b investigated using the same energy to make each of the samples. Natural samples taken from Essex were also tested from Star Lane brickworks, near Southend in Essex, NGR: 590 186. The samples were taken from site using the U100 sampling equipment developed by the BGS, described in Culshaw et al. (1993). The equipment for taking undisturbed samples is shown in Figure 3-3. This method is advantageous for a number of reasons including, drying out is virtually eliminated, the samples are simple to remove in the laboratory and oedometer samples can be prepared with the minimum of cutting away while the remainder of the sample can stay supported within the tube.

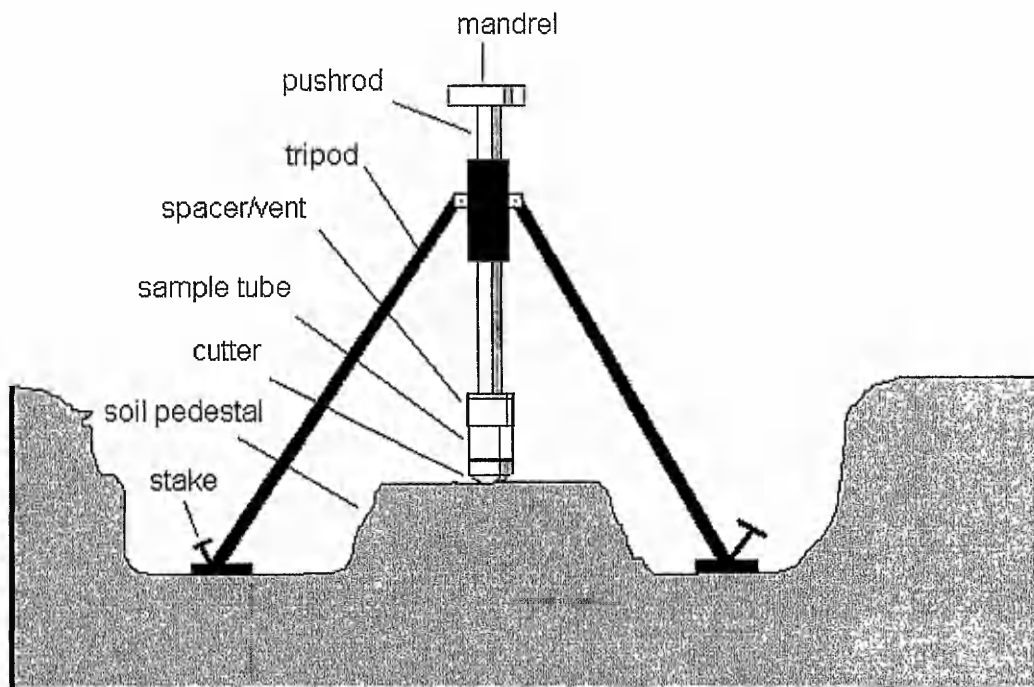


Figure 3-3 Schematic representation of the tripod sampler

### 3.6.3 Testing for hydrocollapse: Single oedometer test

Specimens were prepared and loaded using the oedometers. In the single oedometer test only one specimen is required. The specimen was stressed in increments, typically to 200kPa, and then saturated. The specimen was subsequently stressed to 1600kPa. The deformations at each stage were measured using a vertical dial gauge and transducer (LVDT), which allowed the readings to be logged over the duration of testing. Calibration of the LVDT's was carried out by comparing the readings to the vertical dial gauge, which in turn, was tested using a Vernier scale. The percentage change in height from before to after flooding was calculated and is expressed as the percentage hydrocollapse.

The sample was weighed before and after the test, to calculate the water content for each of the samples. Weighing the wet sample is not a true indication of the saturation ratio because during unloading in the oedometer, the specimen will draw in more water from the surrounding container. Even if the surrounding water is removed before unloading, the water from the porous disk is drawn into the sample. After weighing, the sample was oven dried for 24 hours at 105°C and then weighed again in order to find the dry mass of the sample.

### 3.6.4 Testing for potential hydrocollapse: Double oedometer test

The second test is the double oedometer test. This test requires two identical specimens, something very difficult to guarantee in natural samples due to sampling effects (Culshaw et al.1992) and the material variability. One of the specimens is loaded in its unsaturated state and the other is flooded before loading. Deformations are recorded for the saturated and unsaturated specimens with a vertical dial gauge. The difference between the settlements observed in the two specimens at a given stress, represents the amount of collapse that would be observed in a single oedometer test. The coefficient of collapse ( $i_c$ ) was used by Abelev (1948) and Lutenegger and Hallberg (1988) and is often determined for stresses of 200 or 300kPa.

$$i_c = \Delta e / (1 + e') = (e' - e'') / (1 + e') = \Delta h / (1 + h') = (h' - h'') / (1 + h') \quad (3.1)$$

where,  $\Delta e$  = change in void ratio

$e'$  = void ratio before wetting

$e''$  = void ratio after wetting

$\Delta h$  = change in height

$h'$  = height before wetting

$h''$  = height after wetting

Generally, if  $i_c > 0.02$ , the soil is considered to be collapsible.

Collapse coefficient can also be obtained from:

$$i_c = \Delta e_v / (1 + e_0), \quad (3.2)$$

Where,  $\Delta e_c$  is the change of void ratio upon wetting and  $e_0$  is the natural void ratio. This latter calculation takes in to account the deformation due to loading as well as the collapse observed due to wetting, Knight (1963). The coefficients vary with stress at wetting, so it is important to quote what the saturation stress was, as well as the method for calculating the collapse coefficient. This project has used the former definition (3.1) for collapse coefficient at a stress of 200kPa.

### 3.6.5 Procedure

All experiments were carried out in a temperature controlled room, to ensure repeatability. Loading was carried out using modifications to BS 1377:1990 (BSI, 1990). A stressing sequence of 5, 10, 25, 50, 100, 200, 400, 800 and 1600kPa was used. The required load was added to the loading arm after 1 hour in most cases, long enough for the structure to densify under each applied stress (Dibben, 1998). After flooding the specimens were left for up to 12 hours to allow for complete hydrocollapse. A summary of the oedometer tests undertaken are given in Table 3-1.

### 3.6.6 Testing the oedometer for creep

To make sure the deformations recorded are from the settlement of the sample and not from creep of the apparatus, the following procedure was followed every 6 months. A steel plate with a known stiffness was tested in the oedometers. The apparatus, with the steel plate, was left with no load for one hour and the displacements are recorded. A vertical stress of 5kPa was applied to the steel plate. The applied stress was increased in increments (10, 25, 50, 100, 200, 400, 800, 1600kPa) every hour, and the displacements recorded. Creep can then be worked out from the recorded displacement minus the expected displacement. Creep was monitored for the equipment and found to be negligible for the short duration of

the loading sequence. At 19°C the oedometers were found to be accurate to  $\pm 0.001$ mm. The test room was kept at 19°C for the duration of the testing program.

Silt Type	Method (preconsolidation pressure)	To test	Preparation water content %
Loess from Star Lane, Essex	-	Typical natural behaviour of UK loess	-
Crushed sand	1 – constant mass	Effect of clay content percentage (0-40%)	steam
Ballotini balls	1 – constant mass	Effect of clay content percentage (0-40%)	steam
Ground Silica	1 – constant mass	Effect of clay content percentage (0-40%)	steam
Ground Silica	2a – constant effort (0, 50, 100kPa)	Effect of clay content percentage (10,20,30,40,50%)	17.5 and 30%
Ground Silica	2b – constant effort (5, 10 50kPa)	Effect of clay content percentage (0,5,10,15,20,25,30,35,40,60, 100%)	10-20%

**Table 3-1 Summary of the oedometer tests undertaken during this project**

### 3.7 TRIAXIAL TESTING

Like the oedometer test, the triaxial test provides data on an element of soil. However the loading conditions can be more readily compared to the stresses that occur in the ground, as they involve three-dimensional pressures which can be controlled. Unconsolidated, undrained triaxial tests were performed to suggested practice in the testing soil manual volume 2, Head (1990). The conventional method of determining strains in soil samples in triaxial tests is to measure the displacement of the loading piston relative to the machine platen or cell body. This is assumed to be equivalent to measuring the displacement of the top cap relative to the base pedestal. Strain measurements of this kind are referred to as

end-cap measurements. This method is usually satisfactory if large strains occur and if only the failure criterion is relevant.

The main sources of error in end-cap measurements of strain are as follows:

- 1) Deflection of load cell, or bedding of load ring contact seatings.
- 2) Deflection of loading system, including bedding of cell base.
- 3) Tilting of sample.
- 4) Consequent reorientation of top cap.
- 5) Bedding of top cap and base pedestal on to sample.

Deflection of the equipment was found to be negligible compared to the relatively large movements found in the sample. It was necessary to make sure that the sample was centred on the equipment to avoid tilting and reorientation of the cap. This was done by forming the samples in a tube and placing the end caps in the tube during the formation of the sample. The bottom cap was placed on the base plate of the equipment and the top cap, which had a locating ball on the top, fitted into the hole at the top of the equipment to ensure adequate centring of the sample.

### 3.7.1 Samples

Artificial samples were made using method 2a. A small number of natural samples were also tested. The samples were taken from block samples taken from Pegwell Bay, near Ramsgate in Kent, NGR: 635 165.

### 3.7.2 Method for Undrained Triaxial Tests

A number of undrained triaxial tests were performed on samples with 30% kaolinite content to further test the stiffness of the soil, as this clay content was found to give a good representation of the behaviour of natural loess, see chapter 4. Formation of the samples was carried out on a similar basis to the oedometer tests. Samples were compacted, using the same effort as for the oedometer tests. Specimens of 38mm diameter and 76mm in height were formed in the triaxial membrane, which was inserted in a metallic tube on the triaxial cell base. This allowed the sample to keep its shape until it had dried sufficiently. The samples were left to dry in air for 1, 2, 3 and 4 days and some for up to 3 months, to produce samples with different initial water contents and bonding strengths.

Minor principal stresses of 100, 200 and 300kPa were used and axial stresses were applied until failure. These stresses were used to represent the stresses of a heavy foundation on the soil. The strain rate was 1.5mm/min, as for traditional quick undrained triaxial tests. These tests were performed on saturated and unsaturated specimens to produce Young's Moduli for both saturated and unsaturated states. This gave an idea of how much the sample would collapse if loaded and then wetted as for the oedometer tests. A range of water contents were tested to get an idea of how much settlement to expect as ground water level is raised and water content is therefore increased. This is important for the next stage of testing and prediction, which involved a model foundation on loess soil with increasing ground water level

### 3.7.3 Elastic Parameters

A small number of tests were carried out using the triaxial apparatus to get an approximate idea of the stiffness compared to that in oedometer apparatus where vertical displacement can only take place.

Young's Modulus,  $E$ , and Poisson's ratio,  $\nu$ , are needed for use in the stress analysis. A vertical stress  $\sigma_v$  produces a vertical strain  $\epsilon_v$  equal to  $x/L$ , where  $x$  is the deflection and  $L$  is the original length. Within the elastic range, change of strain is related to change of stress by the equation

$$d\sigma_v = E \cdot d\epsilon_v \quad 3.3$$

Where  $E$  is defined as the Young's modulus of elasticity.

$E_u$  for undrained

$E'$  for drained conditions

Derivation of the elastic moduli can be done in one of three ways. The tangent modulus can be derived by drawing the tangent to the stress-strain curve at a selected stress or strain. The secant modulus is the slope of the line connecting the origin to a particular point at a particular stress value. These moduli are normally found for the plastic part of the stress-strain curve. The elastic modulus, or Young's modulus, can be found for the straight line part of the curve, where initial loading causes elastic behaviour.

The derived modulus value varies with the selection of the relevant points on the stress-strain curve. In traditional practice the modulus is related to a realistic stress range, or to a specified fraction of estimated or measured failure stress. For many applications it is the

behaviour at very small strains that is most significant, as foundations will be designed to produce the lowest settlements possible in the soil. The chosen method will depend on the shape of the stress-strain curve. For loess it will be the difference between the unsaturated and saturated curves that will prove most significant.

Young's Modulus is related to the constrained modulus found from the oedometer tests. The constrained modulus (confined compression),  $D$ , is defined as, change in normal stress/change of strain.

### **3.8 SUMMARY**

This chapter has looked at the methods used to generate a physical model of loess soil. It has also looked at the methods used to validate this model by comparing it to natural loess. The methods used to determine the geotechnical properties, soil structure and collapse mechanisms of both the natural and artificial loess were discussed. The results from these tests are given in the following chapter.

## 4

## Element Test Results

This chapter presents the results of the index, oedometer compression and triaxial compression tests that were carried out on artificial loess specimens prepared using the methods discussed in chapter 3. A summary of the element tests carried out is shown in Table 4-1.

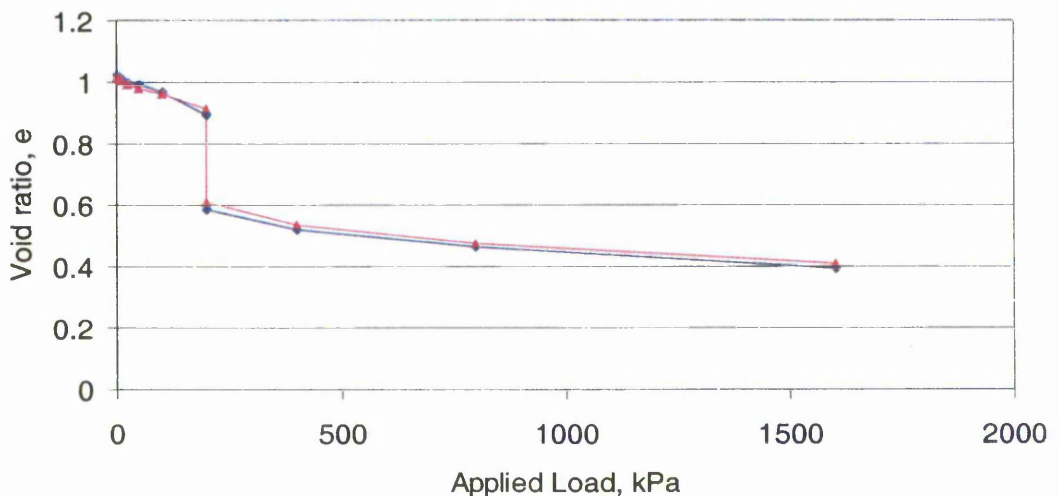
Test	To examine	On natural	Number	On artificial	Number
SEM, photography	Particle shape, bonding	no (see Smith, 1999)	-	yes	3
Atterberg limit	Liquid and plastic limits	yes	-	yes	3
SediGraph	Particle size distribution	no (see Dibben, 1998)	-	yes	1
Oedometer	One-dimensional compression. Using method 1 of production	-	-	yes	27
Oedometer	One-dimensional compression. Varying clay content, preparation water content, overburden pressures, method of making the sample	yes	2	yes	61 (using production methods 2a and 2b)
Oedometer	Hydrocollapse due to different flooding water contents (method 2a)	no	-	yes	9
Oedometer	Unloading in same increments as loaded (method 2a)	no	-	yes	2
Triaxial	Three-dimensional compression	yes	2	yes	5

Table 4-1 Summary table of the element tests carried out

The oedometer and triaxial tests were used to identify the key parameters that control collapse behaviour and enabled investigation of their influence on the magnitude of collapse. The methods of producing the artificial soil have been developed to a point where the following soil parameters can be controlled during production:

1. Clay content
2. Void ratio
3. Overburden pressure
4. Degree of saturation
5. Moisture content

Points 2-5 were achieved with a major development of the work by Assallay (1998) and Dibben (1998). The artificial material produced controllable and repeatable results that were used to validate computational models of the collapse behaviour. The repeatability of the oedometer tests are shown in Figure 4-1, where the preparation water content and mass of the samples were the same and the void ratios throughout the test are similar in the two samples. The new techniques of producing the artificial loess overcome the problems associated with the original methods, i.e. production of samples with natural void ratios, simulation of depth of deposit and control of the level of saturation. A summary of the tests undertaken for this project are shown in Table 4-1.



**Figure 4-1** Oedometer results for two similar artificial samples, showing the repeatability of the results. Water contents were 18-19%.

#### 4.1 SHAPE OF THE PARTICLES

Scanning Electron Microscope pictures show the silt and clay particles in an undisturbed sample of natural loess, as seen in **Plate 4.1**. The clay component between the silt forms bonds to hold the particles in a metastable state. **Plate 4.2** shows a more clayey sample. Both of these samples were collected for a Master's project and were found in Kazakstan, detailed in Smith (1999). The full width of the photograph is 500 microns and therefore a large number of the silt particles can be observed. Voids between the particles can clearly be seen. These SEM pictures provide a reference on which to base the artificial soil. The effect of clay bonding was recreated in the artificial loess in the laboratory. Ballotini balls, crushed natural sand and industrially ground silica flour (HPF4) were all used to simulate the silt-sized fraction of loess. These particles were mixed with clay binder to form a collapsible deposit.

The Ballotini balls are glass spheres and were used by Dibben (1998) and Assallay (1998) to make an artificial loess soil. The shapes of all the particles have been examined under the SEM. The spherical glass balls have been used to represent the silt particles of loess, but do not have the same characteristic blade-shape. However, the glass spheres are a useful link to the particle packing ideas which have mainly been developed using spheres see, for example, Nobari and Duncan (1972), Dijkstra et al. (1995). The ballotini spheres are shown in **Plate 4.3**, mixed with 20% clay fraction. A clay bridge can clearly be seen in the SEM photograph. The width of the photograph is 45 microns and therefore only two particles can be seen.

Spherical particles readily adopt their closest packing whereas angular and blade shape particles interlock. Rounded grains tend to roll over one another rather than interlock, and therefore tend to shift under load. Angular particles resist shear better due to the interlocking of the particles. In fact, angular and blade shaped particles of loess can stand in very steep cuttings due to the interlocking of the grains. The voids between the spherical and angular particles are also different. Pathways for water flow will be larger and more open for the rounder particles, compared with the smaller more tortuous routes around the angular particles. This will affect the way the particles behave when infiltrated by water. Crushed sand was also used as to represent typical silt-sized particles in loess. The crushing process produces very angular particles, see **Plate 4.4**. The loess silt particles are more

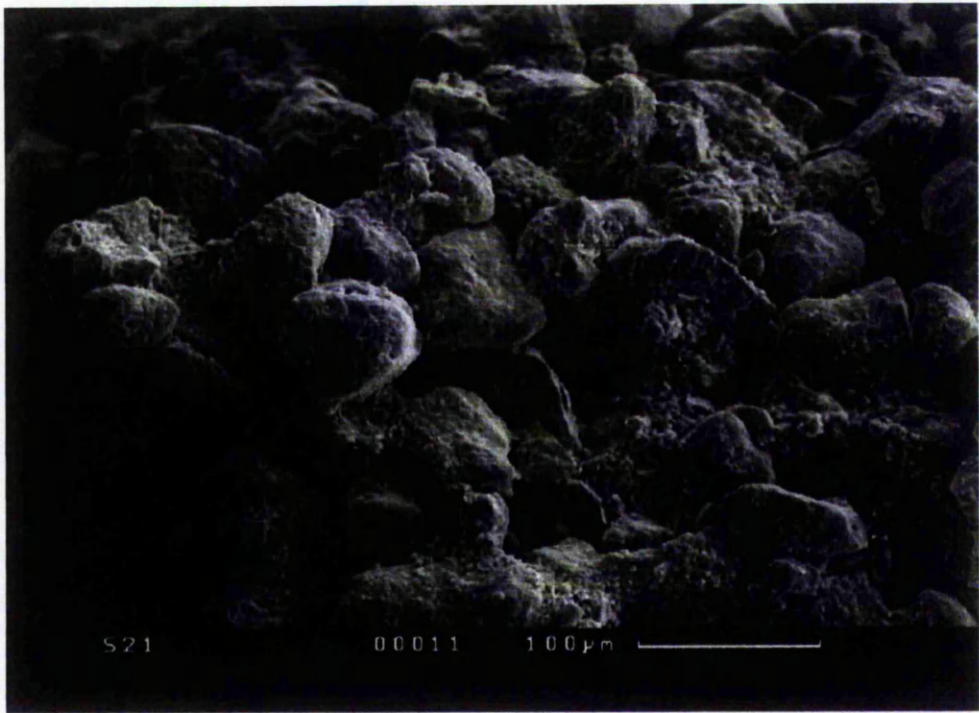


**Plate 4-1. Natural Loess from Kazakstan, (Smith, 1999)**

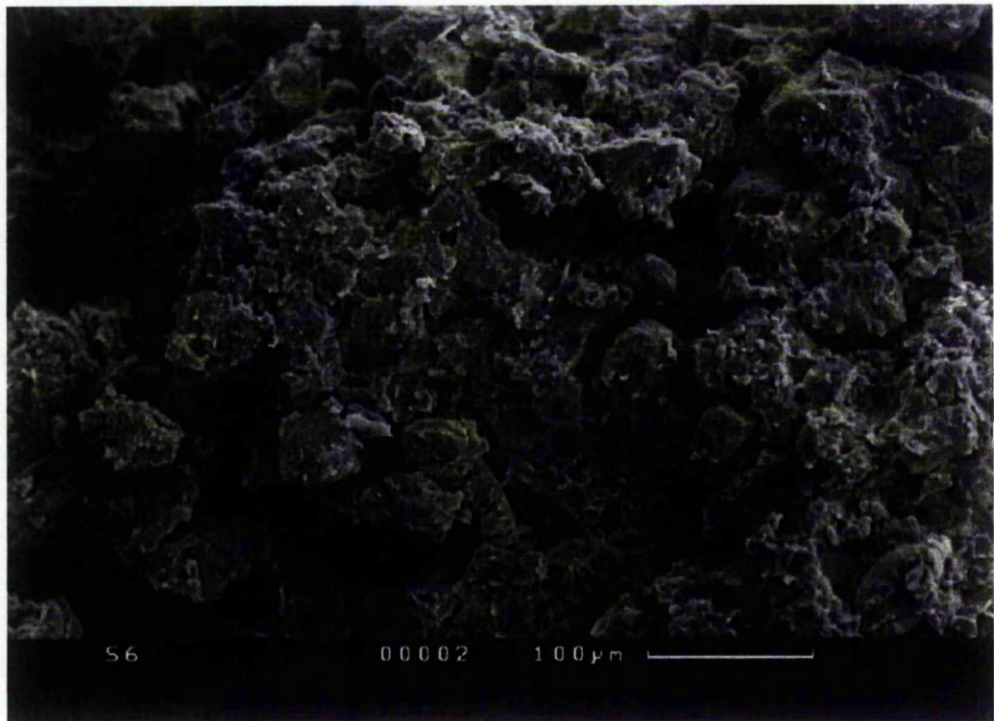


**Plate 4-2. Clayey Natural Loess from Kazakstan, (Smith, 1999)**



**Plate 4-3. Artificial Loess made from Ballotini Balls and Kaolinite**

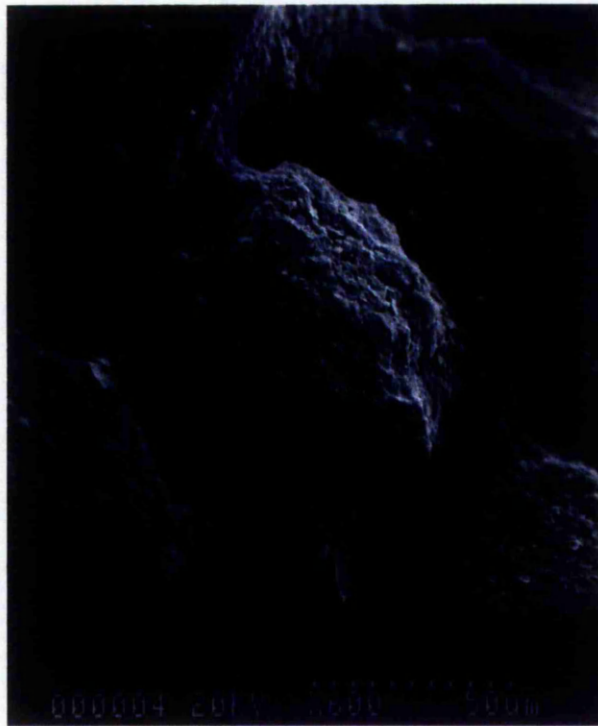


**Plate 4-4. Artificial Loess made from Crushed Sand and Kaolinite**

rounded than the newly crushed sand due to the weathering and transportation processes undergone during formation of the deposit, Smalley (1996). A mixture of crushed sand and clay (20%) is shown in **Plate 4.4**, which clearly shows clay coatings and bridges on and between the silt particles. The width of the photograph is 150 microns. The specimen was prepared by mixing the silt and clay with water and then the specimen was dried as in method 2a, Chapter 3, Section 3.5.2. Although this specimen was dry when photographed, the bridges have formed in the same shape as a meniscus, which must have occurred when the soil was wet. The clay has stayed in position, post-drying. The same shapes and coatings were also observed for the ground silica and clay mixture. **Plate 4.5** shows the ground silica flour mixed with 30% kaolinite. The kaolinite particles have coated most of the silica particles. The photograph is 300 microns across. A large void can be seen in the centre of the photograph, in **Plate 4.5**. Voids like these were formed naturally when the particles were mixed with water. Similar voids have been observed in natural loess and have been attributed to old root holes or other organic matter, Dibben (1998). However, some of these voids could have been made during the formation of deposit just as in the artificial loess, rather than being made by organic matter.

In **Plate 4.6** the shape of the HPF4 particles can be seen, the width of the photograph is 90 microns. The crushed sand and the ground silica material are both fairly angular. These particles are not as rounded and weathered as natural loess silt but display the characteristic blade shape. The ground silica was chosen for the bulk of the experiments due to the convenience of not having to crush the material. The particle size of the silica, according to the manufacturers guide lines, are within the required range for loess silt (about 20-60  $\mu\text{m}$ ) and therefore no crushing was needed. A chemical analysis, provided by the manufacturers, shows that 98.5% of the particles are quartz, with a small amount of impurities.

## 4.2 INDEX TESTING

Index properties for natural loess were given in Table 2-1, in Chapter 2. Liquid and plastic limit (LL and PL respectively) tests have been performed on all three types of artificial loess and on natural loess, obtained from the Star Lane site, Essex (see Figure 3.3) for comparison. Plasticity index (PI) is difficult to obtain for the artificial loess as the PI (LL-PL) is low. The material is very brittle, especially for low clay contents. While undertaking the Plastic and Liquid Limit tests it was observed that at water contents of up to



**Plate 4-5 Artificial Loess Prepared Using HPF4 Silica Flour and 30% Kaolinite**



**Plate 4-6. The Shape of the HPF4 Silica Flour Particles**

15% the material remained very brittle and crumbly. A change in the behaviour was observed in the artificial soil with water contents above 20%. The material becomes very soft and has very little strength. The index properties obtained for the artificial loess are similar to natural loess (Table 2.2, Chapter 2) and are shown in Table 4-2. A value for the PI for the ballotini balls could not be obtained as it was non-plastic.

<b>Artificial material</b> <b>Silt/Clay ratio</b> <b>Method of preparation</b>	<b>LL</b> <b>%</b>	<b>PL</b> <b>%</b>	<b>PI</b> <b>%</b>	<b>G<sub>s</sub></b>
Kaolinite (Grade 50)	56	37	19	2.60
80/20, Ballotini and kaolinite (Grade 50) <b>Air fall method 1</b>	-	-	-	2.50
90/10, Crushed sand/ kaolinite (Grade 50) <b>Air fall method 1</b>	22	21	2	2.65
80/20 CS/k (Grade 50) <b>Air fall method 1</b>	21	18	3	2.64
80/20, HPF4/kaolinite (Grade 50) <b>Air fall method 1</b>	25	17	8	2.64
80/20, HPF4/kaolinite (Grade 50) <b>Wet method 2a</b>	25	17	8	2.64
70/30, HPF4/kaolinite (Grade 50) <b>Wet method 2a</b>	27	18	10	2.64
70/30,HPF4/kaolinite (Grade 50) <b>Bonding method 2b</b>	27	18	10	2.64

**Table 4-2 Artificial loess index properties**

Where, LL = Liquid limit, PL = Plastic Limit, PI = Plastic index, G<sub>s</sub> = Specific gravity.

The specific gravity, G<sub>s</sub>, for each of the artificial materials is also shown in Table 4-2. The specific gravity of the ballotini balls was less than for the silt size particles of natural loess. The crushed sand and ground silica were both mainly quartz and therefore had specific gravity of 2.65, this was confirmed with the specific gravity testing carried out in the laboratory, carried out as discussed in Chapter 3.2.2. This value is more comparable to natural loess than for the Ballotini balls. The specific gravity is lower than generally found for natural loess. This will affect the mass of the samples but should not affect the packing characteristics of the grains.

A particle size analysis of the silt-sized particles was performed using the SediGraph at the British Geological Survey (BGS). Results are shown in Figure 4-2 and Figure 4-3. Based on the particle size classification given by BSI, 1990, the silica material consists of 40% coarse silt, 28% medium silt, 10% fine silt and 4% clay-sized particles. This compares to the crushed sand, which had 64% coarse silt, 30% medium silt, 4% fine silt and 2% clay-sized particles. The much coarser Ballotini which had 80%, 12%, 3% and 0% respectively.

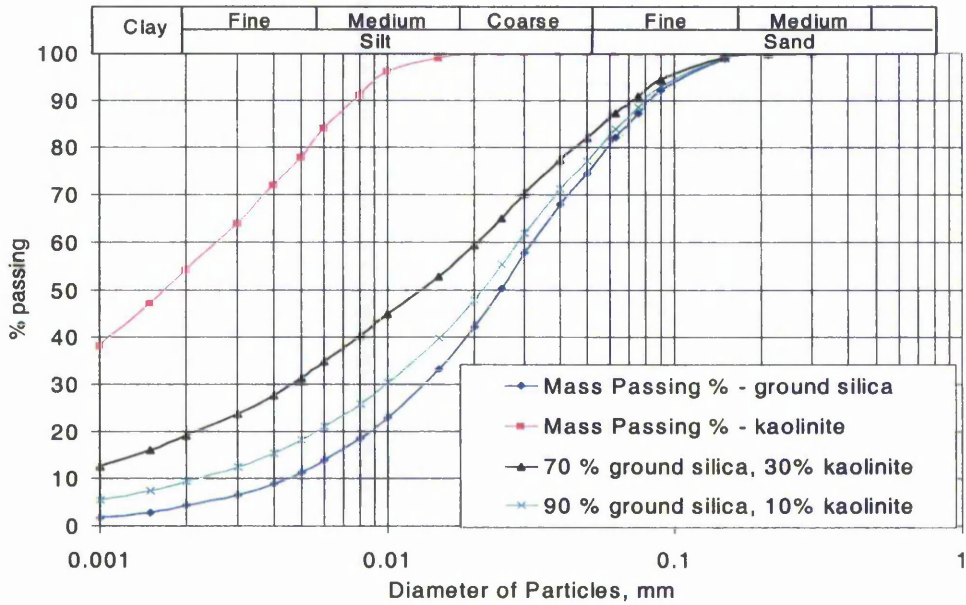


Figure 4-2 Particle size analysis results for kaolinite and silica

The kaolinite had 84% of its particles finer than the fine/medium silt boundary. All the kaolinite particles were finer than 20µm. By combining these two results it was possible to estimate curves for any clay content. The calculated particle size distribution curves for 10% and 30% clay are shown in Figure 4-2. Figure 4-3 shows the comparison of the particle size distribution curves for 30% clay artificial loess and for the Essex loess. Also shown are the boundaries found by Derbyshire and Mellors (1988) for Lanzou loess, China. The Essex loess and the artificial loess fit between these boundaries for Lanzou loess. This indicates the close comparability of loess from artificial sources to those around the world.

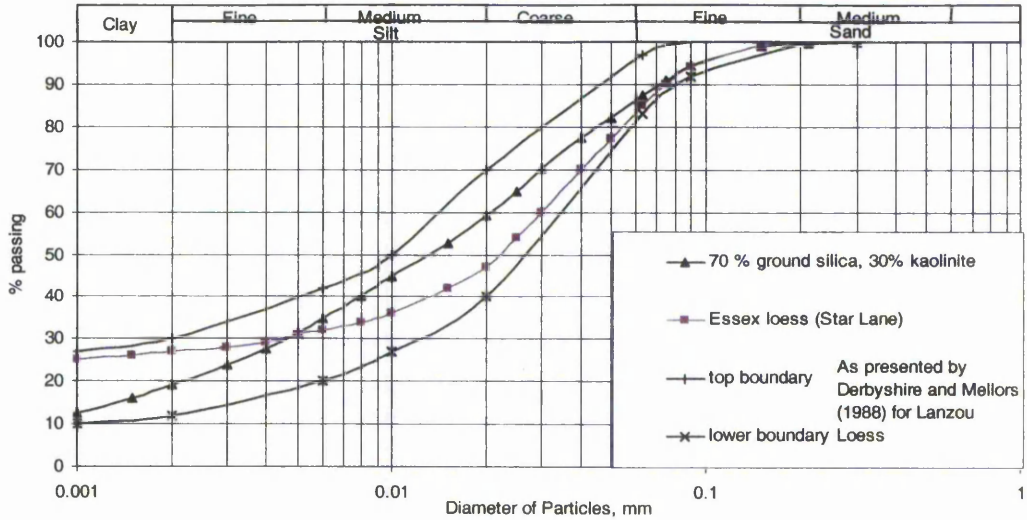


Figure 4-3 Comparison of particle size distribution for natural and artificial samples

Assallay, (1998) showed that kaolinite was an effective clay mineral to use in laboratory tests. Kaolinite has limited surface activity and is less chemically interactive with pore water than other minerals. This means the physical mechanisms of collapse can be assessed without chemical mechanisms confusing the issue. A chemical analysis of the kaolinite used is given in Table 4-3. The quoted mineralogical composition was derived from x-ray diffraction measurements and calculations based on chemical analysis produced by the manufacturers. Mineralogical analysis of the natural Essex loess, from Star Lane brick pit, is provided in Table 4-4. Clay content is around 32% with kaolinite and illite-smectite being the clay minerals present. However, since smectite is a swelling clay mineral, as discussed above, it was decided that kaolinite would be used to simulate the clay bonds for simplicity.

Mineral	Puraflow (Grade 50)
Kaolintie	65
Potash Mica	24
Quartz	2
Soda Mica	6

Table 4-3 Mineralogical analysis of Kaolinite (Grade 50)

[Source: Manufacturers data sheet - WBB Devon Clays.]

Mineral Type	Mineral	Star Lane, Essex
Quartz	Quartz	56
Carbonate	Calcite	0
	Dolomite	0
Clay mineral	Kaolinite	4
	Illite-smectite	28
Feldspars	Pagioclase	8
Total		96

**Table 4-4 Mineralogical Analysis of Natural Loess found in Essex, Star Lane site.**

### 4.3 OEDOMETER TEST RESULTS

A summary of the oedometer test results is given in this section and the main points of interest highlighted. Three methods of producing the artificial loess were used, as discussed in Chapter 3. Method 1 is the method used by Dibben (1998), where an air fall deposit is created and the same mass is used to produce each sample. Using the same mass has a number of limitations associated with it (as discussed in Chapter 3, Section 3.3.1), so a second method using the same compressive effort was developed, in order to produce the 'natural' void ratio for each sample. Wetting by steaming, as in method 1, is practical for a small sample, but an alternative to steaming was also investigated that could be used to prepare larger samples. Firstly, by simply mixing the dry materials with water and forming the sample wet (2a) and secondly, by spraying the sample as it was formed (2b). A summary of the production methods is given in Chapter 3.

Results from oedometer tests on the artificial loess have been compared with results from natural loess specimens, to check the validity of the artificial loess model. Typical oedometer results for the natural loess obtained from Essex are shown in Figure 4-4. Three curves are shown, one sample was loaded unsaturated up to an applied stress of 1600kPa, one sample was saturated and loaded up to an applied stress of 1600kPa (double oedometer test) and the third sample was loaded initially unsaturated and loaded with an applied stress of 200kPa, then saturated and finally loaded to 1600kPa (single oedometer test). The results from the single oedometer test are similar to the results of the unsaturated specimen up to an applied stress of 200kPa. After saturation, the results are similar to the results of the saturated specimen in the double oedometer test. This shows that the soil reaches the same stress-strain point independent of the order or wetting and loading. Similar behaviour is observed for other collapsible soils, for example colliery spoil, Skinner et al. (1999).

The graph shows the normal stress applied to the oedometer sample (x-axis) against the deformation that this stress produces (on the y-axis). It is usual to plot effective stress against void ratio, however, effective stress is not valid for unsaturated materials, as it assumes that the material is fully saturated. Deformation has been plotted instead of void ratio to illustrate collapse of the specimen on saturation. Results for the oedometer tests for the artificial samples are all represented in this way in the following sections. The results from the natural samples provide a comparison with the artificial loess soils produced in the laboratory. Important points to note are, firstly the same state is gained whether the soil is saturated and then loaded or loaded and then saturated. Secondly, the constrained modulus of the oedometer samples increases with applied stress.

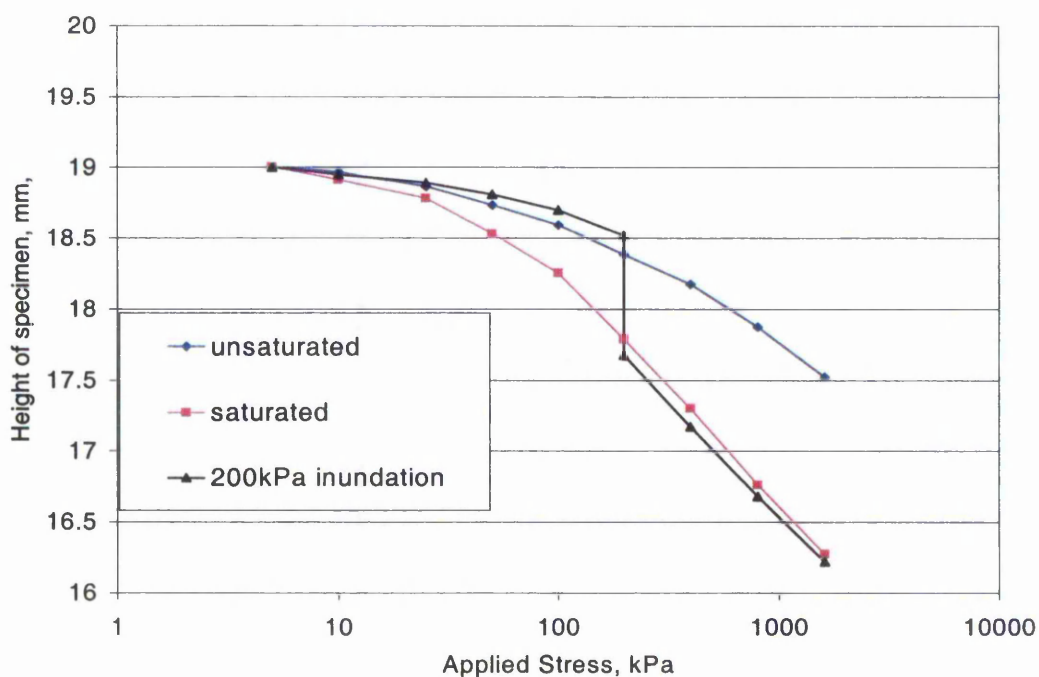


**Figure 4-4** Typical oedometer results for loess samples from Essex, Star Lane site.

#### 4.3.1 Production Method 1 - The air fall method, after Dibben and Assallay

Three types of silt-sized particle were used to produce the samples using method 1. This allowed the effect of the shape of the primary particles on the behaviour of the samples to be assessed. All of these samples were made using the Dibben (1998) method using varying proportions of silt and clay. The samples were all made with the same mass (105g)

of material. This produced samples with similar void ratios in each of the specimens with varying clay contents.

During production of the samples it was observed that as the clay content increased over 25% it became harder to fit the same mass of material into the oedometer ring. The specimens with higher clay contents required far more effort to pack the particles into the oedometer ring. This may have been due to repelling forces in the clay or perhaps because of the way the smaller and larger particles pack together. This observation was investigated further in methods 2a and 2b and using a computational model explained in Chapter 5.

Typical oedometer results for the ballotini balls are shown in Figure 4-5. The solid line illustrates the behaviour of the ballotini and the dotted line shows the behaviour of the Essex loess from Star Lane Brickworks, which is provided for comparison. It was observed that the artificial loess produces more strain for low applied stresses than the natural loess. This was thought to be due to a number of factors, the shape of the particles, the smoothness of the glass surface, which may prevent strong bonds from developing, the lack of time available to develop bonds, and the lack of brittle carbonate bonds in this simplified artificial loess. The bonding between the particles in the artificial samples is not as strong as in the natural loess samples in the unsaturated state. The particles pack closely due to their spherical shape and initial void ratios were low (0.84). Collapsed void ratios are also low, for the same reason.

Typical oedometer results for the crushed sand are shown in Figure 4-6 and for the ground silica in Figure 4-7. The results show more settlement than was observed for the natural Essex loess. This was perhaps due to the weaker bonding for the reasons discussed above. Also, initial void ratios are very high, 1.26 and 1.36 for the crushed sand and ground silica respectively. High void ratios in the samples were observed when low compressive stresses and low water contents were used to form the specimens. The crushed sand and HPF4 samples (see Figure 4-7) are more comparable to natural loess than the ballotini balls because they have the same specific gravity as the silt fraction of natural loess and have a more natural shape. All three methods produce similar curves on the height versus applied stress graphs. Collapse is far greater than in the natural loess because the initial void ratios are high. Of course, the void ratios could be reduced by initially compacting the specimens using a known stress.

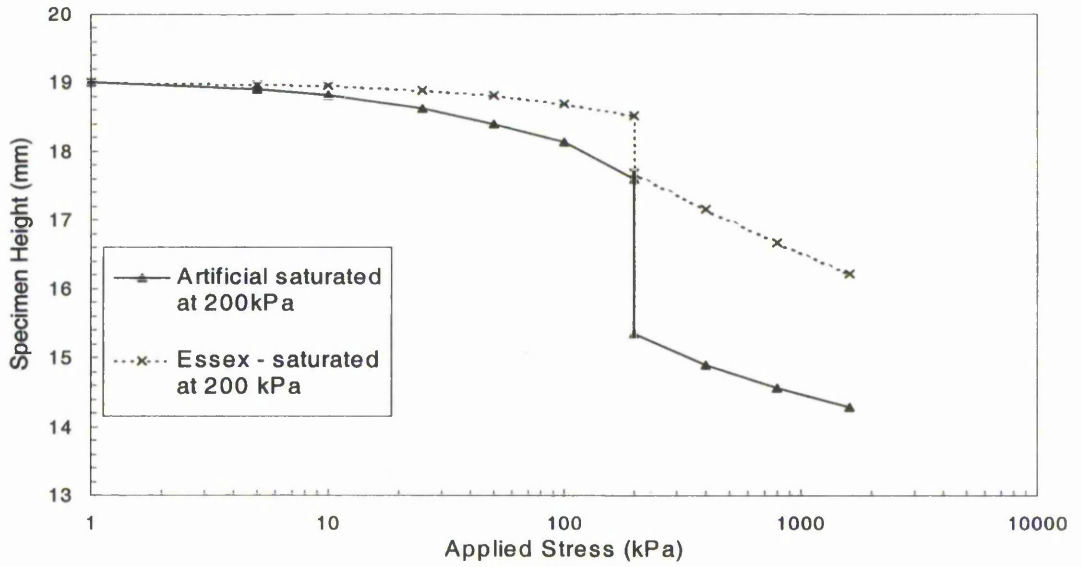


Figure 4-5 Oedometer results for artificial samples made with Ballotini balls/kaolinite 80/20 method 1, compared to natural loess from the Star Lane site, Essex.

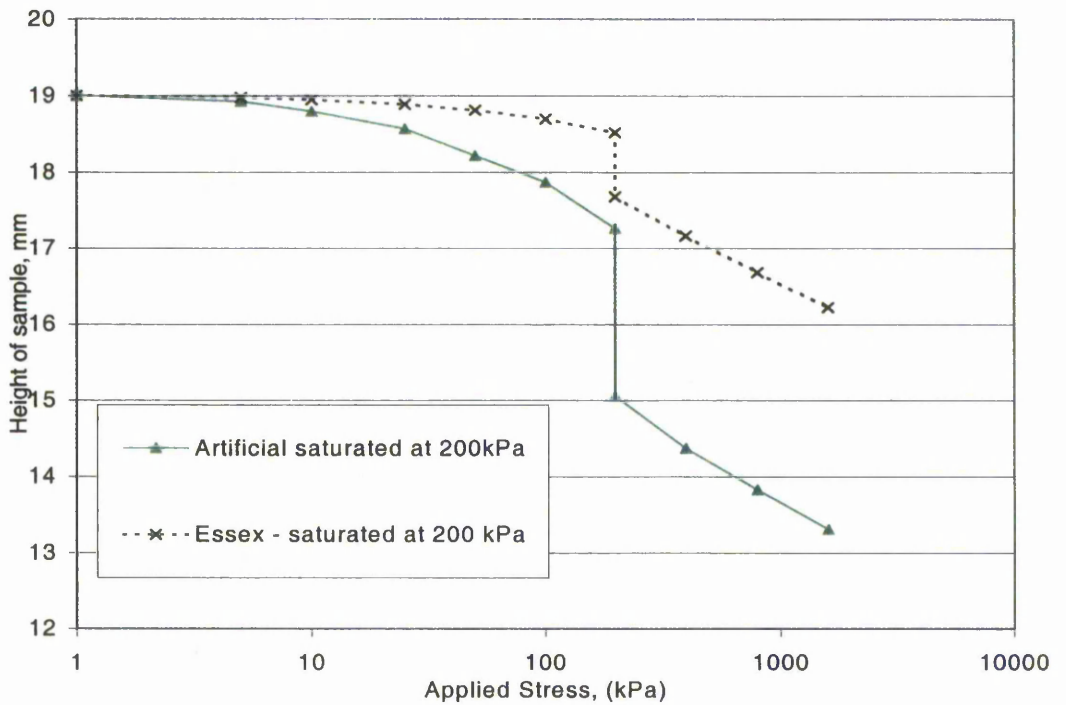


Figure 4-6 Oedometer results for artificial samples made with crushed sand/kaolinite 80/20 Method 1, compared to natural loess from the Star Lane site, Essex.

## 4.3.1.1 Particle Shape

The Essex loess had a hydrocollapse value of 4.5%. The artificial loess exhibited much higher values of hydrocollapse for all three types of silt. The ballotini had around 12.8% hydrocollapse, the crushed sand also had 12.8% and the ground silica had 14%. All these samples were made with 105g of dry material and were made with 20% kaolinite. The values obtained for hydrocollapse are consistent with specimens made from different shaped particles, even though the void ratios are not. This indicates that the particle shape will affect the void ratio of the sample but will not affect the amount of collapse settlement. The influence of the particle shape on the void ratio of the unsaturated specimen is the same as the influence over the void ratio of the saturated specimen and therefore the magnitude of the hydrocollapse is almost unaffected. The amount of hydrocollapse is not greatly affected by particle shape, but magnitude of hydrocollapse was different in the artificial and natural samples, this was probably due to the combination of higher void ratios and weaker bonding in the artificial samples.

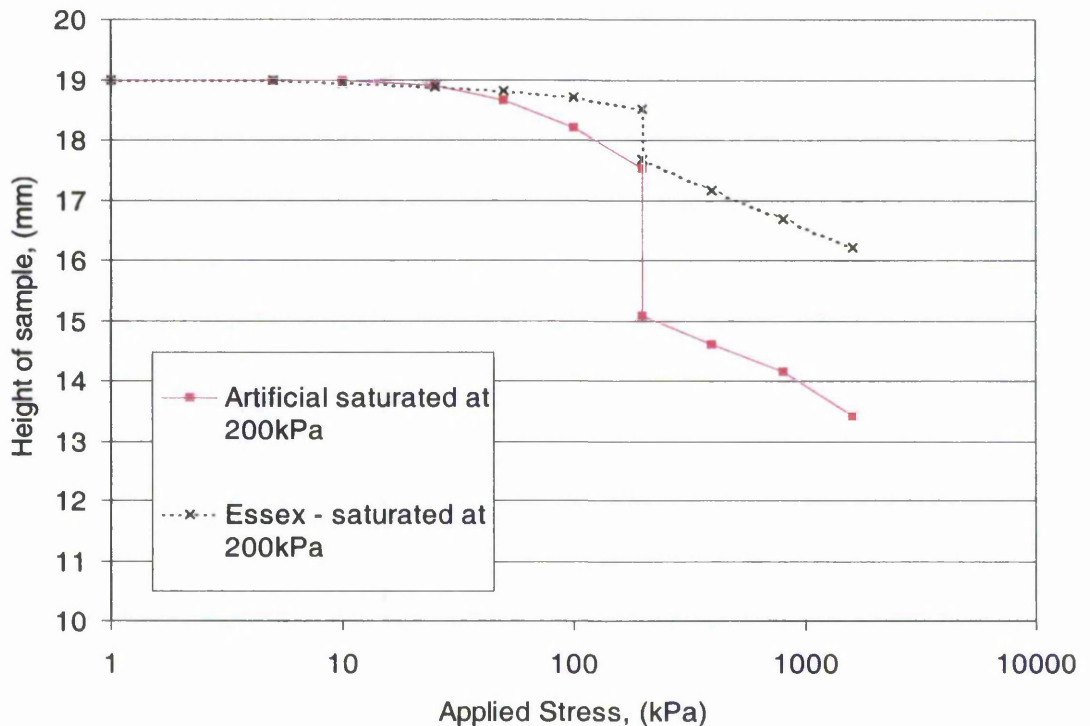
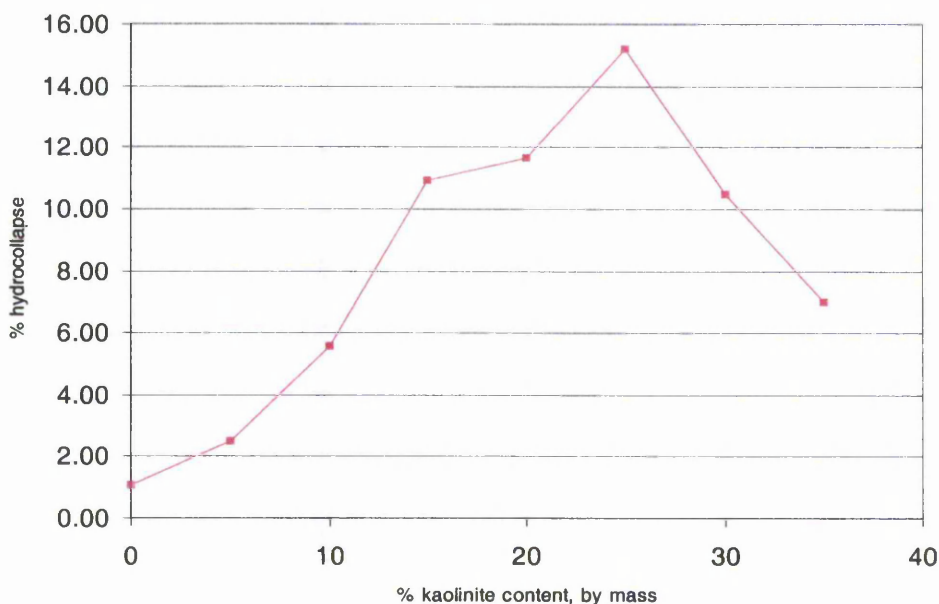


Figure 4-7 Oedometer results for artificial samples made with ground silica/kaolinite 80/20 Method 1, compared to natural loess from the Star Lane site, Essex.

## 4.3.1.2 Hydrocollapse and void ratio

Oedometer tests were carried out on specimens made using method 1 and clay contents of 0, 5, 10, 15, 20, 25, 30 and 35%. The hydrocollapse of each specimen was found for an applied stress of 200kPa and compared for different clay contents. For all three different artificial silts, the largest hydrocollapse is observed for clay contents of around 25%, this is shown in Figure 4-8. This trend is not observed in natural samples, see the discussion in Section 4.3.4.



**Figure 4-8 Percentage hydrocollapse for varying kaolinite content for samples prepared using method 1. Crushed sand and Kaolinite specimens.**

The explanation for observing this in the laboratory specimens seems to lie in the way the particles pack. The same mass was used for each specimen, regardless of its clay content. It was noted that greater effort was needed to pack the same mass of sample into the oedometer ring for higher clay contents. The formation process and the way the particles naturally pack affected the collapse potential of the specimens. It was therefore necessary to further examine the relationship of clay content and particle packing to test this hypothesis. The effect of clay content on void ratio and hydrocollapse is discussed in Section 4.3.6.

Figure 4-9 shows the changes in void ratio during the oedometer tests on the artificial specimens prepared using Method 1. As the samples are compressed the particles rearrange

and pack together more closely. The graph indicates that the samples with 25% clay content pack most densely on hydrocollapse. This explains the peak of hydrocollapse at this clay content, seen in Figure 4-8. The results indicate that specimens would naturally pack at different densities for different clay contents. It is therefore proposed that specimens should be formed with the same energy to encourage these natural densities to develop in the samples during preparation. This approach should mean that the samples are formed with void ratios more in line with those that would be found in a natural sample.

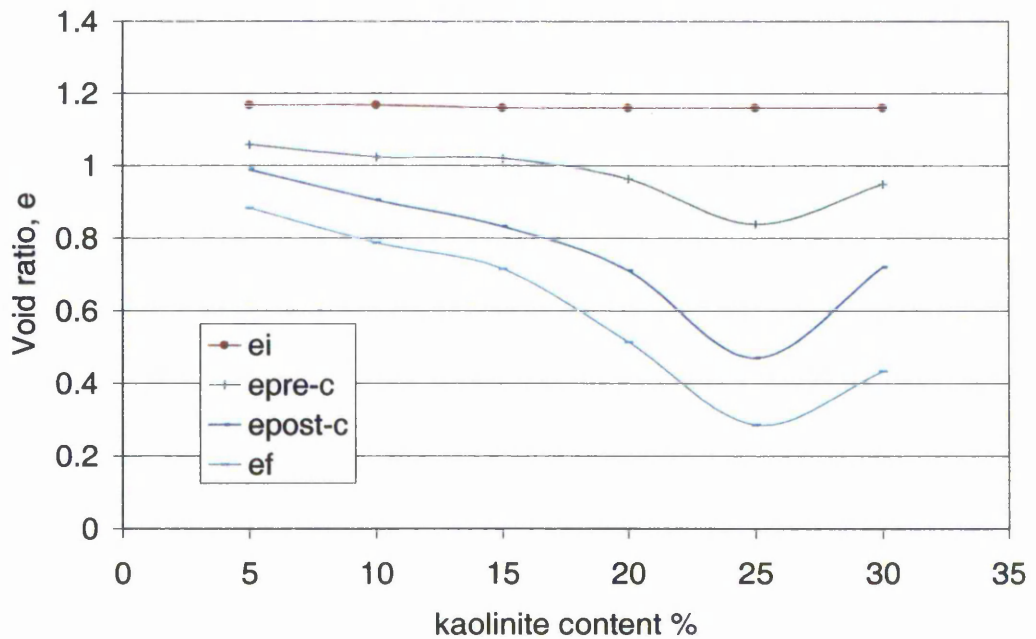


**Figure 4-9 Void ratio at the four stages in an oedometer test. (Method 1 - constant mass, Crushed sand and Kaolinite)**

Where,  $e_i$  = initial void ratio,  $e_{pre-c}$  = voids ratio before wetting at 200kPa,  $e_{post-c}$  = void ratio after wetting at 200kPa,  $e_f$  = final void ratio at 1600kPa applied stress

#### 4.3.2 Production Method 2a - The wet method

Instead of using the same mass, the same compressive effort was used to make the samples. In method 2a the silt particles, clay particles and water were mixed together before forming the sample.

##### 4.3.2.1 Preparation water content

The preparation water content was investigated to ensure that the sample was wet enough to produce bonds within the material but dry enough so that shrinkage of the samples did not

occur. The optimum water content was determined by using the same compressive effort to make samples with different moisture contents. The results of these tests are illustrated in Figure 4-10. This graph shows that a peak density is achieved with preparation water contents of around 25%. Specimens were dried in the oven to create the bonds needed between the silt particles. Shrinkage of the samples occurred when they were prepared with water contents above 20%. A water content of 17.5% was chosen for preparation of the majority of the samples which is low enough to avoid shrinkage of the specimens but high enough to allow bonding to develop during drying.

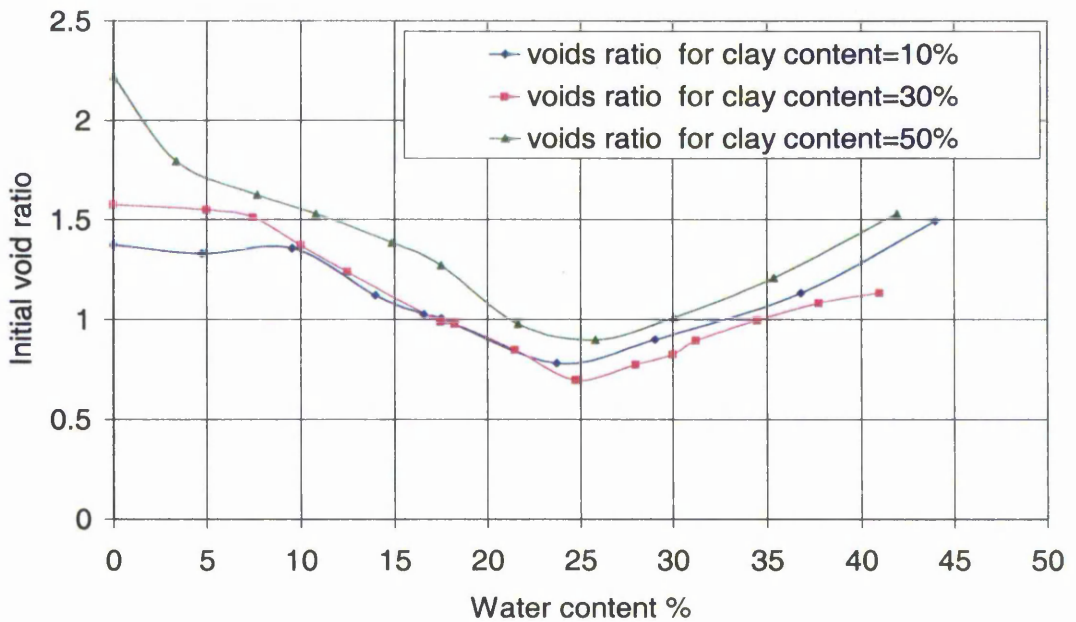


**Figure 4-10 Comparison of initial voids ratio of samples made with different preparation water contents with ground silica and 10, 30 and 50% kaolinite content.**

A small number of samples were made using the optimum preparation water content for which the samples produced their lowest void ratios. Results for typical oedometer tests on this artificial material are shown in Figure 4-11 and Figure 4-12 for 20% (sample a) and 30% (sample b) clay content respectively. Sample (a) was made with 27% preparation water content and had an initial void ratio of 0.72. Sample (b) was made with 25% preparation water content and has an initial void ratio of 0.81. Hydrocollapse values compare favourably with the Essex loess. Sample (a) showed 4.3% hydrocollapse and sample (b) had 5.3% hydrocollapse. This method introduced a strong structure and low void ratios that compare favourably with the Essex natural loess samples from the Star

Lane brick works site. However, the samples produced at this water content shrunk when dried. They therefore had to be made in larger rings and transferred to the smaller oedometer rings for testing once they had been dried. This meant that the samples had to be disturbed from where they were made, and one of the advantages of the artificial loess was that it did not have to be disturbed and therefore is not affected by sampling effects.

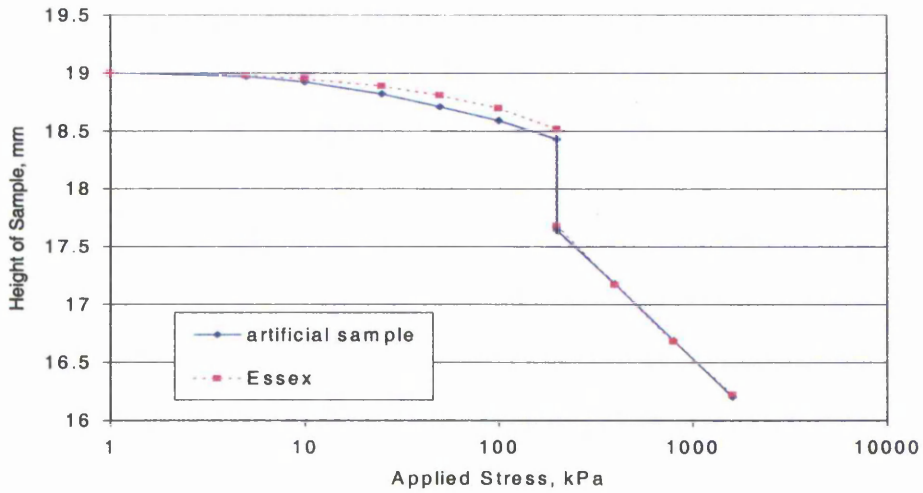


**Figure 4-11 Oedometer results for samples made using method 2a. Ground silica/kaolinite content 80/20. Preparation water content 27%. Initial voids ratio,  $e=0.72$**

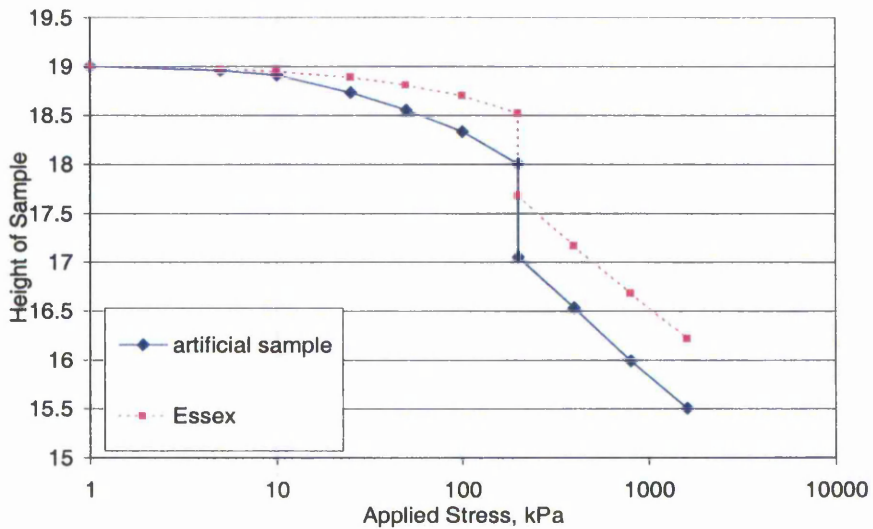


**Figure 4-12 Oedometer results for samples made using method 2a. Ground silica/kaolinite 70/30. Preparation water content 25%. Initial voids ratio,  $e=0.81$**

The next stage of the research was to make a larger sample of artificial loess as this would be required for the model footing test (see Chapter 6). The specimens above suffered from shrinkage during drying. However, shrinkage of the samples does not happen if the samples are made with less water. A water-content of 17.5% was used throughout the rest of the testing, as samples prepared with this water content did not shrink during drying. Figure 4-13 shows the oedometer results of samples made with 17.5% water content. This shows collapse behaviour similar to that shown by method 1, as the void ratios are similar. The initial void ratio of this sample was 1.0. This method provides a much simpler way of making the samples and produces very similar results to the method used by Dibben (1998). Much more collapse is observed than for samples prepared with the optimum water content due to the higher initial void ratios. The preparation water content affects the initial void ratio and therefore the magnitude of the hydrocollapse.

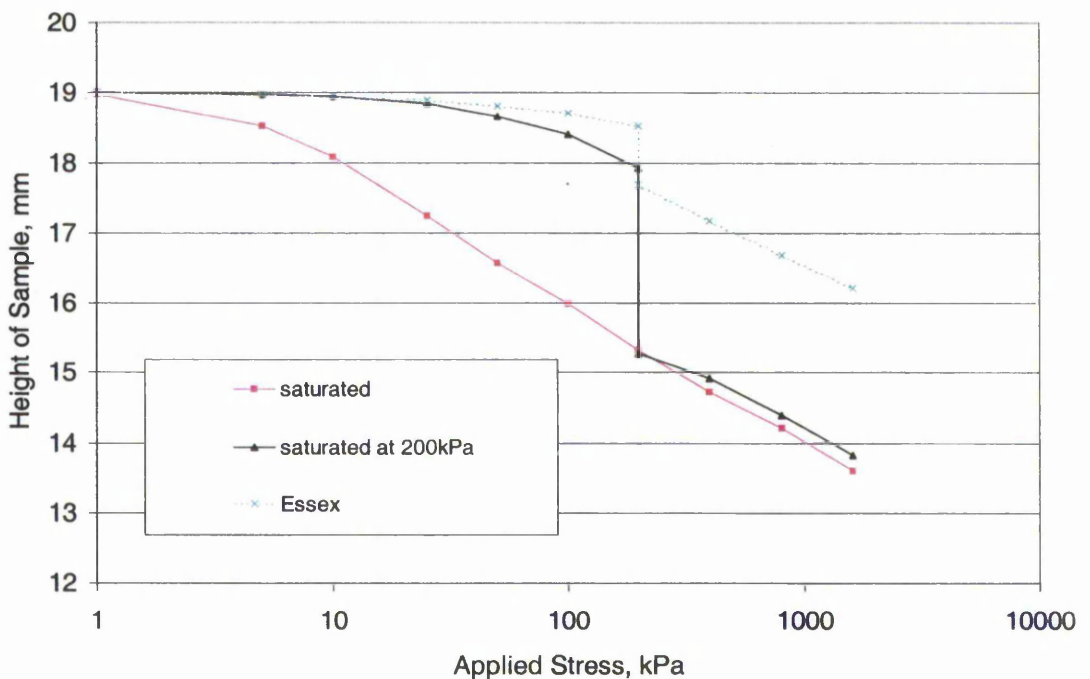


**Figure 4-13 Oedometer results for samples prepared using method 2a. Ground silica/kaolinite 70/30. Preparation water content = 17.5%. Initial voids ratio,  $e=1.0$**

#### 4.3.2.2 Water content causing collapse

The influence of water content on hydrocollapse was investigated in a series of oedometer tests, where the samples were loaded with an applied stress of 200kPa and wetted with

different amounts of water. A known quantity of water was added to the oedometer ring after the sample was loaded. The porous discs and samples were weighed separately pre- and post-collapse to obtain the water content causing collapse in the specimens. Specimens were produced using method 2a with clay contents of 30%. The results from this test showed an increase in hydrocollapse up to a saturation ratio of 0.5. For saturations greater than 0.5 there is almost no additional hydrocollapse, see Figure 4-14. Results are reasonably close to those found by El-Ehwany and Houston (1990), who report that 85% of full collapse is produced at 50% saturation. After 50% saturation it is suggested that the bonding has been reduced between the particles allowing movement between the particles, so that they can pack as closely together as possible. Any further increase in water content merely fills the voids and does not facilitate any more movement of the particles.

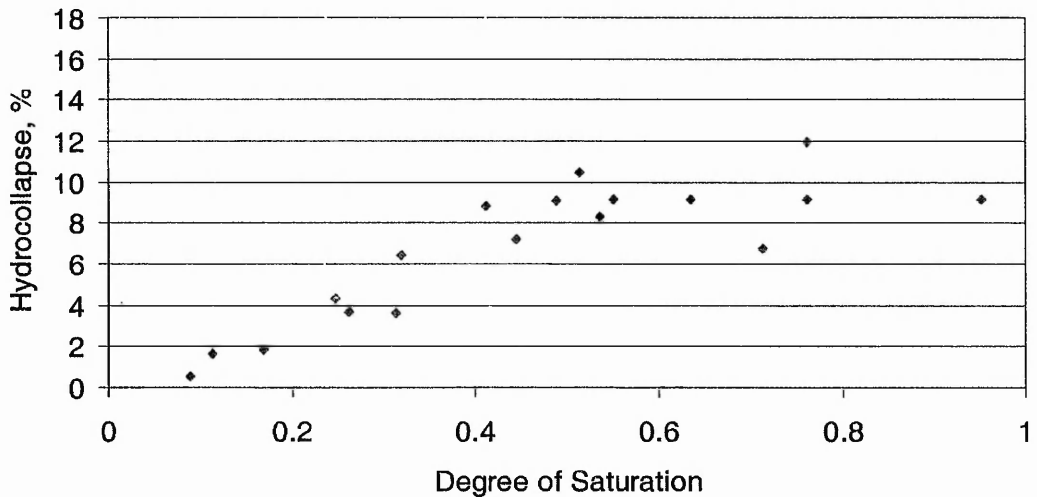


**Figure 4-14 Graph to show the relationship between saturation ratio at the time of collapse and amount of hydrocollapse, for specimens prepared with 30% clay content.**

#### 4.3.3 Preparation Method 2b - Spraying Method

Specimens were formed in layers. Each layer was sprayed with water before adding another layer as explained in Section 3.5.3, Chapter 3. A summary table of results is shown in Table 4-5. The results are ordered by preparation method, then clay content percentage and then preparation moisture content. Results are shown in Figure 4-15 for typical results for samples produced using method 2b. The initial void ratio for this sample was 1.17 and the preparation water content was 13.5%. The hydrocollapse observed in this sample was

13.7%. Again this behaviour is similar to that observed for methods 1 and 2a for similar void ratios and preparation water content.

#### 4.3.4 General Observations for both methods 2a and 2b

Swelling occurs during saturation of an artificial sample if the applied stress is below 25kPa. Swelling has been shown to occur in natural samples too, Assallay (1998). The reasons for this could be due to swelling in the clay minerals in some samples, however, in these tests kaolinite is used which is not a swelling clay mineral. Alternatively, the soil has been initially over-consolidated and when the soil is wetted it attempts to find its natural equilibrium. These results are consistent with observations on compacted kaolin, see Zakaria et al. (1995).

Method	Percentage Clay	Mass g	Moisture Content %	Initial Void ratio, e	Preconsolidation pressure kPa	Void ratio pre-saturation at 200kPa	Void ratio after saturation at 200kPa
2a	10	137.75	0.00	0.65	0	0.62	0.59
2a	10	115.72	17.50	1.00	0	0.73	0.60
2a	10	137.48	26.65	0.64	0	0.61	0.57
2a	10	130.85	29.96	0.70	0	0.64	0.60
2a	20	116.03	17.50	0.95	0	0.75	0.57
2a	20	125.98	21.58	0.81	0	0.69	0.61
2a	20	131.63	29.96	0.72	0	0.67	0.60
2a	30	112.28	0.00	1.02	100	0.90	0.68
2a	30	111.96	16.24	1.04	0	0.83	0.57
2a	30	113.92	17.50	0.94	0	0.83	0.56
2a	30	122.07	17.50	0.84	100	0.77	0.53
2a	30	130.85	17.50	0.72	100	0.68	0.58
2a	30	133.40	17.50	0.73	100	0.68	0.55
2a	30	113.96	17.50	0.99	0	0.84	0.56
2a	30	125.75	17.50	0.81	0	0.72	0.61
2a	30	121.31	17.50	0.87	0	0.77	0.64
2a	30	112.50	17.50	1.02	0	0.82	0.67
2a	30	112.14	17.50	1.02	0	0.90	0.83
2a	30	113.96	17.50	0.99	0	0.84	0.56
2a	30	120.65	17.62	0.88	0	0.81	0.62
2a	30	120.21	17.62	0.89	0	0.79	0.58
2a	30	112.90	17.63	1.01	0	0.82	0.51
2a	30	112.90	17.63	1.01	0	0.91	0.61
2a	30	112.43	17.68	1.02	0	0.89	0.58
2a	30	112.90	17.68	1.01	0	0.82	0.51
2a	30	112.90	17.68	1.01	0	0.91	0.61

Method	Percentage Clay	Mass g	Moisture Content %	Initial Void ratio, e	Preconsolidation pressure kPa	Void ratio pre-saturation at 200kPa	Void ratio after saturation at 200kPa
2a	30	112.43	17.68	1.02	0	0.89	0.58
2a	30	131.53	18.75	0.71	100	0.67	0.53
2a	30	127.29	29.98	0.78	0	0.69	0.60
2a	30	125.16	30.00	0.81	0	0.72	0.63
2a	30	123.02	34.50	0.78	0	0.69	0.60
2a	40	104.25	17.50	1.17	0	0.94	0.61
2a	40	127.08	29.99	0.78	0	0.72	0.62
2a	50	102.49	17.50	1.21	0	0.97	0.62
2a	50	124.18	30.00	0.80	0	0.74	0.63
2b	5	93.80	21.00	1.40	0	0.93	0.72
2b	10	92.20	13.90	1.44	0	0.70	0.54
2b	10	98.71	14.90	1.31	0	0.92	0.68
2b	10	111.74	16.61	1.03	0	0.89	0.72
2b	15	94.31	13.34	1.41	0	0.90	0.62
2b	15	97.33	17.05	1.34	0	0.85	0.62
2b	20	99.80	14.69	1.28	0	0.93	0.68
2b	20	110.86	19.53	1.02	0	0.93	0.66
2b	20	103.49	22.42	1.17	0	0.86	0.60
2b	25	103.41	15.10	1.20	10	0.84	0.57
2b	25	106.31	15.90	1.13	5	0.84	0.57
2b	25	113.22	16.76	0.99	50	0.86	0.59
2b	30	98.74	0.00	1.30	50	0.91	0.68
2b	30	97.35	15.56	1.32	10	0.89	0.58
2b	30	98.85	18.67	1.29	5	0.91	0.62
2b	40	96.27	15.59	1.35	10	0.88	0.56
2b	40	86.84	16.51	1.62	5	0.99	0.64
2b	40	103.35	19.75	1.18	50	0.97	0.67
2b	60	94.60	4.65	1.39	5	0.89	0.61
2b	60	97.39	8.47	1.32	10	0.83	0.61
2b	60	96.98	13.98	1.33	0	1.09	0.78
2b	60	96.67	17.50	1.34	0	0.98	0.64
2b	60	85.50	22.49	1.63	50	1.19	0.79
2b	60	126.51	32.11	0.78	0	0.71	0.61
2b	100	94.60	4.65	1.37	5	0.99	0.87
2b	100	96.98	13.98	1.31	0	1.07	0.77

**Table 4-5 Summary table of results for the one-dimensional compression tests for methods 2a and 2b.**

The specimens were also tested in the oedometer during unloading. Having loaded the sample with an applied stress of 1600kPa, the load was reduced in the same increments as it

was increased. The loading was reduced every hour. Elastic deformation is described as the amount of height that is regained during unloading. Plastic deformation is defined as the amount of deformation that can not be regained during unloading. The results for a typical sample formed using method 2a show that a similar amount of plastic deformation occurs in the saturated sample and in the unsaturated sample, 1.19 and 1.275mm respectively. However, there is a lot more elastic behaviour exhibited in the saturated sample, which was allowed to swell due to the water surrounding it during unloading, see Figure 4-16. Swelling occurred in the sample that was saturated under no load. This was due to the low initial void ratio (0.6) and overconsolidation of the sample during preparation.

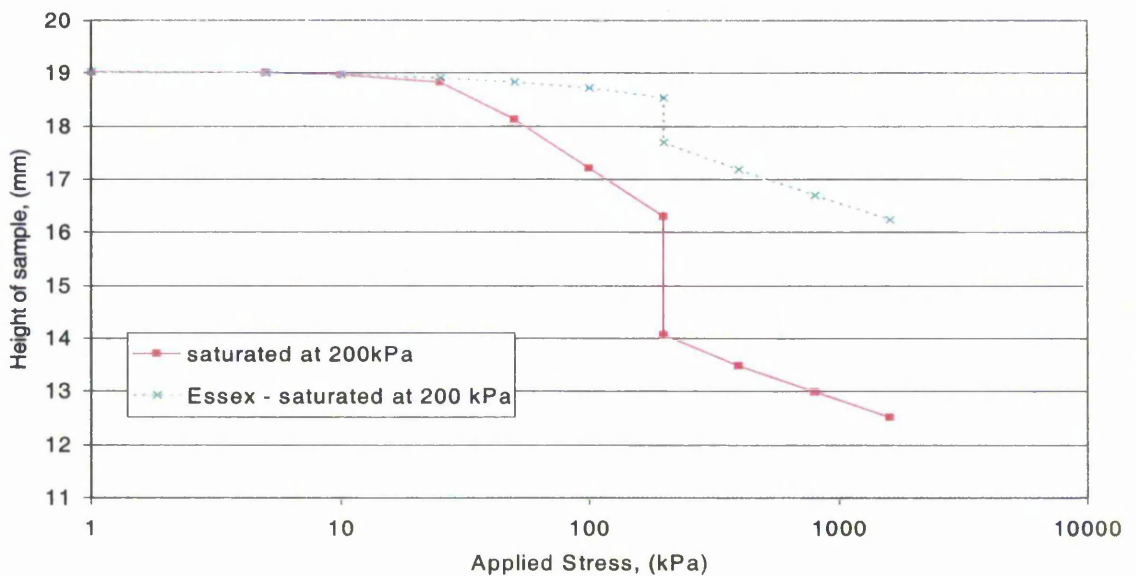


**Figure 4-15 Oedometer results for samples prepared using method 2b. Initial voids ratio,  $e = 1.17$ . Preparation water content = 13.5%.**

#### 4.3.5 Clay Content and Void Ratio

Specimens were prepared with varying clay contents to observe the influence on void ratio and collapse. The initial void ratios for all the tests are shown in Figure 4-17. A large difference in initial void ratio is observed in the results as the specimens were made with different water contents and compressive stresses. A tendency for the particles to pack more densely at 25% clay content can be seen from the results of the specimens made using both methods. Figure 4-18 shows the void ratios of the same specimens at an applied stress of 200kPa, before the wetting stage of the test. Figure 4-19 shows the same results split into

bands according to the initial water content at the start of the test. The range of void ratios is reduced because the influence of the consolidation pressure is reduced at 200kPa.

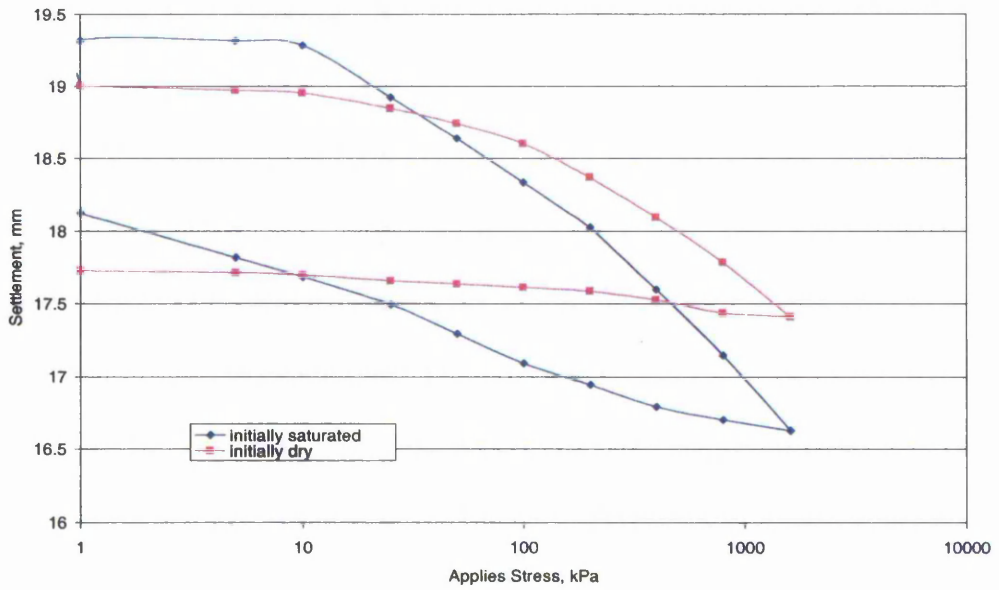


Figure 4-16 Loading and unloading of oedometer samples prepared using method 2a. Preparation water content = 25%, initial void ratio 0.6.

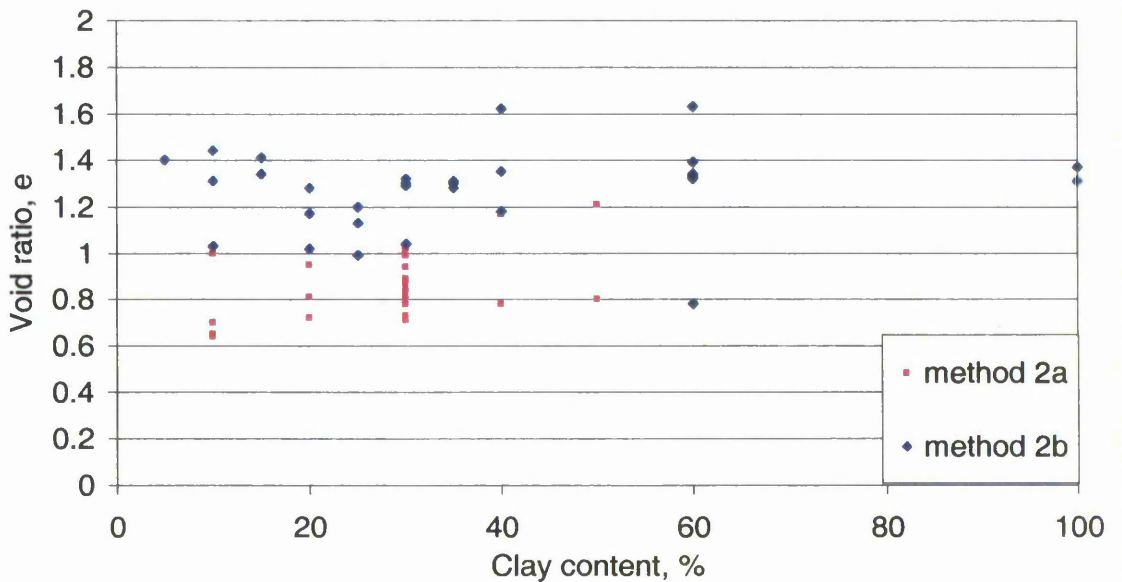


Figure 4-17 Initial void ratio of the oedometer specimens before loading shown for different preparation methods

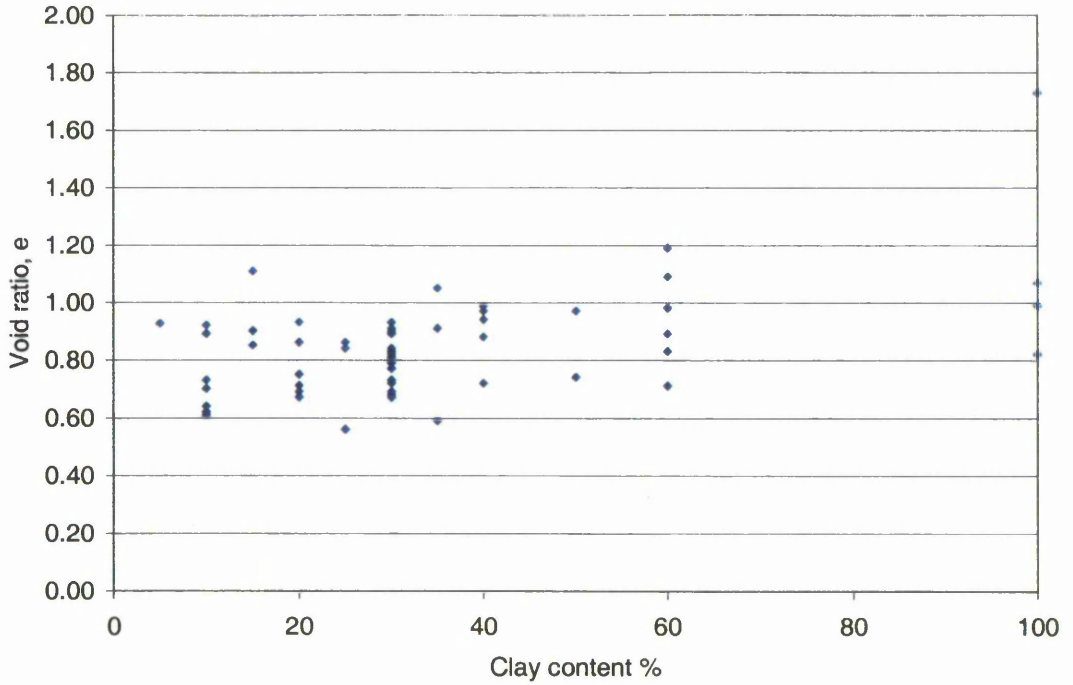


Figure 4-18 Void ratio of specimens at 200kPa before wetting shown for different preparation methods

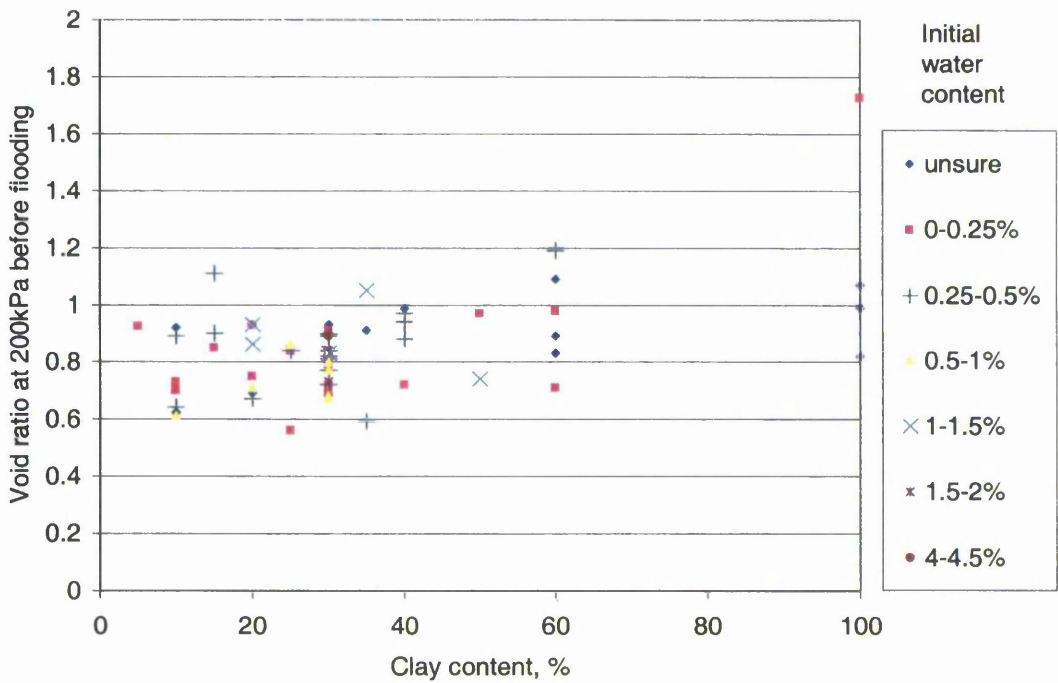


Figure 4-19 Void ratio of specimens at an applied stress of 200kPa before wetting shown for different initial water contents

The void ratios of the specimens at an applied stress of 200kPa are less variable than the initial void ratios. The influence of the preconsolidation pressure is removed, as the stress applied to the soil is greater than the preconsolidation pressure. The specimens were either air dried or oven dried. The differences in void ratio at 200kPa could be due to the small differences in initial water contents, caused by air drying or oven drying. Or due to the drying process itself; using the oven or allowing the specimens to dry more slowly in the air. Alternatively, the differences could be due to the differences in preparation water contents, which could cause the clay bonds to develop differently between the silt particles.

Void ratios are more consistent after the specimens have been wetted as shown in Figure 4-20. The initial water content now has no effect on the void ratios. The differences in void ratios are mainly due to different water contents after flooding. The specimens at 25-40% clay content appear to pack with lower void ratios than the other clay contents. The clay content can be seen to influence the void ratios of the specimens throughout the oedometer test. The variation of the void ratios at this stage is mainly due to different flooding water contents. Generally, the higher the flooding water content the greater the hydrocollapse, as can be seen in Figure 4-21. There will also be a natural variation in the void ratio that can be achieved, due to the interlocking of particles and the different alignments that could possibly be achieved.

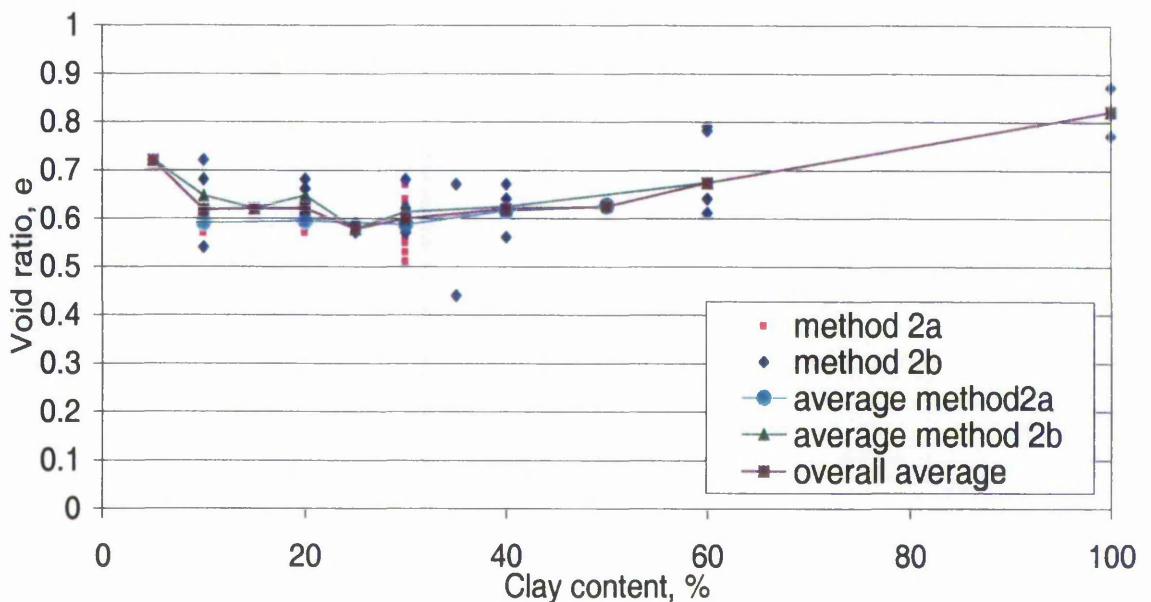


Figure 4-20 Void ratio of the oedometer samples at 200kPa after wetting

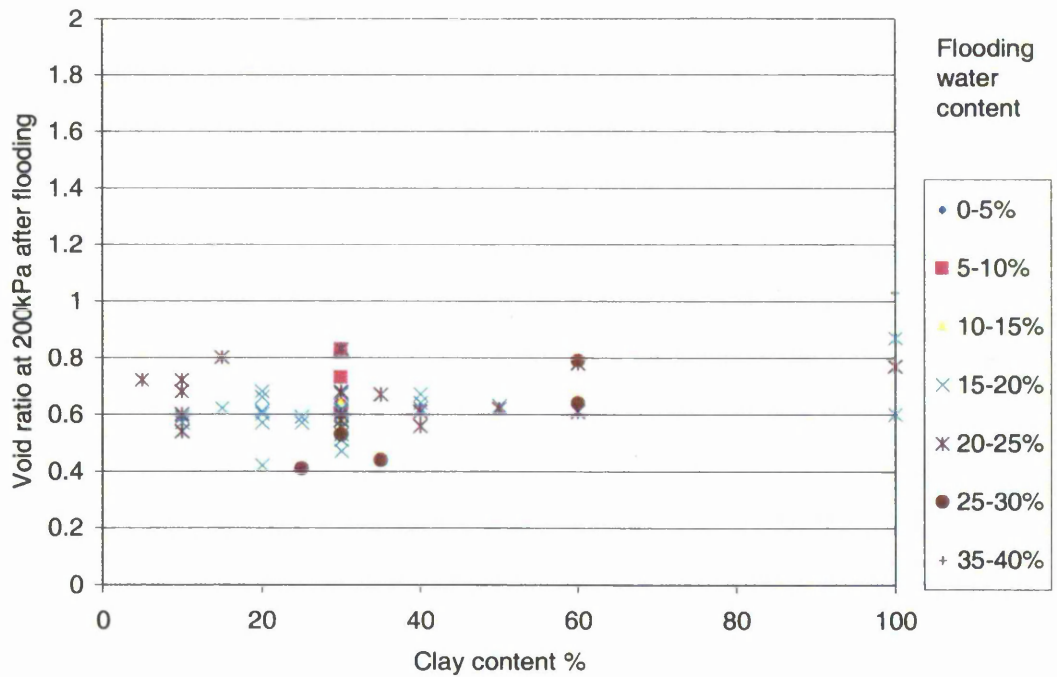


Figure 4-21 Void ratios at 200kPa after flooding of the specimens shown against flooding water content

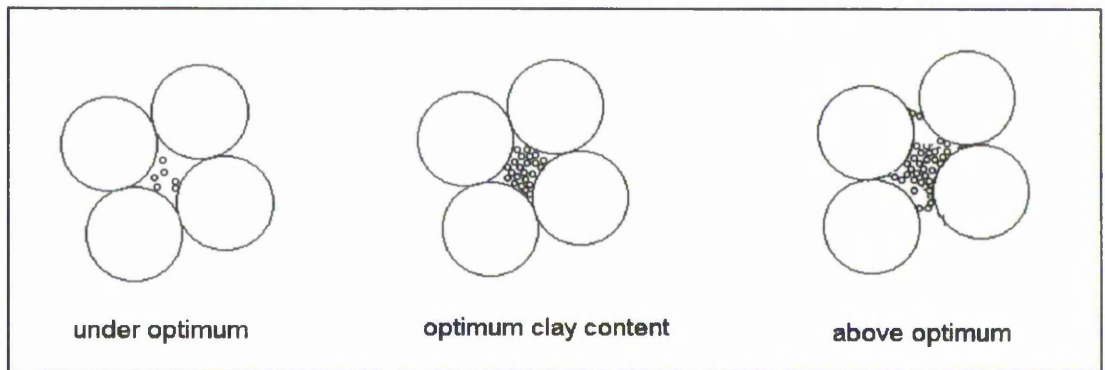


Figure 4-22 Illustration of optimum clay content

Clay content would appear to affect the void ratios of the samples at all stages of the test and therefore the amount of hydrocollapse observed in the samples. The densest initial packing is achieved with kaolinite contents of 25% i.e. this is an optimum initial packing arrangement. Approximately twenty five percent clay is the optimum amount of clay to fill

the voids between the silt particles. Above this clay percentage the smaller particles begin to dominate, the silt particles are pushed apart which creates larger void ratios. Below the optimum 25% clay content, the void ratios may also slightly increase because the clay will not fill as much of the void space between the silt particles. This hypothesis is illustrated in Figure 4-22. A similar effect was observed by Reddi and Bonala (1997) for a kaolinite-sand mix. Samples were compacted in moulds and extruded for testing. 10, 20, 30 and 40% kaolinite were tested, which had void ratios of 0.54, 0.36, 0.37 and 0.57 respectively for samples compacted dry of optimum.

#### 4.3.6 Effect of Clay Content on hydrocollapse

Figure 4-23 shows the percentage hydrocollapse observed in samples with varying clay contents. As clay content increases, hydrocollapse increases, if all other factors are kept the same (i.e. preparation water content and initial compaction). Some of the data on the loess deposits around the world seems to agree with this trend. Some of the deposits with greater clay contents seem to show more hydrocollapse. Other deposits show less hydrocollapse and show no correlation with clay content. The magnitude of hydrocollapse is dependent on many other factors apart from clay content, such as initial void ratio, initial water content, degree of saturation during flooding and bonding from other sources such as carbonates. The variation of natural loess deposits and the number of factors affecting hydrocollapse make it very difficult to compare hydrocollapse from one region to another. Therefore, a relationship between clay content and hydrocollapse can not be seen in the natural samples as it can in the artificial soil, where just one of the constituents can be varied.

The results shown in Figure 4-25 explain the hydrocollapse peak observed at 25% clay content (as shown in Figure 4-8), produced using method 1, where a constant mass is used to form each sample. The specimens also had very near constant initial void ratios due to the small change in their specific gravity caused by the small difference in densities of the silt and clay grains.

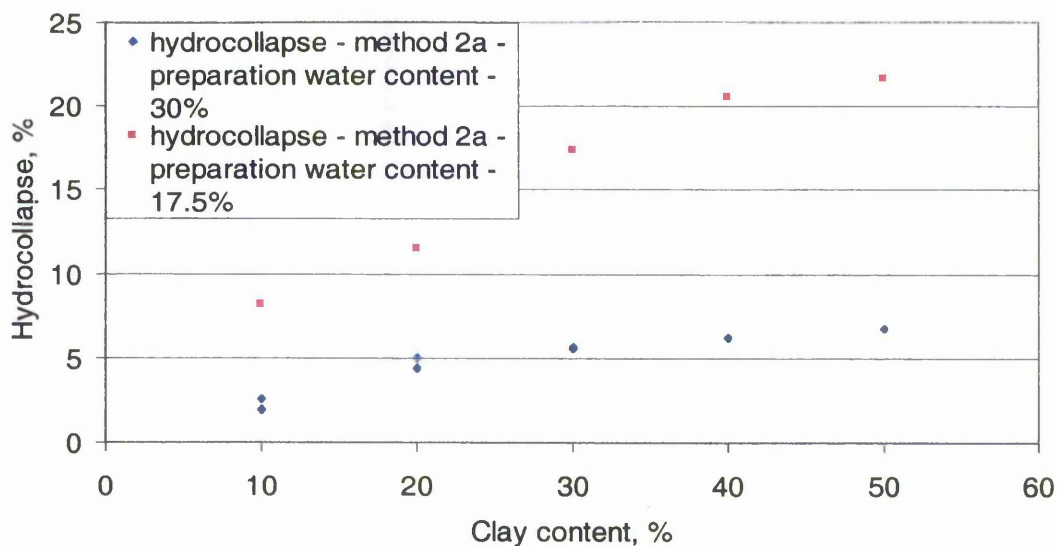


**Figure 4-23 Comparison of hydrocollapse for samples prepared using method 2a with 17.5% water content and 30% initial water content for different clay contents.**

Consider a set of specimens that are forced to pack with a void ratio of 1 for kaolinite contents varying from 0-40%. This void ratio is natural, perhaps for a clay content of 25%, but very dense for clay content higher or lower than this. The specimens formed with a greater percentage of clay than the optimum will also be forced into a denser structure than it would naturally form. Less hydrocollapse will therefore be observed due to the relatively more dense initial packing. It is proposed that the peak hydrocollapse curve observed in Figure 4-8 is, therefore, merely a function of the preparation of the samples and their initial void ratios. In specimens forced to have the same initial void ratio, specimens with the clay content that can be most easily packed will show the greatest hydrocollapse because they will have the potential to pack closest together. When the samples are formed at their natural void ratios, increasing the clay percentage results in an increase in hydrocollapse as shown in Figure 4-23. This shows the influence of the clay content for samples that have been allowed to form at their natural initial void ratios. The increase in hydrocollapse with clay content is not observed in the results from the literature due to the natural variations of other factors that control hydrocollapse.

Similar results were noted by Basma and Tuncer (1992). Sand – clay % was plotted against collapse potential. 0% is equivalent to 50% sand and 50% clay. 100% is equivalent to 100% sand and no clay. As the difference between the sand - clay percent reduced (higher

clay percent), the collapse potential increased, as can be seen in Figure 4-24. They explain their findings by the fact that the fine grains, of clay in this case, act as a bonding material. At low water contents, the clay fraction at the contacts of the larger grains, sand particles in this case, provides the shear strength that resists deformation. The higher the clay fraction the more the resistance is to densification and consequently, the higher the void ratio will be. However, when the soil is allowed free access to water, the clay binder is partially or fully broken, and the soil collapses. There are no results shown for void ratios of the different samples at the different stages, but the clay binder certainly has an influence over these soils. It is interesting to see that the sand and clay material behaves in a very similar way to the silt and clay material tested for this project.

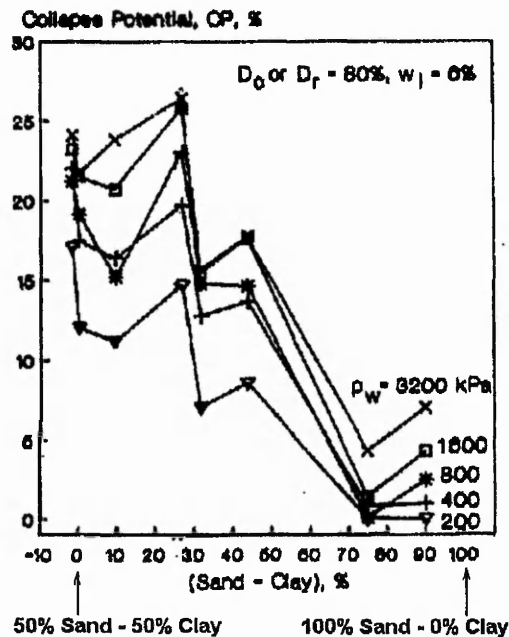


**Figure 4-24** Effect of difference between sand and clay on collapse potential at various wetting pressures (Basma and Tuncer, 1992).

#### 4.3.7 Effect of compressive effort

The depth of a deposit can be simulated in the sample by applying a compressive stress equal to the stress that would occur at a given depth. This reduces void ratio and hence increases the stiffness. For example, if the model soil sample is required to simulate an element of soil from 2m depth, the stress applied would be  $2 \times 15$  (unit weight of sample)

minus the water pressure at that depth. If the water depth is 1m then the applied stress needed is 20kPa.

Methods 2a and 2b have been used to create samples to examine the effect of varying kaolinite content. The same compressive effort was used for each clay content to allow the samples to reach their natural equilibrium. The main influence of compressive effort during the preparation of the samples is to make the samples stiffer due to increased void ratios as can be seen in Figure 4-25.

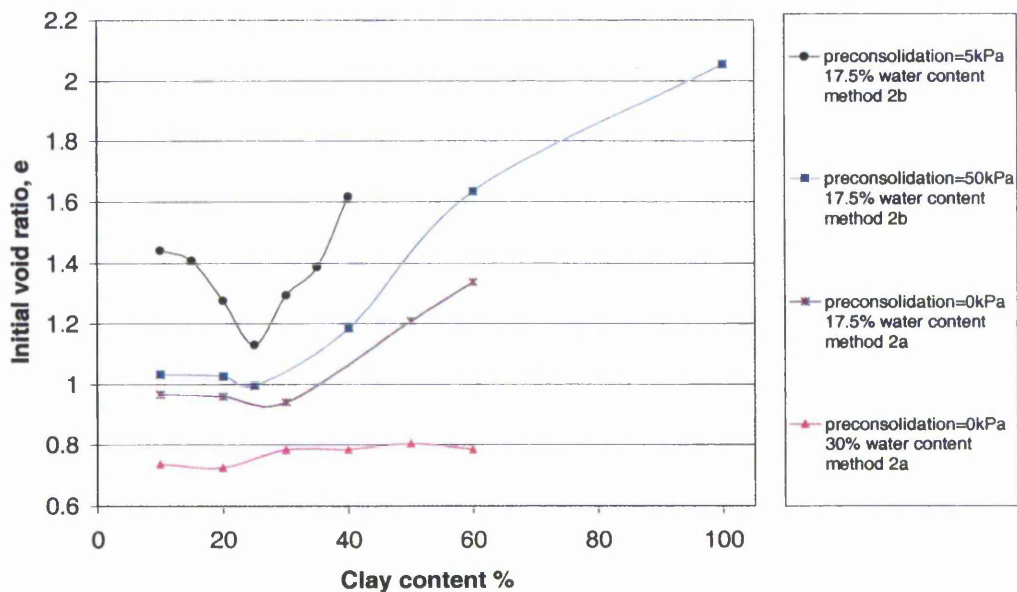


**Figure 4-25 Effect of clay content and preconsolidation pressure on initial void ratio of the artificial samples compacted with the same compressive effort**

#### 4.3.8 Effect of Water content

Preparation water content will affect the initial void ratio of the sample and therefore the constrained modulus. An optimum water content of 25% was shown to produce the samples with the highest density during preparation of the samples, see Figure 4-10. The effect of preparation water content is similar to clay content. As for all soils, there is an optimum water content, which produces the highest density sample. Both clay content and initial water content are significant influences in the formation of an artificial sample.

The behaviour of the samples under load is also affected by water content. As initial water content is increases, samples will become softer. At 50% saturation ratio the samples seem

to reach their densest packing following collapse, see Figure 4-14. Even if more water is added at this stage there will be no further decrease in height of the sample, provided the loading remains unchanged.

Results from El-Ehwany and Houston (1990) and Ishihara and Harada (1994) show similar relationships as seen in Figure 4-26. The latter report that for degrees of saturation above 65-70%, full collapse occurs and for a degree of saturation of 50%, 85% of full collapse occurs. Initial saturation is plotted against the hydrocollapse observed after full saturation of the samples. The shape and position of the partial collapse curve will, of course depend on the particular soil type, the amount of fine particles present and the type of cementation.

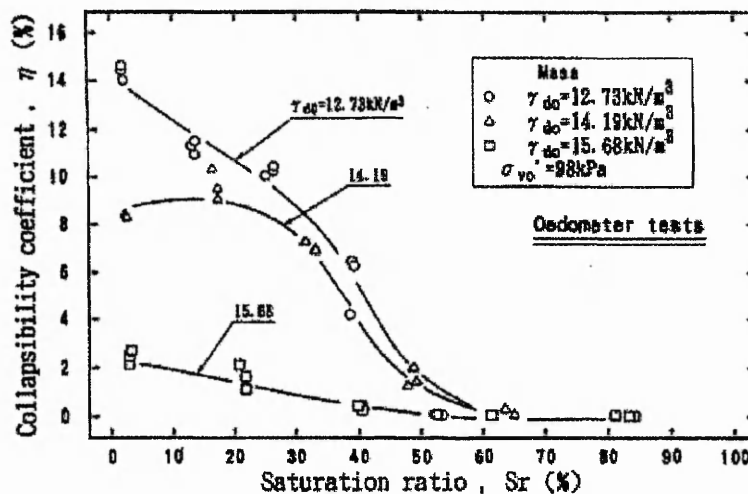
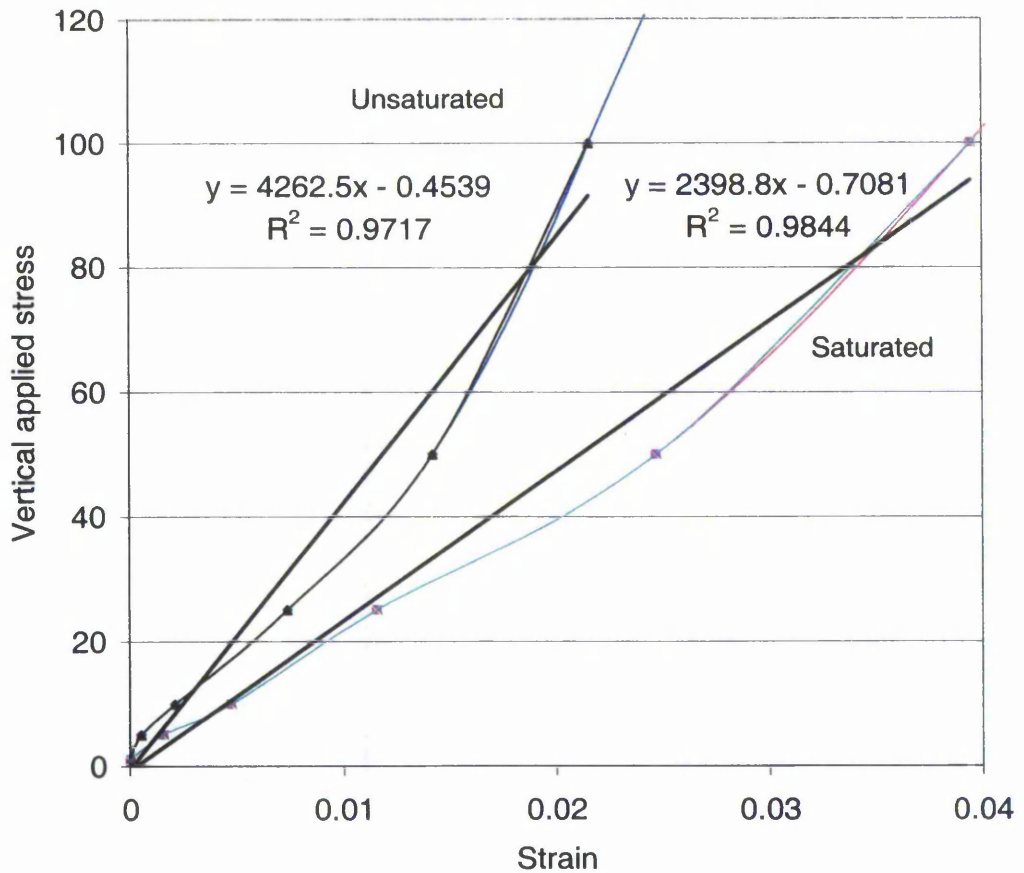


Figure 4-26 Collapsibility versus saturation ratio for test material (Ishihara and Harada, 1994)

#### 4.3.9 The constrained modulus, D

The constrained modulus was found for the oedometer tests by finding the line of best fit through the loading curve between 0-100kPa. Stresses up to 100kPa are of particular interest as this stress will be used in further testing later in this thesis. Values for the constrained modulus were found for both natural and artificial samples. The constrained modulus for specimens collected at the Star Lane site in Essex were around 4300kPa for unsaturated and 2400kPa for the saturated samples for stresses up to 100kPa. After this point the constrained modulus increased as the void particles became more densely packed, see Figure 4-27. The void ratio of these samples were around 0.78.



**Figure 4-27** Constrained modulus,  $D$ , for the Essex samples, 4300kPa for the unsaturated sample and 2400kPa for the saturated sample

For the unsaturated oedometer tests on the artificial loess, the stress-strain curve was near linear where applied stress was between 0-100kPa and the constrained modulus was easily found. Obviously for higher loads a non-linear approach would be more valid. For a sample with a void ratio of nearly 1, the constrained modulus,  $D$ , was around 1900kPa, and a sample with void ratio of 0.87,  $D = 2500$ kPa, see Figure 4-28.

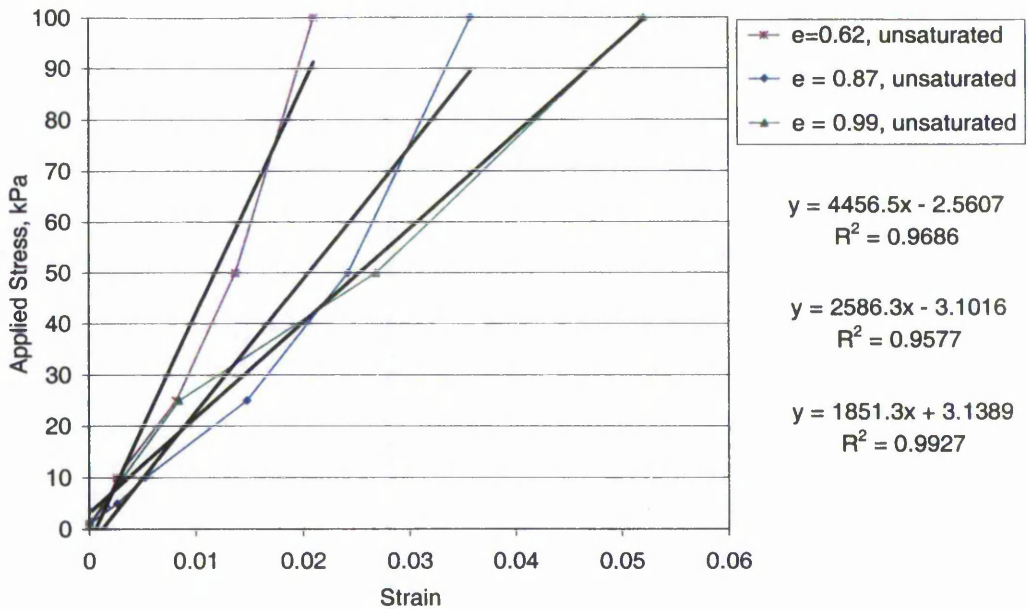


Figure 4-28 Constrained modulus, D, found for unsaturated artificial specimens (method 2a) with different initial void ratios and 30% clay content. Equations are given in order of their gradient.

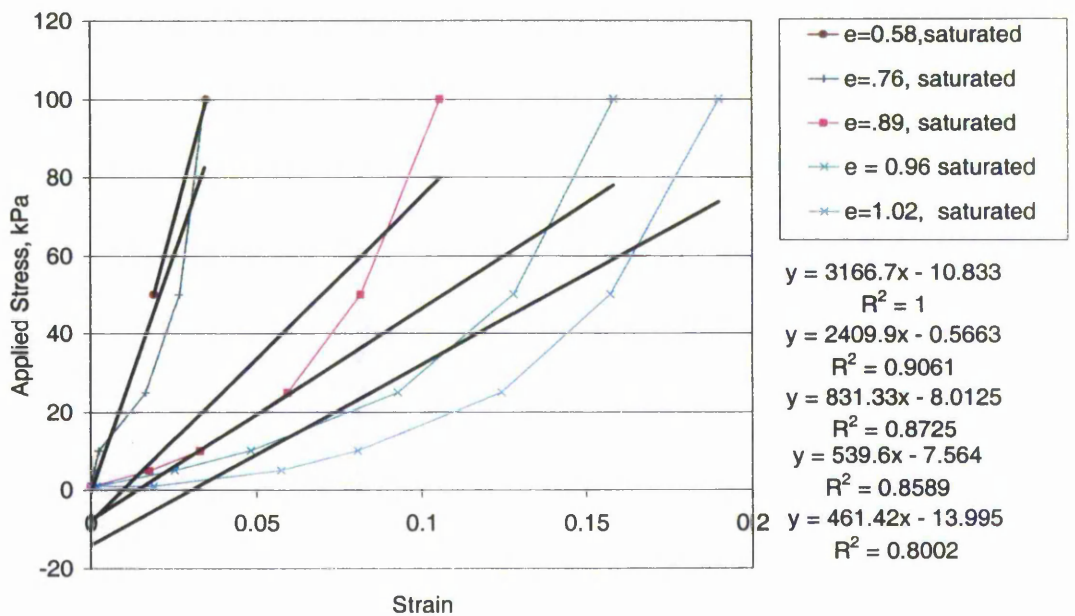
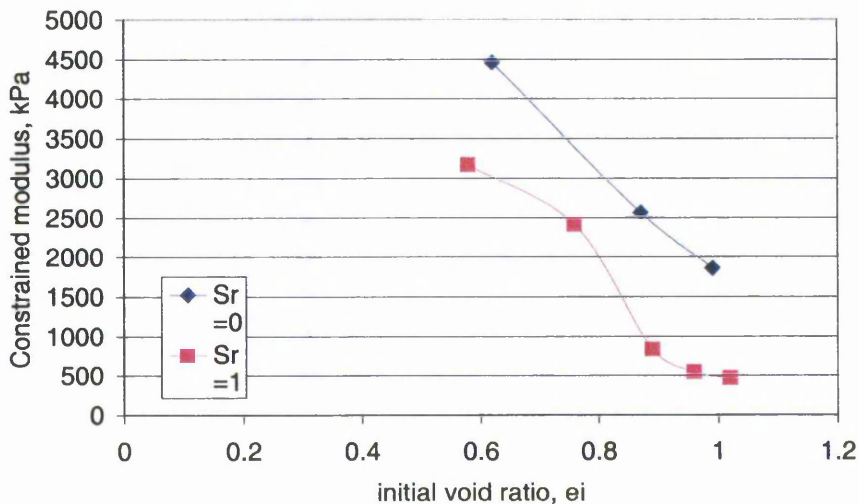


Figure 4-29 Constrained modulus, D, for saturated artificial specimens (method 2a) with different initial void ratios and 30% clay content. . Equations are given in order of their gradient.

The saturated artificial samples were less linear and therefore a line of best fit does not model the behaviour of the samples very well, as can be observed in Figure 4-29. However this approach allows a comparison to be made between the natural Essex loess and the artificial loess. For a saturated artificial specimen with an initial void ratio of 0.76, the constrained modulus was around 2400kPa, compared with the natural loess which had an initial void ratio of 0.78 and a constrained modulus of 2300kPa, for saturated specimens. An artificial sample of slightly lower void ratio,  $e = 0.89$ , had a much reduced constrained modulus of around 830kPa. The samples seem very sensitive to changes in initial void ratio. Constrained modulus decreased considerably with void ratios greater than 0.8.

A comparison of constrained modulus values for different initial void ratios is shown in Figure 4-30. The constrained modulus of the samples is obviously linked to their initial void ratio. Constrained modulus reduces considerably for saturated samples with a void ratio above 0.8. The unsaturated samples were stiffer than the natural specimens with an equivalent void ratio.



**Figure 4-30 Relationship of constrained modulus with initial void ratio for saturated and unsaturated samples, for the results presented in Figures 4.27 and 4.28.**

#### 4.4 TRIAXIAL COMPRESSION TESTS

Results for the undrained, unconsolidated triaxial compression tests carried out on natural loess from Pegwell Bay (see Figure 3.3, Chapter 3) are shown in Figure 4-31. The loess

from the Essex site and the Pegwell Bay site are very similar. The results from triaxial tests on this natural loess are shown for comparison with the artificial loess in Figure 4-32.

Triaxial compression tests were performed on the artificial loess to observe stress/strain behaviour of the samples under more realistic conditions. Method 2a was employed to make the samples, having proved to be the most successful way to make the artificial loess. Methods to produce the triaxial samples are discussed in Chapter 3. Specimens were again made using the same effort, so that the natural void ratio would form for the sample.

The specimens were tested in their unsaturated state. The specimens were tested with 100, 200 and 300kPa cell pressure. As the strain increased the stress was recorded at intervals and plotted on a graph of deviator stress against strain as in Figure 4-31.

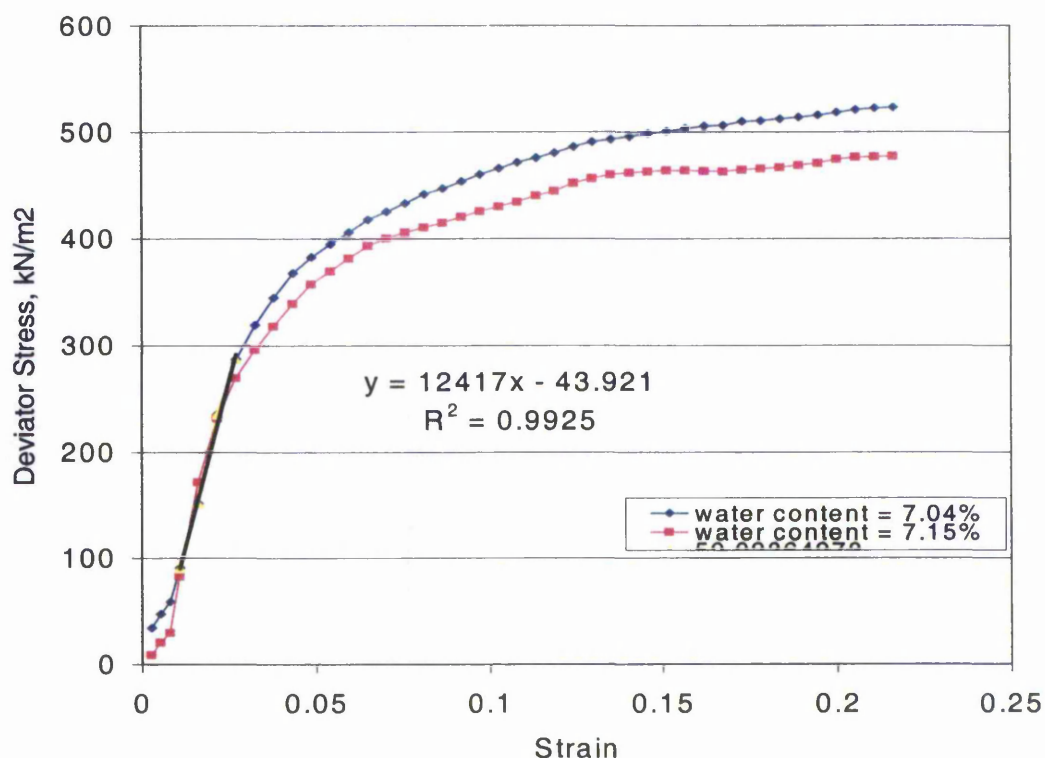
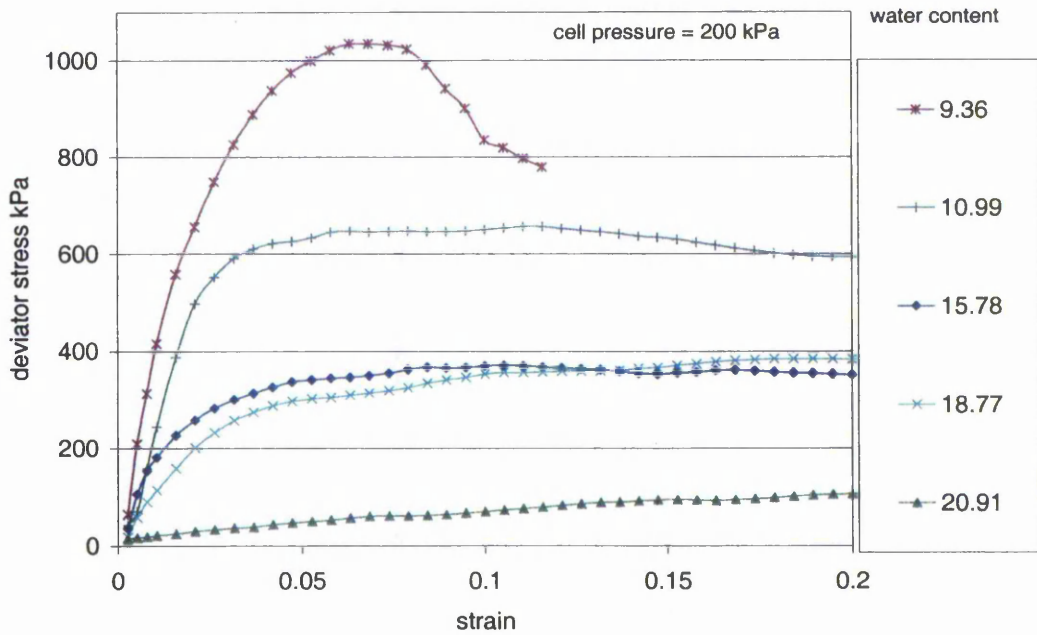


Figure 4-31 Deviator stress-strain curves for triaxial tests performed on loess from Pegwell Bay, Kent.



**Figure 4-32** Typical triaxial tests for artificial loess prepared using method 2a and tests at different initial water contents (%).

The maximum deviator stress,  $q_f$ , for the natural samples was around 500kPa. The maximum deviator stress for the artificial samples depended strongly on the water content that they were tested at, as expected. For artificial samples with water contents close to those tested in the natural samples,  $q_f$  was higher than for the natural samples. For the sample tested at 9.4% water content the void ratio was 0.75. The void ratios in the natural samples were very similar, 0.74 and 0.77. Void ratio was therefore not the cause of the increased strength in the artificial samples.

Once the strain of the specimen had reached over 0.03 (3%), the stress exerted by the equipment did not increase significantly. There is an almost linear relationship between stress and water content. The water content seems to have more of an influence at higher strains.

#### 4.4.1 Effect of confining pressure

Results for 100, 200 and 300kPa confining pressures are shown in Figure 4-33. Samples were made and left for 2 days to dry to a water content of approximately 14-15%. Increasing the confining pressure from 100kPa to 200kPa increased the Young's Modulus.

At 300kPa the Young's Modulus had decreased. It was observed that the samples tested with a confining pressure 300kPa were compressed as the confining pressure was added, before the axial load was applied. This will have disturbed the sample and broken some of the bonds, possibly causing fracture of the sample before it was loaded. This will account for the decrease in Young's Modulus at higher confining pressures.

The failure of the specimens was generally through ductile failure, although some brittle failures were observed for confining pressures of 100 and 200kPa, as shown in Figure 4-33. This was similar to results reported by Tan (1988), for loess in Lanzhou Province in China. For these natural samples, the stress-strain curves showed a peak followed by shear softening for confining pressures below 100kPa. When confining pressure exceeded 100kPa no peak was observed, the vertical strain could exceed 10% and failure occurred by plastic bulging. It is encouraging to observe the similarity in behaviour between the artificial laboratory prepared specimens and the natural deposit that had developed over millions of years.

The Young's Modulus of the artificial samples tested with a confining pressure of 300kPa was reduced compared with the samples tested at 200kPa. This was also observed by Wiebe et al. (1998) for a sand-bentonite mix where Young's Modulus increased with confining pressure up to 1,000kPa but decreased at higher pressures, this is shown in Table 4-6. Young's Modulus of the soil  $E_{50}$  was found for 50% of the maximum deviator stress. The reason for the decrease in Young's Modulus with confining pressure after 1,000kPa was not discussed. It is possible that with higher confining pressures, the structure of the sample is disturbed, perhaps breaking some of the bonds that provide the strength to the structure, and when axial stress is applied the sample is simply less strong. The majority of the tests for this current project were carried out with a confining pressure of 200kPa because there were fewer problems associated with testing at this pressure level.

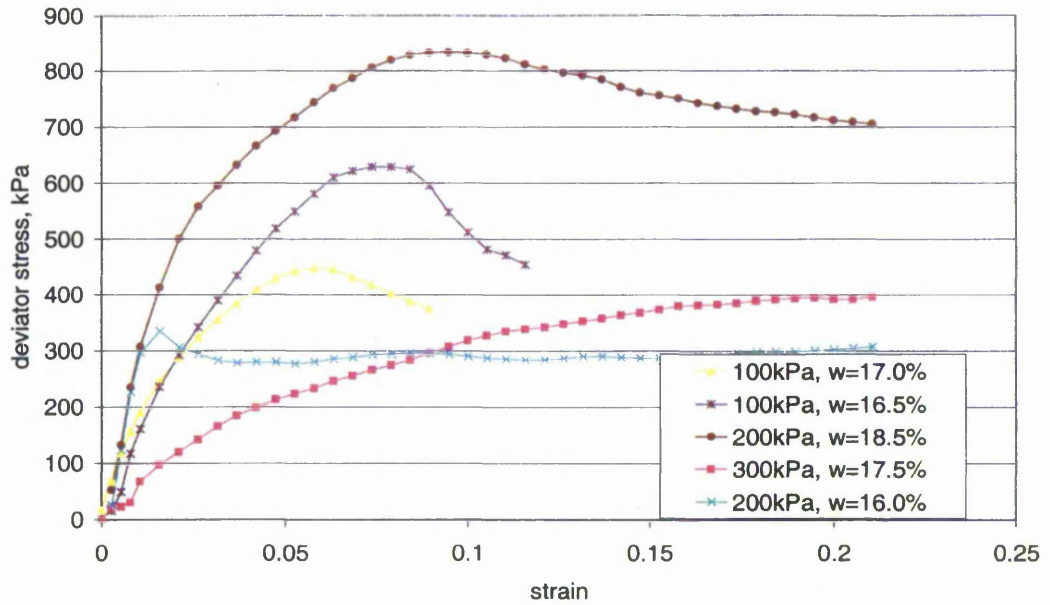


Figure 4-33 A comparison of typical triaxial test results on artificial samples at different confining pressures. Where  $w$  = water content %.

Saturation (%)	Temperature (°C)	Confining pressure, $p_{con}$ (kPa)				
		200	500	1,000	1,800	3,000
50	26	182	197	251	173	80
	65	105	116	108	93	84
	100	89	94	135	108	85
65	26	150	170	196	97	57
	65	102	114	102	56	75
	100	82	78	108	64	80
80	26	-	-	107	55	66
	65	82	85	61	46	102
	100	88	56	122	79	146
98	26	53	86	62	55	55
	65	54	41	48	50	84
	100	71	33	68	81	109

Table 4-6 Young's Modulus  $E_{50}$  (in kPa) related to saturation, temperature and confining pressure (Weibe et al, 1998).

#### 4.4.2 Effect of water content

Figure 4-34 shows the results of a range of triaxial tests, which were performed on samples with different moisture contents. The moisture content of each sample is shown in the key.

The samples were made wet during preparation and left to dry in air for varying lengths of time to produce the different water contents. As initial water content increased the samples had a tendency to bulge rather than shear, as would be expected. The strength of the specimens decreased as water content increased.

This also agrees with data reported by Wiebe et al. (1998) for an unsaturated sand-bentonite mix. Quick undrained compression tests were performed on this mixture under different confining pressures, saturations and temperatures. They reported that shear strengths and stiffness increase as the saturation decreases. Failure modes are predominantly ductile, except at low saturations and confining pressures where some strain softening takes place.

The Young's Modulus of the natural specimens was estimated to be about 12,500kPa using a cell pressure of 200kPa, as shown in Figure 4-31. Estimates of Young's Modulus were also made for the artificial specimens. The Young's Modulus of each sample was calculated by taking the line of best fit through the stress-strain curves, as each sample showed close to straight line behaviour for deviator stresses up to 300kPa. Some of these lines of best fit are shown in Figure 4-34, which are shown for deviator stresses up to 400kPa for different water contents. Figure 4-35 shows how the Young's Modulus of each sample varies with water content. This was considered to be a maximum expected loading for any normal foundation. Samples with water contents less than 15% show stiff behaviour. These samples compare well with the behaviour of the natural samples. Between 15-20% water content, the Young's Modulus begins to reduce considerably. Samples with water contents above 20% show very soft behaviour. These percentage water contents were significant while carrying out the Plastic Index tests. The liquid limit was an average of around 25% and the plastic limit approximately 17%. Therefore this change in behaviour at around 20% water content is expected. Soils with a water content of below 15% will be very susceptible to collapse even if the water content is only increased by a few percent.

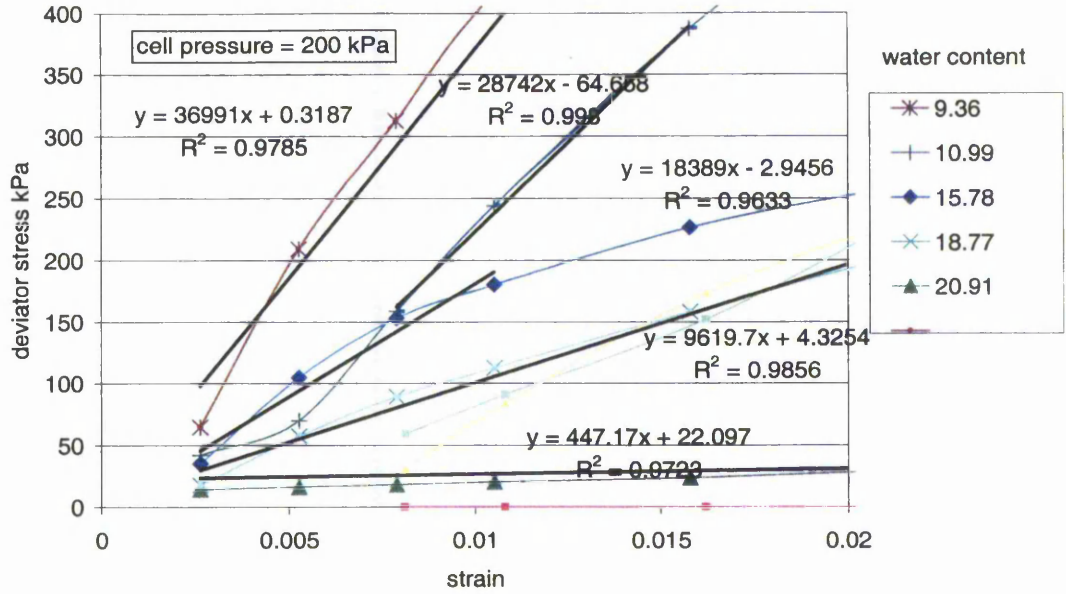


Figure 4-34 Young's modulus found using lines of best fit for the artificial specimens tested in undrained, unconsolidated triaxial tests.

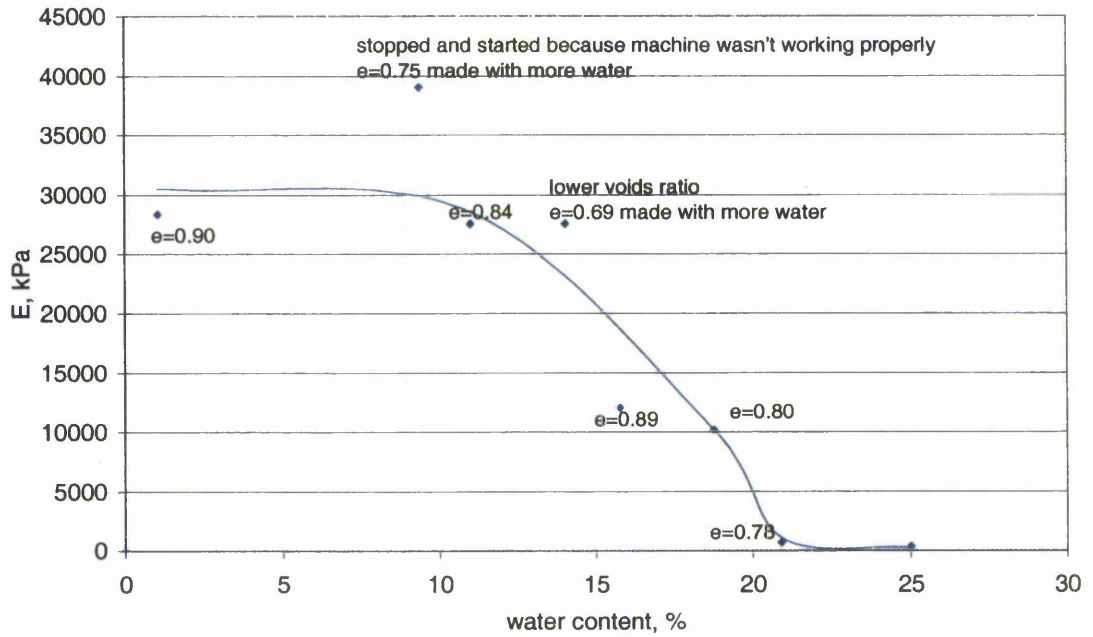
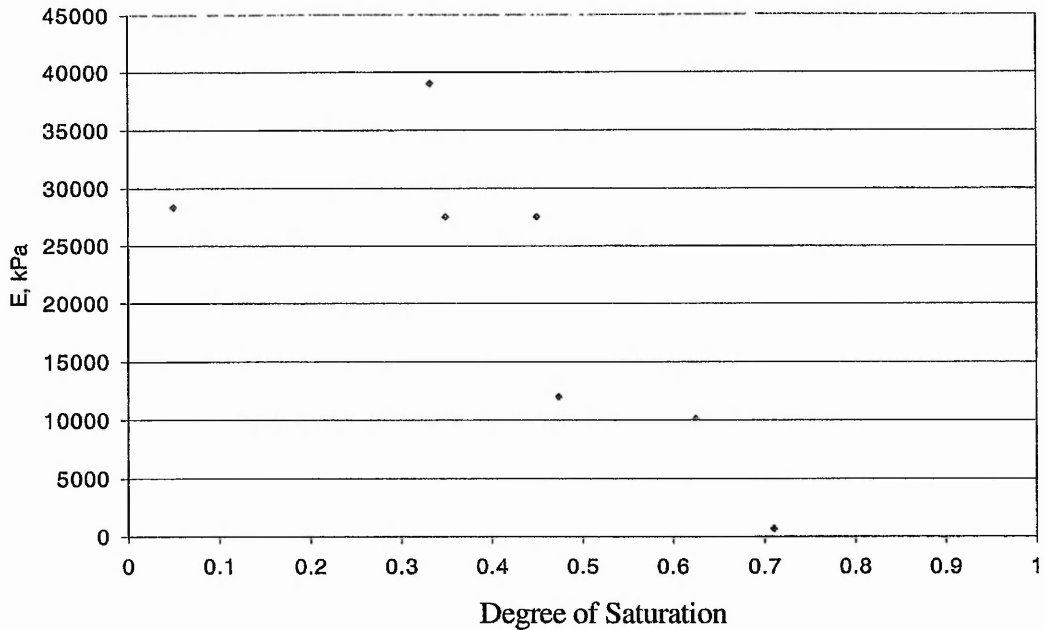


Figure 4-35 Young's modulus, E, values compared to water content of the sample



**Figure 4-36 Young's Modulus (E, kPa) found for the artificial samples against estimated saturation ratio during the test**

Figure 4-35 shows the relationship between Young's Modulus and saturation ratio, this relationship is similar to those found from the oedometer tests, where the majority of collapse was observed with a saturation of 50%, see Figure 4-14. Increasing the water content further in the oedometer tests did not increase the amount of collapse. At 20% water content the saturation ratio is around 0.6, depending on voids ratio, which explains the soft behaviour and is consistent with the behaviour observed in the oedometers. The degree of saturation affected the Young's Modulus of the soil up to a degree of saturation of 70% in the triaxial tests, see Figure 4-36. Above a degree of saturation of 70% the Young's Modulus appeared to be unaffected.

#### 4.4.3 Conclusions from Oedometer Tests

It appears from the oedometer tests that some of the important factors for assessing the magnitude of hydrocollapse are the initial void ratio, the clay content, the specific gravity and the degree of saturation or water content. An additional factor affecting the behaviour of the samples seem to be the method of preparation of the samples

Two observations have been made from the oedometer tests, which have been built into the proceeding numerical model.

1. A trend for increasing constrained modulus as the vertical stress is increased was observed, see Figure 4-4 for results of natural loess specimens taken from the Star Lane site in Essex. This is due to the confining conditions in the oedometer and is not observed in triaxial tests on the same material.
2. Samples that are loaded and then saturated reach the same void ratios as a sample that is saturated and then loaded. This could also be due to the confining conditions.

All the artificial samples were made by wetting (steaming, mixing or spraying) and then drying the material to create the clay bonds. The wetting and drying processes are vital for the production of the bonds (Trofimov, 1990). Re-saturating the sample breaks down the bonds (clay bonds and suction) between the particles resulting in the observed hydrocollapse behaviour.

Method 1 produces samples that collapse in a similar way to natural loess. However, the initial void ratios are higher than for natural loess (around 1.1, instead of 0.8-1.0 found in natural samples, see Figures 4-4 to 4-7) and the shape of the saturated curve is different. Collapse values are higher than in natural loess because of the high initial void ratios and the lack of bonding created by the steaming method.

Method 2a (the wet method) also produces collapsible samples. Both unsaturated and saturated curves have similar shapes to the natural loess curves. With this method the lowest void ratios are produced for samples made with 25% kaolinite. This percentage of kaolinite is the optimum clay content to produce the highest density samples during preparation for a silt-kaolinite mix. Void ratios produced by method 2a are more realistic than produced by method 1 (the air fall method) and collapse values are around the same value as for natural loess for samples prepared with 27% water content. Hydrocollapse of these samples increases with kaolinite content. Method 2b (the bonding method) provides results similar to method 2a but with more collapse upon saturation. Method 2a provides a good way to make larger specimens, which can be directly placed in the footing model.

The clay binder appears to be providing the strength to maintain the high void ratios which later cause collapse. Water degrades the clay bonds and allows rearrangement of the particles to a closer packing. Additional factors affecting the behaviour of the samples besides clay content, initial void ratio, and water content seem to be the method of

preparation of the samples and the particle shape. Particle shape affected the void ratios but had negligible effect on the magnitude of hydrocollapse.

#### 4.4.4 Conclusions from the triaxial tests

Water greatly affects the Young's Modulus and strength of the artificial samples, as with all soils. The Young's Modulus decreases with saturation increase up to 50% saturation. After this the increase in saturation has little effect on the Young's Modulus of the sample. The majority of hydrocollapse of the sample will occur with saturations up to 50%-70%. Any increase in water content above this will not greatly affect the collapse observed in the sample.

Behaviour of the artificial samples was similar to that of the natural samples tested from Pegwell bay. The maximum deviator pressure for the natural samples was lower than for the artificial samples at equivalent water contents (500kPa compared with 800kPa). A confining pressure of 300kPa seemed to destroy the bonds in the artificial sample and, consequently, a much lower strength was recorded for these samples. In general the failure mode was ductile, although some brittle failures were observed in both the natural and artificial samples at low saturations and low confining pressures.

Samples with over 70% saturation ratio had negligible strength, Young's modulus values below 500kPa were found. Increasing the saturation ratio did not significantly alter the Young's Modulus. This has also been observed in the oedometer tests for constrained modulus.

Estimates of stiffness parameters were made for the artificial and natural specimens. The natural loess had a Young's modulus of around 12,500kPa at 200kPa confining pressure. The artificial samples exhibited slightly stiffer behaviour at equivalent water contents. At a water content of 15.5% the Young's modulus of the artificial specimens was around 18,000kPa and at 18.7% water content the Young's Modulus was reduced to 9,600kPa.

## 4.5 GENERAL CONCLUSIONS

This chapter has discussed the physical modelling results for the artificial materials compared to some natural loess deposits from the UK. The silt-size component of loess was represented in the artificial soil by three types of silt sized particle; glass balls, crushed

sand and industrially ground silica. Three methods of forming the artificial loess were also developed. Particle size analysis, microscopic photography, index tests, oedometer tests and triaxial were all carried out on the artificial loess and have been discussed in relation to the natural deposits. The particle size analysis, index tests and SEM's indicated that the ground silica and crushed sand gave a better representation of natural loess than the glass balls in terms of particle shape.

New methods of production of artificial collapsible soils have been developed and tested. The oedometer tests allowed the methods of producing the artificial loess to be assessed. The method that produced the most comparable material to loess was method 2a. The oedometer tests revealed that these artificial specimens gave the best representation of the behaviour of the natural deposits. Method 2a required silt and clay to be mixed with water and then formed into the specimens while wet. Samples were dried either in the oven or in air (for a more natural water content). The specimens were prepared using the same compressive effort for different clay contents to investigate the effect of clay content on void ratio and hydrocollapse of the samples. Different compressive efforts were used to represent samples that had been formed at different depths. This approach allowed the samples to form at their natural void ratios, which was important to investigate particle packing effects.

It was found that there is an optimum clay content for producing the highest density samples during preparation, similar to optimum water content. The clay content that produced the lowest void ratios for the same compressive effort was 25%. The optimum water content was found to be around 25%. Similar behaviour was found in the artificial loess and natural loess. Both samples exhibited hydrocollapse and similar stiffness parameters were observed for the samples in both the oedometer and triaxial tests. The constrained modulus of the oedometer samples was generally lower than that found for the natural loess due to higher void ratios and, possibly, due to lack of carbonate bonds. The specimens exhibited behaviour close to that of UK loess when prepared with water contents of 30%. This made samples that had lower void ratios for the same compressive effort and therefore specimens had a higher Constrained Modulus when tested in the oedometer equipment. The artificial samples prepared with ground silica/kaolinite content 80/20 and a preparation water content of 27% had an initial voids ratio,  $e$ , of 0.72 and behaved very like the loess from the brick works in Essex, UK in the oedometers. The relationships between

degree of hydrocollapse and clay content, water content at collapse and production pressure were discussed. The constrained modulus was found for each of the oedometer specimens and related to the void ratio of the samples. The void ratios depend on preparation water content and the compaction pressure exerted on the sample during preparation.

The favoured method of production, method 2a, and was used to produce the samples for a number of undrained triaxial compression tests. The majority of the specimens were prepared with a water content of 17.5% and clay content of 30% to provide samples with a large hydrocollapse potential. The specimens were allowed to dry for different amounts of time to provide different initial water contents for testing. These tests were carried out to assess the importance of initial water content and confining pressure on the Young's Modulus and strength of the samples. The bonds in the samples tested at a confining pressure of 300kPa were slightly destroyed by the high cell pressures and therefore exhibited lower strengths than the samples at a confining pressure of 200kPa.

Young's Modulus values of around 12,500kPa for unsaturated soil at natural water content and around 400kPa for saturated soil were found from the triaxial tests. The Young's Modulus for the artificial triaxial samples compared very well to the natural samples from Pegwell Bay as the void ratios were very similar. Artificial samples with water contents between 15-17% showed similar strength and stiffness characteristics as for the natural loess with a water content of 7.5%.

The amount of hydrocollapse in natural loess is dependent on many factors such as clay content, initial void ratio, initial water content, degree of saturation after flooding and integrity of other bonds such as from carbonates, oxides or calcite. The number of factors affecting hydrocollapse and the variation of these factors in loess deposits around the world make it very difficult to compare hydrocollapse from one region to another. Things are simplified by taking samples from a single region. Localised samples have much the same mineral content and particle sizes throughout which decreases the number of factors involved. The affect of loading and water content can be determined for these samples in the oedometer and triaxial equipment and used to determine the geotechnical properties for the site. These properties can then be used in further analysis to determine how the soil will act under load and wetting. However, sampling effects on the soil make it hard to test a truly undisturbed soil. The artificial soil has helped to reduce the sampling effects and has

also allowed the effect of clay content on hydrocollapse to be analysed. This could not be done for natural loess due to the natural variation in all the other factors that control the amount of hydrocollapse. The artificial loess has therefore been of great benefit in understanding the affect that the clay content has on the behaviour of loess-like soils. Although the artificial loess lacks some mineralogical content of natural loess, it does produce hydrocollapse and has been proven to behave very like a natural loess deposit.

Both the oedometer and triaxial results from the artificial results compared favourably with results for UK loess deposits. Hydrocollapse behaviour was observed in the oedometer samples when loaded and wetted. The same deformations were found for specimens that were loaded and then saturated as for specimens that were saturated and then loaded. The sequence of loading and wetting for both artificial and natural samples had negligible influence on the final stress-strain point of the soil.

## 5 Computer Models to Simulate Collapsible Soils

---

### 5.1 SUMMARY OF LABORATORY RESULTS

In chapter 4 it was observed that oedometer specimens that were initially made by using the same total mass of clay and silt particles, had approximately the same initial void ratios for each of the samples, following method 1, after Dibben (1998) and Assallay (1998). Figure 5-1 illustrates the void ratios found from the oedometer tests for clay contents of up to 30%. The lines show the initial void ratio,  $e_i$ , the void ratio at 200kPa before wetting,  $e_{pre-c}$ , the void ratio of the sample at 200kPa after wetting,  $e_{post-c}$ , and the final void ratio,  $e_f$  recorded for the sample at 1600kPa. Samples with 25% clay content reduced their void ratios more than any of the other samples. The graph of hydrocollapse<sup>1</sup> against clay content percent is shown in Figure 5-2. This shows how a peak hydrocollapse is observed at 25% clay content. The reasons for this were unclear but were thought to be due to the way that the particles pack for different clay contents, see the discussion in Chapter 4.3.6.

---

<sup>1</sup> Hydrocollapse was calculated for each clay content using the equation: (void ratio pre-collapse – void ratio post-collapse) / void ratio pre-collapse.

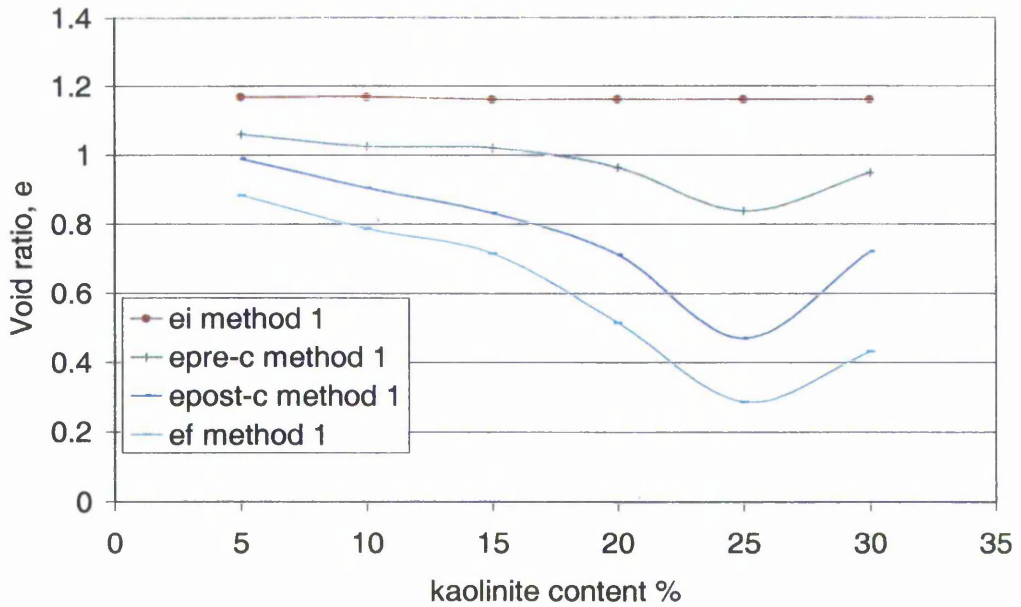


**Figure 5-1 Void ratio vs. kaolinite content for artificial loess specimens prepared using method 1.**

Where,  $e_i$  = initial void ratio,  $e_{pre-c}$  = void ratio before collapse (200kPa applied stress),  $e_{post-c}$  = void ratio after collapse (200kPa applied stress) and  $e_f$  = final void ratio (1600kPa applied stress).

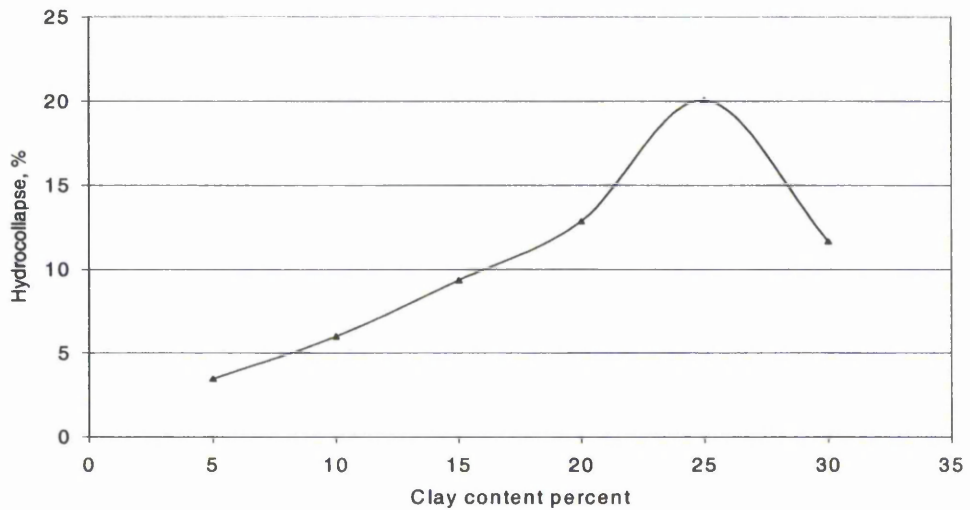


**Figure 5-2 Peak hydrocollapse observed for specimens prepared using method 1**

To investigate this further, samples were made again, but this time the samples were made using the same static compressive effort to form 'natural' void ratios within the samples using method 2, see Chapter 4.3.2. This means each of the samples is formed using the same standard compressive energy and should form in their natural void ratios. The initial void ratios for these samples are shown in Figure 5-3. The lowest natural void ratio was formed approximately between 20 and 30% clay content. This indicates that the samples found their own 'natural' void ratio for different clay contents under different compressive efforts. Producing the sample with the same compressive effort reduced the effect of the clay content on the initial void ratios, allowing the effect of clay content on magnitude of hydrocollapse to be investigated. In fact, hydrocollapse steadily increases as clay content increases if all other properties are kept constant. Forming the samples using the same energy completely removed the peak hydrocollapse that was found at 25% kaolinite content for samples prepared using method one. This peak is also not observed in natural samples. This means that initial packing and method of formation of the samples significantly influences the amount of settlement and magnitude of collapse that will occur in a sample. Hence, results in the literature (e.g. Assallay 1998) are more likely to be a function of sample preparation as discussed in chapter 4. Initial packing and void ratios depended on the clay content that the samples were prepared with. It became clear that there was an optimum clay content at which a more dense packing occurred that produced lower initial void ratios, but still maintains hydrocollapse potential within the specimens.

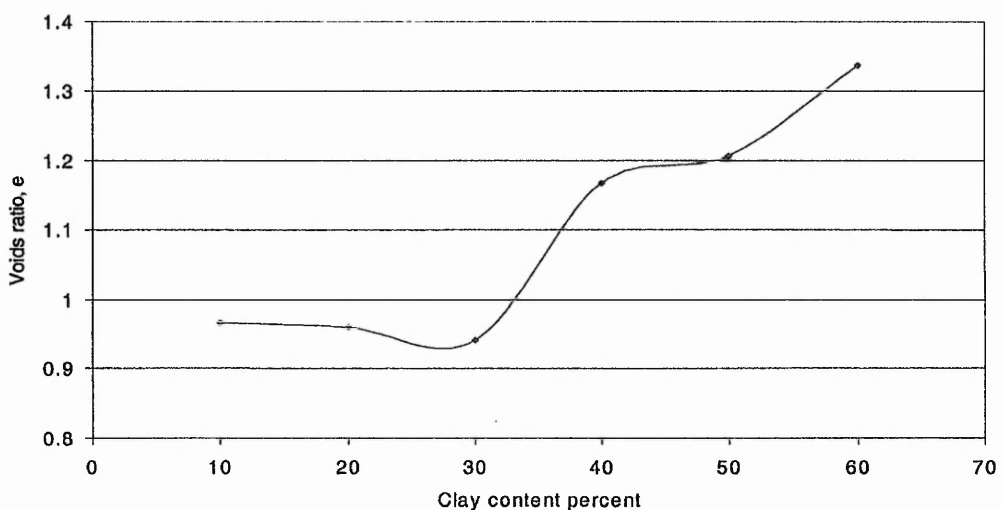


Figure 5-3 Natural void ratios formed in the samples for different clay contents

## 5.2 PARTICLE PACKING

It is proposed that particle packing has a great deal of influence over the behaviour of a collapsible deposit. In particular, it is proposed that the void ratio of the deposit will depend on the clay content. The results from method one indicated that the initial packing of the particles in a sample affects the amount of hydrocollapse obtained in a typical oedometer collapse test. The new methods of producing artificial loess, developed and discussed in this thesis, have further indicated that packing has a large effect on void ratios and on the magnitude of collapse when the sample is wetted. The following computer models were developed to investigate the influence of packing indicated by the oedometer tests.

This chapter discusses the aims, objectives and theory behind a computer model developed to simulate a collapsible soil. The model was developed to simulate a collapsible deposit with randomly arranged clay and silt particles. The logic of the program is discussed as well as the simplifications and assumptions needed to make the model. The assumptions make it possible to devise such models but also limit the extent to which the models can be realistic.

The debate in Ground Engineering November 1999 on the motion that 'constitutive models are past their sell by date' showed the merits of both particle packing and finite element methods and suggested that both approaches can be valid and useful. A particle packing approach, proposed in the following model, can help to elucidate the behaviour on a micromechanical level, whereas finite element approaches look at the deposit as a whole using a more 'macromechanical' approach. Both methods can help to understand the mechanisms of collapse behaviour. Such a combined approach was advocated by Feda (1995).

The question of whether the clay part of loess was created before or after deposition was discussed by Bell (2000). The paper suggests that both are possible sources for the clay component of loess. The idea that clay is deposited at the same time as the silt has been assumed for the following computing exercise. This assumption was based on the fact that some clay mineral must be deposited with the silt in order for the clay bonding to develop, whether or not this component is attached to the silt particles or deposited as separate

grains. The clay mineral groups found in loess are generally, montmorillonite, illite and kaolinite. Kaolinite is generally produced from alkali feldspars under acidic conditions, illites are generally produced from micas or alkali feldspars under alkaline conditions and the montmorillonite group are formed by the alteration of basic rocks or other silicates, low in Potassium under alkaline conditions, providing Calcium and Magnesium are present. This suggests that at least some of the clay minerals found in loess must have been 'carried in' while it was being deposited since they are produced under very different conditions.

The aim of the computer simulations was to investigate:

1. The metastable and stable structures formed in a collapsible soil
2. The peak collapse observed in method 1 (after, Dibben, 1998 and Assallay, 1998) with artificial loess soils.
3. The effect of varying the clay content on particle arrangements

The ultimate aim was to elucidate the role that particle packing has on the collapse behaviour of loess soils.

## **5.3 THE STRUCTURAL MODEL**

### **5.3.1 Introduction**

A fabric model of a collapsible loess deposit has been created using visual basic, which was chosen for its graphical capabilities. This windows based visual language allows representation of the structure on screen during the run time of the program. This helped during development of the program to ensure that the code was working as expected. After running the program the image could also be printed to produce a permanent record of the structure. This allowed the random structures to be examined and assessed by comparing void ratios, packing arrangements and pore shapes. These structures could then be compared to the structures found in the natural and artificial loess in the laboratory.

### **5.3.2 Assumptions**

A loess deposit comprises a random arrangement of particles, deposited on top of the existing bedrock. The main mechanisms for deposition are by wind and fluvial action, which help to transport the particles to produce the blanket deposit. For the computer

model it is assumed that the particles are deposited randomly one by one with clay and silt particles being deposited in set proportions at the same time.

The methods described in Chapter 3 to produce artificial loess specimens have been used to simulate a deposit in the laboratory. The computer program was designed in order to investigate the particle arrangements that occur during the depositional process and address the questions that were generated as a result of the laboratory testing. It was necessary to consider the following questions:

- Why did method 1 produce samples with a peak collapse at 25 % clay content?
- How do the metastable/stable arrangements develop?
- Is the influence of clay content on the particle packing due to its size?
- Was the clay deposited at the same time as the silt?

The computer program was designed to model a two particle sizes representing the clay 'packets' and the larger silt particles. These particles were randomly placed on the deposit in the required proportions to replicate the laboratory tests discussed in chapters 3 and 4. In particular, the computer generated fabric model was useful to investigate the effect of changing the proportions of silt and clay on the arrangement of the particles and explain why the peak in hydrocollapse was produced at 25% clay content.

### 5.3.3 Methodology

A domain of 12,000 units wide and 10,000 units tall was defined in which the particles could be placed. The origin was set at the top left corner with positive directions as right and down. A lower boundary was set at  $y=8,000$  which represents the existing bedrock on which the deposit would accumulate. Each particle was assumed to be circular so that orientation of the particles was not important. The circles were defined using the co-ordinates of the centre of the circle,  $x_c$  and  $y_c$  and radius,  $r$ . The initial location of each particle was defined by allocating a random integer number for the  $x$  co-ordinate of the centre of the circle,  $x_c$ , between 1000 and 11000 units, so that the edge of the grid did not effect the way the particles settled. The centre of the circle,  $y_c$ , was calculated so that the circumference of the circle just made contact with the lower boundary. The radius obviously depends on whether the circle represents a clay or silt particle. As each particle was placed, it was defined as part of the boundary to ensure that they could not be

overlapped by subsequent particles. This placing and then boundary defining process was repeated for as many particles as was desired and in this way each particle becomes part of the random arrangement to form a blanket covering of discrete particles.

The shape of each particle was defined by recording the y co-ordinate for each integer value of x along the width of the particle. For example, if the radius of the particle was set to 10 units, then the shape would be defined as in Figure 5-4. There are 40 points defining the shape of the particle. Nineteen points define the lower part of the shape, nineteen define the top half of the shape and two define the left and right hand sides. This was considered sufficient points to describe the shape of the circle and to avoid too much overlap between each particle.

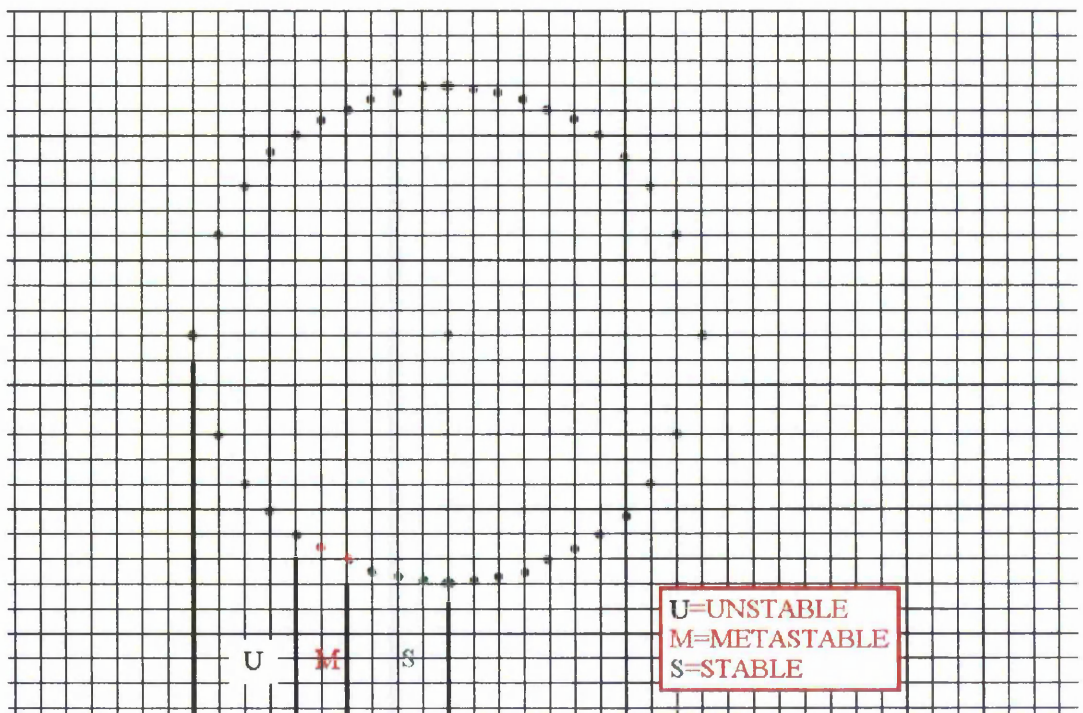


Figure 5-4 Defining the particle shape.

### 5.3.4 Proportion of silt and clay particles

The computer program produces a 2-dimensional structure of random particles, within the set domain. However, a relationship was required between the 2-D slice and the 3-D arrangement that it represents. It was therefore necessary to initially consider the deposit in

three dimensions to determine the relationship that a two-dimensional model would have to a three-dimensional deposit.

The ratio of silt diameter to clay diameter and clay content are specified at the beginning of each run of the program. The silt particles could be simulated as 3-20 times larger than the clay particles. From this information the program calculates the proportion of silt particles to clay particles that would be found in a three dimensional deposit, based on the volume of a sphere. The specific gravity of quartz and kaolinite differ by only 0.1 and therefore the difference can be neglected.

In a 3D model, the percentage of silt would be:

$$P_s = V_s / (N_c V_c + V_s) = R_s^3 / (N_c R_c^3 + R_s^3) \quad 5.1$$

And similarly,

$$P_c = N_c V_c / (N_c V_c + V_s) = N_c R_c^3 / (N_c R_c^3 + R_s^3) \quad 5.2$$

where,  $N_c$  is the number of clay particles for every one silt particle.  $R_s$  is the radius of the silt,  $R_c$  is the radius of the clay.  $P_s$  is the percentage of silt and  $P_c$  is the percentage of clay.  $V_c$  and  $V_s$  are the volume a clay and a silt particle respectively.

which by rearrangement gives the proportion of clay particles to silt particles,

$$N_c = \left[ \left( \frac{R_s}{R_c} \right)^3 / \frac{P_s}{P_c} \right] \quad 5.3$$

However, the 2D image, which is produced by the computer model, only represents a slice of a 3D arrangement. Since the clay particles are smaller than the silt particles, there will be fewer clay particles in the 2D 'slice' than in an equivalent 3D arrangement. It is therefore necessary to reduce  $N_c$  by a relevant factor in order to produce a more realistic proportion of clay/silt particles in the 2D 'slice'. This proportion was estimated by considering a single silt particle in 2- and 3-dimensions. The amount of clay particles that can pack around a

sphere will be greater than the amount of particles that would fit around a circle. Consider the smallest square that could be drawn around a circle, see Figure 5-5. The area outside the circle would be left for clay particles to settle. Similarly, for a 3-dimensional particle, a box could be imagined around the particle and the volume not occupied by the sphere would be available for the clay particles.

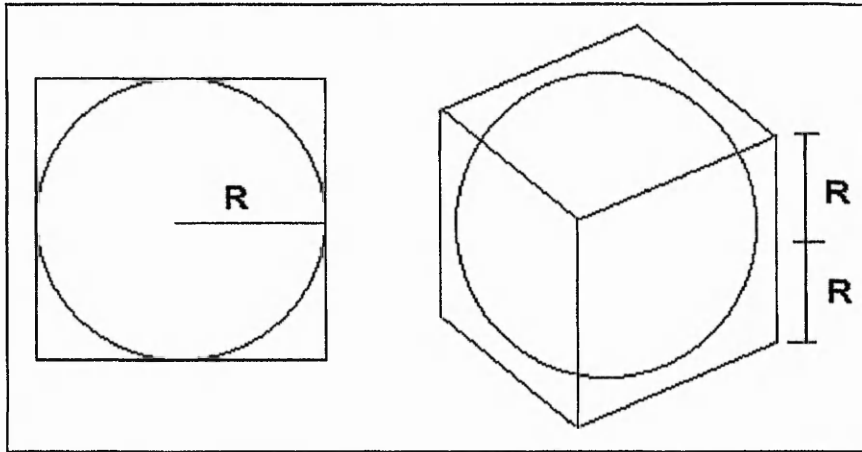


**Figure 5-5. Two and three dimensional representations of the space around a silt particle.**

The area left in the 2-dimensional case is  $4R_s^2 - \pi R_s^2$ . For the 3-dimensional case the volume left is  $8R_s^3 - 4/3\pi R_s^3$ . Assuming that all of this space was available for the particles then,

$$N_{c2}/N_{c3} = (A_{12}V_c)/(V_{13}A_c) = (4R_s^2 - \pi R_s^2)(4/3\pi R_c^3)/(8R_s^3 - 4/3\pi R_s^3)(\pi R_c^2) \quad 5.4$$

And if  $R = R_s/R_c$ ,

$$N_{c2}/N_{c3} = 4/3(4R^2 - \pi R^2)/(8R^3 - 4/3\pi R^3) = f \quad 5.5$$

- Where,
- $N_{c3}$  = number of clay particles in 3-dimensions
  - $N_{c2}$  = number of clay particles in an equivalent 2D slice
  - $A_{12}$  = Area left in 2-dimensions
  - $V_{13}$  = Volume left in 3-dimensions
  - $A_c$  = Area of a clay particle
  - $V_c$  = Volume of a clay particle

Therefore, to reduce the calculated value of  $N_{c3}$  it was necessary to multiply by the factor  $f$  to give  $N_{c2}$ . This means that the proportion of clay /silt particles viewed in the 2D slice is roughly equivalent to the percentage chosen at the start of the program for a three dimensional arrangement. Obviously, this does not take account of the area or volume that would occur between the clay particles, but since the clay particles are significantly smaller than the silt particles this was neglected for this model.

In the simulation, each time 10 silt particles were placed,  $10 \times N_{c2}$  clay particles were placed, until the boundaries of the model were reached. The total number of particles needed to fill the test grid depended on the proportion of clay particles as they took up less room in the grid.

Particle packing is considered in terms of the void ratio. Void ratios of the packing arrangements formed in the model are determined for the rectangle defined between 1500 and 10,500 on the horizontal axis and between 6500 and 3500 on the vertical axis. This reduces edge effects. The void ratios are also based on areas of the particle and not volumes as only 2-dimensional particles have been placed. The void ratio values are therefore not representative of the equivalent 3-D arrangement but can be used as a tool to compare the 2-dimensional structures produced by the model.

### 5.3.5 Unstable, Metastable and Stable Structures

Three stages in loess development can be identified (Dibben 1998). When the particles are first deposited the structure will be unstable. Very soon the particle arrangements will settle under their own weight to a second state, known as metastable. During this stage the deposit is stable providing the external conditions remain unchanged. Finally, with the addition of water and load, the particles will become more densely packed and become stable. These three stages are simulated by three different stages in the computer program.

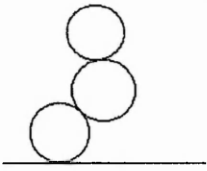
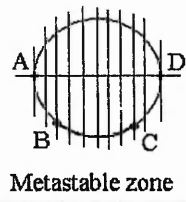
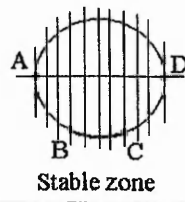
For the unstable simulation, the particles are allowed to rest as soon as any part of the shape contacts with the current boundary. If contact between the shape and the boundary is made anywhere on the circle, the particle will not move any further. In this way a very unstable structure is built as in Figure 5-6(a).

The unstable structure will not exist for long. The self-weight of the soil alone will begin to make the particles shift to a slightly more stable state. This state is known as metastable and the particles will remain in this position, undisturbed, unless the external conditions change. Therefore, to form a metastable structure in the program, the particles do not necessarily come to rest when they first contact with the boundary. Instead, if the particle is in an unstable position, they will move until they find a more stable position. A particle is considered to be unstable if contact occurs further from the centre than point M, in Figure 5-4. Point M is  $3/5$  of the radius away from the centre of the particle. Line BC in Figure 5-6(b) shows the metastable zone for a particle of 10 units diameter. Three fifths was arbitrarily chosen as a sensible division point between the particles being unstable and metastable. The further away from the centre that the particle is supported, the less stable it will be in this position. At around three-fifths away from the centre point the particle should just be stable enough to keep its position, especially if some bonding were present. Three fifths does not hold a mathematical significance it was chosen to produce a slightly more dense structure. Allowing the particles to come to rest  $3/5$ 's of the radius away from the centre of the particle allows a more dense structure to form than the unstable structure above. An open structure is still produced which allows for more movement if the structure was subjected to heavy loads or wetting.

If the point of contact occurs outside the metastable zone, say at point B on the new particle in Figure 5-6(b), the particle would naturally tumble to the right. In the program this movement was simulated by moving one integer space to the right and then moving down until the particle contacted with the boundary again. When contact is made, the program checks for stability and the whole process is repeated until the contact is made within the metastable or stable zones.

Wetting and/or loading causes greater movement of the particles to an even more dense state. The stable arrangement is formed in exactly the same way as for the metastable particles. Instead of the metastable zone, a smaller stable zone is defined as in Figure 5-6(c). B and C are  $2/5$  of the radius away from the centre of the circle in this case. If contact is made with the boundary at an unstable position on the particle, it will move left or right one integer position as before and move down to make contact with the boundary again. The process is repeated until the particle makes contact with the boundary at a stable point on

the particle. This forms a more dense structure, similar to the structure that would be created through loading and wetting of a natural sample.

Type	Unstable Deposit (a)	Metastable Deposit (b)	Stable Deposit (c)
Formation			
Rules	Stop when particle contacts boundary	<p>If contact occurs between A and B fall right.</p> <p>If contact occurs between C and D fall left.</p> <p>Stop when particle contacts boundary in the metastable zone. (B-C)</p>	<p>If contact occurs between A and B fall right.</p> <p>If contact occurs between C and D fall left.</p> <p>Stop when particle contacts boundary in the stable zone. (B-C)</p>

**Figure 5-6 Rules used for the falling particles is the computer simulation**

### 5.3.6 Using the Program

The program has been written as a Windows application using Visual Basic. A screen shot of the program interface is shown in Figure 5-7. Step 1 in the program is to choose how much bigger the silt particles are than the clay particles. The range is from 2 to 20 times larger than the clay particles and the choice is made from the drop down menu. Step 2 is to choose the clay percentage for a (three-dimensional) deposit. The selected clay percentage is for a three-dimensional deposit, therefore this number is converted to the proportion of clay/silt particles that would occur in an average 2D slice of this 3D deposit. From the third drop down menu, a choice of development stage must be made, unstable, metastable or stable. Once all the choices have been made from the options in the drop down menus, the draw button is clicked and calculations commence. Once the deposit has been drawn, the void ratio of the 2D image is written to the screen and the screen may be printed for a future record of the structure.



**Figure 5-7** Screen shot of program interface

The program has allowed examination of the effect of varying the clay percentages on particle arrangement and voids ratio. Each combination of inputs was repeated 30 times in order that the results could be statistically analysed.

## 5.4 RESULTS

The program was initially run for the case where the silt particles are 6 times larger than the clay packets. A typical unstable arrangement is shown in Figure 5-8 for a clay content of 30%. The void ratio was worked out for each arrangement inside the red box so that the calculated values were not affected by the packing at the boundaries of the simulation. Voids are very large and it is easy to see that the particles would rearrange due to their own weight. Figure 5-9 shows a slightly more dense packing produced by choosing to build a metastable arrangement. Voids are smaller, and are often long and thin, a shape often observed in a natural loess deposit. Pores are still large and calculated void ratios are around 0.9. A typical stable arrangement is shown in Figure 5-10, where the clay content was 30%. Typical void ratios were 0.58, i.e. typical of corresponding states found in natural loess soils. Generally, void spaces are again long and thin. An even more stable

arrangement was produced by choosing the stable point S to be  $1/5$  from the centre, instead of  $2/5$ . This produces void ratios of around 0.4, shown in Figure 5-11.

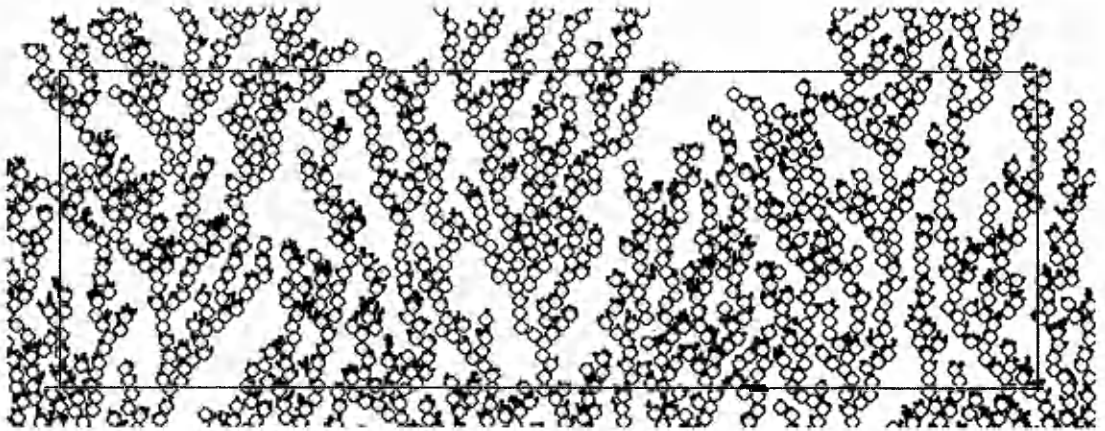


**Figure 5-8 Typical arrangement found from the Air Fall method in the computer program, for a silt diameter six times larger than clay diameter with thirty percent clay.**

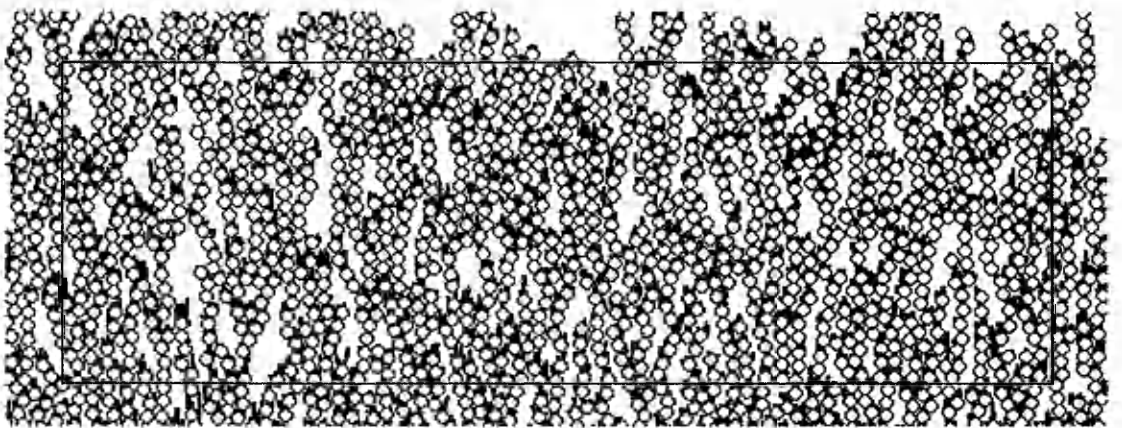


**Figure 5-9 Metastable arrangement, void ratio = 0.95, for a silt diameter six times larger than clay diameter with thirty percent clay.**

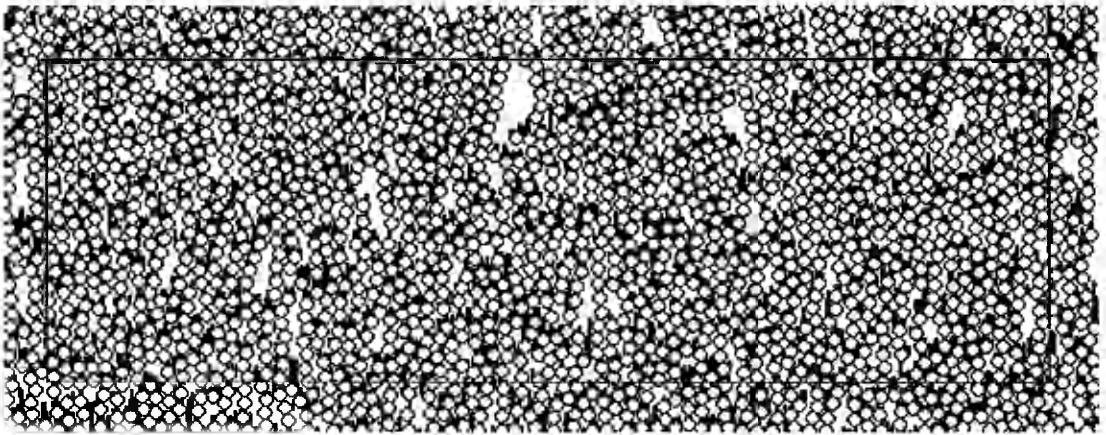


**Figure 5-10** Stable arrangement (2/5), void ratio = 0.56, for a silt diameter six times larger than clay diameter with thirty percent clay.

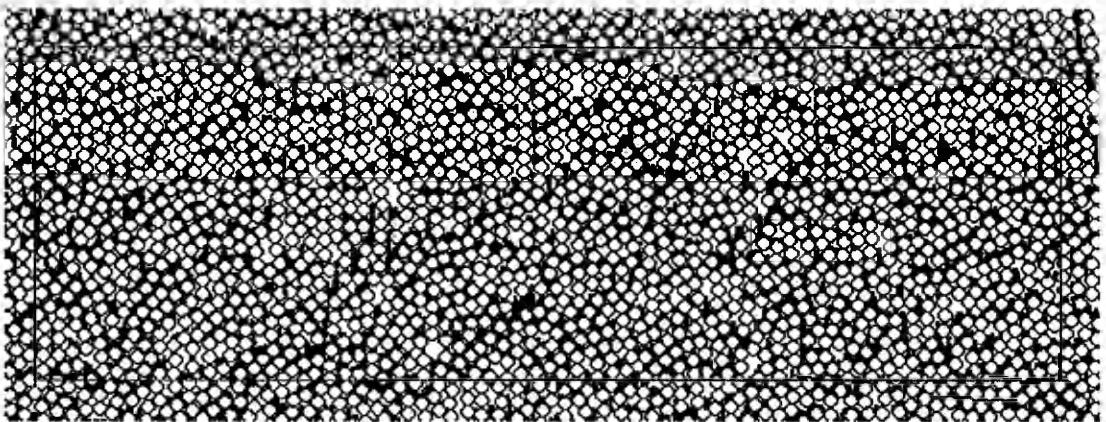


**Figure 5-11** Stable arrangement (1/5), void ratio = 0.367, for a silt diameter six times larger than clay diameter with thirty percent clay.

Figure 5-12 shows results for three different ratios where the silt particles are three, six and ten times larger (most realistic) than the smaller clay particles. The model was run 30 times for each for each combination to obtain an average void ratio. Figure 5-12 shows the average void ratio obtained for each clay percentage. The variation of these results are shown in Figure 5-13, for silt particles ten times larger than the clay packets. All three of the curves show a tendency for the particles to pack more densely at a clay percentage of 20-25%. This 'peak' packing density was observed in the natural samples. Comparing Figures 5.3 (for artificial loess tested in the laboratory) and 5.12 (for the computer

simulation) it is easy to observe a similar optimum packing. The simulation that modelled the silt particles ten times larger than the clay particles is the closest to the proportions observed in natural loess, and also shows a more obvious peak in particle packing. This peak occurs in approximately the same position for both models (laboratory and computer), this is interesting as the computer simulation is only 2-dimensional. However, the fact that a peak is observed, backs up the findings from the oedometer tests, that density of a sample will depend on the percentage of fines in the sample and a peak density can be found at a certain clay content percentage.

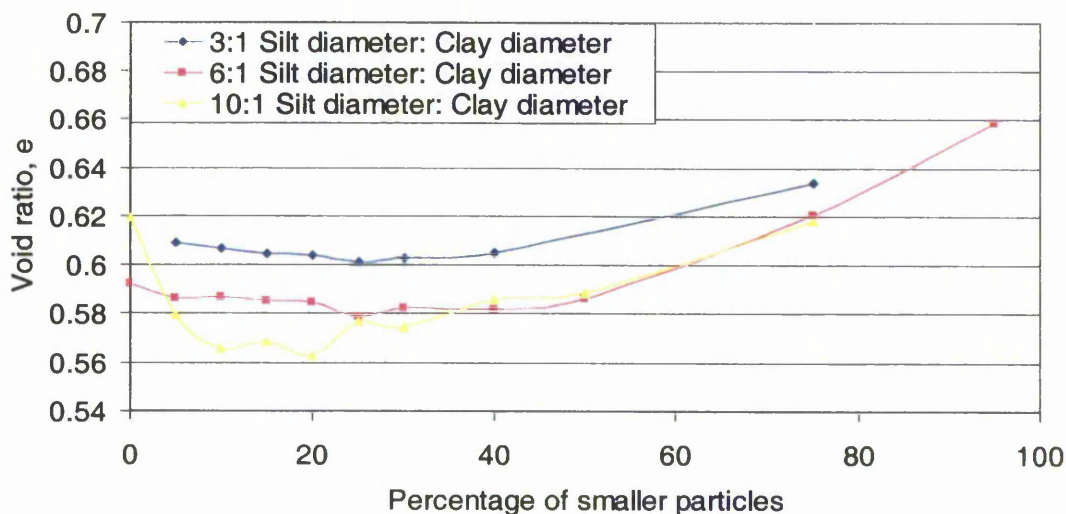


**Figure 5-12 Variation of void ratio for Stokes situation with the percentage of smaller particles (fines)**

The position of the peak density for the computer simulation depended on the relative size of silt/clay diameters. As the ratio of silt/clay diameter ratio reduces the peak occurs at higher clay contents. In natural loess there is a gradual grading of particles, not 2 distinct sizes, however an average particle size for the silt fraction would be around 0.02mm and the clay fraction an average of 0.0015mm. Therefore, an estimate of the ratio of silt/clay size would be around 13. In the computer simulation the peak density was produced at a clay content of 20% for silt particles 10 times larger than the clay particles. For artificial loess in the laboratory the peak was found between 25 and 30% clay content. Figure 5-13 shows the maximum, average and minimum values of void ratio found where the silt particles were 10 times larger than the clay particles.

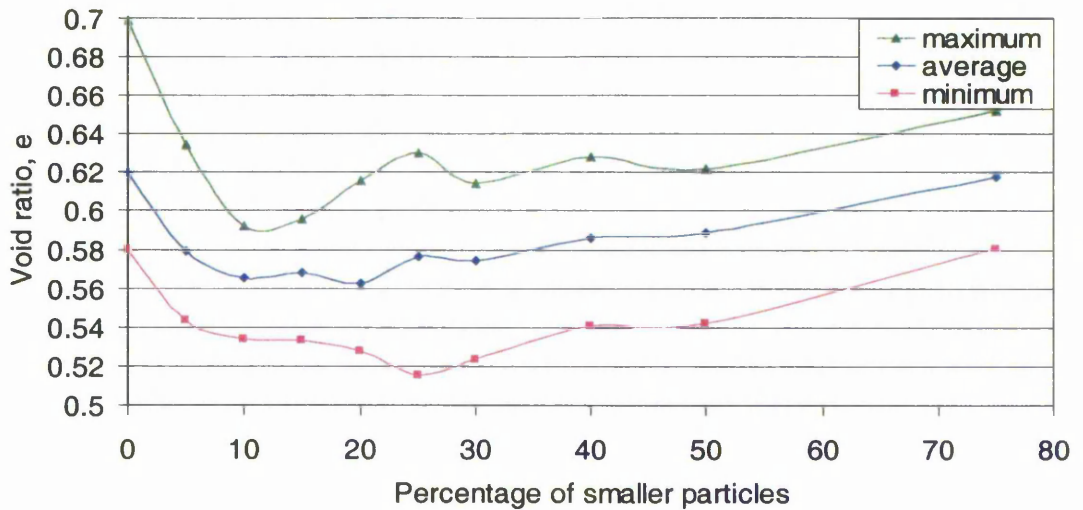


**Figure 5-13** Variation of void ratio with 10 percent small particles, with maximum and minimum values also shown.

An average void ratio for each combination was found so it was also possible to find out the variation of these results. The program was run 30 times for each combination so that the standard deviation could be found. Standard deviation is not statistically relevant below this number of inputs. The standard deviation of void ratio was calculated for each combination of larger/small particles. Figure 5-14 shows the standard deviation from the mean of the results for each of the simulations.

The standard deviation of the void ratio increases as the ratio of silt to clay size increases. This indicates that there are more possibilities of arrangements for larger ratios of silt size to clay size. The standard deviation peaks at 25% for silt particles that are 10 times larger than the clay particles and troughs at 10%. However, for silt particles that are 6 times larger than the clay particles, the peak standard deviation occurs at 10% clay content and troughs at 50%. The peaks show where there was a wide range of possible arrangements for that clay content percentage. The quantity and size of the peaks indicate the influence of the clay (fines) particles. The stability (i.e. fewer peaks) of the lines seems to increase as the silt/clay diameter ratio decreases. As the clay particles get relatively smaller to the silt particles, the chaos of the system is increased and the number of possible arrangements is increased.

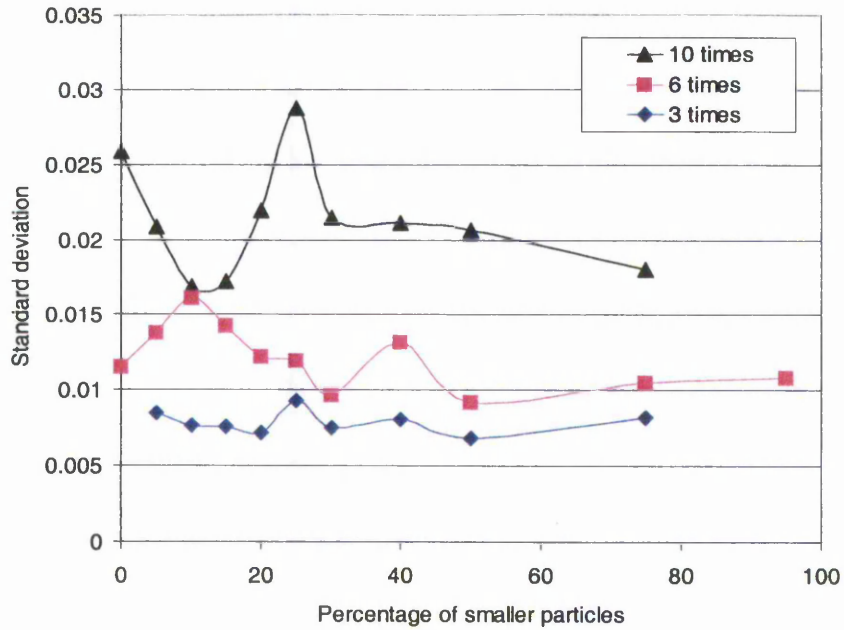


**Figure 5-14** Variation of standard deviation of void ratio with small particle percentage (fines) for three different silt /clay diameter ratios for Stokes situation.

## 5.5 DISCUSSION

The models presented in this chapter are clearly a simplification of a complex interaction of particles. However, despite the simplifications used to create the models, they have enabled many valuable ideas to be discussed. The main simplification was that the models were presented in two-dimensions. This has been partly accounted for by calculating the clay percentages for a three-dimensional deposit and applying this to an average slice of the deposit to give an approximate clay percentage for the two-dimensional slice. Due to the two-dimensional nature of the models, the void ratios are not realistic for each clay percentage. However, the calculated void ratios have provided a useful tool with which to compare the different arrangements.

Another over simplification is that the particles are considered as perfect circles or spheres. The blade shape of the loess particles have been shown to effect the void ratios of each sample. However, the hydrocollapse observed in samples made from spheres and samples made from more realistic shaped crushed silica were similar, see Chapter 4. The overall

effect of using spheres would therefore only have an influence on the void ratios of the computed arrangements.

To examine the effect of the clay and silt particles and the proportions of each, it was decided to have one size for the clay particles and one size for the silt particles. Of course, this is a major simplification as there would be a range of sizes of both the clay and silt particles, as indicated by the smooth particle size graphs in chapter 4, Figures 4.1 and 4.2. To develop the models further, a range of sizes could be used to give a better indication of the arrangements.

The results indicate the same optimum packing as was observed in the laboratory samples. Samples made with smaller 'clay' particles compared to the larger 'silt' particles have a higher standard deviation from the mean than samples with relatively larger clay particles. For example the standard deviation for silt particles that are ten times larger than the clay particles is roughly double that for samples with silt particles three times larger than the clay particles. The standard deviations are approximately 0.02 and 0.01 respectively for these cases. This represents a void ratio of between 0.5 and 0.6. It appears that the packing for the relatively smaller clay particles are more 'chaotic' or less predictable than for particles that are of more similar sizes.

An optimum packing was observed for clay contents of between 20-30%. The position of this peak depended on the ratio of the silt to clay diameters. As the silt particles were made larger in comparison to the clay particles, the percentage clay required to produce the optimum packing was reduced. For clay contents of 0-25%, the clay can fit in between the silt particles and void ratio is slowly reduced. As clay content is increased further, the clay particles will force the silt particles apart as there are too many clay particles to fit in the gaps between the silt particles. The void ratio therefore increases as the clay content increases past 30% clay (smaller particles).

These computer studies give a supporting argument that particle packing has a large part to play in the reasons behind the behaviour of the laboratory samples. As explained from the graph in Figure 5-12, the particles would naturally pack according to the 'natural void ratio' line. This shows a natural tendency to pack more closely if the clay content is around 20-

35%. The peak observed from the method 1 results can be explained from these findings. The specimens all started with the same void ratio (only in method 1) and therefore, for the high and low clay percents, the potential to collapse was less. The samples with clay contents of 20-35% would naturally pack more densely if they were formed at their natural initial void ratio. Since the mass of the sample is restricted these samples have the potential to show the most collapse, as their natural void ratios are lower. For samples with higher clay contents, the material had to be forced into the container to produce the samples in the laboratory. Therefore in these cases, the magnitude of collapse was not as great as if the samples were formed naturally. Most of the collapse potential was reduced during the formation process. When the samples are made using the same compressive effort (as in methods 2a and 2b in Chapter 4) the natural packing is formed during the making of the sample. Since the samples were prepared by allowing their natural void ratio to develop for a certain compressive effort, the peak hydrocollapse is not observed.

## **6 Footing Model Tests - Methods and Results**

---

### **6.1 INTRODUCTION**

Chapters 3 and 4 discussed the methods and results of tests carried out on both artificial and natural loess soils. The tests revealed some similarities in behaviour between the two materials. However, unlike the natural collapsible deposits, the properties of the artificial soil can be controlled. Void ratio, water content, clay content and their variation within the deposit can be regulated and investigated. It was shown that all these factors have a part to play in potential magnitude of collapse of the deposit.

The laboratory tests allowed the identification of important geotechnical properties, such as the Plastic Index and compressibility characteristics, as well as showing that the natural and artificial soils have much in common, see Chapter 4.

Problems from collapsible soils normally arise due to an increase in the water content. This typically may occur due to increasing ground water levels or infiltration from ponded water or from a leaking pipe. It was decided to investigate this phenomenon further, building from earlier work discussed in Chapter 4. To do this a model of a strip footing was built in the laboratory. The strip footing was supported by collapsible loess soil and the behaviour

was monitored. The footing model was designed to emulate a strip footing with a load of 86kPa, to represent an average sized industrial building. A strip footing was chosen so that it could be modelled using a two-dimensional finite element method such as that discussed in Chapter 7. Initially tests were carried out on rising ground water level, as this was the simplest to model, control and monitor. Surface deformations of the soil and footing were monitored, and compared with predictions from the finite element model.

## 6.2 SCALE MODELLING

Scale models permit transformation of problems to manageable proportions that may be too large for direct experimentation. They can shorten the time taken for experimentation and promote (and require) deeper understanding of the phenomenon under investigation.

When devising a model test, it is important to be able to relate the behaviour of the model to the behaviour at full scale. Roscoe (1968), started by considering the equations of equilibrium for the forces acting on a soil element and proceeded to derive relations between a prototype at full scale and a model at  $1/N$  scale and to obtain the critical dimensionless groups. The conclusion reached from this approach was that the model should be made from the prototype soil and tested at the prototype stress level. Although model tests are often carried out under smaller stresses than those occurring in the prototype, the effects of the applied stress on the mechanical properties are not correctly reproduced in the model. This can lead to erroneous conclusions regarding the prototype behaviour.

In a model with dimensions scaled down from the prototype it could be argued, in contradiction to Roscoe (1968), that to retain similarity the soil particles should be similarly reduced. Roscoe (1970) showed that the width of the shear band along the failure surface is a function of grain size. Thus if the prototype and the model are made of the same material the failure zone will be relatively thicker in the model and the localised strain in the failure zone will be under-estimated in the model. He concluded that a more appropriate criterion for choosing model dimensions and test materials is to ensure that the ratio of the grain size to the length of the failure plane is similar to that of the prototype. In most full-scale constructions this ratio is small. However, it was felt for this project the material should be

kept the same as full scale, as it is the behaviour of this particular soil and the inter-particle bonding that is of key importance.

Conflicts between various requirements for complete similarity are common in any modelling technique. If the particle size of the soil is scaled down in the model some properties can be reproduced satisfactorily but others cannot. In soil the size, shape, surface condition and arrangement of the grains are very difficult parameters to control simultaneously.

For the model strip footing the important things to model are:

1. Newton's second law,  $F=ma$  (inertia and gravity)
2. Friction between the particles
3. Cohesion between the soil particles
4. Weight of the soil
5. Elasticity of the soil

Friction, cohesion and elasticity all depend on strain, strain rate, geometry of the foundation/soil interface, and degree of compaction during loading. If there are large strains, elasticity can be neglected and 1-4 are important, as explained by Schuring (1977).

There are, of course, limits on the similarity between the scale model and a prototype built at full scale. A stress of 86kPa was used to represent a substantial factory/industrial building. The model was built by scaling down the dimensions but not scaling down the grain sizes. This allowed investigation of the inter-particle bonding and means that the full stress was needed to cause collapse in the material. The disadvantage of using this approach is that the zone of failure may be relatively thicker in the model than in the prototype and the localised strain may have been underestimated. However, the mechanisms of collapse were still evident and a comparison with the finite element model could be made.

### 6.3 DIMENSIONS

The strip footing was supported by the artificial loess, which was contained in a large tank. The dimensions of the tank had to be large enough to avoid significant boundary effects. The faces of the soil container had to be as far as possible from the zone of interest, with the

walls smooth and the floor rough in an attempt to create similarity (Bolton, 1979). Desai and Abel (1972) report that the depth of the tank must be 10-12 times larger than the width of the foundation. The width of the tank also had to be 8-12 times the width of the foundation to avoid boundary effects. The length of the tank had to be long enough so that the footing could be regarded as a strip footing, for this it had to be greater than 4 times the width of the footing.

Another consideration was that the footing had to be wide enough so that there were enough grains below the footing. As the grains are small the width of the footing could be relatively small. A check was made to prove that the footing is rigid. For this the footing was assumed to act as a uniformly distributed load and the footing was assumed to be fixed where the hydraulic jack was placed, in the centre of the footing. Deflections would therefore be at the ends of the footing, as discussed in Section 6.4.2. Table 6.1 shows the range of deflections expected for different sized strip footings, where,

$b$  = the width of the footing,  $d$  = the depth of the footing,  $I$  = the second moment of area =  $bd^3/12$ ,  $w$  = load per unit width = Load(kPa)\*width(m) and  $df$  = the expected deflection of the footing =  $-wL^4/8EI$ .  $L$  was taken as one half the length of the footing = 175mm,  $E$  was assumed as 200Gpa for mild steel. The load was assumed to be 80kPa.

b(mm)	d(mm)	I(mm <sup>4</sup> )	w(kN/m)	df(mm)
31	10	2.58E+03	0.800	-0.182
31	20	2.07E+04	1.600	-0.045
31	30	6.98E+04	2.400	-0.020
31	40	1.65E+05	3.200	-0.011
40	10	3.33E+03	0.800	-0.141
40	20	2.67E+04	1.600	-0.035
40	30	9.00E+04	2.400	-0.016
40	40	2.13E+05	3.200	-0.009
50	10	4.17E+03	0.800	-0.113
50	20	3.33E+04	1.600	-0.028
50	30	1.13E+05	2.400	-0.013
50	40	2.67E+05	3.200	-0.007

**Table 6-1 The expected deflection of various footing widths and depths**

Where  $b$  is the width of the footing,  $d$  is the depth  $I$  is the second moment of area,  $w$  is the Load per unit area on the footing and  $df$  is the deflection of the footing in mm.

For a 31mm wide footing, 30mm deep, the expected deflection of the footing would be 0.02mm. This deflection was considered negligible as the deflections were measurable to 0.01mm and the expected deflections of the soil were relatively much greater. The strip footing was made as shown in Figure 6-1. The footing dimensions were 31mm by 350mm by 30mm. The deflections were calculated for the half length of the footing, as shown. The internal dimensions of the tank were chosen as 360mmx360mmx360mm, and the tank designed as Figure 6-2. The tank width, was over 11 times the footing width,  $B$ , which was enough for side effects to be regarded as negligible.

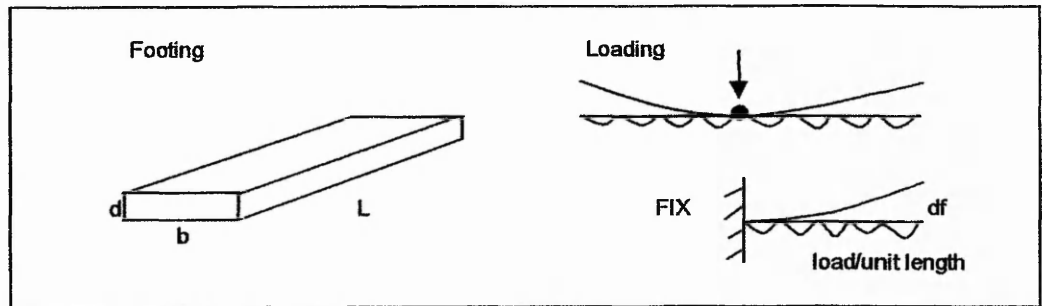


**Figure 6-1 Mode of deflection for the footing. The soil acts as a uniformly distributed load.**

## 6.4 TEST PROCEDURE

### 6.4.1 Setting up the test

The tank walls were made from perspex, as close to frictionless as possible. This reduced the boundary effects to negligible proportions. The loading system was via a loading frame and hydraulic jack. A load cell was calibrated and set up to a data logger and computer to enable accurate determination of the load imposed by the hydraulic jack. The advantage of the hydraulic jack is that it can be set up to exert constant load on the footing. Once set up, the jack adjusts its height in order to exert the required force, even if large settlements occur. Measurement of the vertical displacements of the soil and footing was carried out using dial gauges and transducers as shown in Figure 6-3. Dial gauges were also set up to monitor the deformation of the tank sides.

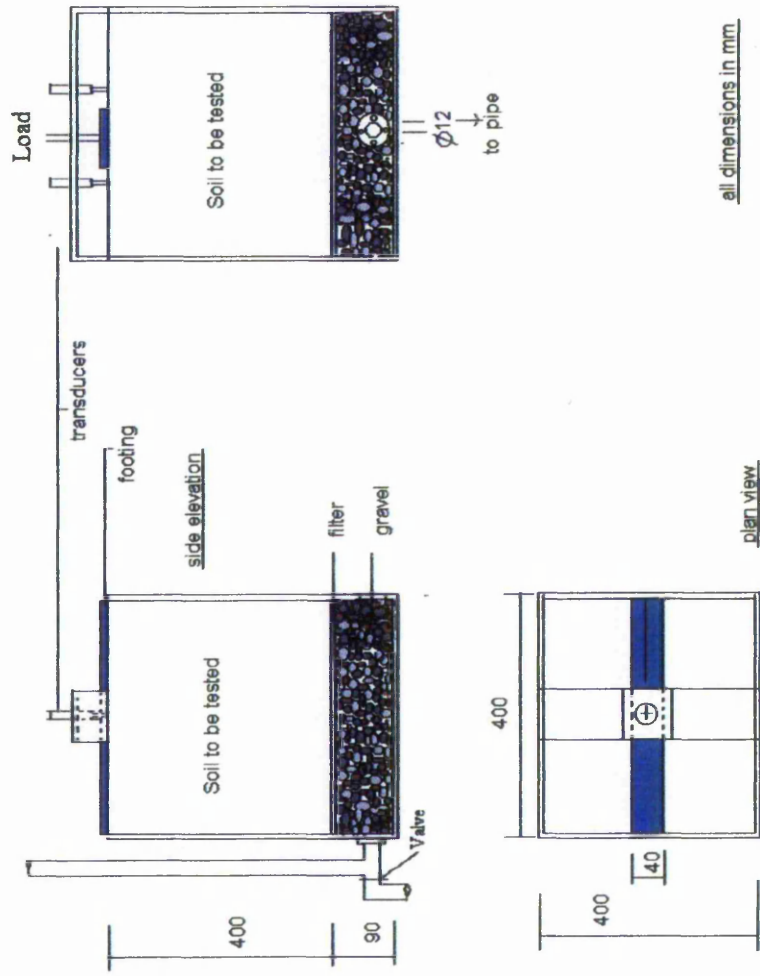


**Figure 6-2 Footing test tank dimensions. The gravel layer was used to spread the water over the base of the model and the filter layer was used to stop the silty material mixing with the gravel layer but allowed water through.**

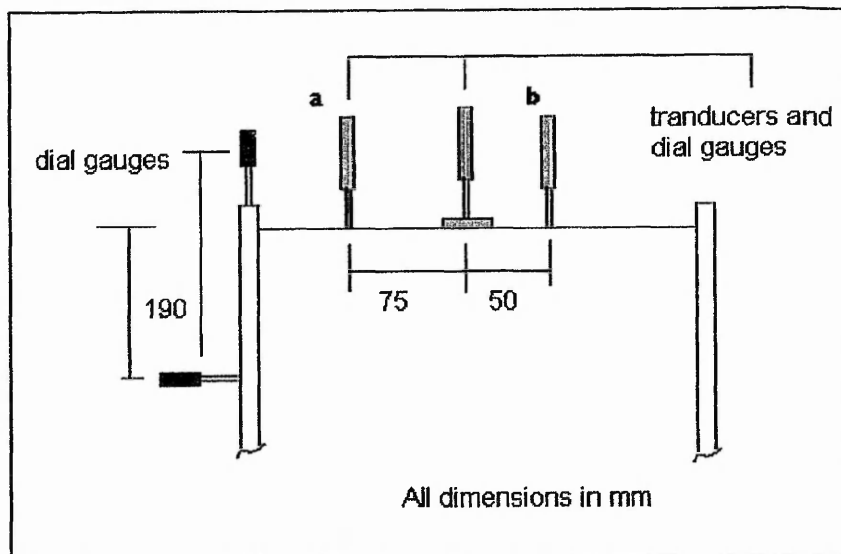


**Figure 6-3 Location of load gauges and transducers on the footing and the soil surface.**

The equipment for the footing test is shown in Figure 6-4. The tank was mounted on a loading frame, which was designed to take a maximum load of 20 tonnes and was therefore more than adequate for loading the footing. The centre of the platen on the loading frame and the centres of the tank sides were marked to ensure that the tank was placed in the centre of the frame. Marking the centre of the sides also ensured that the footing would rest in the centre of the tank and the load would be applied in the centre of the footing. The tank was made of clear perspex so that the deposit could be viewed during testing.

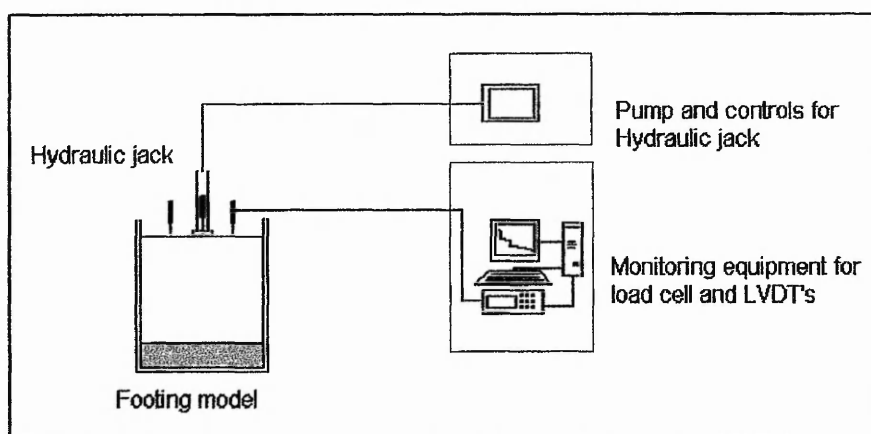


**Figure 6-4 . Equipment for the model footing tests.**

A gravel base was used to disperse the water and allow an even rise in the water level throughout the deposit. Inundation was produced using a water supply from a pipe through a 20mm diameter hole at the base of the tank, see Figure 6-5. This allowed the water to seep through the gravel bed and up into the layers of soil above. Before testing began the gravel was weighed in order to find the void ratio. The gravel layer was placed into the base of the perspex tank. A specific gravity of 2.64 was estimated for the gravel and a void ratio 0.68 was found. The gravel was placed in the perspex tank to form a layer 90mm deep. Distilled water was added to the layer until the water covered the entire layer. The volume of water needed to cover the gravel layer was measured. It was found that 4.8 litres of water were needed to fill the 90mm layer. This agreed with the figure calculated from the void ratio, which means that the gravel was fully saturated when the water was added through the pipe and there were no pockets of air left that were hard to fill. This was important as it enabled calculation of the quantity of water that was added to the soil.

Once the gravel layer was placed and compacted a filter layer made from black geotextile was placed over the top. This layer created a barrier between the artificial soil and the gravel so that the artificial soil could not mix with the gravel layer. It also helped to evenly distribute the water as it rose above the gravel layer.

#### 6.4.2 Fill Placement

It was found that the triaxial samples gained most of their strength in the first 2 days of drying. The soil in the footing model was built up in shallow layers leaving each layer for at least 2 days to allow the soil to dry and the clay bonds to develop. This ensured that the artificial soil had a high enough unsaturated strength to support the footing. The silt and clay were mixed together in the proportions 70:30. The artificial material had shown similar collapse and strength characteristics to the natural loess in the index, oedometer and triaxial tests when mixed in these proportions. Ten kilograms of the dry material was mixed together thoroughly. Water was added to create a mixture with 17.5% water content. This water content had been used for the oedometer and triaxial specimens, which had shown similar hydrocollapse characteristics. This bulk of the oedometer and triaxial tests were carried out using this water content so a direct comparison could be drawn. The distilled water and dry materials were mixed thoroughly until the moisture had become evenly distributed throughout the material. The artificial soil was then placed in small amounts into the tank on top of the geotextile layer. The material was compacted into place

with the wooden tamper as was used for the triaxial samples. A 5kg weight was used to compact the sample, this was used 3 times in each position to ensure the same effort of compaction was used throughout the deposit. Each ten kilogram layer of material was compacted to 50mm deep, giving a calculated void ratio of around 0.9.

The 50mm layer of wet artificial soil was left to dry for 2 days and another layer was added in the same way. Layers were added over a two week period until the artificial deposit was 350mm deep. The top layer needed to be as flat as possible. The flat surface was produced by using the flat based 5kg weight to compact the soil. It was also important to ensure that the top surface was horizontal. This was checked using a spirit level.

The strip footing was placed in the centre of the deposit and the dial gauges and transducers were arranged as shown in Figure 6-3. Transducers were placed on top of the dial gauges so that the data could be logged. The data logger was set to take readings every 15 minutes. A load cell was fitted on top of the strip footing. The loading frame, dial gauges and layers within the footing model are shown in Plate 6-1.

The load cell was calibrated using a loading machine that was calibrated to British Standards Grade A standard. The volts that were read from the data logger were converted to kN using this calibration. This was done by slowly increasing the load on the loading machine in increments and recording the output voltage at each load. The output voltage vs. load (in kN) were plotted on a graph which is shown in Figure 6-5. The calibration showed that for the data logger and cell used,

$$\text{Load (kN)} = (\text{Load (Volts)} - 14.94) / 42.485 \quad 6.1.$$

#### 6.4.3 Running the test

Once the load cell was placed on the footing, the hydraulic jack was lowered into position. The time was recorded, the clock started and the data logger was started to take readings from the transducers. Readings were taken on the dial gauges at the same time to obtain readings for zero load. The load was slowly increased in increments of 10kN every 4 hours, or until the observed deformations did not change. Readings were taken on the dial gauges each hour so that the readings from the transducers could be checked for accuracy.

On the second day the target load of 86kPa was reached and this load was left for 24 hours to allow all the settlement to take place under this load.

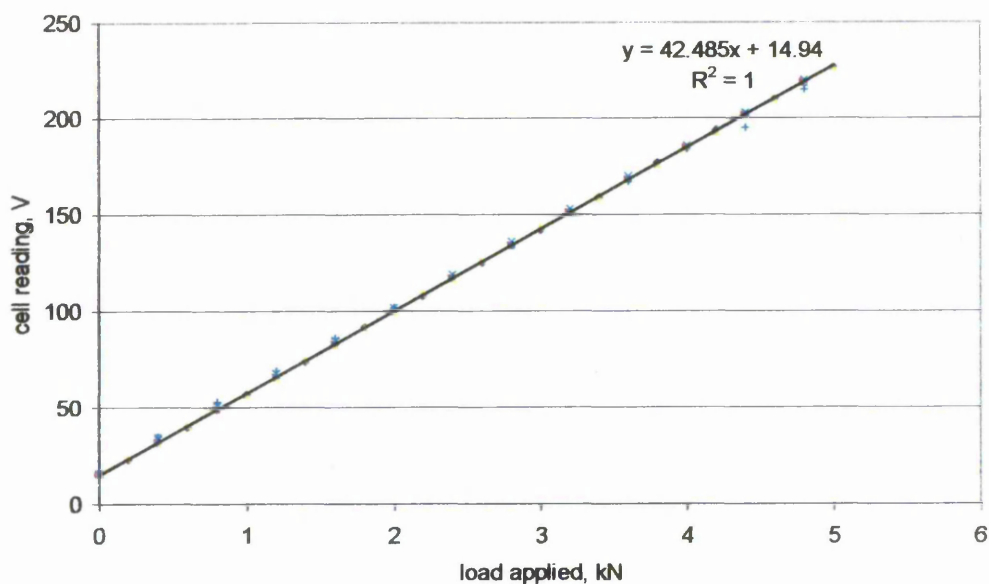


**Figure 6-5 Calibration of the load cell, based on 3 calibration runs.**

Three series of tests were conducted using the footing model to simulate different wetting scenarios: (i) loading the footing and then an increase in ground water level; (ii) increase of ground water level and then loading the footing; (iii) loading the footing and then ponding of water on the surface. An increase in the ground water level was simulated by adding water down the tube, which rose through the gravel and up through the deposit. The water was added in known amounts, so that an estimate of the water content of the deposit could be made. Recordings of the deflections were made over the next 48 hours, or until the monitored deflections were negligible. This procedure was repeated in stages until failure of the deposit was observed. Failure could occur due to punching shear or cracking of the deposit. The settlement of the footing was measured and observed until the limit of the dial gauges was reached. Throughout this process the deflections were recorded by the data loggers from the transducer readings. After failure occurred, soil samples were taken from each 50mm layer throughout the deposit in order to calculate a moisture content gradient for the wetted deposit. In the second case water was added to the deposit and then the footing was loaded. This was to test the assumption that: a soil that is loaded and then

saturated will obtain the same state as a soil that is saturated and then loaded. In the final test, water was added at the top of the deposit. The same procedure was observed for recording displacements and taking the moisture contents of each layer at the end of the test. A summary of the tests carried out is presented in Table 6-1.

Test	No. of tests carried out
Preliminary study. Artificial loess was added to the test box in layers and left to dry for 2 days as it would be in the real test. Water contents were measured throughout the layers of the deposit to determine the initial water contents for the rest of the tests. As this was a destructive test it could not be carried out on the soil in the actual tests.	1
Case 1: The footing was stressed and then the deposit saturated from the bottom up – to simulate rising ground water level	3
Case 2: The deposit was saturated and then the footing stressed to determine the differences in behaviour to Case 1.	1
Case 3: The footing was stressed and then the deposit was saturated from the top and the bottom.	1

**Table 6-2 Summary of tests carried out using the model footing.**

#### 6.4.4 Feasibility tests

Before the main tests were carried out, the material was placed in layers in the tank in exactly the same way as for the other tests. The trial test was carried out in order to refine the methods of mixing and placing the soil and to find any possible problems before carrying out the final tests. It also allowed identification of the initial water content of the soil in the tank. After the material was placed in the perspex tank, it was left for 2 days and then the water content of each layer was tested. The water content was taken at seven levels through the deposit. Approximately 40g of sample was taken from each layer in 5 different positions. Each sample was weighed, dried in the oven and weighed again to obtain the moisture content. This allowed the initial water content profile of the following tests to be approximated, see Figure 6-6. No problems occurred during the trial run and no shrinkage of the deposit was observed, the main tests were then undertaken.

## 6.5 RESULTS

Deflections of the tank were recorded as well as settlements of the soil surface to ensure that the measurement of soil deflection was not affected by the movement of the tank, as shown in Figure 6-3. The largest deflections of the tank were recorded when the water was first added. The water increased the lateral stresses on the walls of the tank. Deflections of the tank did not exceed 0.2mm and were considered negligible compared to the deflection of the soil.

### 6.5.1 Water content profile

The water content profile for the full depth of the deposit is shown in Figure 6-6. This will be referred to as the 'dry' (unsaturated) condition, as it is the condition of the soil before wetting occurred. The material reached an average of 15.1% water content, although the water content was very slightly higher in the middle and less at the top and bottom. This is because evaporation of the water could only occur at the top and bottom of the material.

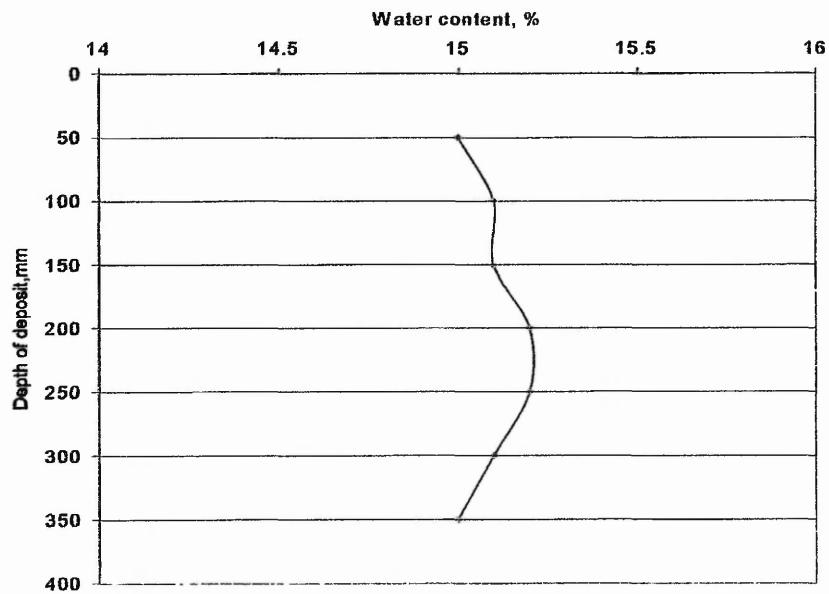


**Figure 6-6 Water content profile for the unsaturated condition**

### 6.5.2 Mechanism for wetting the soil

Water was added to the tank via the tube. The water was added very slowly in order that no air gaps were left between the gravel particles. At each wetting stage the water was added to just above the top of the gravel layer. It was observed that the water was slowly drawn into the soil deposit, above the level of water in the tube. The water level in the tube decreased slowly until it was just lower than the top of the horizontal pipe. This occurred after approximately 30 minutes, see Figure 6-7. This showed that there was a strong suction in the soil that was causing the water to rise up through the deposit. After another 15 minutes, air bubbles began to appear at the top of the gravel layer. This air was introduced through the pipe due to the low water level in the tube. After many hours the water level in the gravel layer and the water level in the tube reach an equilibrium and it can be assumed that no more water could reach the deposit, as an air gap of 30mm existed in the top third of the gravel layer. The air gap was not evident above the geotextile layer as the soil above was wetted. The air gap developed every time water was added, regardless of how much water was added or the speed at which it was added. The size of the air gap will be a function of the suction within the soil but also a function of the size of the gravel. The water content of the soil generally reached 25%, equivalent to a degree of saturation of 90%. This was consistent with the results found by Lawton (1986) who reported an average degree of saturation of 92% after soaking 36 single oedometer specimens. The maximum degree of saturation never reached 100% even though the samples had free access to water throughout their tests.

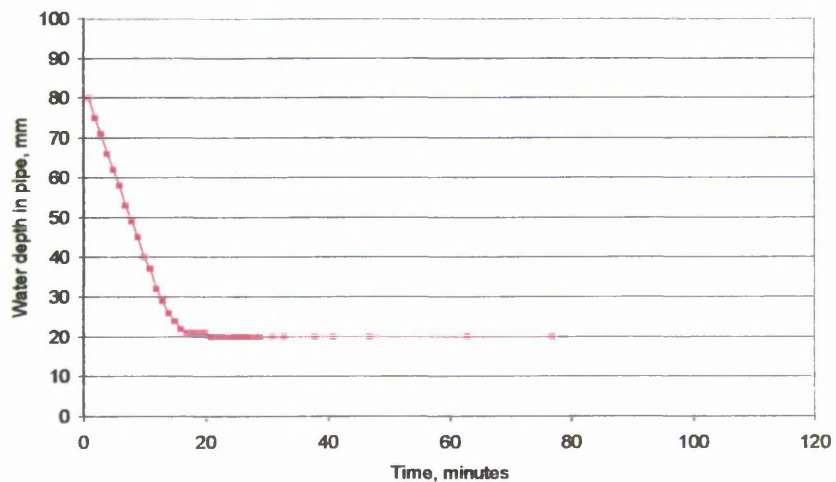
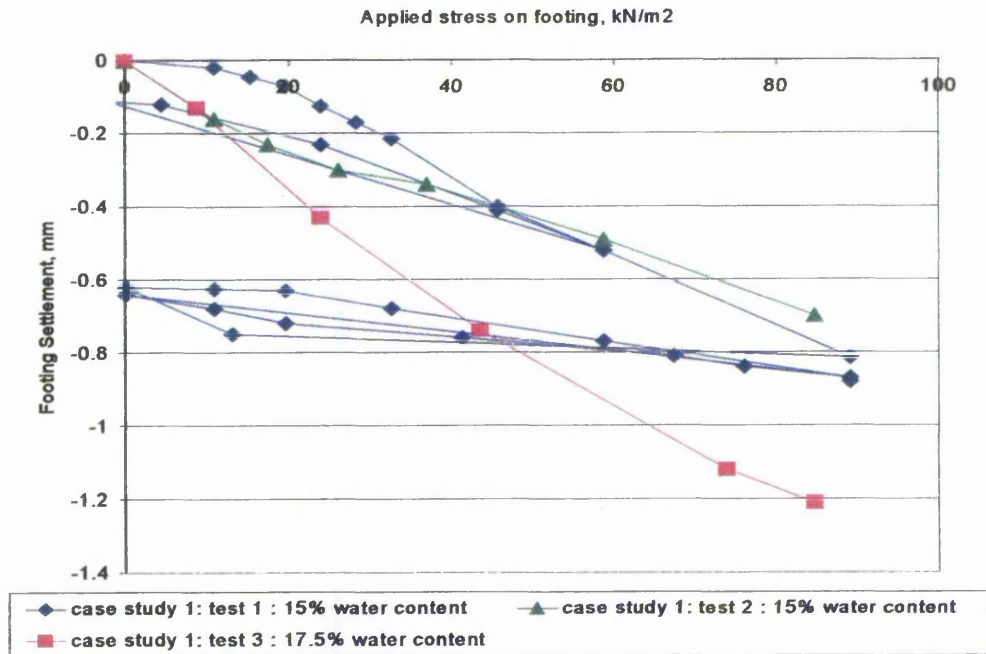


Figure 6-7 Observed water level in the inlet pipe

### 6.5.3 Case study 1: Increasing ground water level

In this study, the footing, supported by the unsaturated soil, was loaded and then wetted from below to simulate an increasing ground water level. Deflections of the footing and soil were recorded as well as deflections of the top and side of the tank, to ensure that the readings taken from the dial gauges and transducers reflected the true deflections of the footing and the soil.

Two similar tests were carried out on increasing the ground water level, which will be referred to as tests 1 and 2. The footing was loaded to approximately 86kPa while the soil was in its initial unsaturated state, with a moisture content of around 15%. A third test was carried out with a slightly higher initial water content of 17.5%. Results for the three tests are shown in Figure 6-8. The behaviour was fairly linear for the loads under consideration. The final loads of the first two tests were slightly different. In test 1 the final load was 89 kPa and in test 2 the final load was 85 kPa. This was due to the high sensitivity of the hydraulic jack. A small movement to increase the load on the hydraulic jack made a large difference to the load imparted to the footing. The recorded deflection of the footing in the second simulation was initially higher than that of the first simulation for low loads. This is probably due to the slightly uneven surface that the footing was placed upon. Once initial settlements had taken place, and the footing had become more firmly in contact with the soil, the observed deformations were more consistent with the first test. In the third test, the moisture content was slightly higher – initially 17.5%. This was done to investigate the effect of starting with a different moisture content. As expected, the soil is softer with a higher water content and greater deflections were recorded.



**Figure 6-8 Settlement of the footing on the unsaturated artificial soil for Case Study 1**

The results from the wetting stages of the first, second and third tests are shown in Figure 6-9, Figure 6-10 and Figure 6-11 respectively. Figure 6-9 shows the deflection of the footing in test 1 due to wetting. Water was added at W1, W2, W3 and W4. The water added at W1 and W2 (total = 7.550 litres) caused an additional vertical deflection of 1.52 mm of the footing (1mm-2.5mm by the end of 80 hours). The water at W3 (0.900 litres) was added but had no effect on the deflection as it did not close the air gap between the gravel and the geotextile. An extra 2 litres of water was added at W4 which was enough to cause failure of the footing.

Figure 6-9 shows the deflection of the footing during the wetting stages of Test 1, Case 1. At W1 (the first wetting stage) collapse is observed as there is a sudden reduction in the height of the footing. At W2 the movement is more gradual and could be considered as consolidation. At W3 no water entered the deposit as the amount of water added did not fill the air gap that had developed within the gravel layer. At W4, the deposit became too wet and failure was observed. The cracking and failure of the deposit is shown in Plate 6-2.

It was hoped that the water level would be clearly visible due to the darkening of the artificial soil when wet. However, this was not the case. An estimate of the height of the water level in the tank therefore had to be made based on the void ratio and the quantity of water added to the model. In proceeding tests (Tests 2 and 3) it was decided to use fluorescene in order to see the level of the water and to track its movement through the soil. The other unexpected result from the first full run of this test, was that an air gap was observed in the gravel layer about one hour after the water was added to the tank. The air gap was around 30mm deep and was fully formed after a few hours, see discussion in Section 6.5.2. The air gap was observed in all the tests and was the result of water being drawn up through the silt. It was therefore necessary to estimate the amount of water added to the deposit by subtracting the quantity of water in the gravel layer from the total amount of water added to the tank.

The graph in Figure 6-10 shows the deflection of two points on the soil and the footing with time for case 1, test 2. Point A was 75mm away from the footing and point B was 50mm from the footing on the other side on the surface of the soil. The deflection of the soil follows the deflection of the footing but is smaller in magnitude, as expected. Water was added at points W1 (4.000 litres), W2 (7.000 litres) and W3 (9.600 litres) marked on the graph.

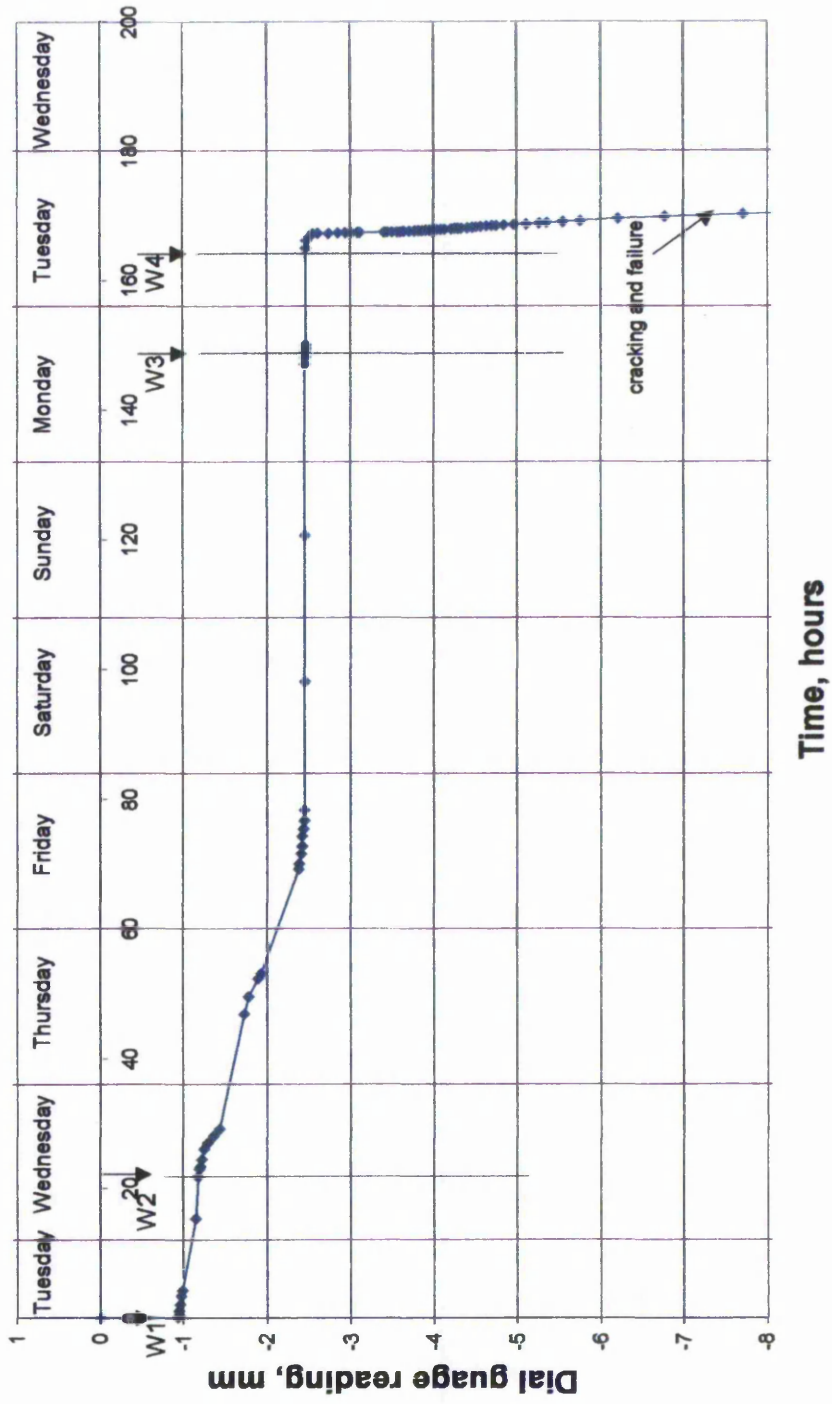


Figure 6-9 Deflection of the footing during wetting Case 1 test1.

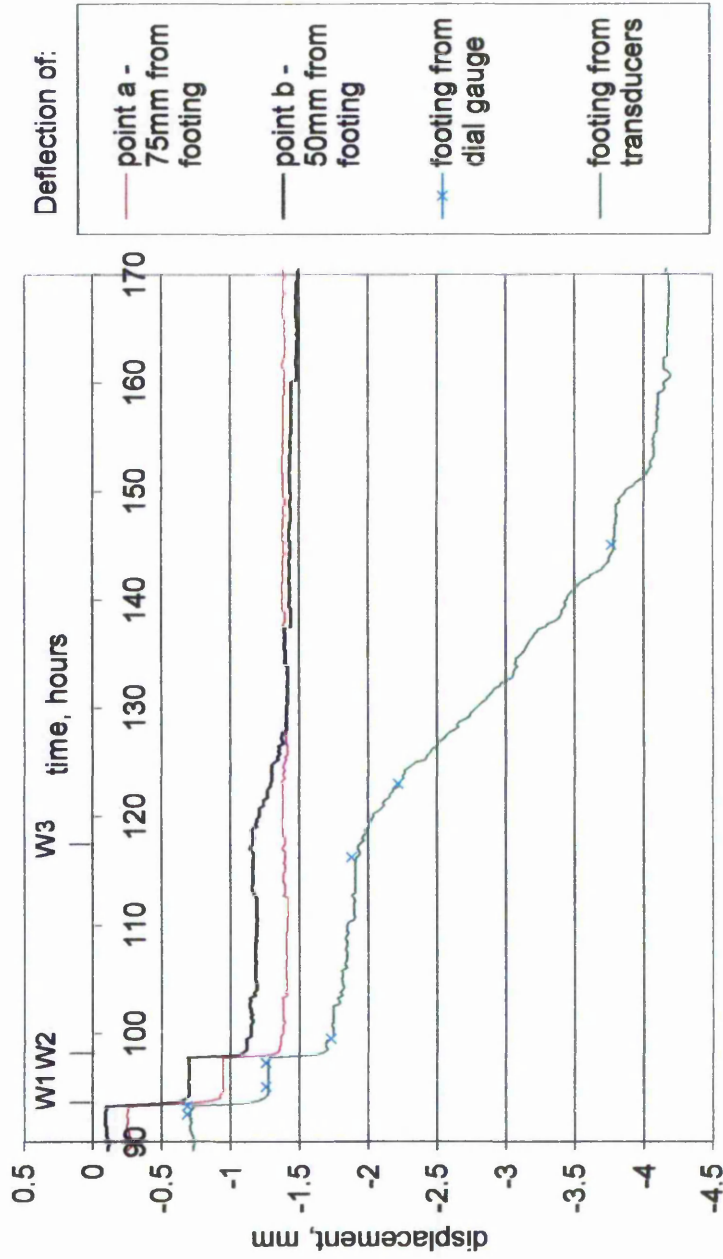


Figure 6-10 Deflection of footing and two points on the soil with time for Case 1, test 2. Water added at W1, W2, W3

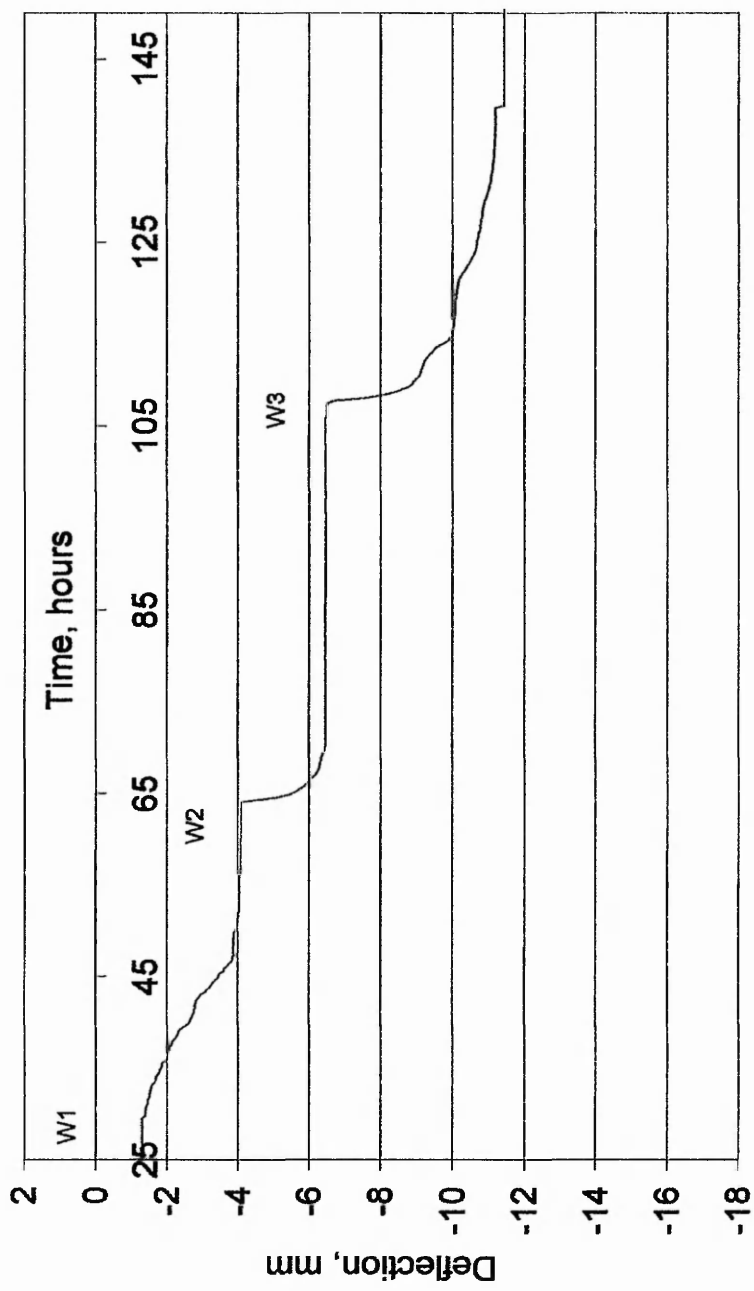
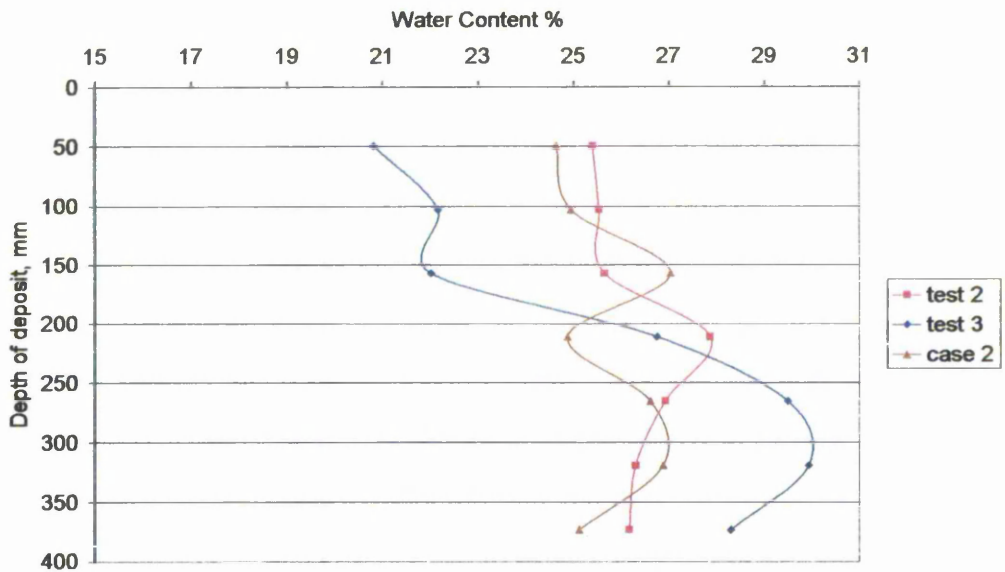


Figure 6-11 Vertical displacement of footing. Case 1, test 3

On the first two occasions that water was added to the soil in Case 1, Test 2, the collapse was fairly sudden with all the movement completed in one hour. When the third wetting event occurred, the movement took considerably longer, i.e. more typical of a consolidation effect. Settlement continued for many hours but had ceased by 50 hours. The settlement recorded at this time was 4.22mm. A small amount of extra water (12.2 litres - not shown on the graph) was added which caused the upper layers of soil to collapse and the footing underwent over 12mm of deflection. The total settlement of the footing was greater than could be measured by the reach of the dial gauges, so the data could not be plotted. It was evident that the footing had 'punched' through the soft upper layer of soil, a typical failure found in soft soil, see Plate 6-3. This small extra addition of water allowed the top 70mm of soil to become wetted and failure took place. The water content of the top layer was 25%, which is equal to a degree of saturation of around 0.77. This is not fully saturated, but is enough cause the soil to soften and will probably be enough to cause complete collapse. The triaxial and oedometer test results presented in Chapter 4 indicated that most of the collapse that could take place will occur in samples with 50% saturation. Further wetting did not increase the amount of collapse observed in the oedometer tests. It is therefore not surprising to see significant settlements with a saturation of 77% in this footing test.

The graph in Figure 6-11 shows vertical deflection against time for the wetting phase of test 3. Water was added in three stages W1, W2 and W3, 7.200 litres was added in stage 1, this total was increased to 8.300 litres in stage 2 and the total added was 10.200 litres by stage 3. Less water was added to obtain the same settlements as in tests 1 and 2 because the initial water content of test 3 was higher. The deflections at these stages were recorded as -4.06mm, -6.43mm and -11.41mm respectively. The changes in height of the footing are relatively sudden and therefore could be classified as collapse, especially at W2 and W3.

The water content profiles of tests 2 and 3 after the final wetting are shown in Figure 6-12. This represents a saturation of between 60-90% assuming a void ratio of 0.9. All of the deposit is above 60% saturation, above which, most collapse has already occurred, see Chapter 4.3.7 on the effect of water content. The water content through the deposit was on average 25%. The wettest part of the soil was found to be at mid-height. It was considered this was due to some water draining downwards, back into the gravel layer.



**Figure 6-12 Final water content profiles for Case 1: tests 2 and 3 and Case 2.**

The water level in the deposit has not been dictated by the water level in the tube but instead by the suction between the particles. This suction is powerful enough to draw water up to the top of the model using capillary action. The highest water content was found in the centre of the deposit at 200mm from the base for test 2. This layer had a water content of 28%, which was equal to a degree of saturation of 0.85. A similar peak was seen at the end of test 3, but this time the peak was lower down the deposit. The reason for this peak in the middle is perhaps due to fact that the water is free to drain at the bottom due to the air gap at the top of the gravel and has not been forced all the way to the top. The mechanisms of producing the wet deposit are not important. The main aim is to be able to model the behaviour of the soil given that it has reached a particular water content.

#### 6.5.4 Observation of the wetting front

Although fluorescene was used as an aid for the observation of the wetting path, the colour was removed from the water at 100mm from the base. The soil seems to filter the stain out of the water and it can no longer be seen from the outside of the tank. An estimate of the water level was made at each stage of wetting. This was calculated by considering the void ratio of the deposit, and the amount of water added. Figure 6-13 shows how the deflection was affected by the quantity of water added to the tank. The figure also shows results for Case 2, which will be discussed in the next section. The estimate of water depth is plotted

against deflection in Figure 6-14. As expected as the water gets closer to the top the increase in settlement becomes far greater.

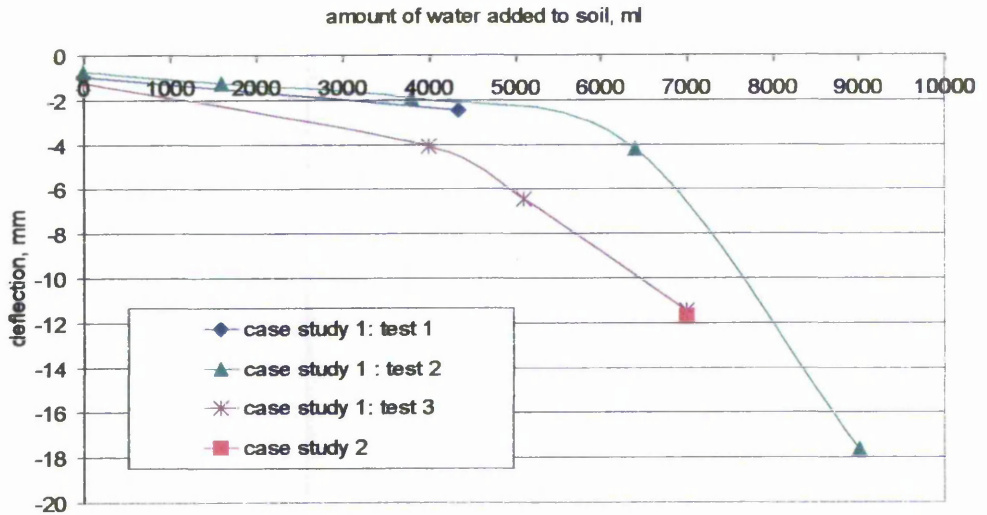


Figure 6-13 Deflection of footing with quantity of water for tests 1, 2 and 3.

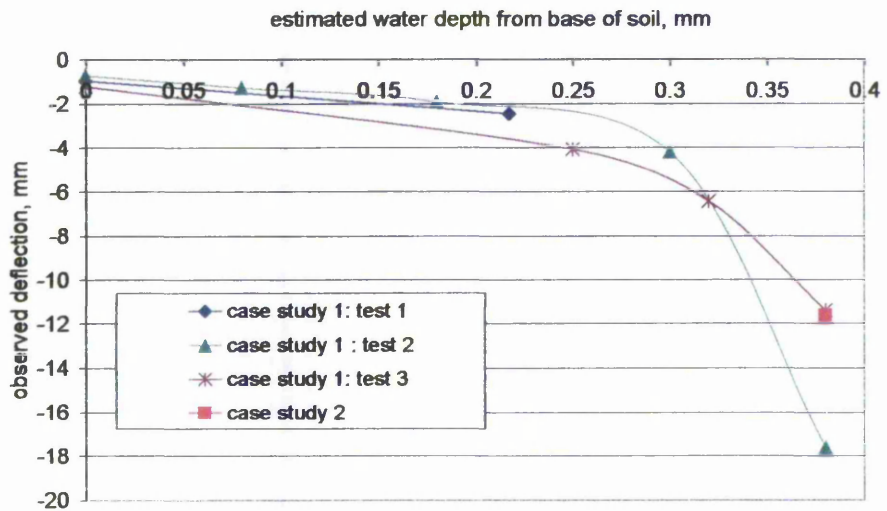


Figure 6-14 Deflection of footing with estimated water depth for tests 1, 2 and 3. Also compared with results for Case 2.

A footing will exert most pressure just below the footing and its influence will decrease as depth increases. Softening the top layers of the soil will obviously have a greater effect on the settlements than wetting the layers below. This was observed in the tests performed in the laboratory. The significance of this is that rising ground water level will only have a significant effect on foundations as it reaches closer to the surface and within the heavily loaded zone of soil. A far greater risk would be from leaking pipes and ponded water on the surface of the soil, which are more likely to affect the top layers of soil where load has the greatest effect on the soil. Greater deflections will occur if these top layers are wetted. There is an extra hazard from these sources, as not only will they affect the top layers where the load has most influence, but they will probably not affect all of the soil around the foundation. It is more likely that a small, localised area of wetting will occur from these sources, which will cause differential settlement of the soil beneath the foundation and consequently cause much more damage to the structure supported by the foundation. Rising ground water is more likely to be more even and therefore deflections may not be as devastating for the structure.

#### 6.5.5 Case study 2: Initially saturated and then loaded

In case study 1 the footing was loaded and then saturated. In case study 2, the soil was first saturated and then the footing was loaded. This was to check the validity of the main assumption: that saturated loaded behaviour results in the same final state as loaded then saturated behaviour. It was decided to add the same quantity of water as in Case Study 1, test 3 so that a direct comparison could be made. The total amount of water used was 10.2 litres. The initial moisture content was 17.5%. The full amount of water was added before any loading began. As the water was added, the deflections of the footing, the soil and the tank were recorded as for all the tests in case study 1. The height of the footing decreased slightly (0.05mm) and the height of the soil increased (heave) slightly (0.2mm). The soil was wetted in stages but no significant deformation of the footing was recorded for any of the wetting stages. The loading stage of the test was commenced after the deposit had been saturated. The water content of the deposit was approximately 26% after the water had been added from the base of the model. The loading on the footing was increased in increments of around 10kPa, as in Case1. The deformation with time behaviour is shown in Figure 6-15. It is possible to directly compare this figure with Figure 6-11, for case study 1, test 3. The deformations fit in well with what would be expected from the previous tests, both deflections recorded 11.5mm at the end of the tests.

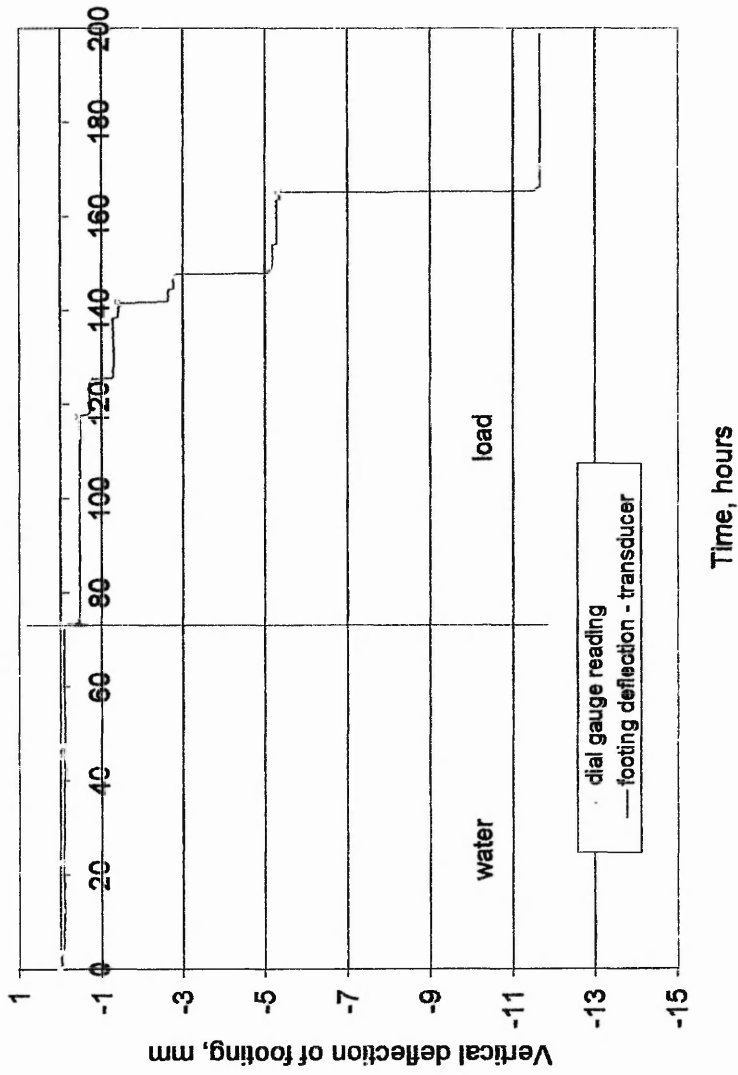
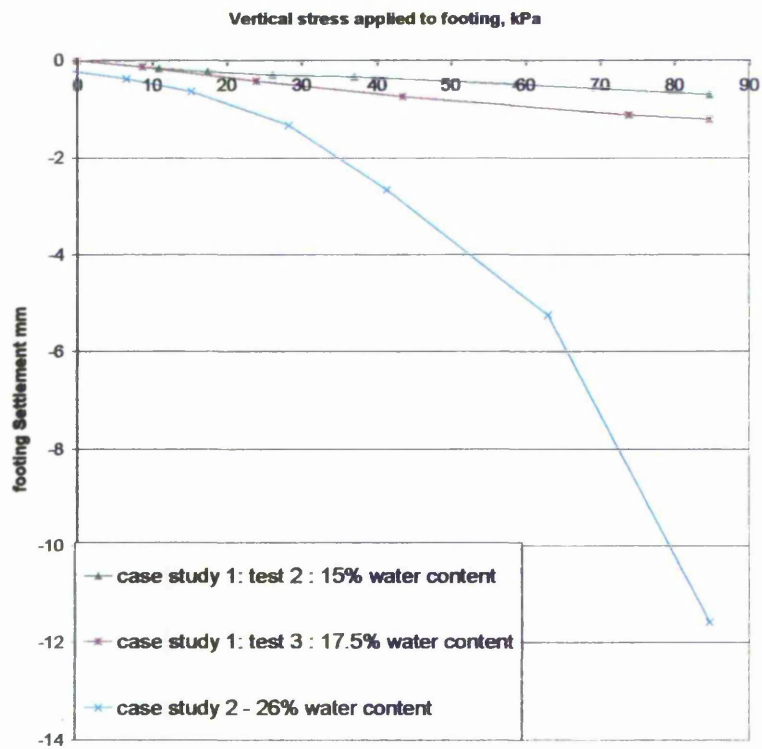
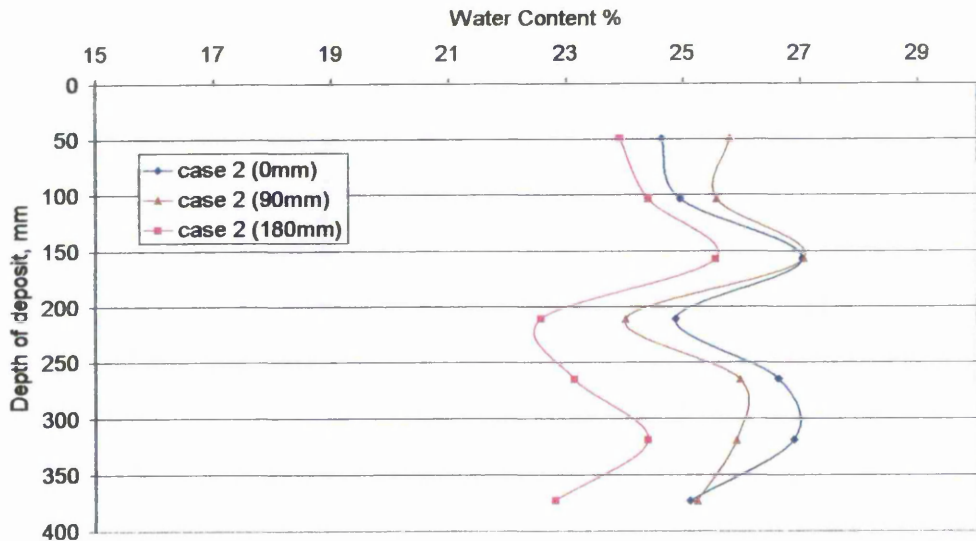


Figure 6-15 Deflection of footing with time for Case 2

Figure 6-16 shows the settlement vs. stress for the footing on the artificial soil at different water contents. The saturated behaviour is less linear than for the drier stages. The same total deflection was gained for case 2 as for case 1 test 3 (11.5mm), where the sample started with the same water content and the same amount of water was added. This confirmed the assumption that a similar stress-strain point is reached whether the soil is saturated and then loaded or loaded and then saturated. The water content profile is shown in. Water contents were taken from seven equal depths and at three positions from each depth. The water contents were taken directly below the footing (0mm), half way between the centre of the footing and the tank sides (90mm) and at the tank sides (180mm). The profiles show that the deposit is slightly drier towards the outside of the model.



**Figure 6-16 Settlement of the footing versus load for various water contents of the artificial material**



**Figure 6-17** Water content profiles for three distances away from the centre of the footing, shown in key.

#### 6.5.6 Case study 3: Ponding at the surface

While undertaking a test for case 1, it was decided to examine the affect of the preparation water content. The soil was placed with a slightly higher water content (19% instead of 17.5%) which caused the soil to contract during each drying stage. This caused a one millimetre gap all around the deposit between the tank sides and the artificial soil. The initial water content was 15% after the drying stage. Water was added in the same way via the tube. Some of the water wetted the lower layers of the soil, but some of the water was forced up through the gap between the tank sides and the artificial soil, which caused the water to pond on the surface of the artificial soil, mostly at W3. It was not possible to control the proportion of water at the top and the bottom of the deposit, so water contents were taken after the test throughout the deposit to assess where the water had infiltrated. Figure 6-18 Error! Reference source not found. shows the deflections of the footing with time. Water was added at W1, W2 and W3. During stage 1 5.400 litres were added, in stage 2 water was added to make the total 6.300 litres and finally a small amount was added to increase the total quantity of water to 6.600 litres. The final total deflection of the footing was -11.4 mm. The deflection of the footing was similar to the deflection observed in case 1. Much less water was needed to cause the same deflection. The settlement at W3 was

very sudden, caused by the water at the surface. The upper layers of the deposit are affected the most by changes in water content, where the majority of the load from the footing is acting.

As expected, far less water was needed to cause the same magnitudes of deflection when water is added at the surface. This is because it is mainly the top layers of soil that will affect the magnitude of deformation.

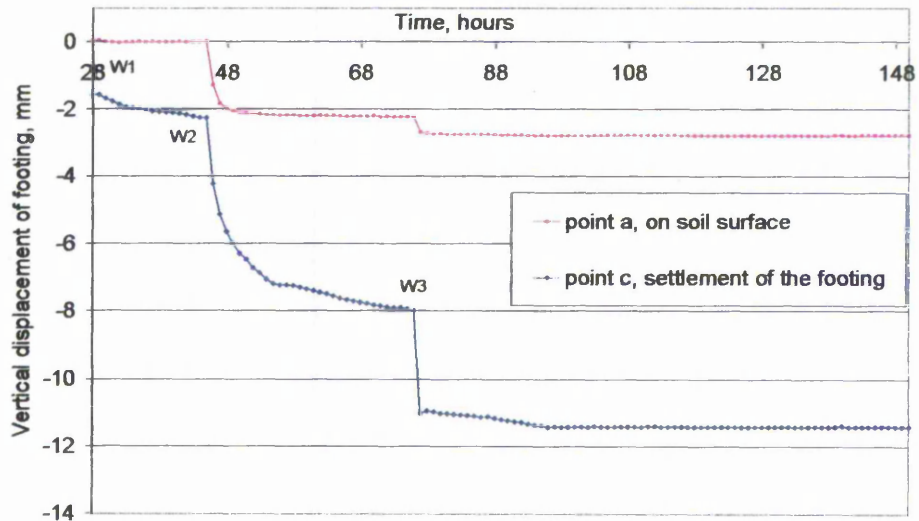


**Figure 6-18 Settlements observed for the footing and the soil surface for Case 3: Saturated at the top and bottom**

The water content profile for this test is shown in Figure 6-19. It can be seen that the top two layers and the bottom two layers have become close to saturated, but the middle three layers have water contents between 16 and 18.5%. The soil still has some strength within this range of water contents but because the upper layers were wetted, the majority of the vertical deformation that was observed in the previous tests was also observed in this case.

#### 6.5.7 Relating the physical footing model to full scale

The physical footing model has distinct differences to a full-scale prototype, but enabled validation of the computer model. The results will be different at full scale compared to lab scale due to the self-weight effects at depth and effects of grain size and footing size. The

void ratios will be less at lower depths and therefore stiffness will increase with depth. This can be simulated within the Finite Element model.

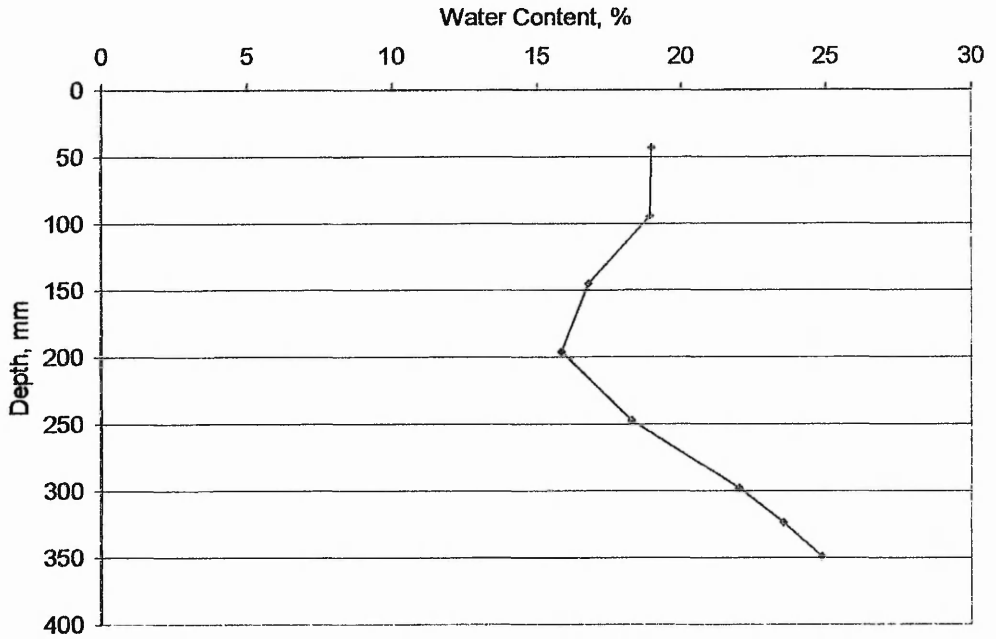


Figure 6-19 Water content profile at the end of Case 3.

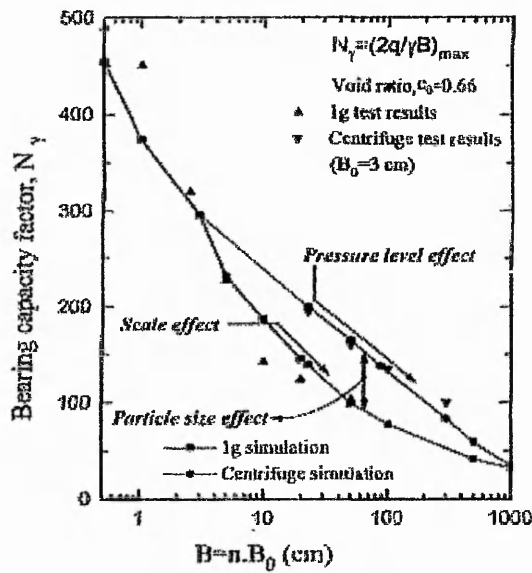


Figure 6-20 Summary of  $N_{\gamma}$  (bearing capacity factor) values from the 1g and centrifuge tests and corresponding FEM simulation, on sand Siddiquee et al (1999)

Other scale effects will also affect the behaviour of a full scale footing. Siddiquee et al (1999) discuss the scale effects present when modelling a strip footing on sand. They explain the scale effect consists of the pressure level effect and the particle size effect. Centrifuge tests and tests at 1g were undertaken on differently sized model footings. The results of the tests are shown in Figure 6-20. The footings ranged in width from 0.5cm to 50cm. The scale effects observed with the increase in the footing size at 1g show that bearing capacity would be over estimated by the scaled down model compared with a full scale model. Caution should be exercised in extrapolating laboratory test results, even for large specimens, to predict field behaviour, Anderson and Blanchfield (1997).

#### 6.5.8 Inaccuracies

It would have been useful to be able to measure internal deflections. A similar test done by BRE on collapsible fill used magnet extensometers to measure the internal deflections. The most accurate extensometer available only gave deflections to an accuracy of 2mm, Skinner (pers. Comm. 2000). This method was not sensitive enough for this model, where movements over 0.2mm were significant. An alternative to this was to use layers of coloured glass beads, which could be photographed to enable an estimate of the deflection at each loading and wetting stage. These also proved inadequate as during the wetting stages the beads were mobilised and readings of deflections were made impossible.

It was expected that, as the water was added to the pipe, the water in the deposit would rise level with the pipe and saturate the soil. This did not occur, as discussed in section 6.5.2. The presence of the air gap meant that the water in the soil rose up through the soil due to capillary action only. The result is that the soil is not fully saturated.

The relative movement of the wetting front is quicker than in a natural full-scale deposit due to the relative thickness of laboratory and field samples. This will result in faster deformations of the footing and possibly larger movements. However, because the natural soil has been used it is expected that the strain zone will be relatively thicker in the model and the localised strain in the failure zone will be under-estimated in the model.

The movements of the tank sides were different depending on whether the soil was loaded or wetted. Typical side movements of the tank for case 1 are shown in . As the load was added a small amount of movement was noticed. The mid-point of the tank side moved

outward (positive direction) and the top of the tank side moved vertically down (negative direction). As the water was added the tank sides deformed further outwards and the tank side decreased further in height. Once the water had all been added, there was no more movement of the tank side or top.

Tank movements for case 2 are shown in Figure 6-22. The movements were less for this case, although the movements are so low for both cases that they could be subject to large errors. The largest horizontal deflection recorded of the tank side was 0.18mm for case 1 and 0.05mm for case 2. The largest vertical deflection recorded of the tank side was 0.10mm for case 1 and 0.03mm for case 2. The larger deflections were observed for the test where loading occurred before wetting. These deflections mean that the reported deflections of the footing may be subject to errors up to 0.1mm. This is 1% of the total deflection recorded in Case 1 test 3 and Case 2 (around 11mm). These deflections are quite significant. If the test was done again it should be repeated in a larger box, so that the soil does not affect the boundaries of the test area.

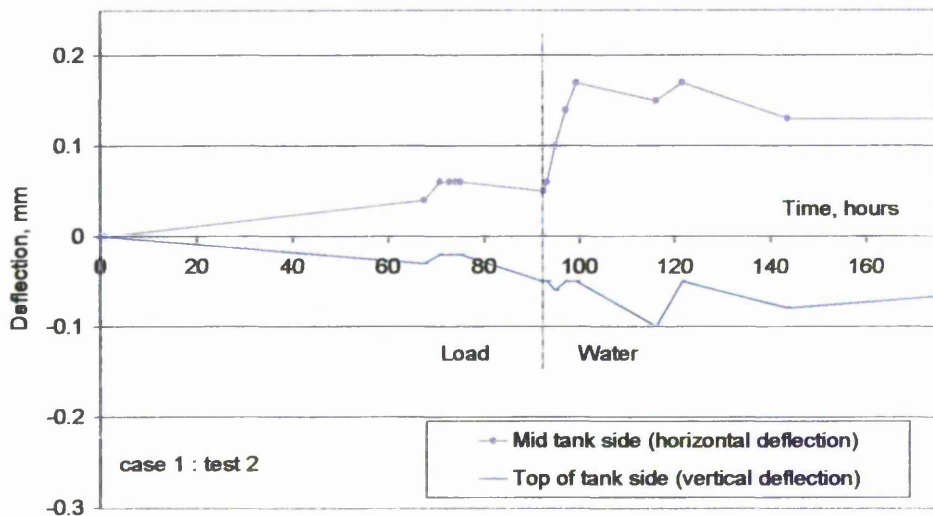
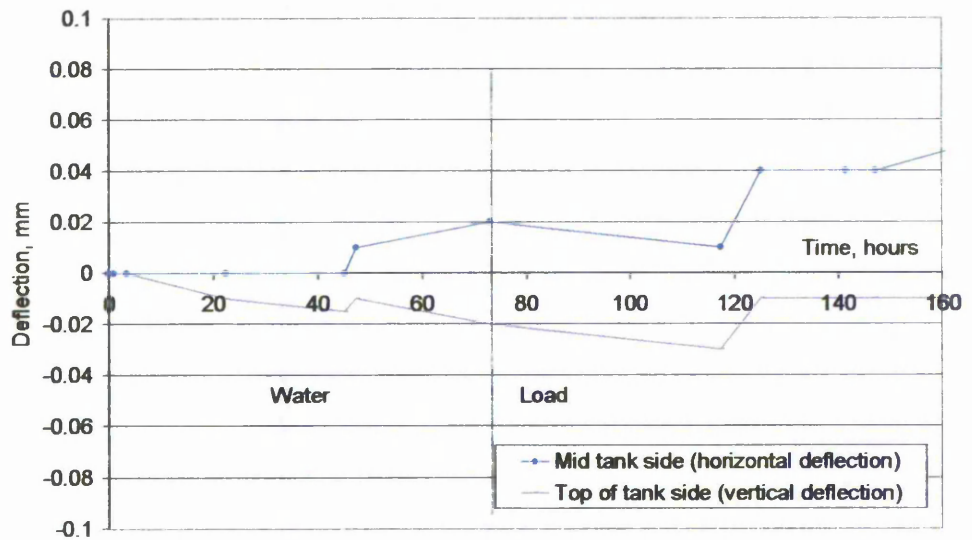


Figure 6-21 Tank movements for Case 1. Loaded then saturated.

## 6.6 DISCUSSION

The flow of water through the deposit and the large voids are key to the collapse process. The large voids in loess aid in the flow of water and enable collapse. Water will naturally fill the larger voids to find the easiest path through the deposit. When a large void is filled with water, the particles around the void are slowly surrounded with water and saturated. This allows movement of these particles and the void is slowly filled with falling particles that were surrounding the void. Globally, this will mean a decrease in volume and therefore vertical deflection under the vertical load.



**Figure 6-22 Tank movements for Case 2. Saturated then loaded.**

Ground water rising can cause collapse of the surrounding soil if the soil is initially unsaturated with a relatively open structure. If the properties of the soil are uniform below the soil, at least in horizontal layers, then differential settlement will not tend to occur, as observed in these experiments. The footing tended to settle uniformly, so it was still horizontal even after the soil had been saturated. Differential settlement could occur if the properties were not laterally uniform or if the rise in ground water was not uniform below the structure or if water had infiltrated from the surface on one side of the building.

The tests show that the deflection of the footing will be the same whether the soil is loaded and then saturated or saturated and then loaded. This confirmed the results of the oedometer tests that the soil same settlement will occur, independent of when the soil is loaded. There must, of course, be the same amount of wetting of the soil in both cases for the same deflection to occur. The moisture content was taken throughout the layers of the footing model after the test had been completed. This allowed a comparison of all the tests. For the tests that were saturated from the bottom the water content was, of course, higher at the bottom than at the top. The range of water contents after the test was 21-29%. The initial water content was around 15%. The change in water content of around 7% resulted in deformations of 11mm. These deformations would be very significant if they were observed on a full-scale footing.

An air gap was observed in all the tests due to the suction in the artificial soil. This means that above the ground water level there will be a layer of soil that will be partially saturated and prone to collapse if it becomes wetted. Any small changes in moisture content could cause significant deformations to structures on the surface. It is therefore important to take moisture contents carefully and assess the risks of rising ground water and any other factors that may increase the moisture content when building on such soils.

Flooding from the top is more devastating than rising ground water level as less water is needed to produce a similar amount of deformation. If there were large variations of voids ratios since flooding at the top would produce large differential settlements as this is where most of the stress is acting from the footing. Localised wetting near the surface would also cause differential settlement. The long thin footing as used for these experiments would further encourage differential movement if the water was not uniformly added.

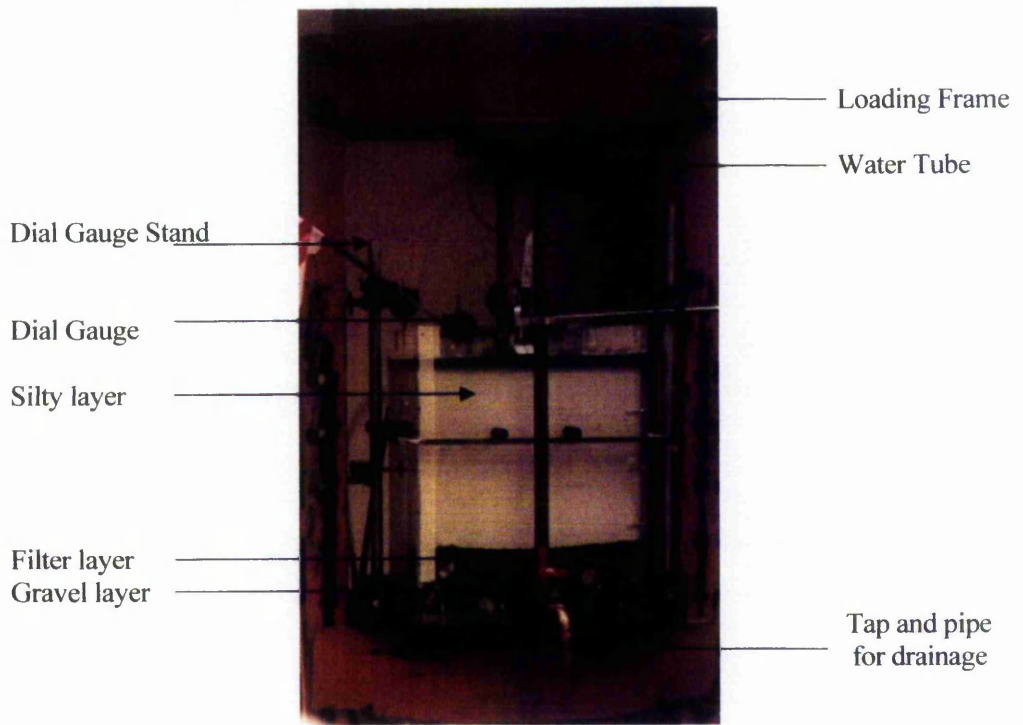


**Plate 6-1 Loading arrangement for the footing test**

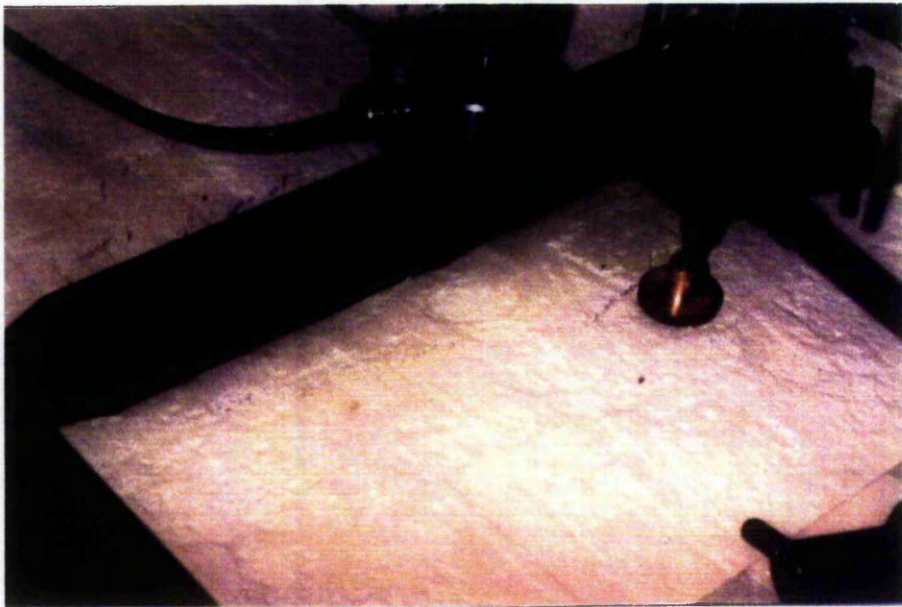


**Plate 6-2 Failure of the deposit after saturation has occurred through rising ground water.**

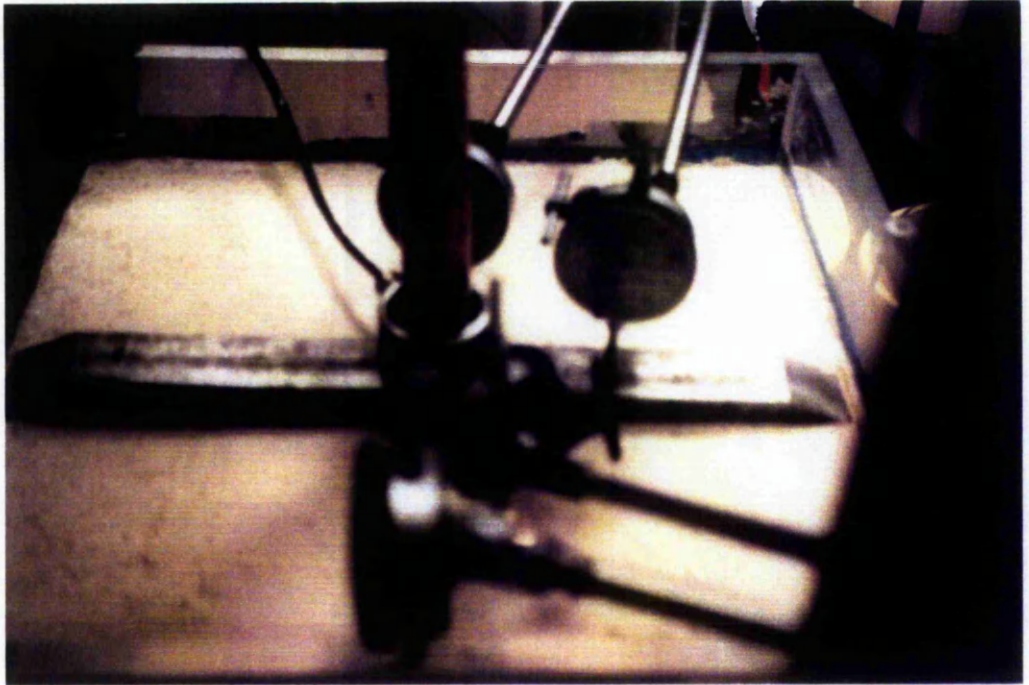


**Plate 6-3. Failure of footing in Case 1 Test 2 – failure mode was punching shear.**

# 7

# Finite Element Models

---

## 7.1 INTRODUCTION

The results of the oedometer tests and triaxial tests indicated the geotechnical properties for an element of the artificial soil. The samples were tested under unsaturated and saturated conditions.

The main points to come from the oedometer tests were:

1. The soil is significantly stiffer in unsaturated conditions than in saturated conditions, as expected.
2. An initial constrained modulus can be assigned to the soil.
3. The constrained modulus of the soil progressively increases as load increases.

The constrained modulus of the soil depends on clay content, water content and preconsolidation pressure.

The triaxial tests showed that:

1. The soil is much stiffer unsaturated than saturated, as would be expected
2. However, the stress strain curve is linear, until yield, unlike the oedometer tests where the behaviour is non-linear from the start of loading.

3. Young's Modulus decreased once yield has been reached (rather than increasing as in the oedometer tests).

The geotechnical parameters indicated by the results of the tests above were used to carry out simple finite element analyses using a linear elastic model. Initially, the oedometer tests and triaxial tests were modelled. The results of the physical testing in the oedometers and triaxial equipment were presented in Chapter 4. Once these were simulated successfully, the same soil parameters were used in the model of a strip footing. The results of the laboratory footing-test were presented in Chapter 6. The laboratory results were compared with the finite element analysis for each situation, in order to evaluate the models.

## 7.2 FINITE ELEMENT MODELLING

### 7.2.1 Background

A finite element program called CRITICAL State Program (CRISP), developed at Cambridge University, was used to simulate the tests that have been undertaken during this study. The code of the existing program is vast. CRISP94 has 6 models, all of which deal with saturated soil problems. These models include elastic, plastic and critical state models. This version does not include any models for unsaturated soils, but can be adapted to include such models. One such model was developed by Alonso et al. (1987) and implemented into Crisp84 by Nesnas (1995). This model extends the traditional cam-clay model to include suctions. This is ideal for granular soils where suction is the only bonding mechanism. However, as already discussed in Chapter 2, the clay and carbonate components in loess provide additional bonding and therefore would need even more complex models to simulate these extra bonding mechanisms. Thus, what is needed is a new way to model collapse, that does not rely on further complicating existing ideas.

### 7.2.2 Unsaturated Soil Modelling

In the last two decades, the unsaturated soil theories have been developed to model clays and sands. Wheeler and Sivakumar (1995) reported on the development of an elasto-plastic critical state framework for unsaturated soils. The general shape of the yield surface is shown in Figure 7-1. The framework enables important features of unsaturated behaviour to be modelled, e.g. an increase of strength with suction and the possibility of collapse (irreversible volumetric compression) on wetting (reduction of suction). In the figure  $p$  is the normal stress,  $q$  is the shear stress and  $s$  is the suction. A soil, which is initially at stress

A, is inside the current yield surface. Yield can be produced by an increase of isotropic loading (path ABC), a reduction in suction (wetting path AFG), an increase of shearing (path ADE) or a combination of the three. The plastic volumetric compression that occurs on section FG of the wetting path is identical to that which occurs on section BC of the isotropic loading path or section DE of the shearing path if all three paths produce the same expansion of the yield surface.

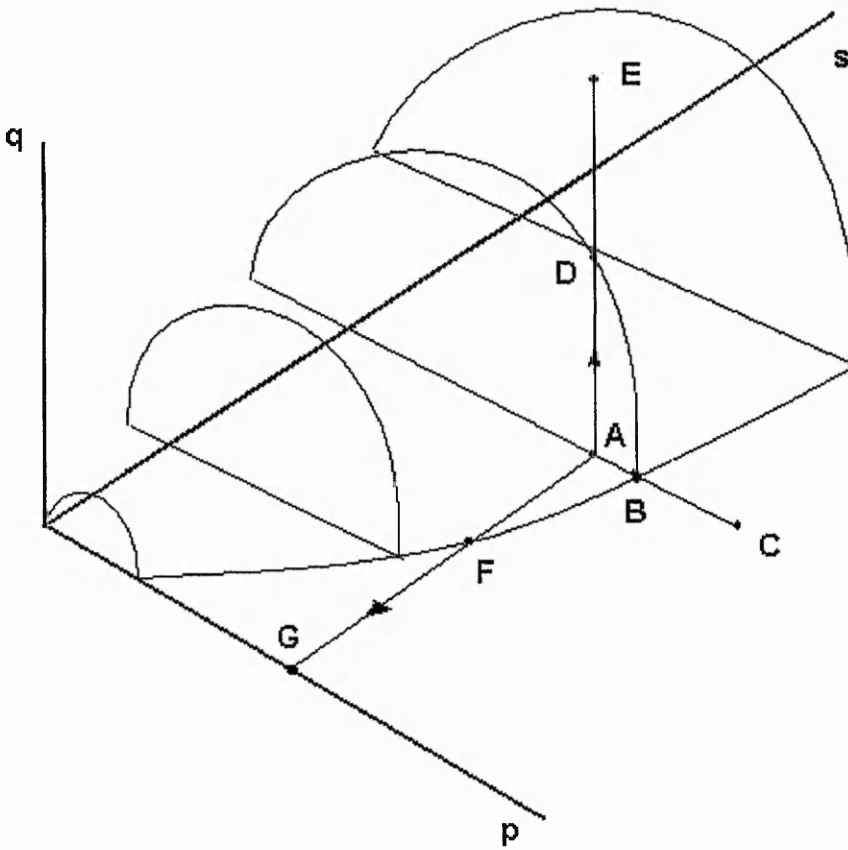


**Figure 7-1 Yield surface (Wheeler and Sivakumar, 1995) where,  $p$  = normal stress,  $q$  = shear stress and  $s$  = suction.**

The yield curve in the  $p,s$  space is represented in Figure 7-2. When the stress path crosses the yield curve, irreversible volumetric strains occur. This may be due to a reduction of suction (C, collapse strains) illustrated by AFG in Figure 7-1 or to an increase in load (L, loading strains) illustrated by ABC. The framework postulates that whatever the origins of the strains, they will have a similar effect on the structure of the material as represented by the movement of the yield curve. In Figure 7-2, both the L and C stress paths take the yield

curve to the same position, and therefore the volumetric strains will be the same in each case. The hardening, implied in this process, is the same as that experienced by a saturated sample moving from A1 to A2. The volume change, therefore can be estimated from the volume change that would be experienced by a saturated normally consolidated sample over the stress increment  $p_o^*1$  to  $p_o^*2$ . The distance between the yield curves increases with suction, which implies that the volumetric stiffness under increasing load also becomes higher with suction. Other stress paths combining simultaneous changes in  $p$  and  $s$  will have similar effects as long as the stress path moves outside the yield curve. To the left of the yield curve an elastic zone is postulated in which reversible deformations occur in response to suction and net total stress changes. This yield curve is called LC (Loading-Collapse) yield curve, Gens and Alonso (1992).

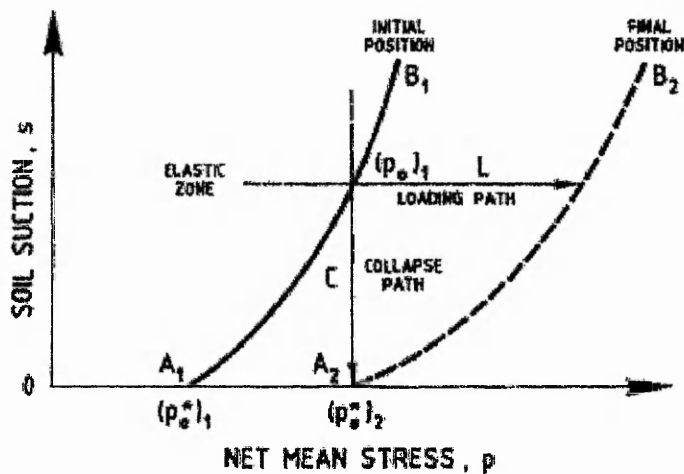


Figure 7-2 LC Yield Surface, after Gens and Alonso (1992)

Figure 7-3a shows the stress paths for five samples schematically indicated and Figure 7-3b shows a probable situation for the relevant yield surfaces controlling soil behaviour. The suction increase (SI) surface at the top of the graph corresponds to the maximum soil suction experienced in the field. Only three positions of the loading-collapse yield surface have been indicated. These are the initial surface LC, the surface corresponding to maximum vertical loading reached in the tests before soaking the samples LC<sub>a</sub>, and the final common surface of all the tests, LC<sub>f</sub>. Figure 7-3c is a qualitative indication of the response of the different stress paths. In this case the model predicts an increase in collapse

with applied stress and a unique  $e-p$  curve for the saturated soil. Laboratory data confirms this uniqueness for loess, Erol and El-Ruwaih (1982), as shown in Figure 7-3d, in the case of collapsing sands, by Blight (1965) and Jennings and Burland (1962), and in the case of a low plasticity sandy clay by Maswoswe (1985).

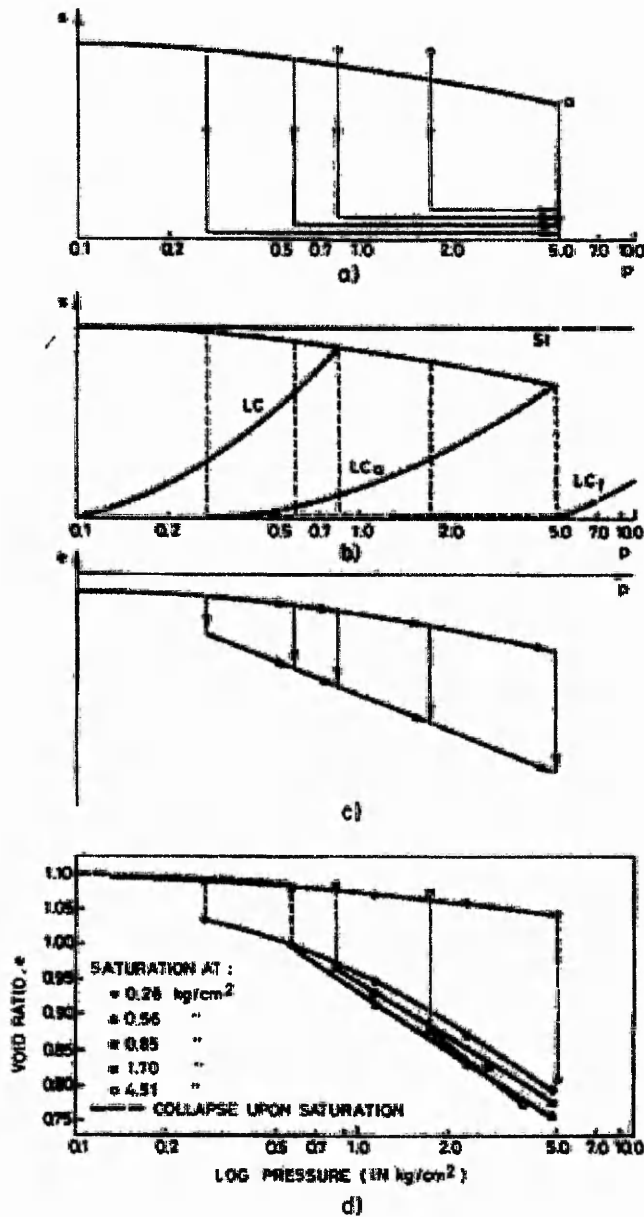


Figure 7-3 Collapse tests on loess under different confining conditions, Alonso et al. (1987). a) Stress path in  $p, s$  space. b) Evolution of yield surfaces. c)  $(e, p)$  relationship d) Typical oedometer test results. (Erol and El-Ruwaih, 1982).

This unique  $e$ - $p$  curve is not observed in expansive soils. This behaviour can also be simulated by the model and is discussed by Alonso et al. (1987). Expansive soil behaviour is not relevant for loess collapse models, as shown by the results of Erol and El-Ruwaih (1982) and so is not discussed further here. The concepts of Alonso et al. (1987) have been explained using two stress parameters  $p$  and  $s$ . The models were also extended to address the effects of shear stress by incorporating the third stress parameter,  $q$ .

A common problem in using a relatively sophisticated constitutive model within a numerical formulation for the solution of real boundary value problems is the difficulty of measuring all the relevant soil parameters. The simplest unsaturated models need three elastic constants and six parameters that vary with suction (Wheeler and Sivakumar, 1995). These models do not include other additions such as the relationship with specific volume of water or any effects of cementation. The idea of including bonding is however discussed by Gens and Nova(1993). The number of parameters needed makes it very costly and time consuming to carry out such analyses.

A rational approach to soil modelling requires the use of the simplest model compatible with the desired accuracy for the particular case under examination. The concepts proposed by Alonso et al. (1987), in their general report, can be split up into different models with increased complexity. Each one of them has a specific role. The volume change behaviour of partially saturated non-expansive soils under stress paths, which typically involve gain in saturation and increase in external loading, can be interpreted in terms of the single Loading-Collapse yield surface. If the suctions were expected to increase, a further addition of a SI yield surface would be needed. Swelling soils require in most cases a joint consideration of the Loading-Collapse and Suction Decrease yield surfaces, which create the non-unique  $e$ - $p$  end results. The full consideration of the three proposed yield surfaces would be required only if an expansive soil, with a complicated history of wetting and drying cycles and varying external load was being considered.

### **7.3 SIMPLE APPROACH TO MODEL COLLAPSE**

It was clear that a pragmatic model was required to overcome the complex nature associated with existing models. Ideas from different areas of soil and rock mechanics have provided the basis for this project. Oedometer tests have traditionally been used to test for

collapsibility of a deposit. The double oedometer and single oedometer tests prove that for an element of soil loaded in one-dimension, the same stress-strain point is reached whether the soil is loaded and then saturated or saturated and then loaded. This was the assumption used in a finite element analysis of the problem.

The ideas of Nobari and Duncan (1972) and Naylor et al. (1989) and later, Farias (1993), showed a simple approach to collapse based on the assumptions above, which used far less parameters than the suction approach discussed in section 7.2.2. They postulated that collapse could be modelled by considering the change in conditions of the soil from unsaturated to saturated. The transformation from one "unsaturated" curve to a "saturated" one needs two groups of parameters to be specified, one for unsaturated and one for saturated soil.

An important experimental finding underlying the technique is that for a given strain, the stress is the same whether the sample is first tested unsaturated to that strain and then saturated (under constant strain) or is saturated from the start. Furthermore, saturation at constant stress after initial loading of a sample followed by further loading will cause the stress-strain curve to revert to that obtained for the same material saturated at the start. This was illustrated for a one-dimensional compression test by Burland (1965). Justo et al. (1984) studied the influence of loading-wetting sequence on the wetting induced volume change of both natural and compacted expansive soils and determined that in the collapse region the volume change was essentially independent of the loading-wetting sequence. The volume changes in the expansive zone, however, were found to depend significantly on the stress at which water was added in the soaked test. Lawton et al. (1992) came to similar conclusions for the slightly expansive clayey sand that they studied. The technique pioneered by Nobari and Duncan (1972) is therefore valid for the estimation of volume change in the collapse zone. This is adequate for the needs of this study.

Unsaturated parameters and saturated parameters can be obtained from the oedometer and triaxial tests. Figure 7-4 illustrates the collapse produced using the method developed by Naylor et al. (1989), following the route A-B-C. Collapse is simulated in two stages. A sample is loaded to point A using the unsaturated parameters, in the first stage, a switch to the saturated stress strain curve is performed without strain changes to point B. The corresponding stress point will be referred to as the clamped stress,  $\sigma^B$ . In the second stage,

equilibrium is restored by the application of the unbalanced stress  $\sigma^A - \sigma^B$  to the saturated material. This produces the desired collapse deformation leading to point C on the second stress strain curve. This procedure was utilised by the Building Research Establishment (BRE) to model collapse of colliery spoil, Skinner et al. (1999).

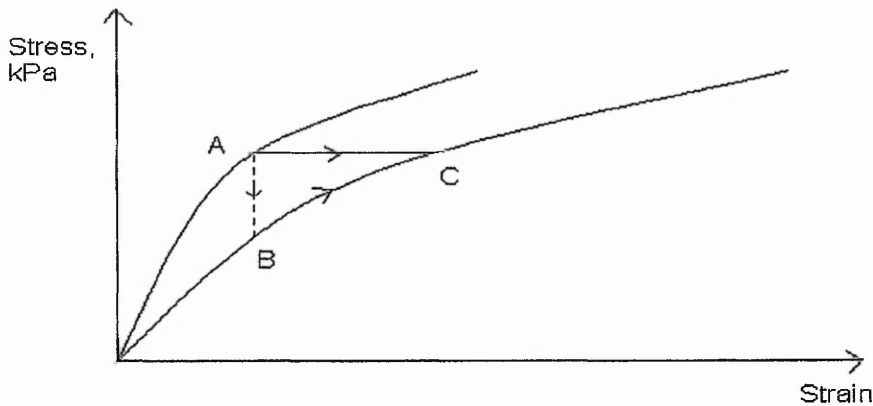


**Figure 7-4 The principle of the new method to move from one state to another**

#### 7.4 METHOD OF MODELLING FOR THIS STUDY

The above procedure was implemented into a finite element program by Farias (1993). The final output of the program gives stresses and strains for a soil loaded to normal stress  $p$ , using the saturated parameters provided by the user.

The cases for this study are simple symmetric models, so it was decided to run the analysis twice, once with unsaturated parameters and once with saturated parameters, would produce the same result as using the above procedure. This uses the assumption discussed above that a sample that is loaded and then saturated is expected to produce the same stress strain state as a sample that is saturated and then loaded. Obtaining the parameters is one of the most important stages in the modelling process. Parameters are usually obtained from triaxial, oedometer or shear box tests. For this study oedometer and triaxial compression tests were carried out on the artificial soil to obtain parameters for both saturated and unsaturated soil, results for which are presented in Chapter 4.

Numerical studies were initially carried out using CRISP in order to validate the results shown in Chapters 4. Modelling the triaxial and oedometer tests allowed a check that the behaviour of a small element of soil could be simulated. The main aim was to model the footing tests, which were carried out and discussed in chapter 6. The analysis was carried out using simple elastic models, however any model could be used with this technique. All that is needed are the properties for saturated and unsaturated soil for the appropriate model. The models were carried out using the saturated and unsaturated parameters collected from the triaxial tests for the appropriate moisture contents. The models were run twice, once using the saturated properties and once using the unsaturated properties. The results for unsaturated and saturated soil were then compared to observe the effect of wetting the soil. Results are shown in Section 7.5 and 7.6.

All the finite element calculations were carried out using eight-noded quadrilateral elements with the two-point Gaussian numerical integration technique utilised by the CRISP finite element program. The artificial soil was modelled as linear elastic for most of the analysis, although a non-linear model was investigated to model the soil in the oedometer tests. This non-linear model was developed to simulate the stiffening behaviour of the soil under one-dimensional loading. However, this behaviour was not observed under any other loading conditions, so a more simple elastic model was used for the majority of the analysis. An elastic model requires the fewest parameters and therefore represents the simplest of the model that could be used.

A one by one grid was used to check the results obtained from the finite element program. The same grid was analysed by hand for both the linear and non-linear elastic models. The results were compared and were exactly the same as those obtained from the finite element program. This gave confidence that the models were working correctly and also that the data was being input correctly

## **7.5 MODELLING THE OEDOMETER TESTS**

The laboratory tests were reproduced using the program CRISP to test the ability of the finite element models to simulate simple conditions. The oedometer tests were modelled using a small number of elements. The dimensions of the oedometer ring were reproduced by the finite element grid. Only half the diameter of the ring was considered due to the

axisymmetry of the problem. The grid was dimensioned as 19mm high and 38mm wide. The loading arrangement is illustrated in Figure 7-5. The top boundary was loaded in stages as carried out in the oedometer tests. The sides were restricted to move only in the y-direction and the lower boundary could only move in the x-direction.

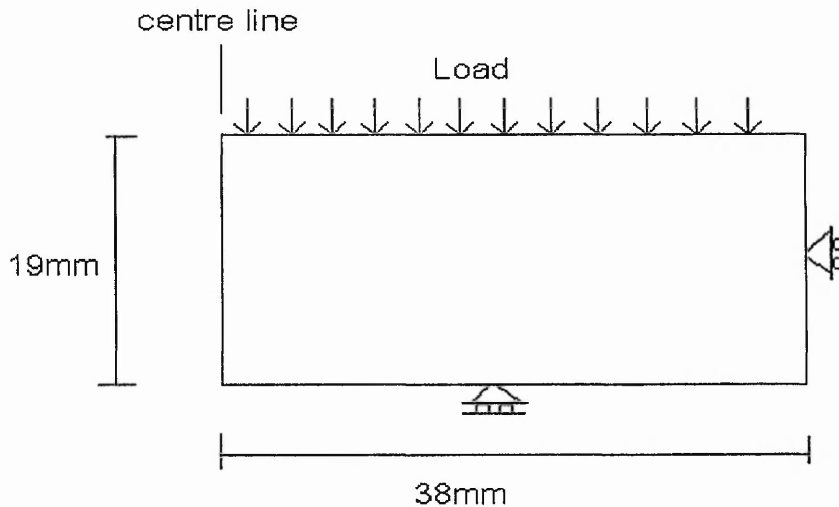


**Figure 7-5 Loading arrangement for the simulation of an oedometer test**

Initially, a value of  $D$  (constrained modulus), the one-dimensional stiffness of the soil, was calculated from oedometer results for both the unsaturated and saturated samples, from Essex.

The constrained modulus is defined as  $D = \Delta\sigma / \Delta\varepsilon$

The artificial samples were made with 30% kaolinite and 70% and tested in the oedometer and triaxial equipment. A best fit line was plotted for the loading curves and was used to estimate the constrained modulus,  $D$ , for the load range 0-100kPa from the oedometer tests. A value of  $D=500\text{kPa}$  was calculated for the saturated artificial soil and a stiffer value of  $D=2000\text{kPa}$  was obtained for the unsaturated material as seen in Figure 7-6. The stress-strain behaviour of the samples is shown on this graph along with the lines of best fit for the curves, and the finite element model results for  $D=500$ , 2000 and 4000kPa.

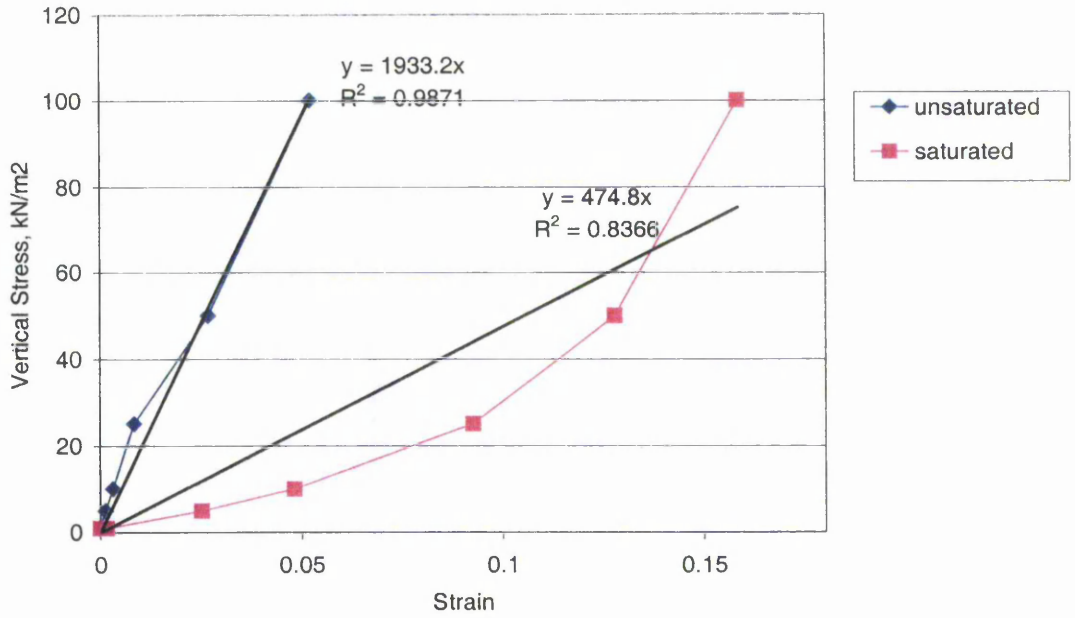


Figure 7-6 Determination of the constrained modulus for the unsaturated and saturated artificial samples with 30% kaolinite content for loads 0-100kPa.

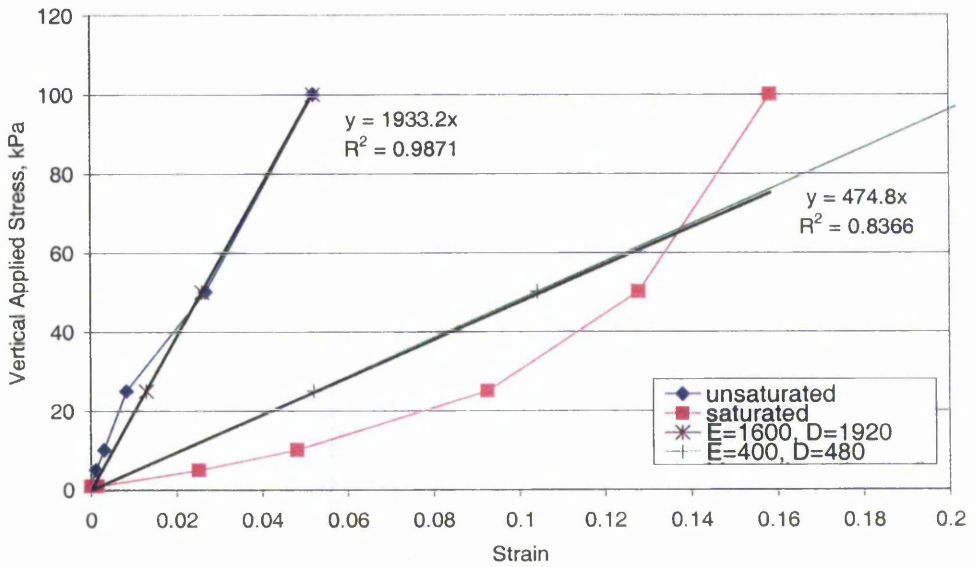


Figure 7-7 Comparison of results for linear elastic model in finite element program with artificial samples 30% kaolinite, over the stress range 0-100kPa

Figure 7-7 shows a comparison of the finite element program results with those of the artificial loess, for stress against height of the sample. The results show that although the elastic model would be too simplistic over the whole range of stress values tested in the oedometer, the predictions are reasonable at small magnitudes of stress, when the material seems to behave nearly linearly. The saturated material did not behave linearly in the oedometer tests. A linear approach is probably an over simplification. Potential hydrocollapse can be estimated from the difference between the unsaturated and saturated curves at a particular stress. At 100kPa the double oedometer predicted a hydrocollapse of 11.2%. The linear model predicted a hydrocollapse of 12.6% by using approximate values of  $D$  of 2000kPa and 500kPa for the unsaturated and saturated samples respectively.

Analysis was also carried out for the samples taken from the Star Lane site in Essex using the method as above. These samples were stiffer and a constrained modulus was estimated as 2,000kPa for the saturated sample and 4,000kPa for the unsaturated sample. These results are shown in Figure 7-8. The difference in stiffness between the artificial and natural specimens was probably due to higher void ratios in the artificial samples and lack of full bonding. Lower initial void ratios were produced in the artificial samples using slightly higher preparation water content or a higher compressive effort to form the artificial samples, as discussed in Chapter 4, sections 4.3.5 and 4.3.7. The effect of the constrained modulus on the vertical deflection of the samples is illustrated in Figure 7-9. As expected, a decrease of constrained modulus causes the vertical deflection to increase.

Instead of this linear relationship, all the oedometer results show that as the load increases, the constrained modulus of the soil increases due to the densely packed particles. With this in mind, a relationship was developed to link constrained modulus with load. It was found constrained modulus and load were related so that,

$$D_n = \frac{D_i P}{x}, \quad (7.1)$$

where,  $D_n$  is the new value of constrained modulus,  $D_i$  is the initial value of constrained modulus found from the oedometer tests,  $P$  is the stress applied and  $x$  is a modifying factor which for the artificial soils tested was 55-60 found by trial and error testing.

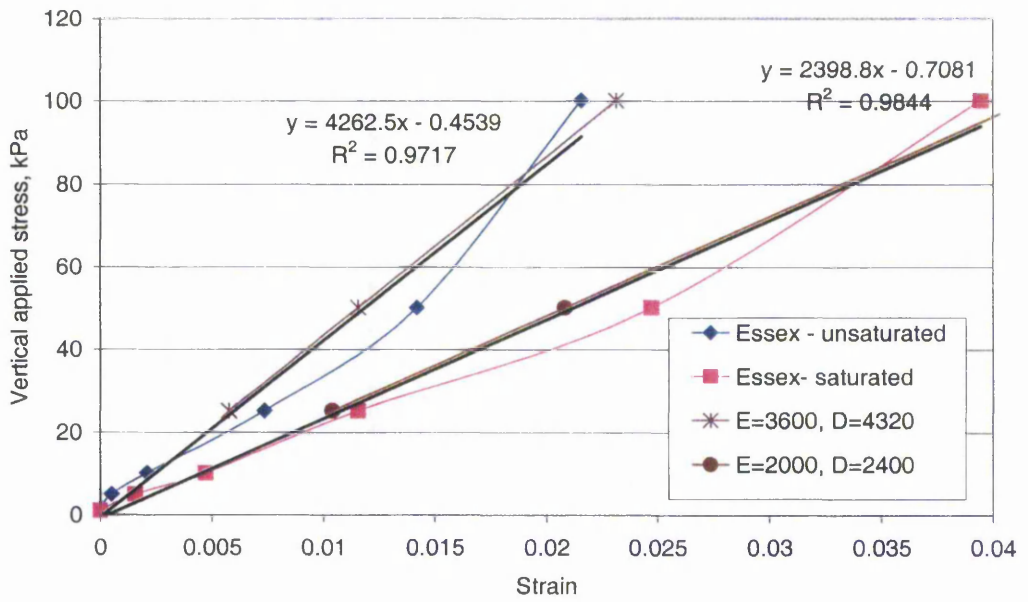


Figure 7-8 . Comparison of finite element results with those from testing undisturbed specimens from the Star Lane, Essex. 0-100kPa. Where, E = Young's modulus and D = Constrained modulus. Values in kPa.

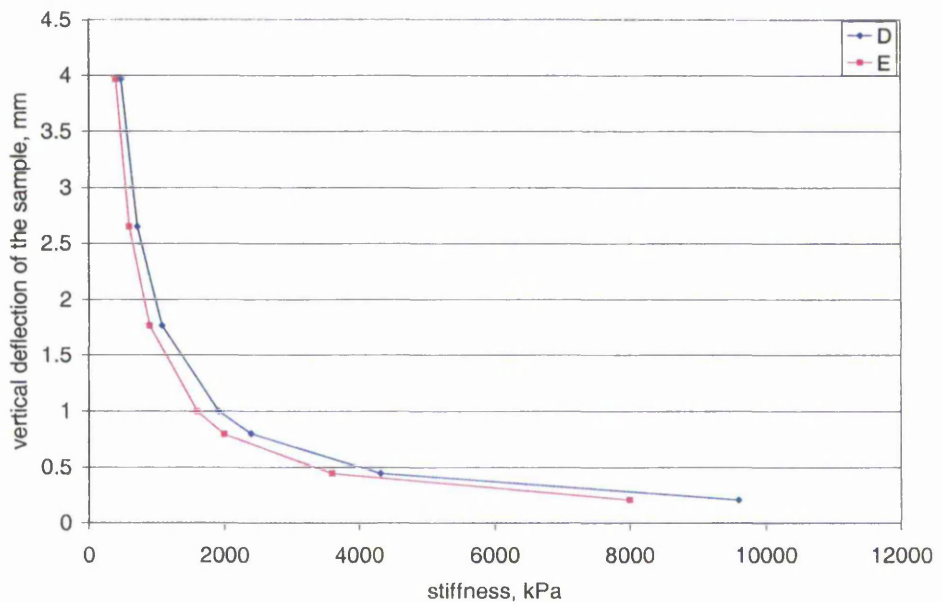
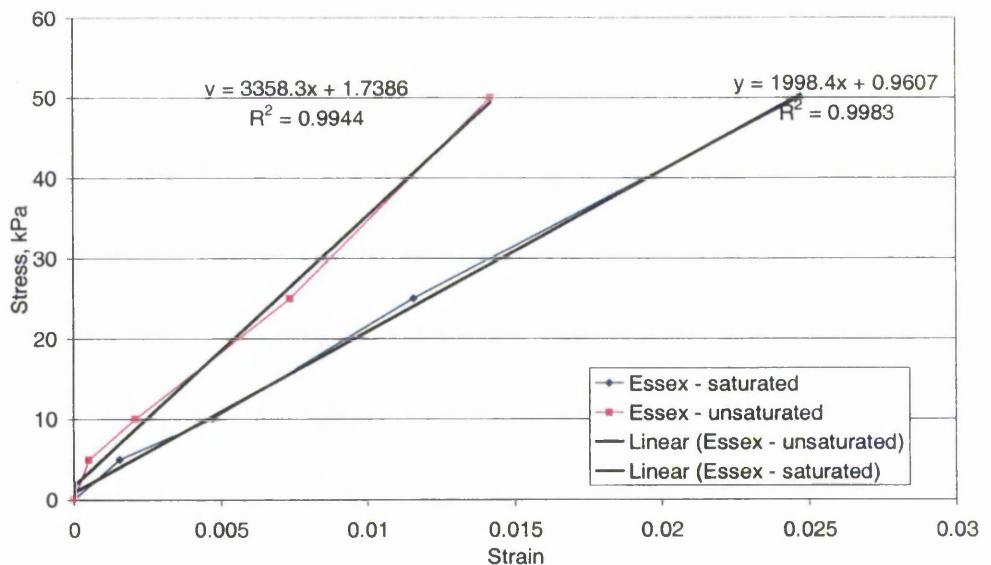


Figure 7-9 Effect of D and E on the vertical deflection of the oedometer sample for 100kPa load. Where, E = Young's modulus and D = Constrained modulus.

A model of the oedometer tests was run using the finite element program with the non-linear model. The boundary conditions were set as before, but the model changed to include the equations above to make the constrained modulus change with the load. An initial value of  $D$  was found for each of the natural samples and used in the Finite Element model ( $D_i$ ).  $D_i$  for the stress range 0-50kPa was around 3400kPa for the unsaturated natural samples and 2000kPa for the saturated natural sample, as shown in Figure 7-10. The values of  $D_i$  were converted to Young's modulus,  $E_i$ , to use in the FE analysis, using the equation,

$$D = E' \frac{(1-\nu')}{(1+\nu')(1-2\nu')} \quad (7.2)$$



**Figure 7-10 Determination of the constrained modulus for the natural samples for loads 0-50kPa.**

However, a range of values were analysed for the constrained modulus to produce the best fit. Poisson's ratio,  $\nu$ , was estimated at 0.25, which is typical for silty clay (Head, 1990). Results from the finite element analysis were compared with the samples from the Essex site. The curves found from the non-linear model gave a very good fit to the natural loess. The curves that gave the best fit were  $E_i=3166$ kPa for the unsaturated sample and  $E_i=1600$ kPa for the saturated samples, for  $x = 55$ , which correspond to values of  $D_i$  of 3800kPa and 1920kPa respectively. The results from the FE analysis gave similar

deflections to the laboratory samples, as seen in Figure 7-11. These values of  $D_i$  used for the analysis were roughly equivalent to the vales of  $D_i$  found from the laboratory oedometer tests, as seen in Table 7.1.

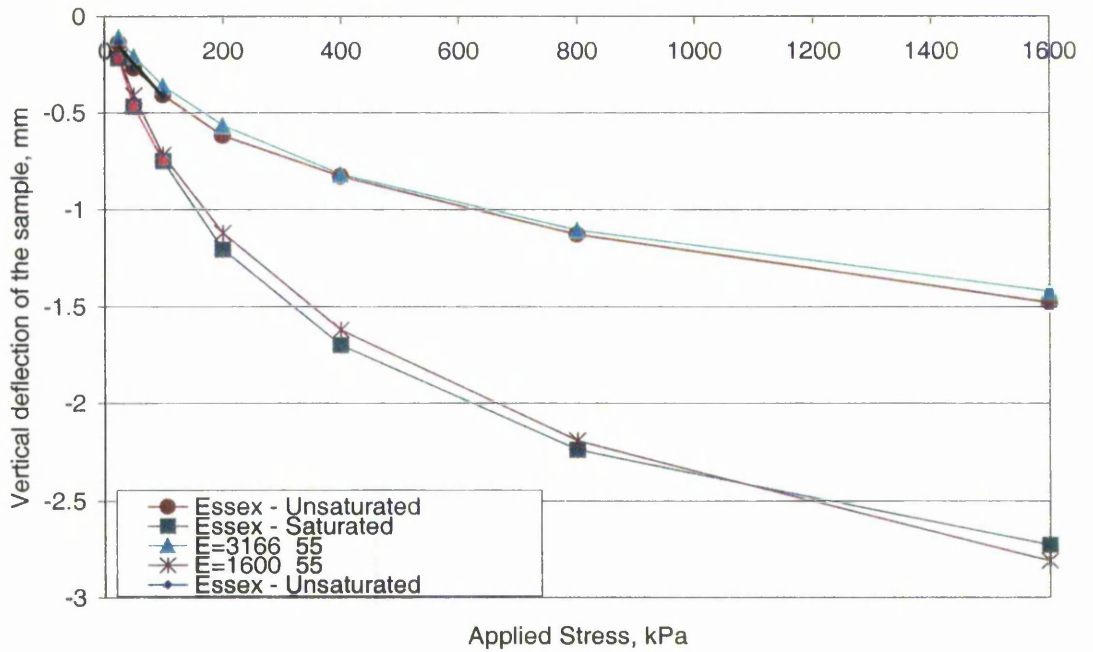


Figure 7-11 Comparison of results for non-linear elastic model in finite element program with samples from the Start Lane, Essex site, over the range 0-1600kPa

Young's modulus, kPa	Poisson's ratio	Constrained modulus, kPa
3166	0.25	3800
1600	0.25	1920

Table 7-1 Values of E for non-linear model for calculated values of D from the oedometer tests.

## 7.6 MODELLING THE TRIAXIAL TESTS

The triaxial tests were also modelled using the finite element (FE) program. The triaxial samples, exhibited linear behaviour in normal stress- strain space until yield. The linear behaviour was observed up to a deviator stress of approximately 200-300kPa, beyond

which the samples began to yield and the Young's Modulus of the samples gradually, or suddenly in some cases, reduced, as seen in Figure 4-30, in Chapter 4. Since the working loads for most buildings are less than 100kPa, it is feasible, especially as a first prediction, to assume linear behaviour. This is often performed in engineering practice to give a first indication of the stresses and deformations that may occur in a system.

The grid used for the finite element analysis of the triaxial tests is shown in Figure 7-12. Again only a small number of elements were used to model this small element of soil. A quarter of the element was considered for the analysis due to the symmetry of the problem. The elements used for this case were six 15 noded CuST (Cubic strain) elements, which are often preferred for axisymmetric analysis. More than 50 load increments are recommended for a finite element analysis which simulates a triaxial test (CRISP manual, 1984). One hundred increments were used for this study. A strain-controlled test was considered, leading to a total axial strain of 20%. The in-situ stresses were specified as 200kPa to simulate the tests that had been carried out in the laboratory. AB was restricted to move horizontally, CD was displaced vertically downwards to simulate a strain controlled test. DB had a pressure loading of 200kPa to model the cell pressure and AC was restricted to moving vertically. The deviator stress was applied at the top boundary, CD.

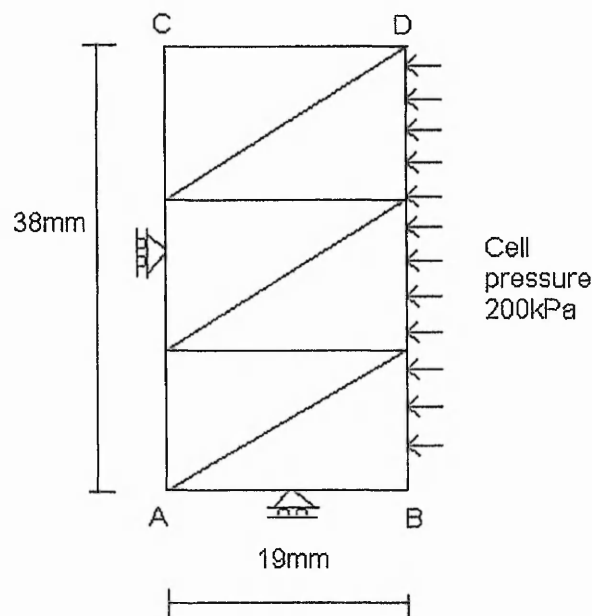


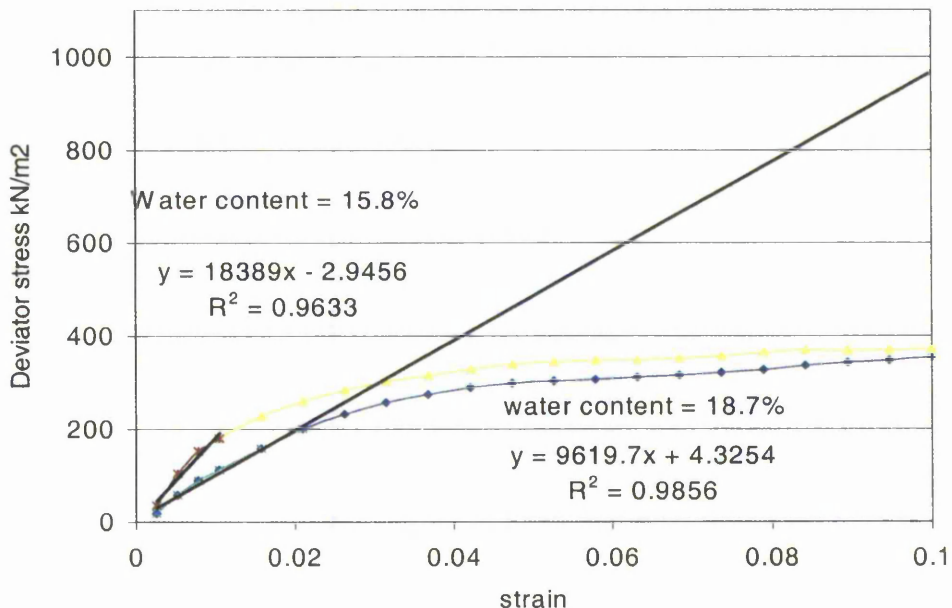
Figure 7-12 Layout of grid and boundary conditions for simulating the triaxial test.

## 7.7 FINDING PARAMETERS FROM THE TRIAXIAL TESTS

The results of the triaxial modelling are shown in Chapter 4, Figures 4-29 and 4-30. These were modelled using a simple linear elastic model using the CRISP finite element program. The advantage of modelling these simple tests using the finite element program was that the effects of varying the parameters could be determined. The triaxial tests were used to find the appropriate Young's Modulus values for the artificial material for different moisture contents.

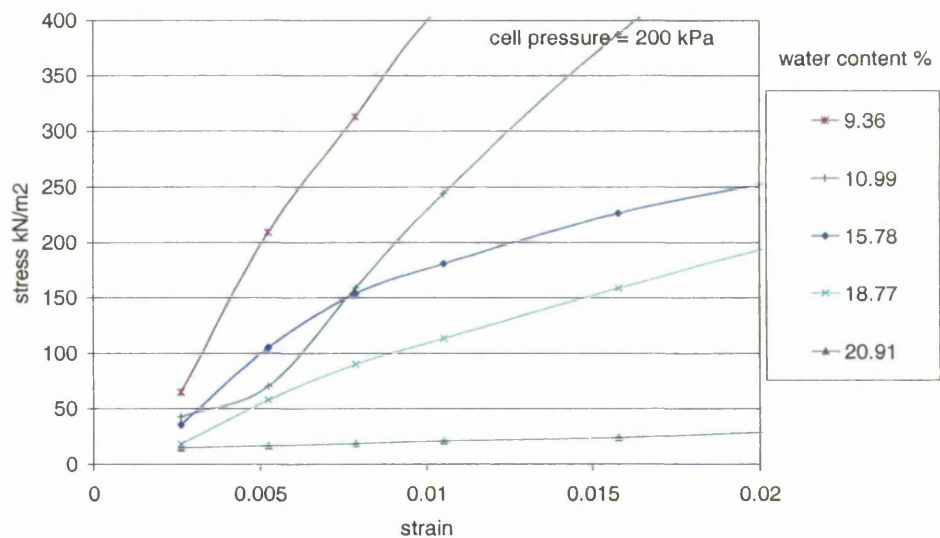
### 7.7.1 Linear Elastic

The main parameters needed for this analysis were  $E$ , the Young's modulus, and  $\nu$ , Poisson's ratio.  $E$  was found from the stress-strain curve for the stress range 0-200kPa, to obtain an approximate initial Young's Modulus for the artificial material, see Figure 7-13. Poisson's ratio is the ratio of strains  $\epsilon_3 / \epsilon_1$  and can be found from measuring the horizontal strains relative to the vertical strains from triaxial tests. Since the simple triaxial equipment in the laboratory did not measure the horizontal strains of the sample, a value of  $\nu$  had to be assumed for the material. An estimate was made between 0.25 and 0.3. This is an average  $\nu$  for rocks such as mudstone and sandstone, which are similar to loess in its natural state.



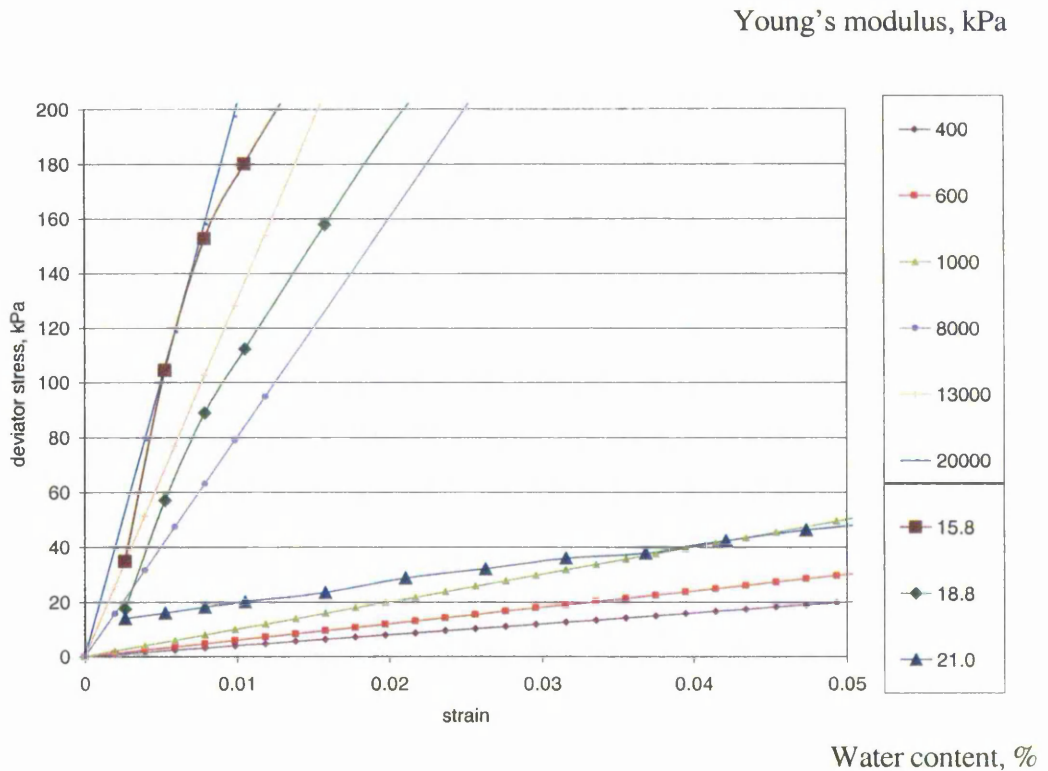
**Figure 7-13 Finding Young's Modulus values from the undrained triaxial tests on two artificial specimens using best fit lines through the data for the results up to 200kPa.**

Figure 7-14 shows the behaviour of the natural samples, taken from Essex brick works, for low loads and for varying water contents. The best fit for each of these lines was taken, shown in 4-34, in Chapter 4. These values were then used in further investigations of the behaviour of the soil beneath a footing as described in section 7.8. Different values of  $E$  were input into the finite element models to compare with the behaviour of the samples in the triaxial tests. The charts in Figures 4-24 and 4-29 in Chapter 4 illustrates how an estimate of  $E$  can be made for specimens tested in the triaxial apparatus with a given initial void ratio and water content. The results of the linear finite element analyses are shown in Figure 7-15.



**Figure 7-14 Triaxial Test Results for artificial specimens with 30% clay content and different initial water contents for lower deviator stress, 0-400kPa**

The sample with 15.78% water content has a Young's Modulus,  $E$ , of 18,000kPa. The finite element analysis shows the behaviour stays within  $E=20,000$ kPa and  $E=13,000$ kPa. For the sample with 18.77% water content, the Young's Modulus was approximately  $E=10,000$ kPa for the stress range 0-200kPa. The specimen with 20.91% water content is around 50% saturated, which means that its behaviour is very soft, with a Young's Modulus of around 1000kPa.



**Figure 7-15** Finite element results for various values of  $E$  (in the range 400 – 20,000kPa) for the triaxial tests, plotted with three of the triaxial test results for specimens with 15.8, 18.8 and 21.0 water content percentages.

### 7.7.2 Other models

For this case the linear model is adequate, as working loads expected for the footing were not above 100kPa. This stress is within the linear region of the stress-strain graph for the artificial soil. However, any model could be used to define the unsaturated and saturated curves of the soil. It is up to the user to find a model which best describes the behaviour of the soil.

## 7.8 PREDICTION OF COLLAPSE BENEATH A STRIP FOOTING

### 7.8.1 Methods

Continuing from the simulations of the oedometer and triaxial tests, the footing test was also modelled using the finite element techniques. The elements were quadrilateral eight noded elements. The grid was designed as illustrated by Figure 7-16. This figure shows the loading arrangement and the geometry. These non-linear divisions were used as well as 10

and 20 equally spaced (linear) divisions across the grid, which were used for comparison. The side boundaries of the grid were set so that the movement could only take place in the y direction. At the top, a width equal to the half width of the footing was loaded in stages up to 100kPa. The grid was sized the same as the artificial soil in the tank. Only half the tank needed to be modelled due to the symmetrical nature of the tank. The footing is long compared to its width so the finite element analysis could be performed in 2-D in plane strain.

The grid was divided into smaller elements in two different ways, linearly and non-linearly. This gave an indication of the influence of divisions of the grid. The grid was also approximately doubled in size (400x800) to gain an insight into how the geometry and formation of the grid affected the results of the finite element analysis.

The grid was split into eight horizontal layers, each with its own, definable, material properties. This enabled layers with different properties to be specified within the analysis, which allowed examination of the effect of a rising, or falling, water table.

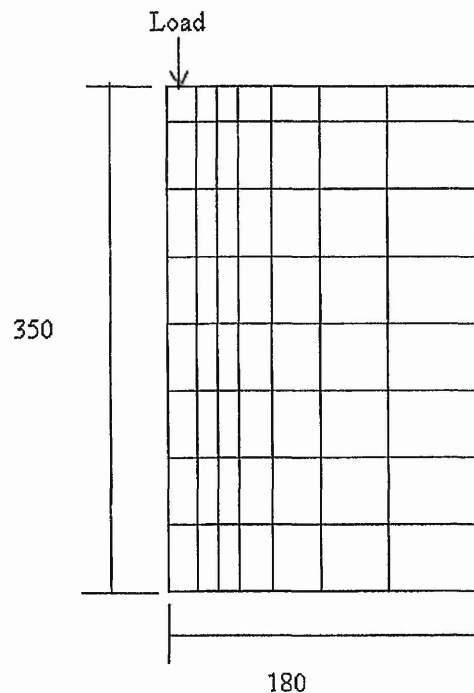


**Figure 7-16 Finite element model grid used to predict the deformations of the footing model**

### 7.8.2 Case 1: Loaded then saturated

For Case 1, initially the finite element analysis was run using a linear model, utilising the unsaturated parameters obtained from the triaxial tests. An estimate of the Poisson's ratio was made as 0.25. This was based on published data for similar materials. Poisson's ratio for consolidated kaolin is around 0.1, for Keuper marl it is 0.12, and for Bunter sandstone-0.27, but for normally consolidated clays it is 0.49, Head (1990). A range of Poisson's ratios were tested in the model to check the sensitivity of the results to this parameter.

The unsaturated water contents of the soil layers ranged from 15-17% in the three physical footing tests that were performed for this case. From triaxial tests, the Young's Modulus of the soil was estimated to be between 20,000kPa (15% water content) and 13,000kPa (17% water content). This value is close to the expected range for normally consolidated clays (5,000-30,000kPa) or a medium dense silt (loose 3,000-80,000kPa dense) (Head, 1990). The finite element analysis was initially run using 13,000kPa to represent the Young's Modulus for the unsaturated condition of the artificial soil for all eight layers of the soil. The deflection of each of the layers was recorded. In order to model the rising water levels the properties of each layer could be changed. The properties of the lowest layer were then changed to those of the saturated soil. At a water content of 20-25%, where all the collapse would have occurred, the Young's Modulus is expected to be around 400-600kPa. This represents a soil with very little strength or stiffness. This value of E was used in the data file for the second run of the analysis in the bottom layer of soil for the footing model. The analysis was rerun and again the displacements of the footing and surrounding soil were recorded. This process was repeated, changing the properties of one layer at a time from the unsaturated parameters to the saturated parameters, up to the top of the deposit. This gave a representation of the wetting front moving up through the deposit and allowed assessment of the influence of the level of water on the deflection of the footing.

### 7.8.3 Case 2. Saturated and then loaded

For the case where all the layers had been changed to reflect the properties of the saturated soil, this represents case 2, for a saturated (due to rising ground water level) and then loaded footing. This uses the assumption that the sequence of wetting and loading does not affect the amount of collapse observed in the soil.

#### 7.8.4 Case 3. Loaded and then saturated from above

Case 3 was investigated the affect of water ponding on top of the deposit and infiltrating through the deposit from above. The wetting front in this case moves down through the deposit. This was simulated using the same procedure as above, but progressively changing the properties of each layer moving down the deposit rather than up. The limitations of this test were that the source of water could not be controlled and the wetting was more localised.

The stiffness values were used to predict the behaviour of a foundation model. The model was able to simulate the change in Young's Modulus with depth as well as the stiffness changes between unsaturated and saturated.

### 7.9 RESULTS AND COMPARISON WITH FOOTING MODEL DATA

As the wetting front moved up the deposit it was simulated in the finite element analysis by changing the properties of the next layer from unsaturated to saturated. The analysis was then rerun. The analysis was run for each wetting stage using the unsaturated and saturated parameters in the appropriate layers of the model. The results for each stage were compared, which showed the effect of an increasing ground water level on the amount of deflection expected from the model.

#### 7.9.1 Case Study 1: Loaded then saturated from bottom

As a linear elastic model was used, the deflection increased linearly with load for each case. The load against deflection graph is illustrated in Figure 7-17 for the two unsaturated cases; an initial unsaturated condition of 15% water content and 17% water content. The value for Young's modulus was estimated to be 20,000kPa and 13,000kPa respectively for the two cases, lower values of E are shown for comparison. Also shown for comparison are the results for the three loading stages for tests 1, 2 and 3 from the laboratory footing model for case 1. The graph indicates that the estimated values for Young's modulus were too high for the soil in the tank. The tests carried out at 15% initial water content, show the same deflections as that modelled by the finite element analysis where  $E=8,000\text{kPa}$ . The third test, with 17.5% initial water content followed the  $E=4,000\text{kPa}$  line from the FE analysis. Values of  $E = 20000 - 13000\text{kPa}$  were expected from the results of the triaxial tests. It is proposed that this was due to the placement of the footing as it was only placed on the

surface of the soil. This meant that only some of the soil was in contact with the footing. The top layer of soil was not totally flat which meant that higher stresses were acting on the soil that was in contact with the base of the footing due to the reduction in contact surface area.

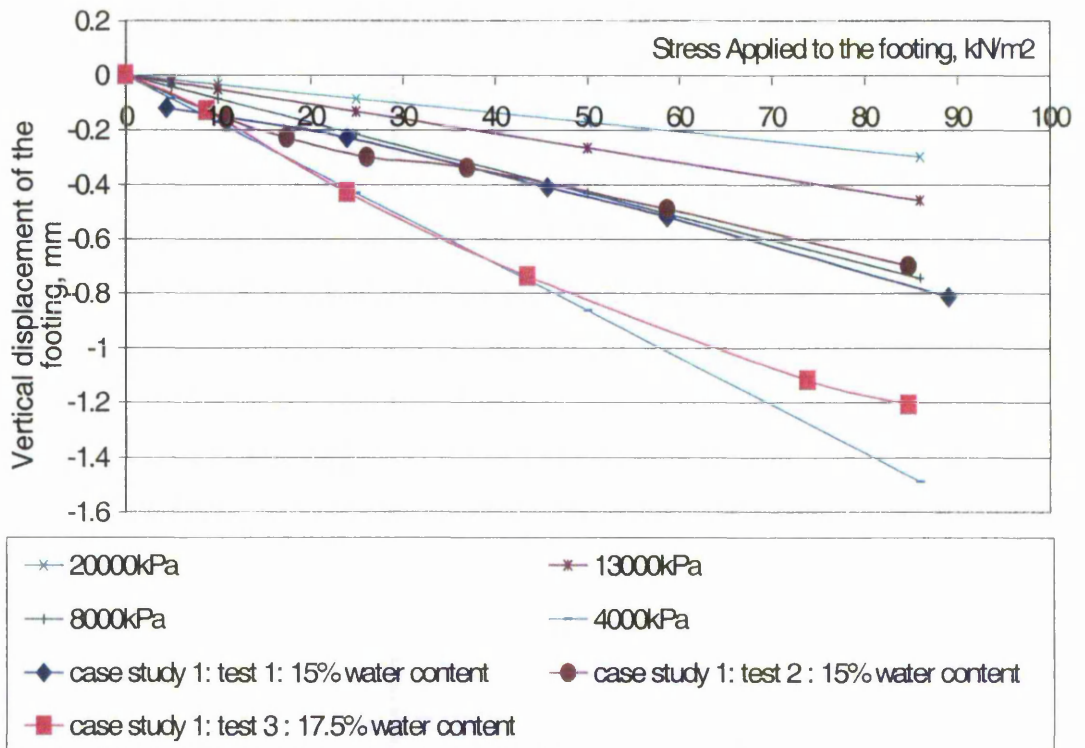


**Figure 7-17 Applied Stress against deflection for the Finite Element model and the laboratory footing model. Finite element results are shown for values of Young’s modulus of 20,000kPa, 13,00kPa, 8,000kPa and 4,000kPa.**

As expected, as the soil properties were made softer, in line with the higher water contents, the deflections became greater. Softer layers at the bottom of the deposit caused the footing to move slightly. As the water was simulated to rise higher through the deposit, this made an increasing affect on the footing deflection. The change in height increased as each layer was wetted. This is shown in Figure 7-18, along with the results from the footing tests for case 1. The laboratory results are illustrated by the un-joined points on the graph and finite

element results are shown by the lines. The footing in the laboratory test was loaded up to 86kPa. The finite element results are presented for loads up to 86kPa. For this analysis, the values for Young's Modulus were taken as 13,000kPa for unsaturated and 400kPa for saturated, as found from the triaxial tests. The finite element results compare favourably with the results found in the laboratory simulation. The same shape curve is observed as the wetting front rises up the deposit and the deformations are very similar in size. It should also be noted that the three tests in the laboratory show good agreement to each other, showing good repeatability of the tests.

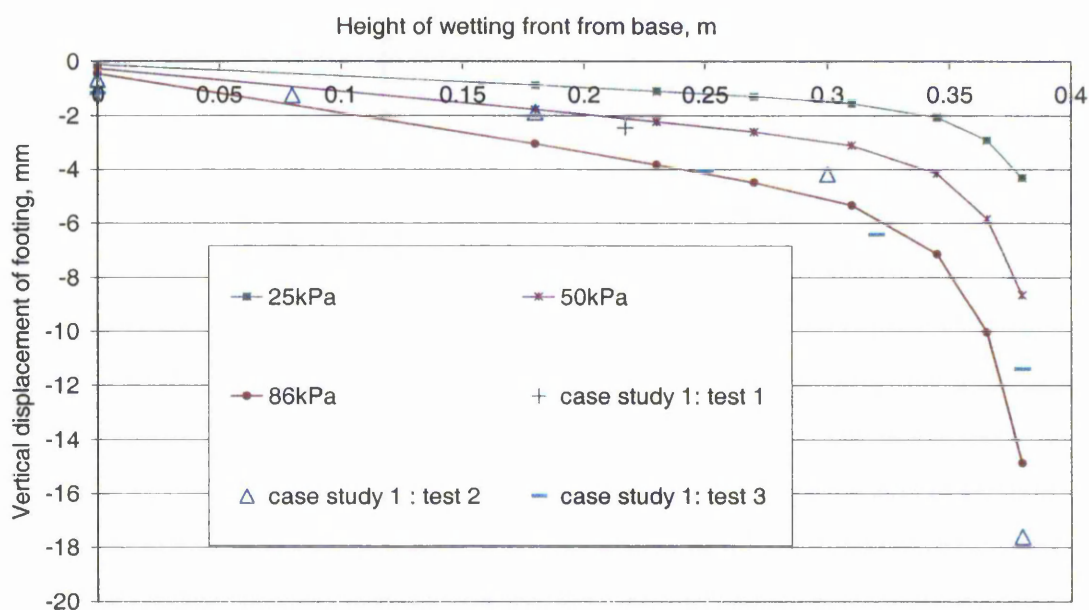


**Figure 7-18 Case 1 comparison of Finite Element results and laboratory footing models. Laboratory footing was loaded to 86kPa.  $E = 400\text{kPa}$  for saturated and 13000kPa for unsaturated material.**

### 7.9.2 Case Study 2: Saturated and then Loaded

In the laboratory footing tests, case 2 indicated that a saturated and then loaded footing would result in a similar stress-strain point as if the footing was loaded and then saturated. This was the assumption for the finite element modelling, so case 2 was modelled in the same way as case 1. The loading curve is shown in Figure 7-19, where the Young's modulus was simulated as 400kPa. Poisson's ratio was again 0.25 for the finite element analysis.

The loading curve was much less linear for the softer soil as observed in the oedometer tests. This may have been due to the softening of the soil as load was added, in which case an elasto-plastic model would have been more appropriate for this case. Alternatively, at the start of the loading stage, the water level in the deposit may not have reached its final height. The softening may have been caused by the progression of the water front through the deposit as the water found equilibrium in the deposit by rising higher. Certainly, the shape of the loading curve is consistent with the curve produced by the wetting front moving progressively further up the deposit. The Young's Modulus up to an applied load of 55kPa was around 1000kPa, but at 86kPa the deflection is equivalent to a soil with a Young's Modulus of 500kPa.

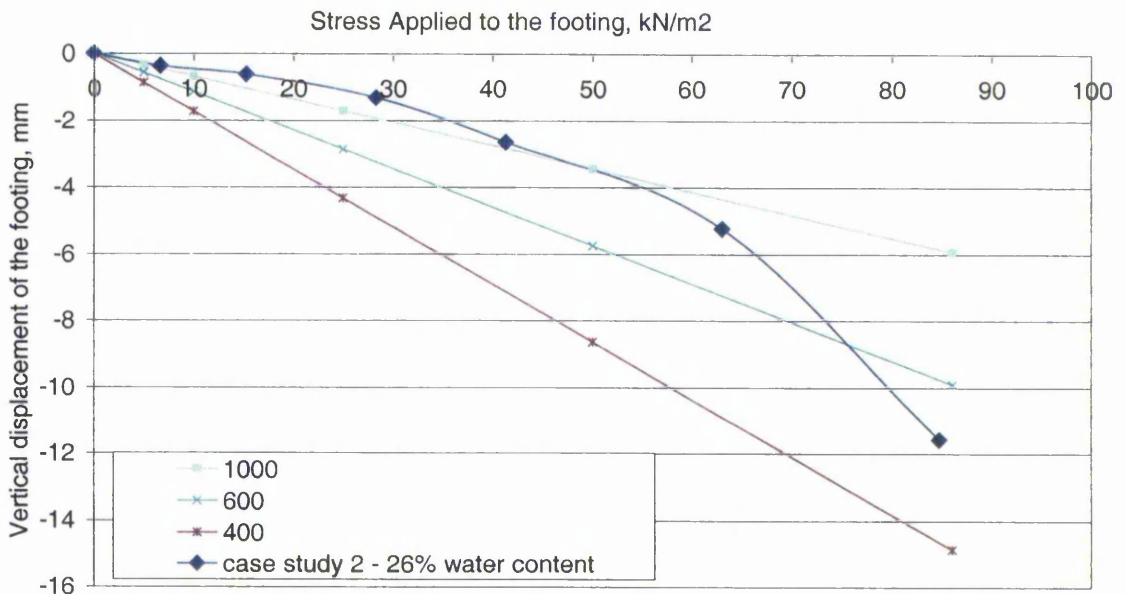


**Figure 7-19 Case 2 - Loading against displacement. A comparison between the laboratory footing model and the finite element model, for  $E = 400, 600$  and  $1000\text{kPa}$ .**

The analyses can predict the footing test reasonably well, even though a simple linear elastic model has been used. The analysis gave a particularly good prediction of the deflection of the footing due to the change in water level. The deflection due to load is less well predicted. It may have been better to use an elasto-plastic model, which can predict the

plastic deformation of the soil. However, these models take at least nine parameters, which must be accurately obtained and therefore are costly to collect.

### 7.9.3 Case Study 3: Loaded then saturated from top and bottom

In the laboratory model, the water was added from the top and the bottom. This gave the water content profile as shown in Chapter 6, Figure 6-19. This was also simulated by the finite element analysis. An estimate of Young's modulus was made for the water content of each of the layers in the soil from the values indicated by the triaxial tests. These properties were used in the analysis for each layer of the model.

For this more speculative case the soil was simulated by progressively softening each layer from top to bottom. As the water moved down the deposit, the change in height decreased as the effect of the load from the footing reduces. Figure 7-20 indicates how the deflection was affected by the depth of the water front moving down from the top finally producing the water content profile that was shown in Figure 6-19. The estimate of final deflection for the footing was less than the observed deflection in the laboratory model. The final deflection was estimated at 10mm, compared to 11.4mm which was observed in the footing model in the laboratory. This may be due to the over estimate of the unsaturated strength as seen from case 1 Figure 7-17 and an oversimplification of the wetting front.

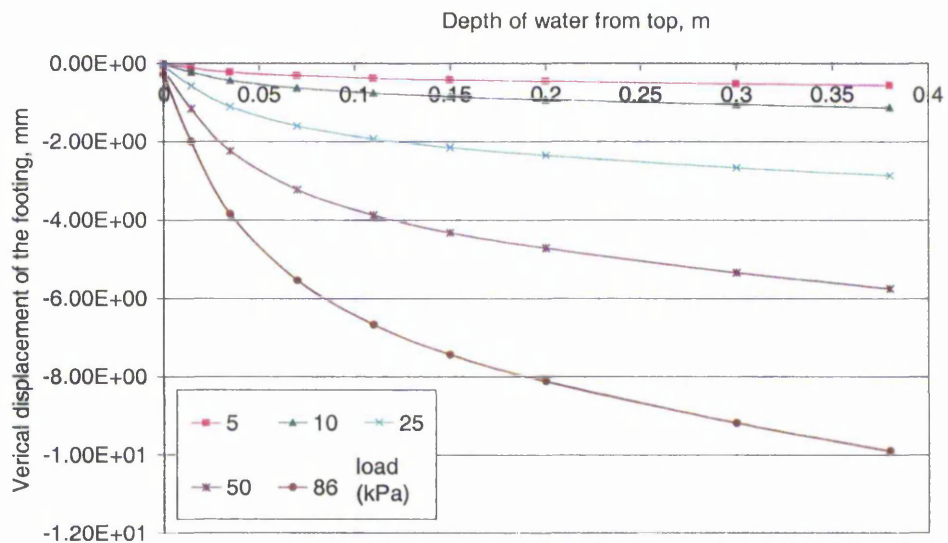
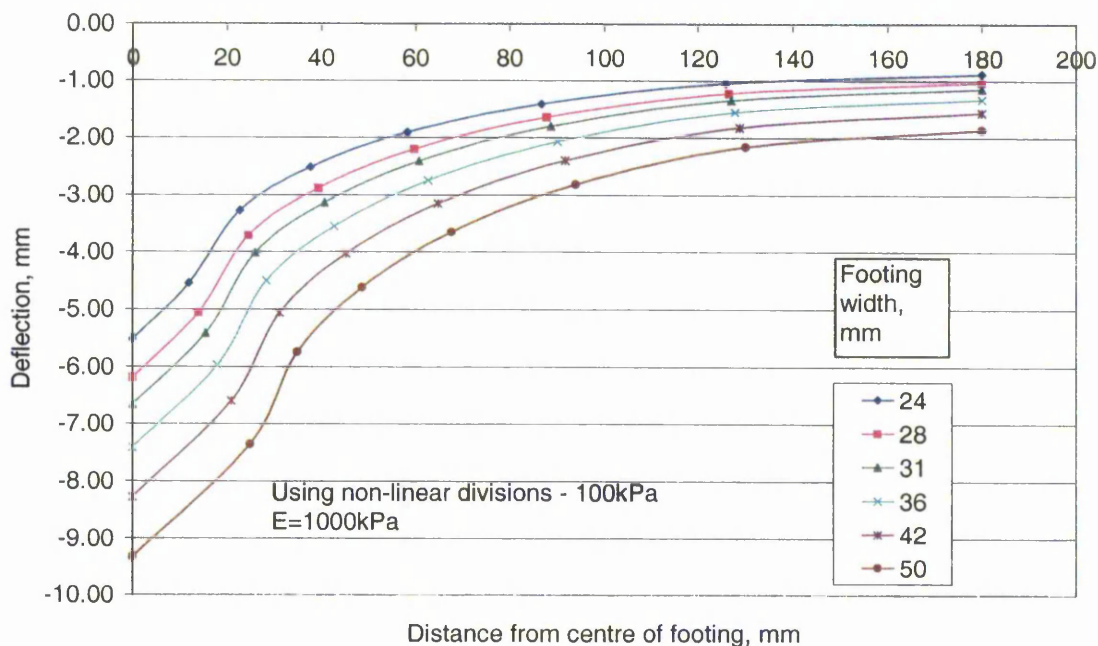


Figure 7-20 Case 3: deflections of footing due to wetting from the top

## 7.10 PARAMETRIC STUDIES

A sensitivity analysis using the finite element model was carried out to examine the effect of increasing the footing width and changing  $E_u$ . Using the elastic model the boundary effects were observed to reach around twelve times the width of the footing as shown in Figure 7-21. As the footing width increases the settlement increases but not quite linearly as shown in Figure 7-22. As expected, as Young's Modulus values decrease (i.e. as the soil becomes wetter and softer) more settlement occurs, as shown in Figure 7-23. The effect of varying Young's modulus,  $E$ , is much greater on the deflections when  $E$  is greater than 2500kPa, where a sudden change in deflection is observed. The value chosen for Poisson's ratio,  $\nu$ , for the finite element analysis also greatly affects the deflection of the soil as shown in Figure 7-24. The deflection is doubled by doubling Poisson's ratio,  $\nu$ . Poisson's ratio has more effect on the soil as the load increases as shown by Figure 7-24.



**Figure 7-21 Effect of footing width. NB 31mm was chosen for the laboratory footing model**

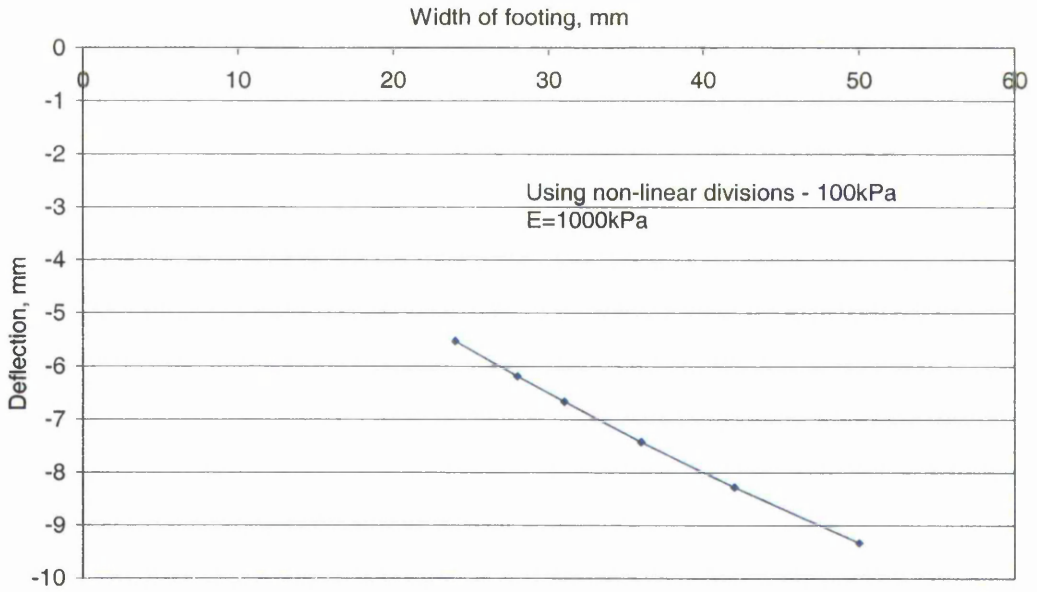


**Figure 7-22** Effect of the footing width on the deflection of the footing for a load of 100kPa and an Elastic modulus of 1000kPa.

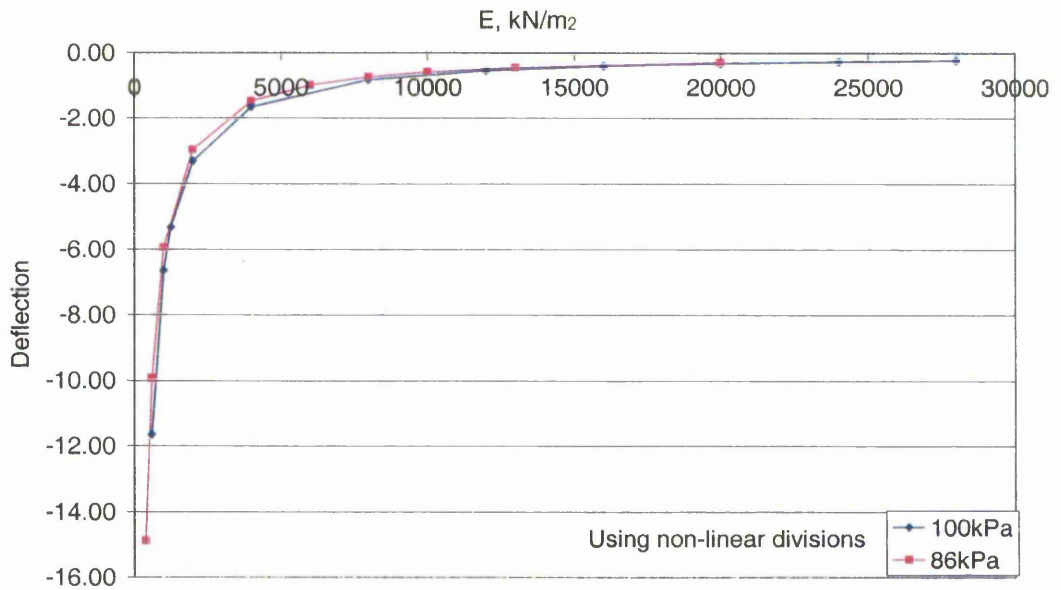


**Figure 7-23** Effect of the Elastic Modulus (E) on the deflection of the footing, for loads of 86kPa and 100kPa.

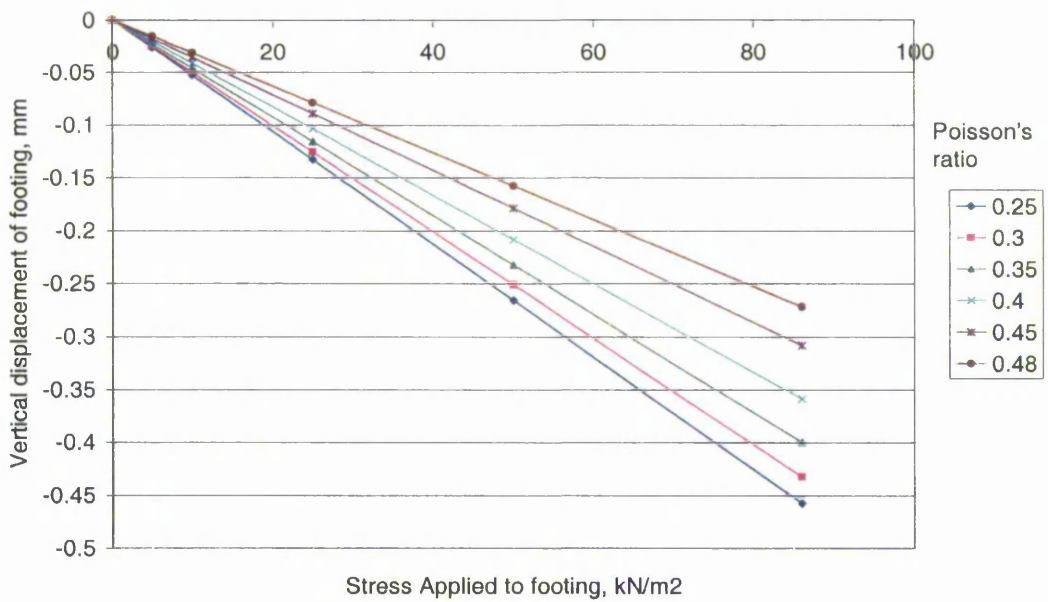


**Figure 7-24** The effect of Poisson's ratio on the deflection of the footing

### 7.11 SCALING EFFECTS

Non-linear and linear divisions of the finite element grid were examined. Both these methods gave the same results for deflection because of the simple elastic model used. A larger grid (400x800) was also examined, which did affect the results. The number of divisions along the width of the grid (10 and 20) did not affect the results given by the analysis. If a more complicated constitutive model was used then more elements would be needed and the number of elements would have an effect on the results. The main effect on the results, apart from  $E$  and  $\nu$ , was the size of the grid. At 86kPa, the deflection was 0.46mm and 0.53mm on the small and large grid respectively, illustrated in Figure 7-25. The boundary effects had a far greater effect on the results for the size of grid used than was originally expected. It is therefore important to choose large dimensions compared to the dimensions of the zone of interest. Figure 7-26 shows the deflections of the footing with load as modelled by the finite element analyses. The results for the double sized grid are shown as well as the grid used during the majority of the modelling. The method of dividing the grid did not affect the results given by the finite element analysis. The 7 non-linear divisions gave approximately the same result as for the 10 and 20 equally spaced divisions, however the larger grid affects the deflections significantly. Another point to note

was the difference in the predicted settlement from the finite element models for near the boundaries compared with those observed in the laboratory model.

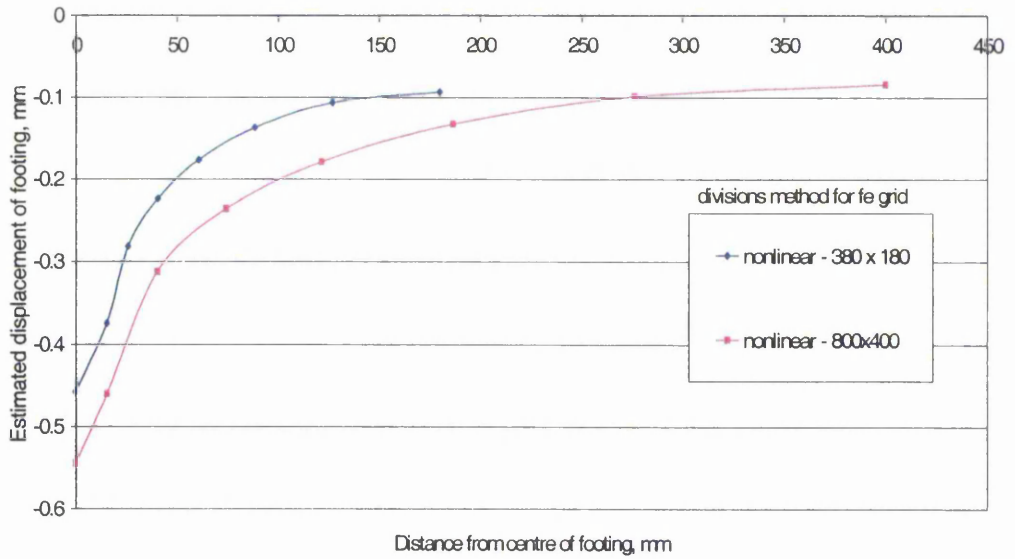


Figure 7-25 Effect of the size of the grid in the finite element analysis.

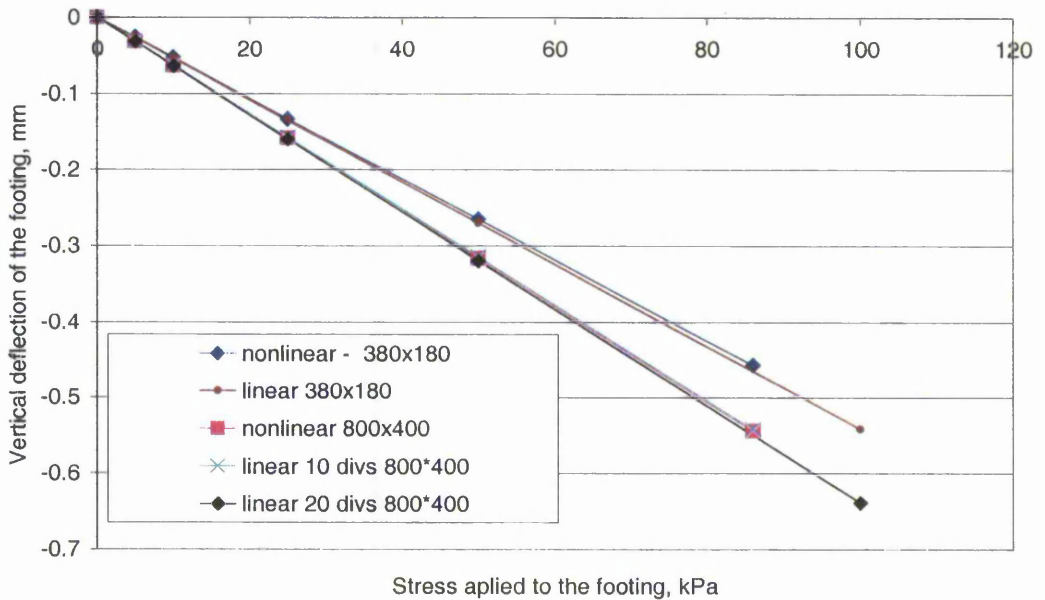
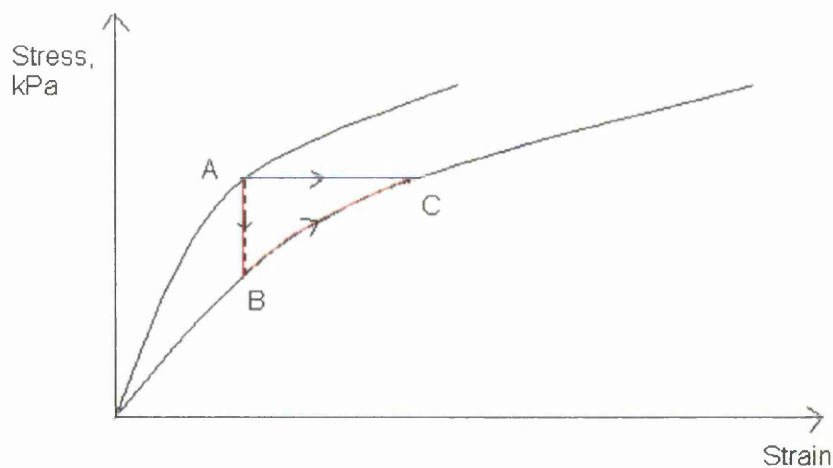


Figure 7-26 The effect of the division methods in the finite element analysis. Where the grid was divided into equal segments (linear) or into smaller segments nearer the footing (non-linear).

## 7.12 DEVELOPMENT OF COMPUTER MODELS

These experiments have shown how a simple finite element study could aid the understanding a soil's potential for collapse. Two sets of parameters should be obtained for the given soil, one for unsaturated and one for saturated. Unsaturated in this case would mean the current (low) moisture content and saturated is an estimate of the likely moisture content of the soil after wetting. Two simple stages of finite element analysis could be used. A model simulating the current state of any loading situation could be set up using known data on the unsaturated material. Then the same model could be run using the parameters obtained for the saturated material. The difference between the deformations at any given load would be the amount of collapse that could be expected if the deposit was wetted at this load. This process allows an estimate of the potential collapse for any situation where a soil is wetted. This is slightly different to the process employed by Naylor et al. (1989), where the soil elements are firstly loaded using the unsaturated parameters, secondly, the stress is reduced by an amount equating to a pseudo reduction in pore water pressure, with no changes in strain (A-B), see Figure 7-27. The stress is then increased by an amount equivalent to the excess pore water pressures using the Young's Modulus appropriate for the saturated soil (B-C). In the finite element analyses carried out in this project, two runs of the model were carried out, one for unsaturated and one for saturated soil up to the load that was of interest. The difference in deformation recorded for each run was assumed to be the amount of collapse that would be observed at that load (A-C).



**Figure 7-27 Stress-strain route to model collapse**

### 7.13 DISCUSSION

In this Chapter, a finite element program was used to model oedometer and triaxial tests, discussed in Chapter 4 and the footing tests, discussed in chapter 6. Simple linear elastic models were used for the majority of the tests. The collapse was modelled by defining two sets of properties, one for unsaturated material and one for the saturated material. The collapse obtained at any pressure was defined as the difference in strain between the results for the unsaturated and saturated material, at that pressure. A range of Young's Moduli were calculated for different water contents, so that varying water contents and therefore stiffness could be represented in the layers of the finite element model.

The linear elastic models did not simulate the stress-strain behaviour of the soil perfectly as the behaviour was not linear for the whole stress range tested. In the oedometer tests the soil became stiffer with load and in the triaxial and footing tests the soil became less stiff with load. However, for the low loads under consideration for the footing model, it was considered that an elastic model was adequate. Even though the linear model was an oversimplification of the behaviour of the soil, the transition from one stiffness to another modelled the collapse phenomenon well.

The simple elastic model could be changed for any constitutive model. The more complicated the model the more parameters that are needed to model the soil. Generating the parameters is a time consuming and costly process, so a simple model may be the more cost effective.

Figure 7-18 shows a comparison between the footing model and finite element model. Even though the soil was modelled with the linear elastic model the change in deflection with rising ground water level is modelled remarkably well. An estimate of the collapse that could occur below a footing can be made using this approach by estimating Young's Modulus values of the soil at the relevant moisture contents. A change in water content from 10-20% would be modelled by estimating the Young's Modulus values at these two water contents and running the finite element model for both of these cases. The difference between the strains that occur in the dryer material and the strains that occur in the wetter material represents the amount of collapse that would be expected if the water content

changed to the new wetter conditions. This approach is advantageous as very few parameters are needed and a good estimate of collapse can be made.

It has been shown from earlier research (e.g. Vanapalli et al. 1996) that wetting cycles can cause the material to behave differently. If a sample is wetted and then dried, the wetting curve on a graph plotting water content against suction is not the same as the drying curve. The suction for the drying curve is higher than for the same water content for the sample being wetted. Therefore, different Young's Modulus may be obtained for same water content. This has been neglected for this model where only one cycle of wetting has been considered. Since collapse occurs during wetting and once the sample has collapsed it will not collapse again, this assumption is adequate for modelling collapse in loess.

#### **7.14 APPLICATIONS**

The simple non-linear elastic model was intended to provide an easier way to model footing behaviour, without having to estimate critical state parameters and measure suctions. To use the conventional unsaturated soil models with any degree of certainty, months of testing are needed to provide the parameters for the model. Large factors of safety are usually used in bearing capacity calculations, of around 2.5-3 and months of testing can rarely be justified.

The model can be used for the following applications:

1. Any structure built on loess where the ground water may rise.
2. Movement of the ground due to inundation from above and below.
3. Effects on buildings supported by cemented collapsible soils.

## **8 Artificial Loess and its Correlation with World-wide Loess Deposits**

---

Despite the variety of origins and differences in thickness and age, loess is a remarkably uniform soil, in terms of minerals and geotechnical behaviour. In general loess around the world has a similar grain size distribution, mineral composition, open texture, low degree of saturation and bonds between the grains that are not resistant to water. Typical properties were given in Chapter 2, Table 2-1. The table shows the small range of values expected for world-wide loess deposits for LL, PL, PI, density and natural void ratio.

The common properties and composition were replicated in the artificial soil. The artificial soil was compared with loess from the UK during all stages of its development, using loess from sites in Essex and Kent. The materials behaviour was compared using Atterberg limits, tests in the oedometers and in triaxial equipment. The material was developed to behave like loess and then tested to evaluate the influencing factors on the magnitude of hydrocollapse observed in each specimen. Initial void ratio, dry density, initial saturation,

degree of saturation on wetting and clay content were all shown to have an influence over the behaviour of the deposit. Individually, it is easy to see the influence that these properties have on the behaviour of the specimens, if all other factors are kept the same. For example, oedometer tests showed that as the degree of saturation increases the hydrocollapse increases, until at 50% saturation, the influence of the water is decreased and above 70% saturation no additional hydrocollapse is observed, if no other factors are changed. However, if clay content and void ratios were initially different in each of the samples tested then a prediction of the effect on hydrocollapse would be more difficult. The artificial loess has been useful because such factors can be varied and controlled, enabling the factors to be evaluated one at a time. It is useful to quantify the degree to which the various factors affects the hydrocollapse, so that the behaviour of the soil can be predicted. The artificial loess is the first step to determining the relative influence of all of the parameters on the hydrocollapse behaviour of world-loess deposits.

### **8.1 BEHAVIOUR OF ARTIFICIAL LOESS**

From index tests, oedometer and triaxial tests on the artificial loess it was possible to examine the behaviour of the artificial material, designed to replicate collapsible loess soil. The artificial soil has been successful at replicating the following characteristics.

- Bonding – as seen in the SEM photographs. Clay bonds were observed between the larger silt particles. The clay particles provided strength when the soil had a low saturation, however, they broke down and provided little strength on wetting.
- Typical geotechnical characteristics such as, liquid and plastic limits, strength and stiffness tested in the oedometers and triaxial equipment were tested and compared with natural loess and values for the artificial loess lay within the ranges found for loess soils from the literature. Liquid limit and plastic limit were 27 and 17.5 respectively for the artificial soil and around 30 and 20 for the loess soil in Pegwell Bay. The Young's modulus for the unsaturated samples was 12.5 and 18kPa for the natural and artificial samples respectively. The strength,  $q_f$ , from the triaxial tests for both samples on unsaturated specimens was similar for both materials, around 500-600kPa, depending on water content.
- Collapse on wetting was also replicated in the artificial soil.

The artificial soil lacks carbonate bonding and organic matter that is often found in natural loess. However, this simplification allowed the influence of the clay content to be evaluated, other parameters may have clouded the issues. Now that the role of clay has been examined it would be possible to add other constituents to evaluate their role in the behaviour of loess-like soils.

## 8.2 COMPARISON OF ARTIFICIAL LOESS WITH WORLD DEPOSITS

### 8.2.1 Properties of the Artificial Material

Many specimens of artificial loess were tested in oedometer tests. A sample of the results are shown in Table 8-1. Clay content, moisture content and void ratio were varied and tested for hydrocollapse. The values for hydrocollapse ( $i_c$ ) of each specimen, saturated at 200kPa, are also shown in the table. Where,

$$i_c = \text{Percentage hydrocollapse} = \frac{100 (\text{Void ratio before flooding} - \text{void ratio after flooding})}{(1 + \text{void ratio before flooding})}$$

In Chapter 4, the influence of the properties in the artificial material were presented and discussed. The results from the oedometer tests have been used to further investigate the relationship between the properties of the soil and the magnitude of hydrocollapse observed in the tests. It was shown that water content, clay content and initial void ratio had a large influence over the void ratios that would occur in the specimen due to their influence over the way the particles pack. These properties were investigated to find out if there was a mathematical link between them, which would give an indication of the likely magnitude of hydrocollapse. First, an equation was investigated to find the void ratios before and after collapse, as hydrocollapse is calculated from the void ratio before and after collapse due to flooding. Secondly, an equation was developed to estimate the hydrocollapse directly.

All the results were combined into simultaneous equations, which were solved using Excel's Solver Add-In. Solver was used to find the values of the coefficients for a number of equations. The 'best' solution for each of the coefficients was evaluated by:

1. Minimising the sum of the difference between the predicted and actual void ratios for each of the specimens before and after collapse at 200kPa.
2. Minimising the sum of the differences between the predicted and actual hydrocollapse values at 200kPa.

Percentage Clay	Bonding Moisture Content %	Initial Void ratio, e	Void ratio pre-saturation at 200kPa	Void ratio after saturation at 200kPa	Initial water content %	Flooding water content %	$i_c$
10	29.43	0.74	0.64	0.6	0.41	17.96	2.44
10	25.73	0.64	0.61	0.57	0.74	17.99	2.48
30	16.38	1.02	0.898	0.83	0.41	8.81	3.58
30	16.86	0.88	0.8	0.73	0.55	9.39	3.89
20	29.6	0.72	0.67	0.6	0.28	19.58	4.19
30	29.86	0.81	0.72	0.63	0.11	8.53	5.23
30	29.82	0.78	0.69	0.6	0.12	21.85	5.33
40	29.9	0.78	0.72	0.62	0.07	19.31	5.81
60	31.93	0.78	0.71	0.61	0.13	22.27	5.85
30	16.8	0.72	0.68	0.58	0.66	13.89	5.95
50	28.62	0.8	0.74	0.63	1.08	16.83	6.32
30	17.08	0.81	0.72	0.61	0.36	19.45	6.40
30	17.05	0.87	0.77	0.64	0.38	12.95	7.34
10	17.27	0.97	0.73	0.6	0.2	23.02	7.51
30	17.73	0.71	0.67	0.53	0.87	28.14	8.38
10	16.13	1.03	0.89	0.72	0.42	20.11	8.99
10	13.4	1.44	0.7	0.54	0.17	20.89	9.41
35	16.13	1.28	0.59	0.44	0.31	28.87	9.43
25	15.96	1.24	0.56	0.41	0.12	29.28	9.62
20	17.39	0.95	0.75	0.57	0.09	19.81	10.29
30	17.18	0.88	0.81	0.62	0.37	15.81	10.50
5	21.11	1.4	0.926	0.72	0.1	21.96	10.70
30	17.36	0.89	0.79	0.58	0.22	22.94	11.73
15	16.98	1.34	0.85	0.62	0.06	19.2	12.43
20	14.62	1.28	0.93	0.68	0.07	18.76	12.95
30	16.34	0.84	0.77	0.53	0.99	17.7	13.56
20	21.06	1.17	0.86	0.6	1.13	18.67	13.98
20	17.94	1.02	0.93	0.66	1.35	18.49	13.99
25	16.01	0.99	0.86	0.59	0.65	17.07	14.52
25	15.53	1.13	0.84	0.57	0.32	15.51	14.67
25	15.06	1.2	0.84	0.57	0.04	18.13	14.67
15	25.98	1.35	1.11	0.8	0.3	20.04	14.69
15	13	1.41	0.9	0.62	0.31	17.67	14.74
30	16.14	0.94	0.83	0.56	1.17	17.12	14.75
30	15.68	0.86	0.73	0.47	1.57	18.58	15.03
30	18.47	1.29	0.91	0.62	0.17	17.46	15.18
30	16.94	0.99	0.84	0.56	0.48	15.98	15.22
40	19.22	1.18	0.97	0.67	0.45	19.77	15.23
30	13.08	1.02	0.89	0.58	4.07	18.29	16.40
30	15	1.32	0.89	0.58	0.49	17.8	16.40
20	17.47	1.28	0.71	0.42	0.97	17.15	16.96
40	17.09	1.17	0.94	0.61	0.35	20.33	17.01
40	15.14	1.35	0.88	0.56	0.39	20.01	17.02
30	17.31	1.01	0.82	0.51	0.26	19.26	17.03
60	17.48	1.34	0.98	0.64	0.02	25.64	17.17
50	17.46	1.21	0.97	0.62	0.04	21.8	17.77
60	22.12	1.63	1.19	0.79	0.31	29.02	18.26
35	20.99	1.31	1.05	0.67	1.04	21.35	18.54

Table 8-1 Properties and collapse coefficient,  $i_c$ , at 200kPa for the artificial loess

Solver uses an iterative procedure to solve the simultaneous equations. The results from 50 specimens were used to find the coefficients, as shown in Table 8-1.

### 8.2.2 The Void Ratio Approach

Firstly an equation was found to predict the void ratio of a deposit, depending on its initial void ratio, moisture content, and clay content. The equation which showed the best fit to the data was as follows

$$e_{200} = 0.412338 + 82.7798e_i - 0.003m + 6.48E-05c + 2.71E-06c^{2.701153} - 82.1863e_i^{1.001791} - 0.11839m^{-0.2421} - 0.1195e_i/m^{-0.37586} + 0.050041m/c^1 \quad (8.1)$$

where,  $e_{200}$  = void ratio at 200kPa,  $e_i$  = initial void ratio,  $m$  = water content %,  $c$  = clay content %

The initial void ratio,  $e_i$ , was included because it will affect the void ratio at 200kPa. The void ratio of two similar specimens will get closer as applied stress increases but at 200kPa the void ratio will still be influenced by the initial void ratio, as illustrated in Figure 8-1.

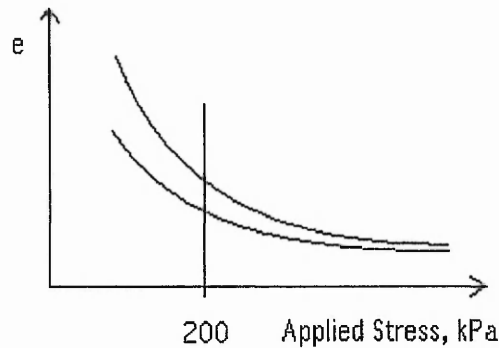


**Figure 8-1 Relationship between void ratio and applied stress for two samples with the same constituents but different initial void ratios**

The moisture content,  $m$ , also influences the void ratio of the sample. As shown in Chapter 4, the rate of change of void ratio decreases as the water content increases, as illustrated in Figure 8-2. It was therefore expected that the equation would have a  $m^{-0.5}$  element. This was later altered so that the  $-0.5$  could be changed as one of the coefficients, which provided a better fit to the actual values. Solver found the best solution for  $m^{-0.24}$ .

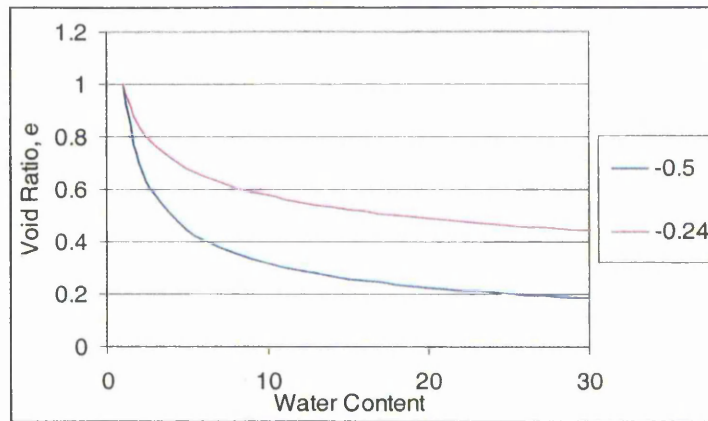


**Figure 8-2 Proposed relationship between moisture content and void ratio for different powers of m, -0.5 and 0.24.**

The clay content,  $c$  has also been shown to govern the packing void ratios throughout the oedometer tests. Initially, the equation was developed to have  $c^2$ , as illustrated in Figure 8-3. After this the power was used as another changeable coefficient, which helped the answers get closer. The final solution has  $c^{2.70}$ .

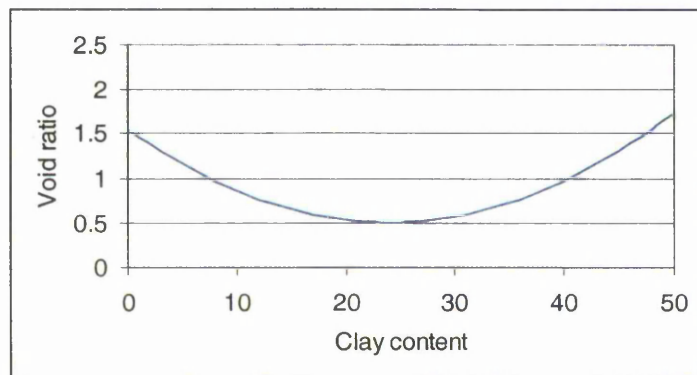


**Figure 8-3 Proposed relationship between Clay content and void ratio**

The ratio,  $e_i/m$ , was introduced because it was noticed that, as moisture content increased,  $e_i$  has less influence, as can be seen by the attenuation of the lines in Figure 8-1. The ratio  $m/c$  also increased the fit of the equation to the actual values. This was included because different moisture contents will have different influences depending on the fines, or clay, content.

The void ratios of the artificial specimens before and after wetting at 200kPa are shown in Figure 8-4. The estimated void ratio's given by the equation above are also shown.

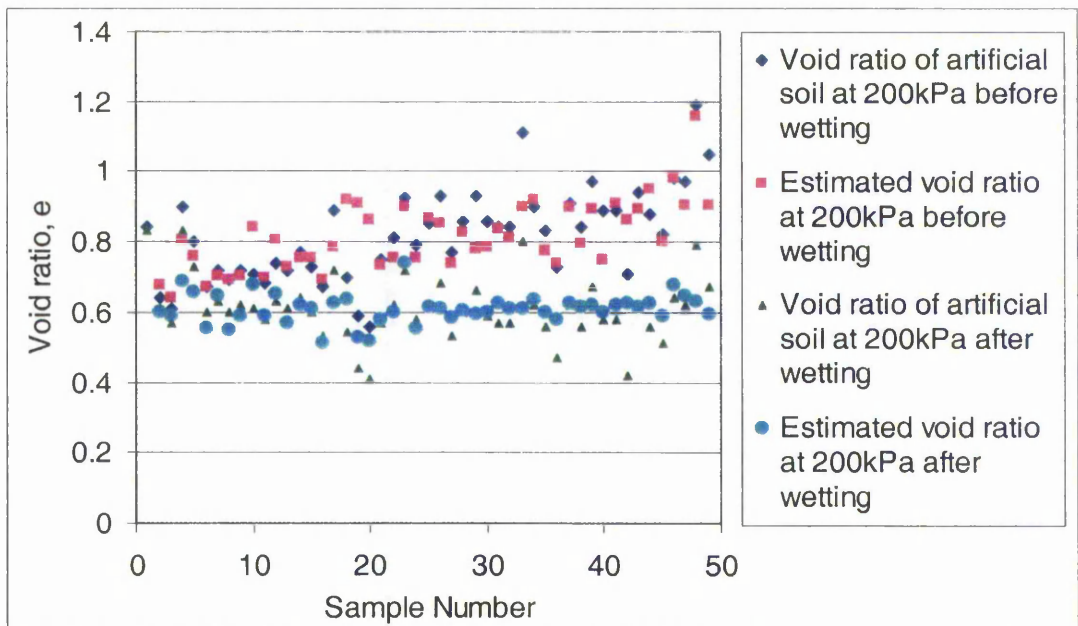


**Figure 8-4** Void ratios of specimens and the predicted void ratios given by Equation 1

The general magnitudes of the void ratios are predicted by the equations fairly well. There is more variance in the void ratios in the artificial soil specimens than in the estimated values.

The estimated void ratios were used to calculate the estimated hydrocollapse for each of the specimens. The estimated and actual hydrocollapse values are shown in Figure 8-5. The equation does not predict hydrocollapse particularly well, in some cases it is half the expected value and in others it is twice as much.

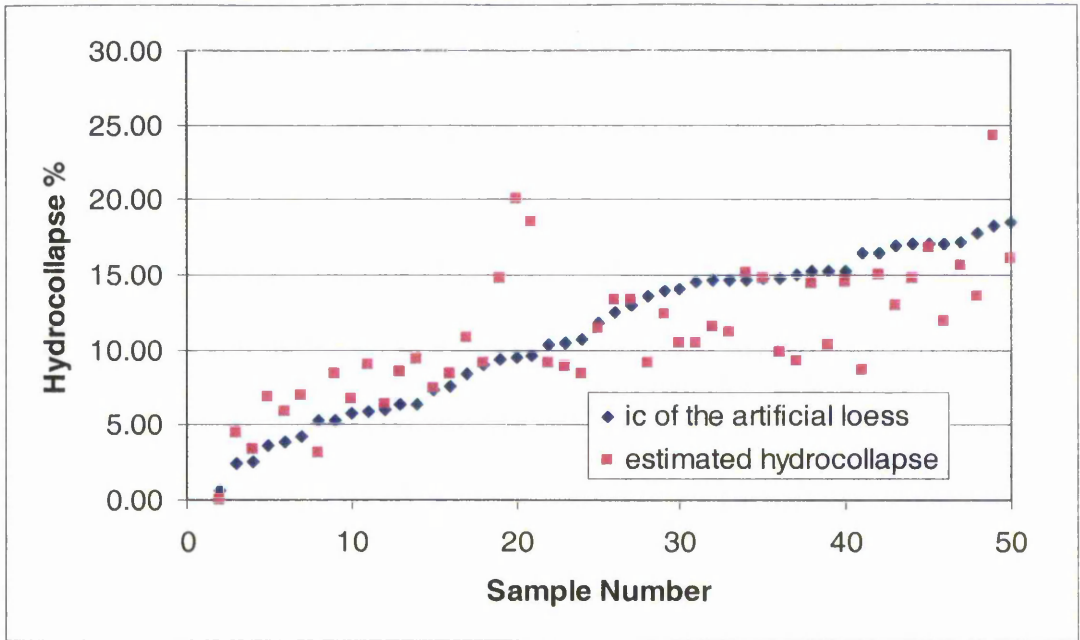


**Figure 8-5 Hydrocollapse as observed in the artificial soil specimens tested in the oedometer and estimated hydrocollapse calculated from equation 1.**

### 8.2.3 Hydrocollapse Approach

Solver was also used to predict the hydrocollapse values directly, rather than predicting the void ratios. This approach gave the equation:

$$\begin{aligned}
 &=1763.833 + 2394.171e_i + 1000.693m_i + 167.7314m_w - 2.84604c - 1346.76e_i^2 + 19.1797m_i^2 + \\
 &22.17579m_w^2 - 0.00346c^2 - 2720.3e_i^{0.5} + 2.185233m_i^{0.5} + 922.149m_w^{0.5} + 158.6231c^{0.5} + 295.9695e_i^3 \\
 &- 2.02565m_i^3 - 0.07104m_w^3 + 0.000109c^3 - 5059.04e_i^{0.018566} - 1004.02m_i^{1.026118} - 58.0026m_w^{1.751192} + \\
 &42.57121c^{0.4681}.
 \end{aligned} \tag{8.2}$$

This equation is a bit cumbersome and would not be very practical to use. The hydrocollapse values for the artificial soil were predicted slightly better using this approach, as can be seen in Figure 8-3. The estimated values for hydrocollapse follow the actual values fairly well, although the values can still vary by up to 30%.

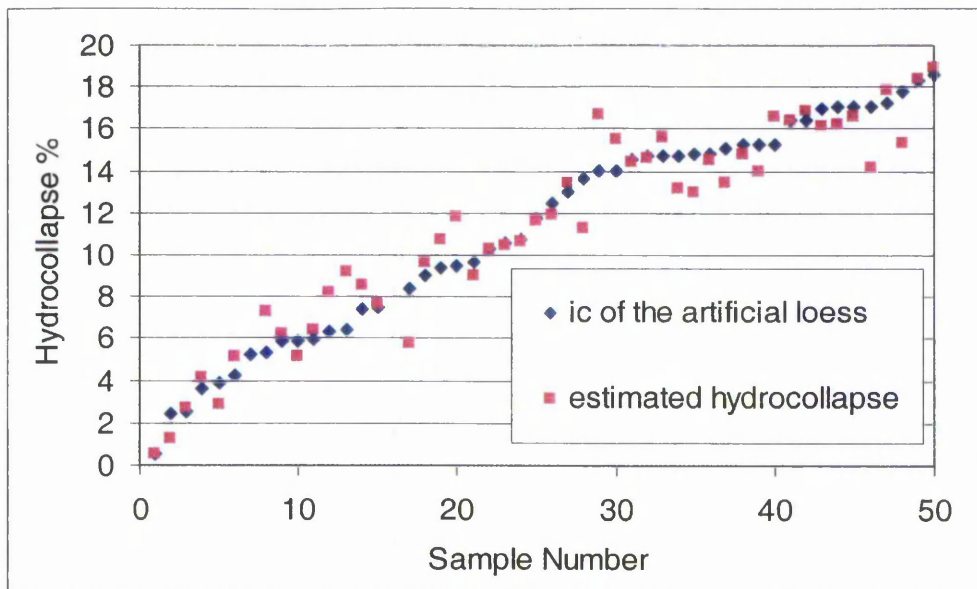


**Figure 8-6 Hydrocollapse values for oedometer specimens made with artificial soil compared to the estimated values of hydrocollapse given by equation 2.**

#### 8.2.4 Properties of Loess

To investigate how successful the artificial loess had been at replicating world deposits, the results from the artificial specimens were compared with results reported in the literature for natural loess around the world. There was a problem getting specific specimen data to compare against the artificial material. Many papers give a list of geological and mineralogical content of their samples but no collapse data, others give some coefficients of collapse but no data on the properties such as clay content. Alternatively, many papers give average properties over a whole range and 'typical results' of collapse tests, so the exact properties of the specimens can not be determined and directly compared with the artificial loess.

Kie (1988) report on a series of tests at stressed to 200kPa in the oedometer and flooded at different water contents. These results were ideal to compare with the equations that had been estimated using the artificial loess. Table 8-2 shows the results of this comparison. As can be seen, Equation 1 gives reasonable numbers for void ratios and hydrocollapse, although hydrocollapse is over estimated. Equation 2 gives very strange results. Although Equation 2 tied in very well with the results from the artificial specimens it was not useful for predicting the behaviour of the Chinese Loess presented by Kie (1988).

$e_i$	1.15	1.15	1.15	1.15
$m_i$	8.50	8.50	8.50	8.50
$m_w$	12.00	16.00	24.50	31.00
$c$	22.00	22.00	22.00	22.00
$i_c$	1.46	3.40	4.85	5.83
$e^l$	1.06	1.06	1.06	1.06
$e^l$	1.03	0.99	0.96	0.94
Equations:				
Estimated e-before wetting (1)	0.70	0.70	0.70	0.70
Estimated e-after wetting (1)	0.66	0.62	0.55	0.51
Estimated hydrocollapse (1)	2.32	4.58	8.57	11.16
Estimated hydrocollapse (2)	-378.95	-376.23	-374.456	-387.472

**Table 8-2 Estimated hydrocollapse for specimens reported in the literature in Kie (1988). Where  $e_i$  = initial void ratio,  $m_i$  = initial water content,  $m_w$  = flooding water content,  $c$  = clay content,  $i_c$  = collapse coefficient,  $e^l$  = void ratio before wetting,  $e^l$  = void ratio after wetting.**

### 8.2.5 Conclusions from the predictive equations

Unfortunately, much of the literature does not generally give enough information on specific specimen properties to compare the prediction of the equations to actual collapse data. This work shows that it may be possible to build such equations for prediction, but these equations need careful consideration. The equations that work well for one type of deposit may not work for another.

This preliminary work shows that there is a link between world loess deposits. The amount of hydrocollapse for a given applied stress is the product of a very sensitive and intricate combination of all the properties in loess. The artificial loess could be further developed to include carbonate bonding and organic content. Further oedometer tests on this artificial soil could provide comprehensive data to produce predictive equations of the type shown in this discussion. These equations would be useful for engineers who know the properties of the ground but have not undertaken oedometer tests to test for collapsibility.

## 8.3 PARAMETERS AFFECTING COLLAPSE

The artificial material has been very useful to determine the influence of clay content and water content of the specimens. During formation of the sample, clay content, water content and compressive stress affected the void ratio. The water content during testing affected the stiffness of the sample. The clay content, moisture content and applied stress affected the

final void ratio. All these factors therefore have an effect on the amount of hydrocollapse observed in the sample.

It was shown that soils with a water content of 10-15% are particularly sensitive to collapse as a change in water content of just a few percent will cause significant collapse of the deposit. Once the deposit has become more than 50% saturated, most of the collapse of the voids will have occurred and an increase in water content will not have a significant affect on the deformation of the deposit.

The formulation of the equations above, show that there are many more factors affecting the collapse. Their relationship with magnitude of hydrocollapse is complicated and not easily determined, however, the fact that some correlation has been observed between the individual deposits means it could be possible to predict the amount of hydrocollapse from the properties of the soil. The equation would have to be formed using a large number of tests, with carefully controlled samples with known constituents. This would be an excellent role for the artificial soil, whose constituents can easily be varied and most importantly, controlled.

As was shown in the oedometer tests and with the computer simulation in chapter 5, clay content will affect the void ratio of a deposit, water content was also shown to affect the void ratio of the deposit. It has been shown that the hydrocollapse phenomenon is intrinsically linked to particle packing.

#### **8.4 SUGGESTED METHOD FOR ASSESSING THE COLLAPSE OF A DEPOSIT UNDER LOAD**

1. Find the initial water content profile for the depth of influence of the proposed load.
2. Estimate the changes in water content that could occur around the footing. This may be a change due to changes in ground water level or ponding of water at the surface.
3. Triaxial tests (unconsolidated, undrained) should be performed on specimens at their natural void ratios on varying water contents from natural water content up to saturated. Use the water contents that are relevant to the estimated water contents that could be expected in the problem being modelled.

- The soil will soften with increasing water content, as illustrated in Figure 8-7. The properties for each of the specimens at different water contents should be calculated. Find Young's modulus,  $E$ , for the deposit for each water content, if an elastic analysis is to be used. This should be done by taking the gradient of the linear part of the stress-strain graph for low stresses (less than 100kPa) for each of the triaxial tests.

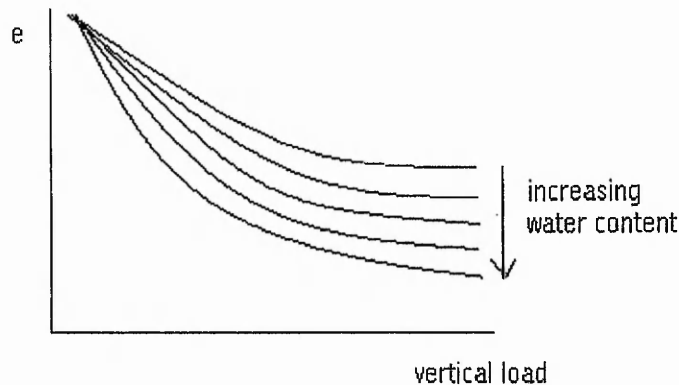


**Figure 8-7 Change of void ratio with vertical loading for various water contents**

- Analysis of the problem can be performed according to the expected increase in water contents. First perform the analysis using the parameters for the natural water content of the soil. The analysis can be split into layers so that different water contents and therefore different soil properties can be modelled for the different layers. The properties of each layer can then be changed to represent a softer layer and the analysis is run again. The difference in settlement observed between the runs of the analyses will give an indication of the amount of collapse that could be expected from the increase in water content being modelled. This process can be repeated until all stages of saturation have been modelled.
- The difference in deformations between the analyses represents the amount of collapse that is likely to occur due to wetting of the soil while under load.

## **9 Conclusions and Recommendations for Further Research**

---

Loess is probably the best known and one of the most widely spread collapsible deposits. This thesis has concentrated on this particular collapsible deposit. However, the methods of testing and modelling that are discussed, could equally apply to other collapsible soils.

Collapsible soils significantly reduce in volume when wetted under load, a phenomenon commonly called hydrocollapse. Hydrocollapse can lead to building collapse, landslides and consequently loss of life. Collapsible soils are therefore a significant concern for construction engineers, who need to design safe, robust and cost effective buildings. Hence, they present a major geohazard to the built environment.

Laboratory tests indicate parameters that relate to an element of soil. The values obtained from the oedometer and triaxial tests can be used in various analyses to determine the soil behaviour under different loading conditions. From the oedometer tests, values for the one-

dimensional constrained modulus  $D$  were found. Triaxial tests provided values for Young's modulus,  $E$ , for low stresses, where stress-strain behaviour was near linear. Although Young's modulus is an elastic parameter it was used to describe the stiffness of the material during loading up to 100kPa. This is a simplification but the behaviour of the soil up to this stress was near linear, especially for the dry soil. The oedometer and triaxial data has enabled a simple FEM analysis of a footing to be carried out. Results from this analysis have been compared with the laboratory footing model. The FEM studies were able to predict the compression of the soil very well.

The aims of this project have been to:

1. Further develop the artificial soils developed by Dibben (1998) and Assallay (1998), to evaluate the key parameters that effect collapse.
2. Investigate the findings from the laboratory tests using a computer simulation.
3. Use the developed artificial soil in a laboratory footing model, to investigate the effect of rising ground water level on a strip footing and to provide data for comparison with a FEM analysis of the same problem.
4. Use FEM techniques to model the collapse of the laboratory footing model.

## **9.1 DEVELOPMENT OF ARTIFICIAL LOESS**

### **9.1.1 Conclusions**

An artificial collapsible deposit was successfully developed to mimic the behaviour of natural loess soils. The preparation of the artificial soil could be controlled and the properties varied to enable an evaluation of the influence of the constituent parts. The main points are discussed below.

Liquid limit and plastic limit tests were performed on the artificial loess and compared to that of natural loess. The Plasticity Index (PI) for the artificial soil was very similar to that of the natural soils. PI for natural loess soils varies between around 5-30. The PI for the artificial material was around 10. The artificial soil was in the lower range for PI.

Samples were made with the same compressive stress to ensure the specimens formed at their natural void ratio. This was a considerable benefit for evaluating the effect of clay content on the magnitude of hydrocollapse. Samples were previously prepared with the

same void ratio or same mass in each sample, this resulted in a peak hydrocollapse observed at 25% clay content. This peak was not observed for samples prepared with the same compressive effort.

Lower void ratios were observed for samples prepared with a higher water content (up to 30%), however, samples prepared using a water content of 20% or higher shrunk when dried, leaving the sample smaller than the oedometer ring that it was formed in. This problem was resolved by forming the samples in a slightly larger ring so that they could be transferred to the oedometer ring for testing. This was only carried out for a small number of samples. One of the main advantages of the artificial loess was that it could be formed in the oedometer ring thereby not be disturbed before testing, unlike a natural sample where sampling effects can affect the properties. Water contents of 17.5% were therefore used for majority of the tests. This produced samples with void ratios of about 1. The samples did not shrink when dried and therefore could be tested easily without disturbing them from where they were prepared.

Natural samples exhibit collapse when loaded and wetted as observed in the artificial loess. Hydrocollapse was observed in the artificial material for tests undertaken in the oedometers. The magnitude of the observed hydrocollapse was around 10%. Hydrocollapse was rather higher in the artificial soils compared to that of the natural loess, due mainly to slightly higher void ratios. Void ratios in the artificial soil were around 1.0 rather than around 0.8. When samples were made with void ratios of around 0.8, the magnitude of hydrocollapse in the artificial and natural specimens were similar. An artificial sample made with ground silica/kaolinite content 80/20 and a preparation water content of 27% had initial voids ratio,  $e$ , of 0.72 and exhibited hydrocollapse of 4.3 %. This specimen behaved like the specimens from Essex that were tested for comparison, where the void ratio was 0.78 and a hydrocollapse of 4.5% was observed.

Swelling behaviour was observed in both the natural and artificial samples when the samples were wetted at low loads in the oedometers. The swelling in the artificial samples could not be attributed to the clay mineral in the sample as kaolinite is not a swelling clay mineral. In the artificial samples it was likely to occur when a high compressive stress was used to compact the samples and/or a high water content was used in preparing the sample. Since the sample was over consolidated before the first stages of testing in the oedometers,

the samples swelled to find their natural void ratios and produce a more naturally consolidated material.

For samples that were prepared with the same compressive effort, increasing the clay content resulted in an increase in the observed magnitude of hydrocollapse of the specimens tested in the oedometers. This is something that could not be observed in the natural samples as all the other properties that could affect hydrocollapse were not controllable.

The influence of the saturation ratio after wetting on hydrocollapse was also tested. It was found that after 50% saturation most of the hydrocollapse has occurred. Increasing the saturation further only contributed a further 15% of hydrocollapse in the samples. At saturations greater than 70%, no further hydrocollapse was observed. This was observed using the oedometer tests and the triaxial tests.

Values for confined modulus,  $D$  and elastic modulus,  $E$  were obtained from the oedometer and triaxial tests. Linear constants such as these do not fully describe the behaviour of the samples, especially at higher loads, however, they were adequate for the low stress (up to 100kPa) that were important for this project. The values found for elastic modulus,  $E$ , were used to estimate the behaviour of a footing modelled in the FEM analysis.

The artificial loess modelled the behaviour of natural loess very well as shown by the comparisons to the UK loess in chapter 4 and the comparisons to world-wide loess deposits in chapter 8.

### 9.1.2 Further research

Carbonate bonds and organic matter could be added to the artificial material to make it more realistic. The addition of these factors would enable the evaluation of these constituents just as the clay content has been evaluated for this project. The continuation of this work would enable the influence of all the properties of the soil to be evaluated. A predictive equation like the ones developed in chapter 8 could be determined from tests on this soil. The constituents can be varied and controlled so a full range of properties could be tested. The tests should also be carried out for a wide range of wetting loads, in order to find the peak hydrocollapse for each combination of materials.

## 9.2 COMPUTER SIMULATIONS

### 9.2.1 Conclusions

A 2-dimensional simulation of the particles in the deposit was created in a computer program using the programming language visual basic. The program allowed different percentages of small particles (fines) to be simulated with larger particles (silt). The particles fell randomly and formed different packing structures, to produce unstable, metastable and stable arrangements. The unstable structures were created by allowing the particles to fall and land on the other particles. It was assumed that the particle was supported if any part of the particle came into contact with another particle. The metastable structures were simulated by assuming that a particle could balance if the contact point occurred up to  $3/5$  of the width of the particle. For stable structures the assumption was that particles could only balance if up to  $2/5$  of the particle width was supported. An even more stable arrangement was created by changing this value to  $1/5$  of the width.

The two-dimensional nature of the simulation limited how realistic the computer simulation could be. However, the clay contents were calculated so that the number of particles in the 2-dimensional simulation represented a slice of a three dimensional deposit. This made comparing the results from the simulation with the collapsible material in the laboratory much easier.

The void ratios of the metastable structures were around 0.9, which is very similar to the void ratios found in metastable loess deposits. The stable structures had void ratios of around 0.5 and the 'more' stable structure had void ratios of around 0.36. These void ratios are very similar to those found in collapsed natural loess.

The size and shape of the voids were also compared to those of natural loess. The elongated voids that were observed in the computer simulation are also observed in natural loess specimens.

### 9.2.2 Further Research

The particles were modelled as circles. It would be more realistic to extend the models to be more blade shaped, like the shape of the silt particles in loess. The particle orientation would also have to be considered. Particle orientation could be ignored for the current study

as the particles were circles. It would be more realistic to consider a three dimensional arrangement of particles. The void ratios of the simulations could then be compared to the void ratios in natural samples.

### **9.3 LABORATORY FOOTING MODEL**

#### **9.3.1 Conclusions**

The order of wetting and loading did not effect the amount of deformation recorded in the footing. The tests where the soil was loaded and then saturated showed 11mm of deformation under a load of 86kPa. The test on an initially saturated material, which was then loaded to 86kPa, also showed deformations of around 11mm.

An air gap was produced in the gravel layer due to suctions in the silty material. The suctions in the material drew the water up simulating the area just above the water table. The moisture contents of thin layers of the soil were taken after the test to find out the moisture content profile for the soil. The moisture content increased with depth below the footing but at the base of the soil the moisture content was lower. This was possibly due to the water draining back into the gravel layer because of the air gap that existed in the gravel layer.

It was difficult to track the water level in the model as the water lost its fluorescence as it rose up the material. Taking the moisture content at the end provided valuable information for modelling the soil in the FEM studies, however, it would have been advantageous to know exactly where the level of the water was for each stage of the test. The water level was back calculated using the amount of water that had been added, the known void ratio of the material and the final moisture content profile.

Ground water rising did produce collapse in the soil, which therefore created movement of the footing. Potentially far more damaging is the threat of water ponding at the top and making the top layers of soil collapse, as seen from the test that was wetted from the top and the bottom. The top layers of soil have the most load acting upon them and are therefore susceptible to larger collapse deformations when wetted. Also, the ground water rising is likely to be more uniform, whereas flooding from the top could occur at one side of the footing. This would produce differential settlement, which is far more threatening to the

structure built on the footing. Cracking and failure of the structure is more likely to occur from these differential settlements. It is therefore vital that remedial measures are taken to improve the ground below the footing, especially the layers of ground at the top where the load from the footing is the highest.

### 9.3.2 Further Research

The model tests would benefit from using different footing widths to estimate the scale effects that occur in the model. This would enable the model to be related to full –scale more easily.

The water level during the test could not be observed as the fluorescence in the water reduced as the water rose up through the deposit. The model would benefit from better monitoring of water level. This would enable better prediction of the water content in each of the layers, which was used in the later FEM studies of the footing test.

Monitoring of deformations within the soil at depth would be an advantage. This would enable better understanding of the depth of influence of the load and better comparison with the FEM studies. The footing model would possibly need to be larger with larger footing and larger deformations in the system to be able to pick up the deformations within the soil. The extensometers used by the BRE, for example, could measure internal deformations but only had an accuracy of 2mm, which would not have been accurate enough for this small-scale study.

## 9.4 FINITE ELEMENT ANALYSIS OF THE FOOTING

### 9.4.1 Conclusions

The footing test was modelled using an elastic analysis. This was a simplification of the problem, as the soil does not behave elastically, especially for high loads. The footing in the model was loaded to 86kPa. At these loads in the triaxial test the stress-strain behaviour of the artificial material was close to linear. The elastic analysis was therefore valid for these low stresses.

The artificial soil was tested in the triaxial apparatus at different water contents. Values for the stiffness,  $E$ , were estimated for each of the water contents from the stress-strain graphs

produced from the triaxial tests. Properties are needed for the soil at different water contents to model the soil as the ground water was raised and the soil reached saturation.

The soil and footing were modelled by using the different material properties for different water contents and simulating the load applied to the footing. The procedure assumes that the loaded and then wetted soil will reach the same stress-strain state as if it were wetted and then loaded. This was confirmed by the footing test carried out in the laboratory. The difference between the dry analysis and the saturated analysis provided the amount of collapse that should be expected from the system.

The footing in the laboratory test was loaded up to 86kPa. The finite element analysis was also carried out for stresses up to 86kPa. The finite element results compare favourably with the results found in the laboratory simulation. The values for elastic stiffness were taken as 13,000kPa for dry and 400kPa for wet, as found from the triaxial tests. The FEM analysis produced deformations of around 15mm. The same shape curve is observed as the wetting front rises up the deposit and the deformations are very similar in size. The final deformation in the footing test was around 17mm for test 2 and 11.5mm for test 3. The difference in deformations was due to the differences in initial and final moisture content profiles of the materials.

Any soil model can be used in the analysis. In this case an elastic model was used, but any model which describes the behaviour of the soil could be used, such as elastic plastic models or cam-clay. All that is needed is the relevant parameters for the soil model to be determined for different water contents. The situation can then be modelled by using these parameters and finding the difference in deformations for the analyses using the different water contents.

#### 9.4.2 Further Research

More complicated constitutive models could be used to model the soil behaviour. This would be particularly useful for the saturated soil, which did not deform linearly under load. This would enable better predictions of the soil behaviour under higher loads.

## **9.5 OVERALL CONCLUSIONS**

This work has brought together research from a diverse range of areas. The main areas of interest have been particle packing ideas from Earth Sciences, experimental test methods for elements of soil, widely used in Geotechnical Engineering and finite element methods, used by a wide range of disciplines. An important contribution to knowledge was the development of an artificial material which can be used to study collapse behaviour. An artificial soil is useful because the properties can be controlled, and so the behaviour of the soil can be evaluated in terms of its constituent parts. The artificial material has been compared with natural loess and has shown to model the collapse process successfully. The method of producing the artificial soil has been discussed. It is considered most effective to mix the dry silt and clay materials together, then mix in the water, making sure the water content is dry of optimum. Specimens can be formed insitu with the required compressive stress and then left to dry in the air or oven dried. Hydrocollapse of around 10% would be expected from a material prepared with approximately 17% water content and tested in the oedometer at a wetting stress of 200kPa.

Triaxial tests were used to find an estimate of Young's modulus for the artificial material for a range of water contents from dry (0% water content) to saturated (around 30% water content). The artificial material was used to create the founding soil for a model footing test. The tests showed that the order of wetting and stressing did not affect the final amount of settlement of the footing. An adaptation of common finite element techniques was used to model the footing test, using the fact that the same stress-state is achieved whether an element of soil is loaded and then saturated or saturated and then loaded. An estimation of the amount of collapse that can be expected from a footing subjected to increasing ground water levels was made. A linear analysis was carried out using the estimates of Young's modulus for the artificial soil. In the analysis, the soil was divided into layers. First the settlement of the footing founded on dry soil was estimated. Then the first layer of soil was assigned a value of Young's modulus more representative of a softer, saturated soil. The settlement due to an increase of ground water through the first layer was estimated as the difference in the settlement between the first analysis and the second. This process was repeated through all the layers of the deposit. The estimated settlements of the footing test compared well with the actual settlements observed in the scale model of the footing.

## Acknowledgements

---

A big thank you to Dr. Ian Jefferson for his continuing support and encouragement. Also, thank you to Prof. Ian Smalley and Dr. Youcef Djerbib for their advice and supervision.

I would also like to thank:

Judy for her help with the oedometer and triaxial tests and the technicians, Mark and Alan for building the footing model box.

Mum and Dad for their motivation and especially to Mum for typing all those references out.

And finally, to Chris for keeping my feet on the ground and for his long suffering patience.

REFERENCES

---

- Abelev, M. Yu. [1948]. *The essentials of designing and building on macroporous soils*. Stroivenmorizdat Moscow 203p (in Russian).
- Abelev, M.Yu. [1988] *Loess and its engineering problems in the USSR*. In Proc. Of Conf. on Engng. Problems of Regional Soils, 1988, pp 3-6.
- Alonso, E.E. and Gens, A. [1993] *On the mechanical behaviour of arid soils*. In: Proc. 1<sup>st</sup> Int. Symp. On Engng Characteristics of Arid Soils, London, 173-206.
- Alonso, E.E., Gens, A. and Whight, D. [1987] *Special Problem Soils* General Report 9<sup>th</sup> European Conference on Soil Mechanics and Foundation Engineering, Durban, South Africa, Vol. 3, pp 1087-1146.
- Anderson, W. F. and Blanchfield, R. [1997] *Settlement of opencast mine backfill in large scale laboratory tests* Proceedings of International Conference on Land Reclamation and Rehabilitation, Penang, Malaysia, pp 406-417.
- Anderson, W.F., Pyrah, I.C., McKinlay, A. and Salmon, T.H. [1993] *The deformation behaviour of partially saturated granular fill at low stress levels*, Engineered Fills, Thomas Telford, London pp153-167.
- Assallay, A.M. [1998] *Structure and hydrocollapse behaviour of loess*. Unpublished PhD Thesis, Loughborough University of Technology.
- Bally, R.J. [1988] *Some specific problems of wetted loessial soils in civil engineering*. Eng. Geol., Vol. 25, pp 303-324.

- Barden, L., McGown, A. and Collins, K. [1973] *The collapse mechanism in partly saturated soil*. Eng. Geol. Vol. 7, pp 49-60.
- Basma, A.A. and Tuncer, E.R. [1992] *Evaluation and Control of Collapsible Soils*. Journal of Geotechnical Engineering, Vol. 118, No.10, pp 1491-1503
- Blanchfield, R. and Anderson, W.F. [2000] *Wetting collapse in opencast coalmine backfill*. Proceedings of the Institution of Civil Engineers, Geotechnical Engineering, Vol 143, pp. 139-149.
- Bell, F.G. [2000] *Silt, Loess and Brickearth*. Engineering Properties of Soils and Rocks, Blackwell Science, 4<sup>th</sup> Edition, Chapter 3, 47-67
- Bell, F.G. and de Bruyn, I.A. [1997] *Sensitive, Expansive, Dispersive and Collapsible Soils*. Bulletin of the International Association of Engineering Geology, Vol. 56, pp. 20-37
- Blight, G.E. [1965] *A study of effective stress for volume change*. In: Moisture Equilibria and Moisture Changes in Soils Beneath Covered Areas, Australia, 1965, pp 259-269.
- BSI [1990] Methods of test for soils for civil engineering purposes. *British Standard 1377*, British Standards Institution, London, U.K.
- Bolton, M.D. [1979] *A guide to soil mechanics*. Macmillian, London
- Burland, J.B. [1965] *Some aspects of the mechanical behaviour of partly saturated soils*. In: Moisture Equilibria and Moisture Changes in Soils Beneath Covered Areas, Australia, 1965, pp 270-278.
- Charles, J.A. and Watts, K.S. [1996] *The assessment of the collapse potential of fills and its significance for building on fill*. Proc. Instn. Civ. Engrs. Geotech. Engng, Vol 119, pp 15-28
- Culshaw, M.G., Hobbs, P.R.N. and Northmore, K.J. [1992] *Engineering Geology of Tropical Red Clay Soils Technical Report*. Report WN/93/14 Manual Sampling Methods British Geological Survey
- Culshaw, M.G., Hobbs, P.R.N. and Northmore, K.J. [1993] *Engineering geology of tropical red clay soils:- manual sampling methods*. BGS Technical Report No. WN/93/14 (ODA/BGS R and D PROJECT 91/18).
- Denisov, N. Ya. [1951] *The engineering properties of loess and loess loams*. Gosstroizdat, Moscow, Vol. 136. (In Russian).

- Derbyshire, E. and Mellors, T.W. [1988] *Geological and geotechnical characteristics of some loess and loessic soils from China and Britain: a comparison*. Eng. Geol. Vol. 25, pp 135-175.
- Derbyshire, E., Meng, X. and Dijkstra, T.A. [2000] *Landslides in the thick loess terrain of north-west China*. John Wiley & Sons Ltd, Chichester, UK
- Desai, C.S. and Abel, J.F. [1972] *Introduction to the finite element method; a numerical method for engineering analysis*. Van Nostrand Reinhold, New York.
- Dibben, S.C. [1998] *A Microstructural Model for Collapsing Soils*. Unpublished PhD thesis, Nottingham Trent University.
- Dibben, S.C., Jefferson, I.F. and Smalley, I.J. [1998] *The 'Loughborough loess' Monte Carlo model of soil structure*. Computers and Geosciences, Vol. 24, No. 4, pp 345-352.
- Dijkstra, T.A., Smalley, I.J. and Rogers, C.D.F. [1995] *Particle packing in loess deposits and the problem of structure collapse and hydroconsolidation*. Eng. Geol. Vol. 40, pp 49-64.
- Dineen, K. and Burland, J.B. [1995] *A new approach to osmotically controlled oedometer testing*. In Alonso, E.E. and Delage, P. (Editors) Proc. 1<sup>st</sup> Int. Conf. on Unsaturated Soils, Paris, France. pp 459-465.
- Dudley, J.H. [1970] *Review of collapsing soils*. Journal of the Soil mechanics and Foundations Division. ASCE. Vol. 3, May, pp 925-947.
- El-Ehwany, M. and Houston, S.L. [1990] *Settlement and Moisture Movement in Collapsible Soils*. Journal of Geotechnical Engineering Vol. 116, pp 1533-1534
- El-Ruwaih, I.A. and Touma, F.T. [1986] *Assessment of the engineering properties of some collapsible soils in Saudi Arabia*. In Proc. 5<sup>th</sup> Int. IAEG Congress, Buenos Aires, pp 563-569.
- Erol, O.A. and El-Ruwaih, I.A. [1982] *Collapse behaviour of desert loess*. In: Proc. 6<sup>th</sup> Congress Int. Assoc. of Engng Geol., Vol. 1, New Delhi, India, pp 443-448.
- Evstatiev, D. [1995] *Design and treatment of loess bases in Bulgaria*. In: Derbyshire, E., Dijkstra, T. and Smalley, I.J. (Editors). Proc. of the NATO Advanced Workshop on Genesis and Properties of collapsible soils. pp. 375-382.

## References

---

- Farias, M.M. [1993] *Numerical analysis of clay core dams*. Unpublished PhD Thesis, University of Swansea, Wales.
- Farias, M.M., Assis, A.P. and Luna, S.C. [1998] *Some traps in modelling of collapse Problematic Soils*. In: Proc. of the Int. Symp. on Problematic Soils, Yanagisawa, E., Moroto, N. and Mitachi, T. (Eds). Sendai, Japan, October, pp 309-312
- Feda, J. [1966] *Structural stability of subsident loess soils from Praha-Dejvice*. Eng. Geol. Vol. 1, pp 201-219.
- Feda, J. [1995] *Mechanisms of collapse of soil structure*. In: Derbyshire, E., Dijkstra, T. and Smalley, I.J. (Editors). Proc. of the NATO Advanced Workshop on Genesis and Properties of collapsible soils. pp 149-172.
- Fookes, P.G. and Best, R. [1969] *Consolidation characteristics of some Late Pleistocene periglacial metastable soils of East Kent*. Quarterly Journal of Eng. Geol. Vol. 2, pp 103-128.
- Fredlund, D.G. and Morgenstern, N.R. [1977] *Stress state variables for unsaturated soils*. Journal of geot. Eng. Division, ASCE, Vol. 103, pp 447-466.
- Fredlund, D.G. and Rahardjo, R. [1993] *Soil Mechanics for Unsaturated Soils*. John Wiley & Sons, Inc., New York
- Gourui, G. [1988] *Formation and development of the structure of collapsible loess in China*. Eng. Geol. Vol. 25, pp 235-245.
- Gens, A. and Alonso, E.E. [1992] *A framework for the behaviour of unsaturated expansive clays*. Canadian Geotechnical Journal. Vol. 29, pp 1013-1016
- Gens, A. and Nova, R. [1993] *Conceptual bases for a constitutive model for bonded soils and weak rocks* In: Geotechnical Engineering Proceedings of the International Symposium on Hard Soils – Soft Rocks, Athens. pp 485-494
- Gibbs, H.J. and Bara, J.P. [1962] *Stability problems of collapsing soils*. ASCE Journal of Soil Mechanics and Foundation Division, Vol. 92, pp 577-594.
- Graton, L.C. and Fraser, H.J. [1935] *Particle Packing* Journal of Geol. Vol. 43, pp 785-909.
- Handy, R.L. [1973] *Collapsible Loess in Iowa*. Soil Science Society of America Vol. 37, pp 281-284.
- Head, K.K. [1990] *Manual of soil laboratory testing*. Vol. 2, Permeability, shear strength and compressibility, Pentech Press, London.

## References

---

- Holtz, W.D. and Gibbs, H.J. [1951] *Consolidation and related properties of loessic soils*. Am. Soc. Text. Mat. Spec. Tech. Pub. Vol. 126, pp 9-33.
- Houston, S.L., Houston, W.N. and Spadola, D.J. [1988] *Prediction of Field Collapse of Soils due to Wetting* Journal of Geotechnical Engineering Vol. 114, No.1 pp 40-58.
- Houston, S.L., Houston, W.N., Zapata, C.E. and Lawrence, C. [2001] *Geotechnical engineering practice for collapsible soils*. Geotechnical and Geological Engineering, Vol. 19, pp 333-355.
- Ishihara, K. and Harada, K. [1994] *Cyclic Behaviour of Partially Saturated Collapsible Soils subjected to Water Permeation* pp 34-49
- Jennings, J.E. and Burland, J.B. [1962] *Limitations to the use of effective stress in partly saturated soils*. Geotechnique, Vol. 12, pp 125-144.
- Jennings, J.E. and Knight, K. [1975] *A guide to Construction on or with Material exhibiting additional settlement due to collapse of grain structure*. In: Proc. of the 6<sup>th</sup> regional conference for Africa on soil mechanics and foundation engineering, Durban South Africa. pp 99-105.
- Justo, J.L. Delgado, A. and Ruiz, J. [1984] *The influence of stress-path in the collapse-swelling of soils in the laboratory*. In: Proc. of the 5<sup>th</sup> International conference Exp Soils: Adelaide. pp 67-71.
- Kane, H. [1969] *Consolidation of two loessial soils*. Highway Research Record No. 284, pp 26-36
- Kane, H. [1973] *Confined Compression of Loess*. In: Proc of the 8<sup>th</sup> International Conference on Soil Mechanics and Foundation Engineering Moscow Vol. 2, pp 115-122
- Kerr, P.I. and Drew, I.M. [1968] *Quick-Clay Slides in the U.S.A.* Engineering Geology Vol. 2, pp 215-238
- Klukanova, A. and Frankovska, J. [1995] *Monitoring of collapsible soils in Slovakia*. Slovak Geological Magazine, Vol. 5, pp 53-61.
- Knight, K. [1963] *The origin and occurrence of collapsing soils*. In: Proc. 3rd African Reg. Conf. Soil Mech. & Found. Eng. Vol. 1, pp 127-130.
- Lawton, E.C. [1986] *Wetting induced collapse in compacted soil* Ph.D. Thesis, Washington State University, Pullman, Washington.

- Lawton, E.C., Frigaszy, R.J. and Hardcastle, J.H [1989] *Collapse of compacted clayey sand*. ASCE, Journal of Geotechnical Engineering Vol. 115, pp 1252-1267.
- Lawton, E.C., Frigaszy, R.J. and Hetherington, M.D. [1992] *Review of Wetting-Induced Collapse in Compacted Soil*. Journal of Geotechnical Engineering Vol. 118, pp 1376-1392
- Leroueil, S. and Vaughan, P.R. [1990] *The general and congruent effects of structure in natural soils and weak rocks* Geotechnique Vol. 40, pp 467-488
- Lloret and Alonso, E.E. [1985] *State surfaces for partially saturated soils*. In: Proc. 11<sup>th</sup> Int. Conf. Soil Mech. and Found. Engng, Vol. 2, San Francisco, 557-562.
- Luttenegger, A.J. and Hallberg, G.R. [1988] *Stability of loess*. Eng. Geol. Vol. 25, Nos. 2-4, pp 247 – 261.
- Luttenegger, A.J. and Saber, R.T. [1988] *Determination of collapse potential of soils*. Geotech. Testing Journal, Vol. 11, No. 3, pp 173-178.
- Mackechnie, W.R. [1993] *General report/ discussion session 7:- collapsible and swelling soils – part 1:- collapsible soils*. Proc. of the 12<sup>th</sup> Int. Conf. on Soil Mech. and Foundation Eng. Vol. 4, part 122, pp 2485–2490.
- Maswoswe, J. [1985] *Stress path for a compacted soil during collapse due to wetting*. Unpublished PhD thesis, Imperial College, London.
- Matyas, E.L. and Radhakrishna, H.S. [1968] *Volume change characteristics of partially saturated soils*. Geotechnique, Vol. 18, pp 432-448.
- Mellors, T.W. [1978] *Geological and engineering characteristics of some Kent brickearths*. Unpublished PhD thesis, University of London
- Morrow, N.R. and Graves, J.R. [1969] *On the Properties of equal sphere packings and their use as ideal soils*. Soil Science Vol. 108, pp 102-107
- Naylor, D.J., Tong, S.L. and Shahkarami, A.A. [1989] *Numerical modelling of saturation shrinkage*. Numerical Models in Geomechanics (NUMOG3), Elsevier, pp 636-648
- Nesnas, K. [1995] *A Finite Element Implementation of a Critical State Model for Unsaturated soil to simulate Drained Conditions*. Unpublished PhD Thesis, University of Sheffield.
- Nobari, E.S. and Duncan, J.M. [1972] *Movements in dams due to reservoir filling*. Special Conf. on Earth Supported Structures, ASCE, Vol. 1, No. 1, pp 797-815.

- Nolan, G.T. and Kavanagh, P.E. [1992] *Computer simulation of random packing of hard spheres*. Powder Tech. Vol. 72, pp 149-155.
- Northmore, K.J., Bell, F.G. and Culshaw, M.G. [1996] *The engineering properties and behaviour of the brickearth of South Essex*. Quarterly Journal of Eng. Geology, Vol. 28, pp 147-161.
- Osipov, V.I. and Sokolov, V.N. [1995] *Factors and mechanisms of loess collapsibility*. In: Derbyshire, E., Dijkstra, T. and Smalley, I.J. (Editors). Proc. of the NATO Advanced Workshop on Genesis and Properties of Collapsible Soils. pp 49-63.
- Phienweij, N., Nutalaya, P. and Udomchoke, V. [1992] *Properties of problem soils of arid north eastern Thailand*. In Proc. of 13<sup>th</sup> Int. Conf. On Soil Mech. and Foundation Eng., New Delhi, India, pp 374-380.
- Pye, K. [1995] *The nature, origin and accumulation of loess*. Quaternary Science Reviews, Vol. 24, pp 653-667.
- Qian, H.J. and Lin, Z.G. [1988] *Loess and its Engineering Problems in China*
- Reddi, L.N. and Bonala M.V.S. [1997] *Critical shear stress and its relationship with cohesion for sand-kaolinite mixtures*. Canadian Geotechnical Journal, Vol. 34, pp 26-33
- Redolfi, E.R. and Oteo Mazo, C. [1994] *Relative collapse of a loess soil*. In: Proc. of 13<sup>th</sup> Int. Conf. On Soil Mech. and Foundation Eng., New Delhi, India, pp 474-481.
- Rogers, C.D.F. [1995] *Types and distribution of collapsible soils*. In: Derbyshire, E., Dijkstra, T. and Smalley, I.J. (Editors). Proc. of the NATO Advanced Workshop on Genesis and Properties of Collapsible Soils. pp 1-17.
- Rogers, C.D.F. and Smalley, I.J. [1993] *The shape of loess particles*. Naturwissenschaften, Vol. 80, pp 461-462.
- Rogers, C.D.F., Dijkstra, T.A. and Smalley, I.J. [1994a] *Hydroconsolidation and subsidence of loess: studies from China, Russia, N. America and Europe*. Eng. Geol. Vol. 37, pp 83-113.
- Rogers, C.D.F., Dijkstra, T.A. and Smalley, I.J. [1994b] *Particle packing from an earth science viewpoint*. Earth-Science Reviews Vol. 36, pp 59-82.
- Roscoe, K.H. [1968] *Soils and model tests*. J. Stain Analysis, Vol.3, No. 1, pp 57-64.
- Roscoe, K.H. [1970] *The influence of strains in soil mechanics*. Geotechnique, Vol. 20, pp 129-170.

- Sajgalik, J. and Klukanova, A. [1994] *Formation of Loess Fabric*. Quarternary International Vol. 24, pp 41-46
- Schuring, D.J. [1977] *Scale Models in Engineering, Fundamentals and Applications*, Pergamon Press, Oxford.
- Schwartz, K. [1985] *Problems of soils in South Africa – state of the art – collapsible soils*. The Civil Engineer in South Africa, June.
- Siddiquee, M.S.A., Tanaka, T., Tatsuoka, F., Tani, K. and Morimoto, T. [1999] *Numerical Simulation of Bearing Capacity Characteristics of Strip Footing on Sand*. Soils and Foundations, Vol. 39, pp 93-109
- Skinner, H.D., Charles, J.A. and Watts, K.S. [1999] *Ground deformations and stress redistribution due to a reduction in volume of zones of soil at depth*. Geotechnique Vol. 49, pp 111-126.
- Skinner, H.D. [2001] *Construction on fill*. In: Problematics Soil (Jefferson, I., Murray, E.J., Faragher, E. and Fleming, P.R. eds.), Nottingham, Nov. 2001, pp 127-143.
- Smalley, I. J. [1970] Variations on the particle packing theme of Graton and Fraser. Powder Technology Vol. 4, pp 97–101.
- Smalley, I.J. [1971] *In-situ theories of loess formation and the significance of the calcium carbonate content of loess*. Earth. Sci. Rev. Vol. 7, pp 67-85.
- Smalley, I.J. [1991] *Possible formation mechanisms for the modal coarse-silt quartz particles in loess deposits*. Quaternary International, Vols. 7/8 pp23-27.
- Smalley, I.J. [1992] *The 'Teton Dam': Rhyolite formation and loess core = disaster*. Geol. Today, Vol. 19, pp 19–22.
- Smalley, I.J. [1996] *Making the material: the formation of silt-sized primary mineral particles for loess deposits*. Quat. Science Reviews, Vol. 14, pp 645-651
- Smalley, I.J., Bentley, S.P. and Moon, C.F. [1975] *The St.Jean Vianney Quickclay* The Canadian Mineralogist Vol. 13, pp 364-369
- Smalley, I.J. and Smalley, V. [1983] *Loess material and loess deposits: formation, distribution and consequences*. In: Eolian Sediments and Processes, (Brookfield, M. and Ahlbrandt, T.S, eds), pp. 51-68.
- Smith, L.F. [1999] *Loess in Kazakstan*. Masters Dissertation, University of Leeds, UK.
- Tan, T.K. [1988] *Fundamental Properties of Loess from Northwestern China*. Engineering Geology Vol. 25, pp 103-122

- Trofimov, V.T. [1990] *Loess Subsidence Models*. Geology Bulletin, Moscow University Vol.15, No.2, pp 5-18
- Tye, C., [2000] *A distribution model to assist ground characterisation of a problem soil- an example, loess in the UK*. In: Proc. of GeoEng 2000, Int. conf. On Geot. and Geol. Engng, Australia, Nov. 2000. CD
- Udomchoke, V. [1991] *Origin and engineering characteristics of problem soils in the Khorat Basin, Northeastern Thailand* Asian Institute of Technology, Thailand
- Vanapalli, S.K., Fredlund, D.G., Pufahl, D.E. and Clifton, A.W. [1996] *Model for the prediction of shear strength with respect to soil suction*. Canadian Geotechnical Journal Vol. 33, pp 379-392
- Vaughan, P.R., Maccarini, M. and Mokhtar, S.M. [1988] *Indexing the engineering properties of residual soil*. Quarterly Journal of Engineering Geology Vol. 21, pp 69-84
- Wheeler, S.J. and Sivakumar, V. [1995] *An elasto-plastic critical state framework for unsaturated soil*. Geotechnique Vol. 45, pp 35-53.
- Wiebe, B., Graham, J., Tang, G.X. and Dixon D. [1998] *Influence of pressure, saturation and temperature on the behaviour of unsaturated sand-bentonite*. Canadian Geotechnical Journal Vol. 35, pp 194-205
- Wright, J., Smith, B. and Whalley, B. [1998] *Mechanisms of loess-sized quartz silt production and their relative effectiveness: laboratory simulations*. Geomorphology, Vol. 23., pp 15-34.
- Yu, C.Y. [1982] *The characteristics of loess collapse in Lanzhou Area*. In: Proceedings of IV Congress International Association of Engineering Geology, New Delhi, India, Vol. 1, pp 449-462
- Zakaria, I., Wheeler, S.J. and Anderson, W.F. [1995] *Yielding of unsaturated compacted kaolin, unsaturated soils*. In: Proc. 1st Int. Conf. on Unsaturated Soils, Paris, France (ed. Alonso, E.E. and Delage, P.), Rotterdam: Balkema, Vol. 1, pp 223-228.

## Dissemination of This Research

---

- 1). Miller, H., Djerbib, Y., Jefferson, I.F. and Smalley, I.J. [1998a]. *Modelling the collapse of Metastable Loess Soils*, Proceedings of the 3rd International Conference on GeoComputation, University of Bristol, United Kingdom 17 - 19 September 1998. [www.geocomputation.org/1998/42/gc\\_42.htm](http://www.geocomputation.org/1998/42/gc_42.htm)
- 2). Miller, H., Djerbib, Y., Jefferson, I.F., Smalley, I.J. [1998b] *The modelling of foundations built on metastable loess soils*, Proceedings of the International Symposium on Problematic Soils, Sendai, Japan, October 1998. P 515-518.
- 3). Miller, H. and Djerbib, Y. [1999] *Modelling the Collapse of Quaternary Metastable Deposits*, Conference, Durban – abstract and presentation.
- 4). Miller, H., Djerbib, Y., Jefferson, I.F., Smalley, I.J. [2000] *Collapse behaviour of loess soils* Proceedings of the GeoEng 2000 International Conference on Geotechnical and Geological Engineering, Melbourne, Australia, Sept.
- 5). Miller, H., Jefferson, I.F., Djerbib, Y., Smalley, I.J. [2002] *The Collapse of Quaternary Metastable Loess*. Quarterly Journal of Engineering Geology, ISSN 0481-2085. In press.

# Modelling the Collapse of Metastable Loess Soils

H. Miller, Y. Djerbib, I.F. Jefferson and I.J. Smalley  
Nottingham Trent University, England  
Email: harriet.miller@ntu.ac.uk

## Abstract

Hydrocollapse of loess continues to cause major geotechnical problems the world over. Modelling the behaviour of these soils is still in its early stages. Computer models are often used to model saturated soil behaviour but for collapsing unsaturated loess soils such models are difficult to implement due to the complex nature of collapse. One method that will help overcome difficulties such as the role of clay bonding or soil fabric, is to consider collapse from a particle packing perspective, rather than as a soil suction problem. The way the particles pack together decides whether a soil is metastable or not. Using this philosophy, work is currently being conducted to develop a constitutive model to be incorporated in CRISP90 in order to analyse the behaviour of collapsing loess soils. This paper will discuss the development of this model and the methods used to validate it, which include the use of an artificial loess soil manufactured in the laboratory. This model material has been shown to reproduce loess behaviour very well and enables a full range of reproducible and repeatable tests to be conducted.

## 1. Introduction

Large areas of the earth's crust are covered with loess. China, America, Eastern Europe and Russia all have deposits ranging in depths from 1m to 100's of metres. For example, around 14 % of the total territory of (the old USSR) is covered by loess where the deposits are around 20m and deeper (Abelev, 1988). Consequently, many residential buildings in cities and towns and big industrial enterprises have been erected on loess around the world.

Loess can cause a number of problems associated with its sudden settlement. An example is a three storey building in Xining, Qinghai, destroyed beyond repair due to subsidence of the foundation soils upon wetting (Qian et al., 1988). Problems result because loess undergoes structural collapse when wetted. This happens when the initial dry density is low and initial water content is low (Dijkstra et al. 1995). There is still some argument as to why loess collapses. To elucidate this problem it is necessary to examine both macroscopic and microscopic aspects of loess collapse. (Feda, 1994).

Increasingly, numerical models such as finite element (FE) models are used to examine the behaviour of foundations built on soil. However, loess collapse is still causes a problem as it can not be modelled using conventional techniques. This paper will describe the combined computer and physical model approach currently being used to explore this complex problem.

## 2. The collapse process

Before any models are developed it is first necessary to establish the typical characteristics of loess. From this a universal standard can be produced, which can not only aid the validation of any FE models produced enable the growing body of literature to be better utilised.

### 2.1 Mineralogy

The structure of loess is dominated by 20-60µm quartz particles of 8:5:2 aspect ratio Rogers et al. (1994). Typically, quartz is the most abundant mineral in loess material, feldspar is also present. Of the clay type minerals, mica is more abundant than montmorillonite (average 15%), which is more abundant than illite and kaolinite (average 5%). (Northmore et al., 1996).

### 2.2 The collapse mechanism

Upon deposition, a loose, open structured, metastable soil is formed, composed of quartz particles separated by coatings or aggregates of clay and carbonate particles. In its dry state the structure has significant strength and can withstand high loads.

Upon saturation, however, the bonding disintegrates and a denser structure is achieved by sudden collapse of the soil particles - often known as hydrocollapse. Saturation can occur through infiltration due to pooling of water from above, leakage from pipes and guttering or through rising ground water levels. The collapse of the internal structure occurs when the stresses between particles exceed the bond strength provided by bridging bonds (Holtz and Gibbs, 1951). This kind of soil is considered to be unstable as a foundation material because of the potential for large settlement. In these cases, if differential settlement occurs it can be severely damaging for structures built on loess.

### 2.3 Collapsibility controls

In certain cases destruction of capillary forces may account for the collapse caused on wetting. (Alonso et al., 1987). However, there is still considerable discussion as to the relative roles of suction and clay bond degradation in the collapse process of loess. Added to this, there is a considerable difficulty in obtaining reliable suction measurements in silty soils (Fredlund & Rahardjo, 1993). The main concern of the authors is that suctions may take a long time to equilibrate and even when they do the suctions developed in the clay bonds may be different to the suction developed between the silt grains. To date there is no way of measuring the differences. The suctions measured would therefore give an average value and may not be reliable. Bond degradation probably governs the collapse processes in loess and therefore experiments will be focused on finding a rule that explains the behaviour in terms of the packing parameters such as clay content and void ratio.

The basic mechanism of collapse involves particle rearrangement from metastable open structure to a denser stable hydrocollapsed structure. Whatever the mechanism includes, ultimately it is the way the particles are packed that controls the structure and hence the susceptibility of loess to collapse. This idea was actively promoted by Smalley in the 1960's (Smalley, 1964) and subsequently developed by Rogers et al.

(1994). Since these crude hand generated solutions, computer models have been developed using FORTRAN and similar languages (see Dibben et al., in press) Thus by considering collapse from a particle packing perspective it is possible to avoid problem associated with relative roles of clay degradation or suction in the collapse process. Such an approach could provide useful insight at both macroscopic and microscopic levels, particularly when developing computer models.

### **3. Artificial Loess**

A considerable body of research has been generated to investigate collapse problems. Unfortunately, the results are often variable due to location and depth of the deposit and therefore are difficult to compare directly. An artificial deposit has been produced that has the same general properties of collapse as loess deposits from around the world. The artificial loess provides results which are repeatable, reproducible and controllable.

Artificial loess samples have been produced by adapting work undertaken by Assallay et al., 1998 and Dibben et al. 1998. This artificial loess allows direct control of the material constituents, thus providing a good method of evaluating the effect of varying the constituents, and hence provides a control method of computer validation. Two methods to generate artificial loess are currently being developed.

#### **3.1 Ballotini balls**

An artificial loess has been made by mixing glass ballotini balls with kaolinite. Ballotini balls are uniform spherical glass objects. They are sieved through a 63 (m sieve to create typical loess size particles the smaller balls are removed through a 20(m sieve. Initial studies by Assallay et al., 1998 illustrate the loess like structures formed with these balls. These structures illustrated that kaolinite was the best clay mineral binder to use, producing a greater control on collapse.

#### **3.2 Crushed sand**

Another method of producing artificial loess is to use crushed sand. Impurities are removed from the sand by washing with water. The sand is then crushed in an end runner mill which reduces the sand size to silt size particles. The ground material is passed through a 63(m sieve to retrieve the smaller fraction. It is deflocculated and the fines removed by sedimentation. The resultant material (63-20(m) is then mixed with kaolinite to produce the bonding needed to create a metastable structure. The effect of varying the clay content has been examined the results of which are shown in Figures 1 and 2.

### **4. Hydrocollapse Testing**

Artificial and remoulded natural loess soils are prepared using methods recently established (see Dibben et al, 1998). Once formed, standard double and single oedometer collapse tests have been performed (between stresses of 5 and 1600kPa).

Single oedometer tests are carried out by loading the sample to a certain pressure (between 5 and 1600 kPa), saturating the sample and then continuing the loading up to 1600kPa. Double oedometer tests are carried out on two samples in parallel one a saturated sample and the other an unsaturated sample these are also loaded to

1600kPa.

Two main curves are observed one for unsaturated behaviour and one for saturated behaviour. (See Figure 1.) The same characteristic collapse behaviour is observed in the artificial loess as it is in the natural deposit. See also, Assalay et al., 1998 and Dibben et al., 1998)

**Figure 1: Crushed sand/kaoli**

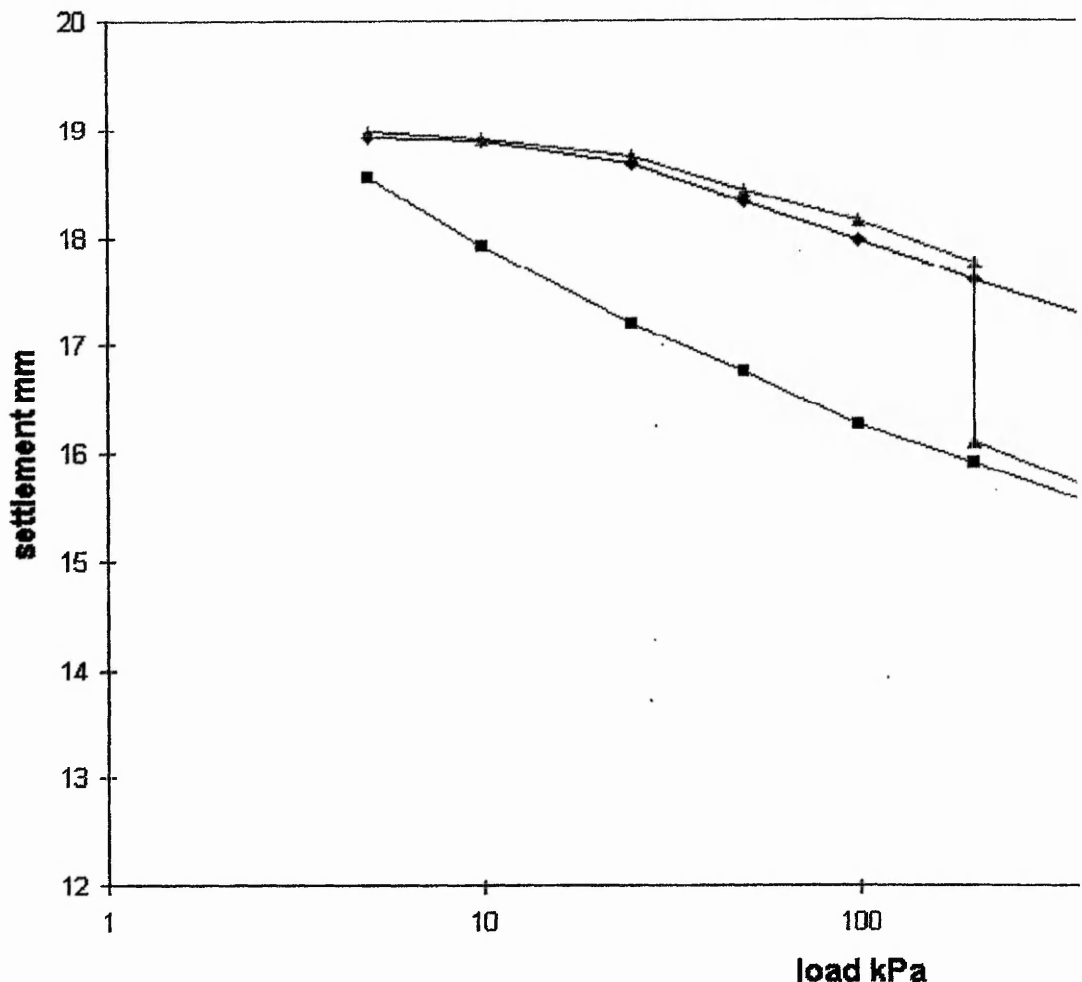


Figure 1: Oedometer tests on artificial loess from crushed sand : kaolinite 85:15. The collapse pressure due to saturation is 200kPa.

Ballotini balls have the advantage that they are rounded, and hence are more representational of natural loess deposits that contain weathered quartz particles as the main building blocks. However they do not have the same specific gravity as the silt particles and therefore exhibit different void ratios for the same mass of soil.

Figure 2 shows how hydrocollapse varies with clay content at 200kPa for the artificial loess samples (crushed sand with kaolinite). Clearly, only a relatively small amount of clay content is required to yield significant collapse. Too much clay and the soil behaves in a typically plastic 'clay like' fashion exhibiting no collapse. Too little clay content and insufficient binder exists to produce the metastable structure required for

collapse to occur. The maximum collapse occurs at 25% clay content which corresponds to approximately 18% clay mineral (kaolinite) content. However, it should be noted that the samples were produced all to have the same mass and therefore, different void ratios result. To make the experiments more realistic the samples will be produced with the same compactive effort which will emulate deposition of loess soils and the effects of overburden pressure. This will enable a true comparison of the effect of the clay content to be assessed. A similar set of results is observed when Ballotini balls are used as the primary mineral constituent. However the magnitude of collapse observed with these samples is lower, due mainly to the spherical shape of the primary particles.

**Figure 2: % hydrocollapse observed for different kaolinite con**

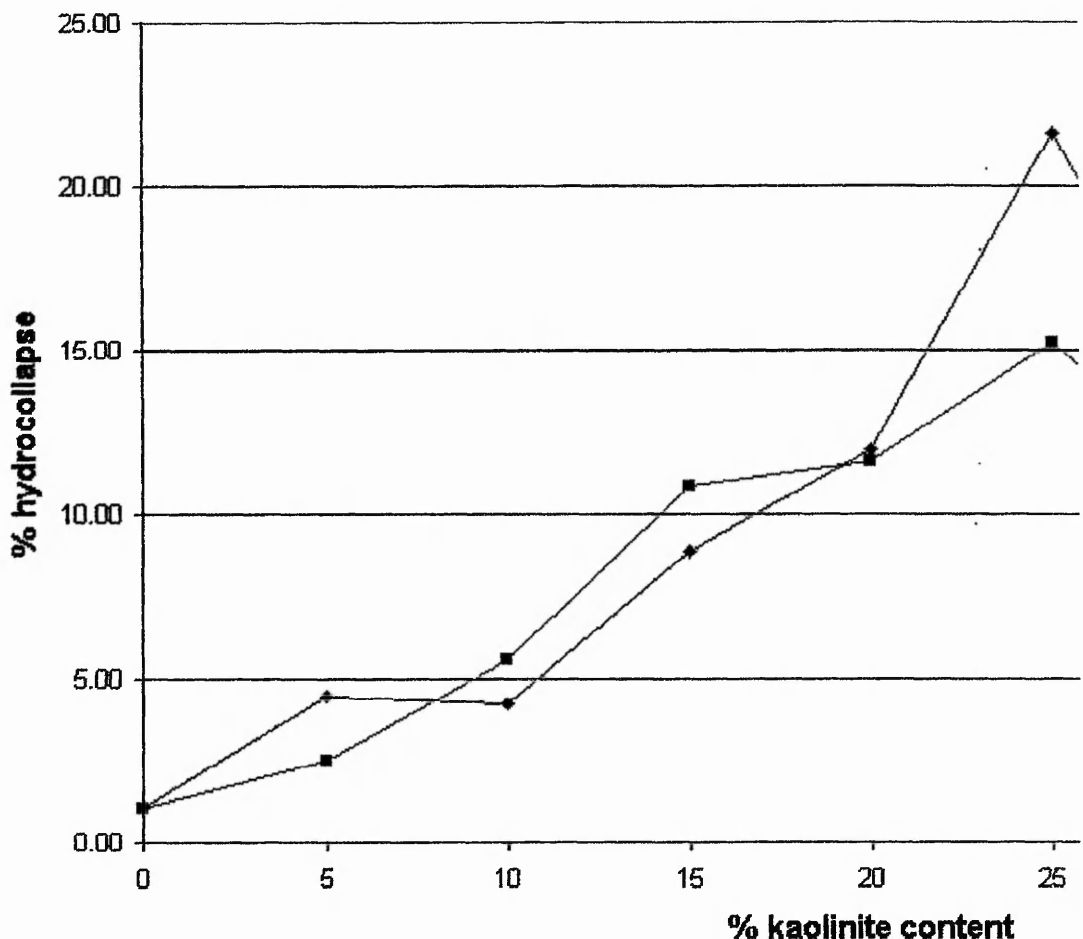


Figure 2: % hydrocollapse for different kaolinite contents.

## 5. Computer modelling

Classical soil mechanics has been developed predominantly from the study of saturated soils. More recent developments in fundamental frameworks of soil behaviour have also been limited to saturated soils. However, loess is an unsaturated soil and new frameworks need to be developed for such soils.

Most approaches use the unsaturated formulation of critical state theory which relies on measurement of suction changes throughout the experiment. Relatively little experimental data on the behaviour of unsaturated soils are available, due to technical difficulties related to both control and measurement of suction (Cui and Delage, 1996). Laboratory equipment for controlling and measurement of suctions has been developed at Imperial College but measurement of suction in the field is still unreliable. If a procedure could be developed based on a more empirical approach without the need for the measurement of suctions, designing for unsaturated soils would be made easier.

A finite element computer package, CRISP90 (CRITICAL State Program), based on the critical state theory of soils will be used to investigate the collapse behaviour of loess subjected to load and/or wetting. The program was written with a provision to incorporate new soil models to suit the problem under study.

Loess displays two different kinds of behaviour. The first is a partially saturated soil. However as the degree of saturation is increased and collapse takes place, the behaviour is typically that of a saturated clayey silt. In its first state, prior to collapse, it is analogous to cemented soil with the bonding between the grains of silt provided by the clay/carbonate elements. Comparison can therefore, be made with the behaviour of weak concrete or rocks.

Nesnas (1995) developed an elasto-plastic constitutive model to predict the behaviour of partially saturated soils including collapse. This model was based on the Barcelona model (a suction based model) Alonso et al., 1990. This model incorporated in the finite element code of CRISP can be modified further and applied to study the behaviour of loess.

Data will be built up from both oedometer tests and a physical model. These models will provide data for calibrating and validating the computer model. The oedometer tests will use both natural and artificial deposits. The natural deposits have been obtained from sites in Southern England, where collapse has resulted in costly engineering problems, e.g. Torquay (Cattell 1997). The artificial loess will also be used to investigate the effect of material variations. Specifically this will allow examination of bonding mechanisms that occur in natural loess systems.

An initial step in implementing the new model will be to introduce threshold stresses at which the deposit will collapse. The lessons learned in the laboratory will be used to calibrate the numerical model. This will be coupled with a code based on a particle packing perspective following on the work of Dibben et al. (1998).

This will overcome the difficulties inherent with critical state models for 3-phase systems which rely on suction measurements. Such measurements are notoriously difficult in silty soils. Ultimately, it is planned to use a scale laboratory model foundation to examine the effects of various water infiltration systems, which will be compared directly to FE analysis. This will be used to validate such models, and hence allow further elucidation of the complex problem of loess collapse.

Application for such a model may include assessment of radioactive waste repositories built in loess, which is currently under consideration in Bulgaria (Jefferson and Smalley, 1997). The FE model developed could help to predict the overall behaviour of foundations and other infrastructure built on or in loess and similar soils.

## 6. Conclusions

This project is currently developing a FE model to assess the behaviour of collapsible loess soils. However, to overcome the arguments of which factor controls the collapse mechanism, collapse is being modelled on a particle packing basis for it is ultimately the way the particles pack that dictate the degree of collapse that occurs. This model will be calibrated using an artificial loess developed to enable full control over the material constituents and hence the collapse that occurs. The artificial loess will be used in the further development of the model, aiming ultimately to enable the full assessment of foundations built on loess and other collapsible soils.

## References

- Abelov, M.Y., (1988), Loess and its Engineering Problems in the USSR, Proc. of the Int. Conf. Engineering Problems of Regional Soils., 11-15 August, Beijing, China, 3-6. Beijing: Chinese Institute of Soil Mech. and Found. Eng.
- Alonso, E.E., A. Gens, & D.W. Hight, 1987, General report. Proc. 9th Conf. Soil Mech., Dublin 3, 1087-1146.
- Alonso, E.E., A. Gens, & A. Josa, (1990), A constitutive model for partially saturated soils, *Geotechnique*, 40: 405-430.
- Assallay, A.M., I. Jefferson, C.D.F. Rogers, & I.J. Smalley, (1998), Fragipan Formation in Loess Soils: Development of the Bryant Hydroconsolidation Model, *Geoderma*, 83, 1-16.
- Cattell, A.C., (1997), The development of loess-bearing soil profiles Permian Breccias in Torbay. Proceedings of the Usher Society, Vol 9, p168-172.
- Cui, Y.J. & P. Delage, (1996), Yielding and plastic behaviour of an unsaturated compacted silt, *Geotechnique*, 46: 291-311.
- Dibben, S.C., I.F. Jefferson, & I.J. Smalley, (1998), The "Loughborough Loess" Monte Carlo Model of Soil Structure. *Computers and Geosciences*. (in press).
- Dijkstra, T.A., I.J. Smalley, & C.D.F. Rogers, (1995). Particle packing in loess deposits and the problem of structure collapse and hydroconsolidation. *Engineering Geology*, 40: 49-64.
- Feda, J. (1994), Mechanisms of Collapse of Soil Structure, In: E. Derbyshire (ed.), *Genesis and properties of collapsible soils*, NATO Series C: Mathematical and Physical Sciences Vol 468. 149-172. Dordrecht: Kluwer.
- Fredlund, D.G., & H. Rahardjo, (1993), *Soil Mechanics for Unsaturated soils*. New York. John Wiley and sons, inc.
- Holtz, W.G. & H.J. Gibbs, (1951), Consolidation and related properties of loessial soils, *ASTM STP 126*: 9-26.
- Jefferson, I. & I.J. Smalley, (1997), Nuclear Waste Poser, *Ground Engineering*, 30

(10): 26-27

Nesnas, K., (1993), A finite Element Implementation of a Critical State Model for unsaturated soil to simulate Drained Conditions. PhD University of Sheffield.

Northmore, K.J., F.G. Bell, & M.G. Culshaw, (1996), The engineering properties and behaviour of the Brick Earth of South Essex, Quarterly Journal of Engineering Geology, 29: 147-161.

Qian, H.J. & Z.G. Lin, (1988), Loess and its Engineering Problems in China. Proc. of the Int. Conf. Engineering problems of Regional Soils. 11-15 August, Beijing, China, 136-153. Beijing: Chinese Institution of Soil Mech. and Found. Eng.

Rogers, C.D.F., T.A. Dijkstra, & I.J. Smalley, (1994), Hydroconsolidation and subsidence of loess: Studies from China, Russia, North America and Europe., Engineering Geology, 37, 83-113. Schwartz, K., (1985), Collapsible Soils, The Civil Engineer in South Africa, July, 379 - 393.

Smalley, I.J., (1964), Representation of packing in a clastic sediment. Amer. J. Science. 262 pp. 242-248.

# The modelling of foundations built on metastable loess

H. Miller

*Department of Civil and Structural Engineering, Nottingham Trent University, UK*

Y. Djerbib

*Department of Civil and Structural Engineering, Nottingham Trent University, UK*

I.F. Jefferson

*Department of Civil and Structural Engineering, Nottingham Trent University, UK*

I.J. Smalley

*Department of Civil and Structural Engineering, Nottingham Trent University, UK*

**ABSTRACT:** Hydrocollapse of loess continues to cause major geotechnical problems the world over. Engineers are increasingly using computer models, such as finite element models to design problems. However, for collapsing loess soils such models are difficult to produce due to the complex nature of loess collapse. One method that will help overcome these difficulties, is to consider collapse from a particle packing perspective, rather than a soil suction problem. The way the particles pack together decides whether a soil is metastable. Using this philosophy, work is currently being conducted to develop a Finite Element model using CRISP90, to analyse foundations built on collapsing loess soils. This paper will discuss the development of this model and the methods used to validate it, which include the use of an artificial loess soil manufactured in the laboratory. This model material has been shown to reproduce loess behaviour very well and enables a full range of reproducible and repeatable tests to be conducted.

## 1 INTRODUCTION

Large areas of the earth's crust are covered with loess. For example, around 14 % of the total territory of Russia is covered by loess (Abelev 1988). A great many residential buildings in cities and towns and big industrial enterprises have been erected on loess.

Loess can cause a number of engineering problems, e.g. settlements in excess of one metre occurred in Lanzhou, Gansu in a terrain composed of 12-14m of collapsible loess underlain by saturated sandy deposits after a test pit of 10m by 10m had been flooded (Qian et al. 1988). Problems result because loess undergoes structural collapse and subsidence due to saturation when both the initial dry density and initial water content are low (Dijkstra et al. 1995).

A considerable body of research has been generated to investigate collapse problems. Unfortunately, the results are often variable and difficult to compare directly. To elucidate this problem it is necessary to examine both macroscopic and microscopic aspects of loess collapse (Feda 1995).

Increasingly, numerical models such as finite element (FE) models are used to examine the behaviour of foundations built on soil. However, loess collapse is still causing problems. This paper will describe the combined finite element

and physical model approach currently being used to explore this complex problem.

## 2 THE COLLAPSE PROCESS

Before any models are developed it is first necessary to establish the typical characteristics of loess in general. From this a universal standard can be produced, which can not only aid the validation of any FE models produced but enable the growing body of literature to be better utilised.

### 2.1 Mineralogy

The structure of loess is dominated by 20-63  $\mu$  m quartz particles of a 8:5:2 aspect ratio Rogers et al. (1994). Typically, quartz is the most abundant mineral in loess, with feldspar is being also present. Of the clay type minerals, mica is more abundant than montmorillonite (average 15%), which is in turn more abundant than illite and kaolinite (average 5%) (Northmore et al. 1996).

### 2.2 The collapse mechanism

Upon deposition, a loose, open structured, metastable soil is formed, composed of quartz particles separated by coatings or aggregates of clay

and carbonate particles. In its dry state the structure has significant strength and can withstand high loads.

Upon saturation, however, the bonding disintegrates and a denser structure is achieved by sudden collapse of the soil particles - often known as hydrocollapse. Saturation can occur through infiltration due to pooling of water from above, leakage from pipes and guttering or through rising ground water levels (Swartz 1985). The collapse of the internal structure occurs when the stresses between particles exceed the bond strength provided by bridging bonds (Holtz & Gibbs 1951). This kind of soil is considered to be unstable as a foundation material because of the potential for large settlement. In these cases, if differential settlement occurs it can be severely damaging for any structures built on loess (Swartz 1985).

### 2.3 Collapsibility controls

In certain cases destruction of capillary forces may account for the collapse caused on wetting. (Alonso et al. 1987). However, there has and still is considerable discussion as to the relative roles of suction and clay bond degradation in the collapse process. This still remains an unsolved problem due in part to the considerable difficulty in obtaining reliable suction measurements in silty soils (Fredlund & Rahardjo 1993)

The basic mechanism of collapse involves particle rearrangement from metastable open structure to a denser stable hydrocollapsed structure. Whatever the mechanism includes, ultimately it is the way the particles are packed that controls the structure and hence the susceptibility of loess to collapse. This idea was actively promoted by Smalley 1960s (Smalley 1964) and subsequently developed by Rogers et al. (1994). Since these crude hand generated solutions, computer models have been developed using FORTRAN and similar languages (see Dibben et al., in press)

Thus by considering collapse from a particle packing perspective it is possible to avoid the problems associated with the relative roles of clay degradation or suction in the collapse process. Such an approach could provide useful insight at both macroscopic and microscopic levels, particularly when developing computer models.

## 3 ARTIFICIAL LOESS

The properties of loess obviously vary due to location and depth of the deposit. This makes experimental data hard to directly compare and hence difficult to use when validating the com-

puter models. An artificial deposit has been produced that had the same overall properties of collapse as loess deposits from around the world. The artificial loess provides results which are repeatable, reproducible and controllable.

Artificial loess samples have been produced by adapting work undertaken by Assallay et al. (in press) and Dibben et al. (in press). This artificial loess allows direct control of the material constituents, thus providing a good method of evaluating the effect of varying the constituents. Hence, provides a control method of computer validation. Two methods to generate artificial loess are currently being developed.

### 3.1 Ballotini balls

An artificial loess has been made by mixing glass ballotini balls with kaolinite. Ballotini balls are uniform spherical glass objects. They are sieved through a 63  $\mu\text{m}$  sieve to create typical loess size particles the smaller balls are removed through a 20 $\mu\text{m}$  sieve. Initial studies by Assallay et al. (in press) illustrate the loess like structures are formed with these balls. These structures illustrated that kaolinite was the best clay mineral binder to use, producing the greatest control on collapse.

### 3.2 Crushed sand

Another method of producing artificial loess is to use crushed sand. Impurities are removed from the sand by washing with water. The sand is then crushed in an end runner mill which reduces the sand size particles to silt size. The ground material is passed through a 63 $\mu\text{m}$  sieve to retrieve the smaller fraction. It is deflocculated and the fines removed by a combination of wet sieving and sedimentation. The resultant material (63-20 $\mu\text{m}$ ) is then mixed with kaolinite to produce the bonding needed to create a metastable structure. The effect of varying the clay content can then be examined.

## 4 HYDROCOLLAPSE TESTING

Artificial and remoulded natural loess soils are prepared using methods recently established (see Dibben et al., in press). Once formed, standard double and single oedometer collapse tests have been performed (between 5 and 1600kPa).

### 4.1 Artificial loess

Single and double oedometer tests have been carried out using the ballotini balls prepared sample. The same characteristic collapse behaviour is ob-

served in the artificial loess as it is in the natural deposit (Figure 1).

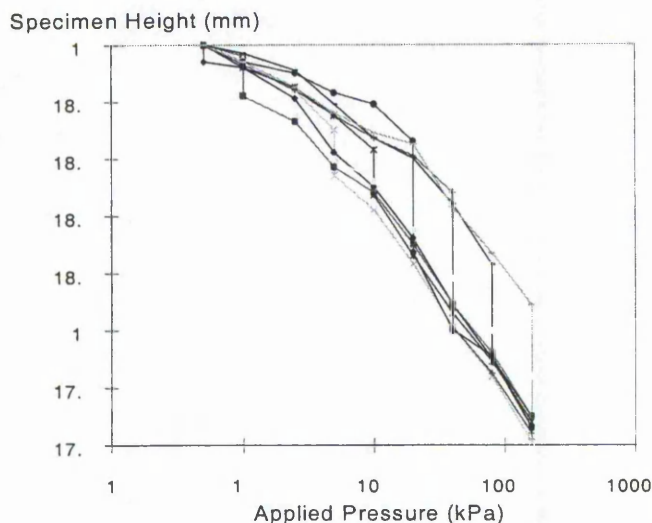


Figure 1: Oedometer tests on artificial loess formed from crushed sand.

The crushed sand sample also produces the characteristic collapse curve that is observed with natural deposits. Ballotini balls have the advantage that they are rounded, and hence are more representational of natural loess deposits that contain weathered quartz particles as the main building blocks.

Similar results have been obtained by Assallay et al. (in press) (Figure 2).

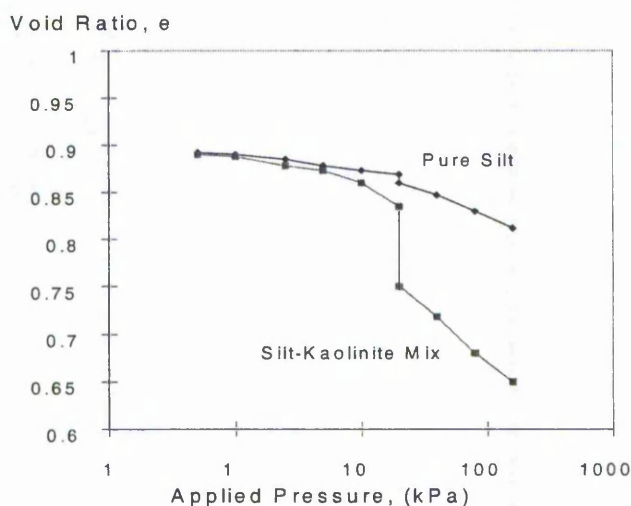


Figure 2: Oedometer tests on artificial loess samples, with and without kaolinite added to the crushed sand (after Assallay et al., in press).

## 5 FINITE ELEMENT ANALYSIS OF THE BEHAVIOUR OF LOESS

### 5.1 Finite element analysis

Classical soil mechanics has been developed predominantly from the study of saturated soils. More recent developments in fundamental frameworks of soil behaviour have also been limited to saturated soils. However, loess is an unsaturated soil and new frameworks need to be developed for such soils.

Relatively little experimental data on the behaviour of unsaturated soils are available, due to technical difficulties related to both control and measurement of suction (Cui & Delage 1996). Shear data from tests on unsaturated soil in which suctions were measured were first reported by Bishop and Blight (1963). The ideas reported by Bishop (1959) were used to interpret the data, and explained the results obtained. The same effective stress concept was extended to volume change behaviour by Blight (1965) but was criticised Burland (1965). Who pointed out that the proposed effective stress law, could not fully explain volume change behaviour.

The first constitutive model able to predict various aspects of unsaturated soil behaviour, called the loading collapse (LC) model, was presented by Alonso et al. (1987). In this work, attention was focused on volume change behaviour, including collapse, and the model qualitatively showed how an extended elasto-plastic theory could satisfactorily account for the main aspects of unsaturated soil behaviour. Alonso et al. (1990) presented a quantitative version of the LC model, where both volume change and shear strength were predicted within the framework of an elasto-plastic theory. Some time later, the first experimental results on volume change behaviour during shear tests appeared, within the general framework of critical state concepts and elasto-plasticity (e.g. Wheeler & Sivakumar 1992).

Most approaches use the unsaturated formulation of critical state theory which still relies on measurement of suction changes throughout the experiment which is difficult to accomplish. If a procedure could be developed based on a more empirical approach this would get rid of the need for the measurement of suctions and therefore make designing for unsaturated soils easier. Liggioia & Nova (1995) have developed a mathematical model which can model collapse for soft rock. However, this model does not consider the infiltration of water which is important for loess collapse.

## 5.2 Model studies

Data can be built up from oedometer tests and a physical model of a footing. These models can provide data for calibrating a validating the computer model. The oedometer tests will use natural and artificial deposits. The natural deposits have been obtained from sites in Southern England, which have been indicated as a cause of foundation problems, e.g. in Torquay (Cattell 1997). The artificial loess will also be used to investigate the effect of material variations.

CRISP90 software is being used to model the oedometer tests. An initial step in implementing the new model will be to introduce threshold stresses at which the deposit will collapse. The lessons learned in the laboratory will be used to calibrate the numerical model. This will be coupled with a code based on a particle packing perspective following on the work of Dibben et al., (in press).

This will overcome the difficulties inherent with critical state models for 3-phase systems which rely on suction measurements. Such measurements are notoriously difficult in silty soils. Ultimately, it is planned to use a scale laboratory model foundation to examine the effects of various water infiltration systems, which will be compared directly to FE analysis. This will be used to validate such models.

Application for such a model include assessment of radioactive waste repositories built in loess, which is currently under consideration in Bulgaria (Jefferson & Smalley 1997). The FE model developed could help to predict the overall foundation stability of loess and hence the viability of such an approach.

## 6 CONCLUSIONS

Unsaturated critical state framework involves suctions (e.g. Wheeler & Sivakumar, 1995) which are hard to measure, particularly in a silt. The other problem is the uncertain role that suction plays in the collapse and therefore difficulties this creates to produce a reliable code for FE modelling which includes suctions.

This project is currently developing a FE model to assess foundations built on collapsible loess soils. However, to overcome the difficulties of what factor controls the collapse mechanism, collapse is being modelled on a particle packing basis, for it is ultimately the way the particles pack that dictate the degree of collapse that occurs. This model will be calibrated using an artificial loess soil developed to enable full control over the material constituents and hence the collapse that occurs. Two methods to produce arti-

ficial loess have proved successful: ballotini balls and crushed sand based mixes. These will be used in the further development of the FE model produce, aiming ultimately to enable the full assessment of foundations built on loess and other collapsible soils.

## REFERENCES

- Abelev, M.Y. 1988. Loess and its Engineering Problems in the USSR. *Proc. of the Int. Conf. Engineering Problems of Regional Soils, 11-15 August, Beijing, China*: 3-6. Beijing: Chinese Institution of Soil Mech. and Found. Eng.
- Alonso, E.E., A. Gens & D.W. Hight 1987. General report, General report. *Proc. 9th Conf. European Soil Mech., Dublin*: 3: 1087-1146.
- Alonso, E.E., A. Gens & A. Josa 1990. A constitutive model for partially saturated soils. *Geotechnique*. 40:405-430.
- Assallay, A.M., I. Jefferson, C.D.F. Rogers & I.J. Smalley 1998. Fragipan Formation in Loess Soils: Development of the Bryant Hydroconsolidation Mode. *Geoderma*. (in press).
- Bishop, A.W. 1959. The principle of effective stress. *Technisk Ukeblad*. 106(39): 859-863.
- Bishop, A.W. & G.E. Blight 1963. Some Aspects of effective stress in saturated and partly saturated soils. *Geotechnique*. 13:177-197.
- Blight, G.E. 1965. A study of effective stress for volume change. *Proc. of the Int. Research and Eng. Conf. on Moisture Equilibrium and Moisture changes in soil beneath Covered Areas*: 259-269. London: Aitchison.
- Burland, J.B. 1965. Some aspects of the mechanical behaviour of partly saturated soils. *Proc. of the Int. Research and Eng. Conf. on Moisture Equilibrium and Moisture changes in soil beneath Covered Areas*: 270-278. London: Aitchison.
- Cattell, A.C. 1997. The development of loess-bearing soil profiles Permian Breccias in Torbay. *Proceedings of the Ussher Society*. 9:168-172.
- Cui, Y.J. & P. Delage 1996. Yielding and plastic behaviour of an unsaturated compacted silt. *Geotechnique*. 46:291-311.
- Dibben, S.C., I.F. Jefferson & I.J. Smalley 1998. The "Loughborough Loess" Monte Carlo Model of Soil Structure. *Computers and Geosciences*. (in press).
- Dijkstra, T.A., I.J. Smalley & C.D.F. Rogers 1995. Particle packing in loess deposits and the problem of structure collapse and hydroconsolidation. *Engineering Geology* 40:49-64.
- Feda, J. 1994. Mechanisms of Collapse of Soil Structure, In: E. Derbyshire (ed.), *Genesis and properties of collapsible soils, NATO SeriesC: Mathematical and Physical Sciences Vol. 468*:149-172. Dordrecht: Kluwer.
- Fredlund, D.G. & H. Rahardjo 1993. *Soil Mechanics for Unsaturated soils*. New York. John Wiley and Sons, inc.
- Holtz, W.G. & H.J. Gibbs 1951. Consolidation and related properties of loessial soils. *ASTM STP*. 126: 9-26.

- Jefferson, I. & I.J. Smalley I.J. 1997. Nuclear Waste Poser, *Ground Engineering*. 30(10): 26-27
- Lagioia, R. & R. Nova 1995. An Experimental and theoretical study of the behaviour of a calcarenite in triaxial compression. *Geotechnique*. 45:633-648.
- Northmore, K.J., F.G. Bell & M.G. Culshaw 1996. The engineering properties and behaviour of the Brick Earth of South Essex. *Quarterly Journal of Engineering Geology*. 29:147-161.
- Rogers, C.D.F., T.A. Dijkstra & I.J. Smalley 1994. Hydroconsolidation and subsidence of loess: Studies from China, Russia, North America and Europe. *Engineering Geology* 37:83-113.
- Schwartz, K. 1985. Collapsible Soils. *The Civil Engineer in South Africa*. July: 379 - 393.
- Smalley, I.J. 1964. Representation of packing in a clastic sediment. *Amer. J. Science*. 262:242-248.
- Wheeler. S.J. & V. Sivakumar 1995. An elasto-plastic critical state framework for unsaturated soil. *Geotechnique*. 45:35-53.

## Modelling The Collapse Of Quaternary Metastable Loess Deposits

H. Miller

Y. Djerbib

I. Jefferson

Civil and Structural Engineering, Nottingham Trent University

Durban, 1999



**ABSTRACT:** Quaternary loess deposits have a metastable, unsaturated open structure that will readily collapse when loaded and wetted. The way that the particles pack is at the heart of the collapse problem. Neglecting the engineering and geological aspects of quaternary deposits can seriously affect the built environment leading to losses of millions of dollars, (Hutchinson, 1997). It is therefore important to be able to predict the behaviour of such soils. Many approaches to modelling soil behaviour have been used, such as the constitutive models used in finite element analysis. These techniques have been successfully employed for saturated soils for many years. Further development over the last two decades has meant that models for unsaturated soils are now available. The main philosophy behind the approach is that suctions are the bond holding the particles in their metastable state, such as in engineered fills. However, the quaternary loess is held in a metastable state by, not only suction, but also clay bonding and carbonate cementation. The complex nature of the bonding makes it difficult to use the new techniques for unsaturated soil behaviour. One method to overcome the uncertainties of the relative roles of suction and clay bonding is to consider the way the particles pack. Using this philosophy, work is currently being conducted to develop a model to be incorporated in CRISP90 in order to analyse the behaviour of metastable collapsing quaternary loess soils. This paper will discuss the development of this model and the methods used to validate it, which include the use of an artificial loess soil manufactured in the laboratory. This model material has been shown to reproduce metastable loess behaviour very well, see Figure 1, and enables a full range of reproducible and repeatable tests to be conducted. The work will help elucidate the behaviour of this quaternary deposit and hence predict the behaviour of this major geohazard, enabling safer designs of foundations and buildings.

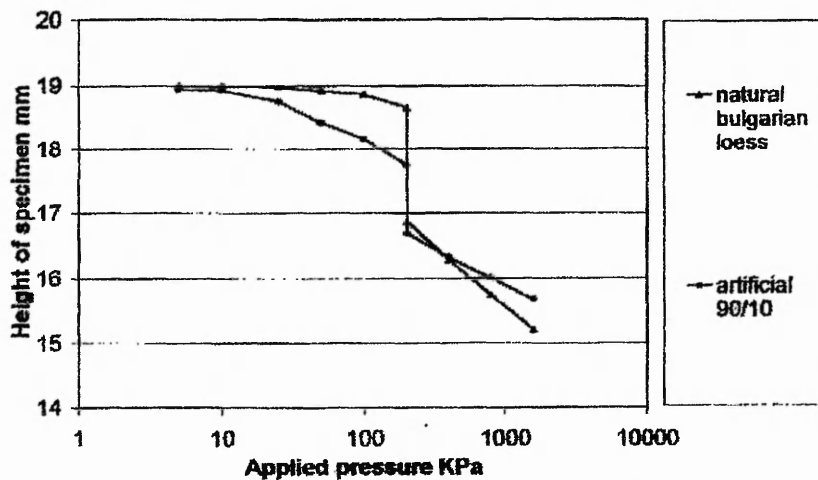


Figure 1. A comparison of collapse for artificial and natural loess samples.

# COLLAPSE BEHAVIOUR OF LOESS SOILS

Harriet Miller<sup>1</sup>, Youcef Djerbib<sup>2</sup>, Ian F. Jefferson<sup>3</sup> and Ian J. Smalley<sup>4</sup>

## ABSTRACT

Loess soils cover approximately 10% of the world's landmass. This quaternary deposit has been studied for many decades, but predicting the collapse behaviour still remains an active subject for discussion and research. For this project, collapse mechanisms have been studied using two techniques; artificial loess, (the physical model) and a numerical model. The physical model is a continuation of artificial soil techniques developed in the literature. The artificial soil is made from silt and clay particles and has been developed to reproduce the collapse characteristics found in natural loess. This artificial loess has been tested using oedometer and triaxial equipment and will be used as the foundation material in a scale model of a footing. Results show that the physical model can reproduce collapse behaviour very well. Secondly, a numerical model has been developed to simulate the collapse behaviour observed in the laboratory tests. This model has been implemented into the finite element program CRISP. Oedometer tests have been accurately simulated and the extension of both of these models to model the behaviour of a footing in plane strain will be discussed.

## INTRODUCTION

The abundant nutrients and low density of loess make it an ideal agricultural soil. However, the open structure that encourages strong root development, makes the soil susceptible to collapse upon the application of load and/or water. In fact, collapse of such open structures can cause reduction in volume by up to 30% (Waltham, 1988). This makes the soil very problematic for engineers. The large voids in the soil are maintained as a result of various bridging and bonding systems between the main structural silt particles. These bonding systems include clay bonding, carbonate cementation and suction (Barden et al., 1973). These components interact in a complex way and therefore modelling the behaviour of these soils is not easy. The relative roles of the bonding components are not clearly understood and models that are based solely on suctions do not account for the various cementing components in natural collapse systems such as loess. Neglect of these various elements has in the past caused considerable problems to the built environment and other associated works, such as the Teton dam collapse in 1976, in Idaho, USA (Smalley, 1992).

A physical model was developed to examine the collapse behaviour of loess soils. This involved the production of an artificial loess soil, made up of varying proportions of clay and primary mineral. Kaolinite has been used as the clay mineral and quartz was used as the primary mineral, crushed to obtain silt-sized particles. Formation of an artificial deposit allows direct control of the constituent parts of the material. This has elucidated the key factors that influence the collapse process. Artificial loess soil reproduces the behaviour of natural deposits from around the world remarkably well.

Since loess is so widespread and there is an increasing demand for infrastructure and housing it is not uncommon to find developments built on these soils. It is therefore important to be able to predict the likely deformations of these systems. Based on the physical model studies, a numerical model has been developed to extend the initial oedometer data towards the assessment of actual foundations built on loess soils. Understanding the processes of collapse will also aid in the evaluation and development of ground improvement methods. Initial results from the numerical model have indicated a high level of comparability to the collapse behaviour of both artificial and natural loess soils found from simple oedometer tests. Further

---

<sup>1</sup> Harriet Miller, Nottingham Trent University, Burton Street, Nottingham, NG4 4BU, UK

<sup>2</sup> Youcef Djerbib, Nottingham Trent University, Burton Street, Nottingham, NG4 4BU, UK

<sup>3</sup> Ian Jefferson, Nottingham Trent University, Burton Street, Nottingham, NG4 4BU, UK

<sup>4</sup> Ian Smalley, Nottingham Trent University, Burton Street, Nottingham, NG4 4BU, UK

study has just started to compare the numerical model behaviour to that of a scale model of a strip footing supported on collapsible loess soil. Initially, the effects of rising groundwater will be examined, before more complex collapse environments are considered. Leaking pipes and inundation are particularly problematic as they can cause differential settlement to occur which causes the most damage to structures. Overall, this paper will discuss both the physical and numerical models, their interactions and how they help elucidate the complex geotechnical problem of loess soil collapse.

## **THE PHYSICAL MODEL:**

A physical model of loess soil has been developed in order to examine the factors that influence collapse potential. The way in which the particles pack has a large influence on collapse. Packing density or void ratio will affect the potential magnitude of collapse. Hydrocollapse is defined as the change in height due to wetting over the height before wetting. Other factors such as water content and clay bonding also effect collapse potential. Producing a model soil enables these factors to be controlled. This allows assessment of the influence of these factors on the soils performance.

Samples were primarily tested in one-dimensional fixed ring oedometers. Oedometer testing is the classic test employed to calculate collapse potential as explained by Luttenegger and Saber (1988). Oedometer data is readily available in the literature for loess deposits around the world. The tests therefore provide a good method of comparing the physical model of loess to natural loess deposits.

### **Method 1 - The Air Fall Method**

The effect of varying clay content on the model soil behaviour was examined. Samples were made with varying proportions of the clay and silt materials. Each sample was produced using the same dry mass (or same void ratio) of material, which was sieved into the oedometer rings. Samples were then steamed to produce a low water content and then placed in the oven to develop the clay bonds, Further details of this method are given by Dibben (1998) (same mass) or Assallay et al. (1998) (same voids ratio).

However, key limitations exist in these methods. The disadvantages are as follows:

1. The steaming method employed by Dibben (1998) could only be used on small samples. If larger samples are steamed the lower layers of the sample collapse under the weight of the higher material due to the high water contents produced lower down in the sample.
2. Moisture contents cannot be controlled using the steaming method.
3. Previous methods compared samples with either the same mass (Dibben, 1998) or the same void ratio (Assallay et al., 1998). The effect of clay content on the initial void ratio is therefore neglected. Initial void ratio will affect the magnitude of hydrocollapse it is therefore important that initial void ratios are not artificial but instead are formed 'naturally'.
4. Since either the mass or void ratio is kept constant, the samples do not relate to natural conditions in the ground. A new approach was needed to produce samples with more natural void ratios.

To overcome these limitations new methods were developed in an attempt to produce more comparable specimens. The following method provided the best results:

### **Method 2 - The Wet Method:**

In this method the clay and silt particles are initially mixed with water to form a paste. This paste is placed in the oedometer ring. The sample was then loaded with a static load (between 5-100kPa) to simulate the overburden pressure. This creates a natural void ratio within the sample, simulating a particular depth of deposit. The samples are dried in the oven to create the bonds between the particles and then tested using oedometers with loads up to 1600kPa. Initial void ratios were compared using different preparation water contents to find the optimum water content for which the material packs with the highest density. Samples were formed dry of this optimum to avoid shrinkage when drying.

## **OEDOMETER RESULTS**

### **Method 1 - Air Fall Method**

Typical oedometer results for natural loess obtained from Essex and saturated at 200kPa are shown by the dotted line in Figure 1. Following the method used by Dibben (1998), a constant mass (120g) of the dry mix

of silt and clay was sieved into the specimen ring. Clay contents between 0-40% were tested. Results were compared to the data obtained from Essex loess and typical results are shown in Figure 1.

The observed behaviour is similar to that of the natural loess. However, some distinct differences can be observed. More settlement is observed for the artificial loess on the addition of each load. This relates to the stiffness of the artificial loess, which is considerably less than for natural loess especially for the saturated samples. The artificial samples show a distinct lack of bonding and also have very high initial void ratios of around 1.3. This causes the greater settlements, especially for loads greater than 25kPa, and more hydrocollapse to occur in the artificial samples than in the natural samples. The lower natural void ratio may have been obtained due to more water present in the system or due to a greater preconsolidation pressure in the field.

Most interestingly, the oedometer results show that the largest hydrocollapse is observed for kaolinite contents of around 25% as shown in Figure 2. The same peak is observed for samples with constant void ratio (Assallay, 1998), but this behaviour is not observed in natural samples. The explanation for this seems to lie in the way the particles pack. The particles naturally pack more closely at around 25% kaolinite content. Therefore, if the samples are forced to have the same initial void ratio, more hydrocollapse will occur at clay contents where the particles can pack most easily, which appears to be the samples with 25% kaolinite content. Thus the formation process and the way the particles naturally pack have affected the collapse potential of the specimens.

### Method 2 - The Wet Method

The advantage of this method is that it produces a more naturally bonded and stiff material. The sample is prone to shrinkage during the drying stage if too much water is added during preparation. A moisture characteristic curve was determined by using the same compactive effort to make samples with different moisture contents. A water content of 17.5% was chosen for preparation of the samples which is less than the optimum water content (therefore avoiding shrinkage) but high enough to allow bonding to develop. Results

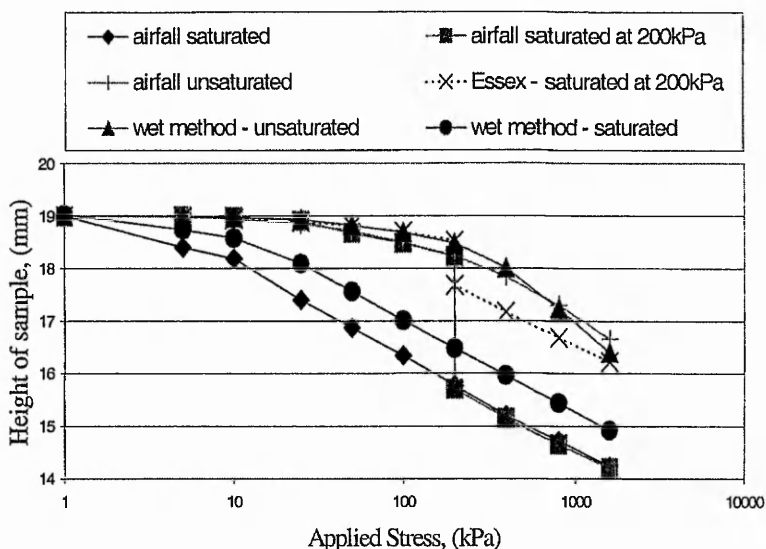


Figure 1 : Essex loess compared to artificial loess formed by the airfall method and the wet method with 30% kaolinite

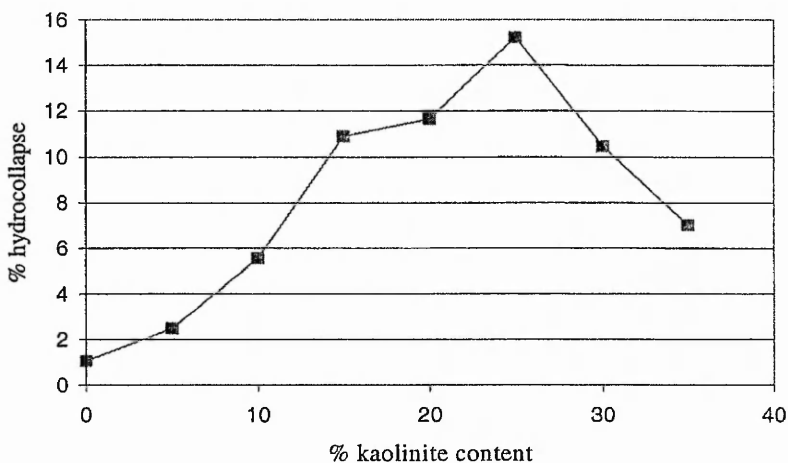


Figure 2 : Peak hydrocollapse observed at 25% kaolinite content using the airfall method

for typical tests are shown in Figure 1 for 30% kaolinite content. The samples show greater strength at lower stresses compared to the airfall method and give a better fit to the natural curves. Void ratios are also much closer to natural loess for loads up to 400kPa than for the previous method. The initial void ratio for the artificial sample in Figure 1 was 0.88 compared to the Essex loess, which had an initial void ratio of 0.8. The natural samples still show a higher strength than the artificial samples when saturated, probably due to length of time that the bonds have had to develop.

Some important factors for assessing the magnitude of hydrocollapse are initial void ratio, clay and carbonate content, specific gravity and degree of saturation or water content. An additional factor affecting the behaviour of the samples seem to be the method of preparation of the samples

Two observations have been made from the oedometer tests, which have been built into the numerical model.

1. A trend for increasing stiffness as the load is increased is observed. This is due to the confining conditions in the oedometer and is not observed in triaxial tests on the same material.
2. Samples that are loaded and then saturated reach the same void ratios as a sample that is saturated and then loaded, in agreement with Lawton et al. (1992). This could also be due to the confining conditions.

It is therefore important to test the soil under different stress conditions. The scale model of a footing will be used for this purpose. It will be used to see if a presaturated soil can be assumed to reach the same state as a dry soil loaded and then saturated and check if the stiffness increases with the load.

#### Saturation Water Content

The influence of water content on hydrocollapse was investigated in a series of oedometer tests, where the samples were loaded to 200kPa and wetted with different amounts of water. Samples were produced using method 2 with clay contents of 30%. The porous discs and samples were weighed separately pre- and post-collapse to obtain the water content causing collapse in the samples. The results from this test showed an increase of hydrocollapse up to a saturation ratio of 0.5. For saturation greater than this there is almost no additional hydrocollapse, see Figure 3. Results are reasonably close to those found by El-Ehwany and Houston (1990), who report that 85% of full collapse is produced at 50% saturation.

#### Clay Content

As clay content is increased, hydrocollapse increases, if all other factors are kept the same (i.e. preparation water content and initial compaction). This is shown in Figure 4. The data on the loess deposits around the world seems to agree with this trend. The deposits with greater clay contents seem to show more hydrocollapse.

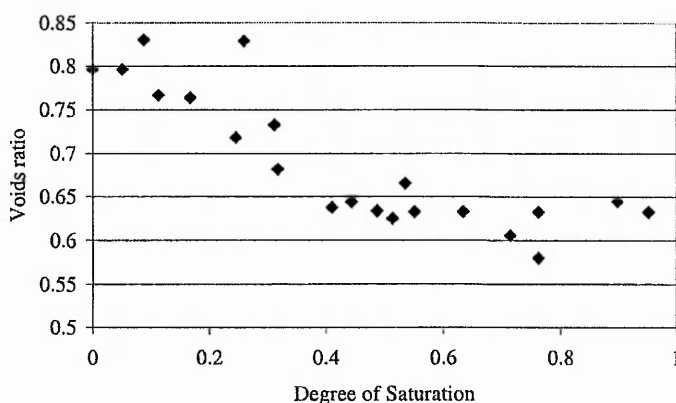


Figure 3 : The variation of post-collapse voids ratio obtained at a stress of 200kPa for different saturation ratios.

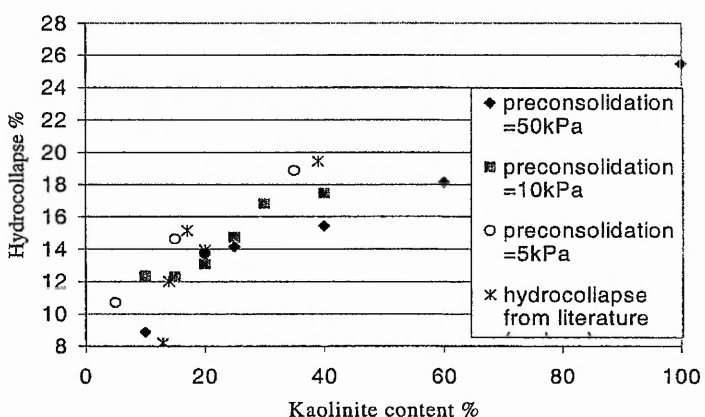


Figure 4 : Hydrocollapse variation with kaolinite content using the wet method. Compared with world data on loess.

## THE NUMERICAL MODEL

Elasto-plastic models such as Cam-Clay and modified Cam-Clay have been used for many years to model saturated soils. New frameworks have been developed to extend these models to include the effect of suctions for unsaturated soils. These ideas were introduced by Alonso *et al.* (1987), Wheeler and Sivakumar (1995) and implemented in CRISP84 by Nenas (1995). The model produced by Alonso *et al.* (1987) is often referred to as the Barcelona model and is intended to describe partially saturated behaviour, using the knowledge of irreversible strains which occur as a consequence of changes in external stresses and suction for non-cemented, non-expansive soils. Equipment for measuring suctions for this purpose has been discussed by Anderson *et al.* (1993). These techniques have been proven to work very well for granular fills. This model has subsequently incorporated increasing numbers of new features (expansion, chemical and thermal coupling, etc.) and is becoming very comprehensive. Additional parameters need to be included in these models, which increases with the complexity and makes them more difficult to use. A great deal of expertise and effort is needed to generate these parameters which renders the problem even more difficult.

An alternative approach to the suction model has been devised which uses the assumption that the soil will obtain the same state, independent of the loading-wetting sequence, as discussed by Lawton *et al.* (1992). Any constitutive model which models the stress/strain behaviour of the particular soil, and for which the required parameters can be assimilated could be used. All that is needed are a set of parameters for the dry soil and a set for the wet soil. A non-linear elastic model was developed to model the increase in stiffness with load observed in the oedometer tests. The model requires values for initial stiffness and Poisson's ratio. The oedometer results indicated that as the load increased, the stiffness of the soil increased due to the densely packed particles. With this in mind, a relationship was developed (equation 1) to link stiffness with load. It was found that as load increased, stiffness also increased so that,

$$E_n = \frac{E_i P^a}{x} \quad (1)$$

where,  $E_n$  is the new value of stiffness,  $E_i$  is the initial value of stiffness found from the oedometer tests,  $P$  is the stress applied and  $x$  is a modifying factor which is material dependent. The factor,  $a$ , is 1 and  $x$  is 55 for the materials tested. This new model has been implemented into finite element program CRISP. Oedometer tests have been simulated and results are shown in Figure 5. The confined stiffness,  $E'_o$ , was found for each of the samples from oedometer tests and used in the finite element program. A good fit to the oedometer curves is obtained using this new non-linear model. The next stage was to further test the capabilities of the soil model implemented into CRISP by predicting the deformation in a plane-strain footing test.

The stiffening behaviour of the artificial soil under load was not observed in triaxial tests, or in the model of a footing. In a triaxial test the stress/strain behaviour was initially linear until yield, after which the samples were less stiff. A linear elastic model was used to predict the settlement of the scale model of the footing. The laboratory model of a footing will be tested to evaluate these findings, and testing will commence shortly. Also, in the oedometer tests, a sample that is saturated then loaded results in the same state as a sample that is loaded then saturated. However, would this be the case in the field? This will also be examined using the scale model of a footing. Initial tests indicate that the saturating and wetting sequence does not have a noticeable affect on the deformation of the footing. Justo *et al.* (1984) studied the loading wetting sequence on the wetting-induced volume change of both natural and compacted expansive soils. They determined that in the collapse region, the volume change was essentially independent of the loading

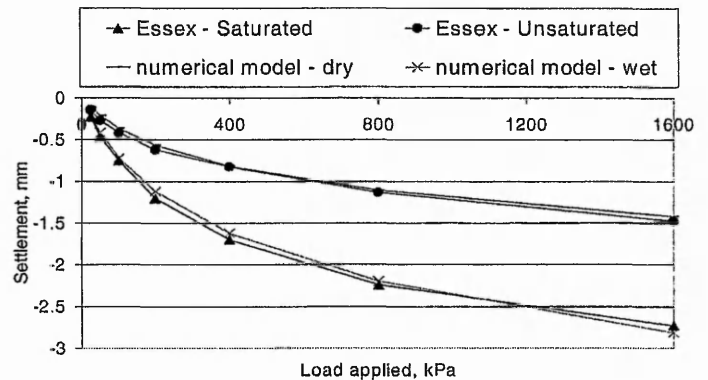


Figure 5: Oedometer data from Essex compared with numerical model results simulating an oedometer test

wetting sequence. The volume changes were only found to be dependent on the stress at which the water was applied in the expansion areas.

## APPLICATIONS

The aim is that the new non-linear elastic model will model any footing situation, without complicating modelling procedures for the engineer in the design office. The simple non-linear elastic model is intended to provide an easier way to model footing behaviour, without having to estimate critical state parameters and measure suctions. To use the suction model with any degree of certainty, months of testing are needed to provide the parameters for the model. These tests are performed on samples taken from the ground that will inevitably have some degree of disturbance. Furthermore, large factors of safety are usually used in bearing capacity calculations, of around 2.5-3. Can months of testing be justified for use with these high safety factors? The finite element model will be used for the following applications:

1. Movement of the ground due to inundation from above and below
2. Effects on buildings supported by cemented collapsible soils.

## CONCLUSIONS

The physical model of loess reproduces classic collapse behaviour very well in the oedometers. An increase of stiffness with load was observed in the oedometer tests. Saturated then loaded behaviour was observed to be the same as loaded then saturated behaviour. A scale model of a footing was built to investigate these two observations under different stress conditions. The physical model of the footing will help to answer a number of questions on how to relate oedometer tests to behaviour of the soil beneath a foundation. Stress/strain behaviour will be examined and compared to oedometer data. The extent to which oedometer data can be relied upon can therefore be assessed. The evaluation of saturated/loaded and loaded then saturated conditions will also be conducted. Using saturated parameters to predict loaded then saturated behaviour may well lead to conservative estimates of settlement and bearing capacity.

The physical footing model has distinct differences to a full-scale prototype, but will enable validation of the computer model. The numerical model and footing model will help to elucidate the collapse mechanisms involved in an increase of ground water level, inundation from above or a leaking pipe.

## REFERENCES

- Alonso, E.E., Gens, A. and Hight, D.W. (1987). "Special Problem Soils. General report". Proc. 9th Conf. Soil Mechanics and Foundation Engineering., Dublin, Vol. 3, pp. 1087-1146.
- Anderson, W.F., Pyrah, I.C., McKinlay, A., Salmon, T.H. and Goodwin, A.K. (1983). "The deformation behaviour of partially saturated granular fill at low stress levels". Engineered fills, Thomas Telford, London, pp. 153-167.
- Assallay, A.M. Rogers, C.D.F. and Smalley, I.J.(1998). "Hydrocollapse in a model loess soil". In : Yanagisawa, E., Moroto, N. and Mitachi, T., (Eds.). Proc. Of the Int. Conf. On Problematic Soils, Sendai, Japan, Oct., pp. 449-452.
- Barden, L., McGown, A. and Collins, K., (1973). "The collapse mechanism in partly saturated soil". *Engineering Geology*, 7, pp. 49-60.
- Dibben, S.C. (1998). "The modelling of collapse in silty soils". PhD Thesis. Nottingham Trent University, UK.
- El-Ehwany M. and Houston S.L. (1990) "Settlement and moisture movement in collapsible soils." *ASCE J. Geotech. Engng.*, Vol. 116, Oct. pp. 1521-1535.
- Justo, J.L., Delgado, A., and Ruiz, J. (1984) "The influence of stress-path in the collapse of swelling soils at the laboratory." Proc. Fifth Int. Conf. On Expansive Soils, 67-71.
- Lawton, E.C., Fragaszy, R.J. and Hetherington, M.D. (1992). "Review of Wetting-Induced Collapse in compacted Soil". *ASCE J. Geotech. Engng.*, Vol. 118, No. 9, September. Pp. 1376-1394.
- Luttenegger, A.J. and Saber, R.T. (1988). "Determination of collapse potential of soils." *Geotechnical Testing Journal*. Vol. 11, No. 3, Sept. pp. 173-178
- Nernas, K. (1995). "A Finite Element Implementation of a Critical State Model for Unsaturated soil to simulate Drained Conditions". PhD Thesis. University of Sheffield. UK.
- Smalley, I.J. (1992). "The Teton Dam: Rhyolite foundation + loess core = disaster". *Geology Today*, Jan-Feb pp. 19-22
- Waltham, A, 1988 "Hydrocompaction of Collapsing Soils". Ground subsidence, Blackie, Glasgow pp.202.
- Wheeler. S.J. and Sivakumar, V., (1995). "An elasto-plastic critical state framework for unsaturated soil". *Geotechnique*, 45, No. 1, pp. 35-53.

## The Collapse of Quaternary Metastable Loess

H. Miller<sup>1</sup>, I.F. Jefferson<sup>1</sup>, Y. Djerbib<sup>2</sup> and I.J. Smalley<sup>1</sup>

<sup>1</sup>Department of Civil and Structural Engineering, Nottingham Trent University, Nottingham, NG1 4BU, UK.

<sup>2</sup>School of Environment and Development, Sheffield Hallam University, Sheffield. UK

### Abstract

Quaternary loess is the archetypal unsaturated, collapsing deposit. An open metastable structure is maintained through clay bonding, cementation and suctions present between the silt particles. If external conditions change, due to increased load during construction or saturation of the deposit, the delicate open structure may collapse. The relative roles of the suctions and clay bonding in the collapse process are not yet fully understood. To overcome these uncertainties this work considers the way the particles pack. A physical model and a numerical model of a collapsing soil are currently being developed to analyse collapse behaviour. The model material has been shown to reproduce metastable loess behaviour very well and enables a full range of repeatable tests to be conducted. The models will help elucidate the behaviour of this quaternary deposit and help to predict the behaviour of this major geohazard, and its consequences for the built environment.

*Key words: Loess, particle packing, collapse, numerical analysis.*

### Introduction

Loess soil is a relatively young deposit that, through aeolian deposition, has a metastable open arrangement of particles. On application of load and/or water the open structure can collapse to form a more closely packed arrangement of particles, a process known as hydrocollapse. These deposits range from a few metres to in excess of 100m deep and cover approximately 10% of the world's landmass. Consequently, many residential and industrial buildings have been erected on the loess ground. Neglecting the engineering and geological behaviour of these deposits can seriously affect the built environment and lead to losses in the order of millions of dollars, e.g. in Bulgaria it has been estimated that over a 30 years some loess related damaged has cost \$(US) 100 million (Minkov 1993).

To elucidate the problems associated with collapsible loess soils, a 'model' loess soil has been developed building on the work of Assallay (1998) and Dibben (1998). The model soil behaves in a similar way to natural loess under load and exhibits the same hydrocollapse behaviour when wetted. The material constituents can be directly controlled, thus providing a good method of assessing the effect of varying the contents on the overall collapse behaviour. Oedometer tests using the artificial loess have been carried out to examine the effect of varying clay content, initial compaction and initial saturation on the collapse process. Further tests using the artificial soil are planned to examine the behaviour of a foundation supported by this soil. In addition to the physical model, a numerical model (using CRITICAL State Program [CRISP94]) has been developed in an attempt to reduce the complexity of existing numerical approaches. The models being produced will help to elucidate the behaviour of this quaternary deposit and its consequences on the built environment.

### Current modelling and prediction techniques

Various approaches have been used to predict the behaviour of collapsible soils. Below is a summary of the most common techniques:

- a. Some authors have discussed collapsibility in terms of fundamental properties of the soil. Criterion based on void ratio (Denisov, 1951), moisture content, Atterberg Limits and dry density (e.g. Gibbs and Bara, 1962), have all been developed. These relationships tend to predict the likelihood of collapse, but not the magnitude of collapse.
- b. Field tests have also been developed to identify potentially collapsible soils. The tests normally involve comparing natural samples with saturated samples. Often, limitations are imposed on the relationships. For example, the saturation must be less than unity and the porosity above 40%

(Fookes and Best, 1969). As above, most prediction criteria are qualitative methods, as they do not provide details on magnitude or rate of collapse.

- c. The amount and rate of collapse can be estimated from oedometer and triaxial tests. The most critical conditions in estimating collapse are the initial water content, dry density and the applied stress. Oedometers can be used in two ways to predict collapse. The first is known as a single oedometer test because only one specimen is required. The specimen is loaded in increments to a certain stress, usually 200kPa, and then saturated. The specimen is subsequently loaded in stages to 1600kPa. The second test is the double oedometer test. This test requires two identical specimens, something very difficult to guarantee in natural samples due to sampling effects (Culshaw, Hobbs and Northmore, 1992). One of the specimens is loaded dry and the other is saturated before loading. The difference between the settlements observed in the two samples at a given stress, represents the collapse settlement over a range of pressures. The coefficient of collapse ( $i_c$ ) is used to classify the collapsibility of a soil and is defined by Lutenegeger and Hallberg (1988). It is often determined for stresses of 200kPa and is defined in equation 1.

$$i_c = \frac{\Delta e}{1 + e'} = \frac{e' - e''}{1 + e'} \quad (1)$$

where,  $\Delta e$  = decrease in void ratio

$e'$  = void ratio before wetting

$e''$  = void ratio after wetting

Generally, if  $i_c > 0.02$ , the soil is considered to be collapsible.

- d. It is generally accepted that the mechanical behaviour of unsaturated soils can be interpreted in terms of changes of two stress variables: net total stress and soil suction, see Matyas and Radhakrishna (1968), and Fredlund and Morgenstern (1977). A three-dimensional plot of  $e$ -void ratio,  $p$ -net normal stress and  $s$ -matric suction can be drawn to show a 'state-surface' for the deformation states of a collapsible soil. From this plot, collapse and swelling conditions are readily interpreted and modelled. The state surfaces only tend to be unique for isotropic and oedometric conditions if the imposed paths always involve a non-decreasing degree of saturation (Matyas and Radhakrishna, 1968), or decrease in load (Lloret and Alonso, 1985).
- e. Finite element analysis is an important technique for predicting stress changes and deformations. Elasto-plastic models such as Cam-Clay and modified Cam-Clay have been used for many years to model saturated soils. New frameworks have been developed to extend these models to include the effect of suctions for unsaturated soils. These ideas were introduced by Alonso Gens and Hight, (1987), Wheeler and Sivakumar (1995) and implemented in CRISP84 by Nesnas (1995). The model produced by Alonso *et al.* (1987) is often referred to as the Barcelona model and is intended to describe uncemented partially saturated behaviour, using the knowledge of irreversible strains which occur as a consequence of changes in external stresses and suction for non-cemented, non-expansive soils. The Barcelona model has subsequently incorporated increasing numbers of new features (expansion, chemical and thermal coupling, etc.) and is very comprehensive.

Both d and e, above, concentrate on frameworks for uncemented soils. Loess is cemented and bonded with carbonates and clay. In uncemented soils degradation of suctions causes collapse. However, in loess it is the degradation of the clay and carbonate bonds as well as suctions that causes collapse. Gens and Nova (1993) proposed ideas for extending the framework to include structure, using theories discussed by Leroueil and Vaughan (1990). However, additional parameters are required for these models, which increases the complexity and makes them more difficult to use. A great deal of expertise and effort is needed to generate these parameters and renders the problem even more difficult.

- f. Particle packings are normally characterised by their packing density and co-ordination number (CN). The packing density is the fraction of the packing volume occupied by its particles and the co-ordination number is the number of particles that contact a particular particle. Dijkstra *et al.* (1995) describe nine uniform packing arrangements in detail based on spherical particles. The

shift from packing to packing, or transformation from state to state is central to the packing problem as applied to loess structure collapse, in which particle arrangements transform from loose to denser packing.

Nolan and Kavanagh (1992) have shown how computer techniques can effectively handle random packings more typical of loess soils. Regions of CN and porosity have been demarcated in which transitions occur. In addition, they have shown some random structures that are directly involved in random packing transitions. These are random loose packing (RLP) and random close packing (RCP). The Nolan and Kavanagh (1992) model simulations showed that packing densities lie between 0.509 (RLP) and 0.638 (RCP).

These densities fit in very well with data on pre-and post-collapsed densities of loess. The loess typically has a void ratio of around 1 in its metastable state, which corresponds to a packing density of 0.5. This compares well to the value 0.509 given for RLP. When the loess sample collapses, the density is increased and the void ratio decreases to around 0.5 - 0.6, equating to a packing density of 0.66 - 0.625. This is close to the RCP value of 0.638. The packing literature can therefore help to elucidate the current understanding of collapse, for it is ultimately the way the particles pack that controls whether a soil will collapse or not.

### **A New Approach**

Ballotini balls, crushed sand and HPF4 have all been used to simulate the silt sized fraction of loess. These particles are mixed with clay binder and compared to natural loess samples. Assallay, (1998) proved that kaolinite was the only viable clay mineral to use in laboratory tests.

The Ballotini balls are glass spheres of 45-90 $\mu\text{m}$  and were used by Assallay (1998) and Dibben (1998). The spherical glass balls represent the silt particles of loess, but do not have the same characteristic blade-shape. However, the glass spheres are a useful link to the particle packing ideas discussed above in point f, which have mainly been developed using spheres.

Crushed sand mixed with kaolinite is shown in Figure 1. Bridges and clay coatings can be observed between the silt particles. HPF4, was chosen to represent the primary silt particles because it comes from the supplier with the required particle size range (100-20 $\mu\text{m}$ ) and therefore further treatment is unnecessary. A chemical analysis of the HPF4 shows that 98.5% of the particles are quartz with a small amount of impurities, e.g.  $\text{Fe}_2\text{O}_3$  and  $\text{Al}_2\text{O}_3$ . Figure 2 shows the shape of the HPF4 particles. Both crushed sand and HPF4 particles have a shape more comparable with those found in natural loess.

### **Sample preparation**

The artificial sample is created using a method developed from Assallay (1998) and Dibben (1998) adapted to overcome key limitations. These limitations were:

- Larger samples could not be made due to the steaming method employed to produce bonding.
- The previous methods compared samples with either the same mass or the same void ratio (Dibben, 1998) and (Assallay, 1998). Samples produced in this way therefore do not relate to natural conditions.
- To examine the effect of clay content it is necessary to have comparable samples. Clay content will affect the mass and the void ratio of the samples. If void ratios are kept constant the true effect of the clay content will therefore not be observed.

To overcome these limitations a new method was developed to produce comparable specimens. Each of the specimens is loaded statically with the same stress. The load represents an equivalent overburden pressure and therefore allows the specimen to form at its natural void ratio and mass. This simulates a sample at a given depth, therefore making the samples more comparable to natural samples and to each other.

Three methods of producing the samples have been tested.

**Method 1: Air fall** - Samples are produced using the same mass for each clay content. Samples are then steamed to produce a low water content and then placed in the oven to develop the clay bonds, see method by Dibben (1998).

**Method 2: The wet method** - In this method the clay and silt particles are mixed with water to form a paste. This mixture is placed in the sample ring. The sample can then be loaded with a static load (between 5-100kPa) to simulate the overburden pressure that would be experienced at a given depth in the deposit. This creates a natural void ratio within the sample, simulating a particular depth of deposit.

**Method 3: The bonding method** - The clay and silt particles are mixed with water and left to dry. The dry material is then crushed and placed into the sample ring in thin layers. A fine mist is used on each of the layers to achieve moisture contents of approximately 20%. The sample is then loaded as in method 2 to simulate the required depth of the deposit. The samples are left dried in the oven to create the bonds between the particles and then tested using single and double oedometer tests with loads up to 1600kPa.

## Oedometer Results

### Method 1 - Air fall method

Following the method used by Dibben (1998), 120g (constant mass) of the dry mix of silt and clay is sieved into the specimen ring. Clay contents between 0-40% were tested. The method of initially compacting the sample to simulate a given depth of deposit was not used. Typical oedometer results for the natural loess obtained from Essex saturated at 200kPa are shown by the dotted line in Figure 3. These results provide a comparison with the artificial loess soils made with crushed sand and kaolinite (80% and 20% respectively). The observed behaviour is similar to that of the natural loess. However, some distinct differences can be observed. The artificial samples show lack of bonding and also have very high initial void ratios of around 1.3. This causes more settlement, especially for loads greater than 25kPa, and more hydrocollapse to occur in the artificial samples than in the natural samples.

Most interestingly, the oedometer results show that for all three different artificial silts, the largest hydrocollapse is observed for kaolinite contents of around 25%, typical results for crushed sand are shown in Figure 4. A peak hydrocollapse is observed at around 25% kaolinite content for samples with constant mass. The same peak is observed for samples with constant void ratio (Assallay, 1998), but is not observed in natural samples. The explanation for this seems to lie in the way the particles pack. The particles naturally pack more closely at around 25% kaolinite content. Therefore, if the samples are forced to have the same initial void ratio, more hydrocollapse will occur in the samples that can pack most easily, which appears to be the samples with 25% kaolinite content. Thus the formation process would seem to have affected the collapse potential of the specimens.

### Method 2 - The wet method

The advantage of this method is that it produces a more naturally bonded and stiff material. The disadvantage is that samples may shrink as they dry and therefore cannot be made in the same container in which it is tested. Moving the sample to a smaller container can cause disturbance in the sample. However, if the sample is made dry of optimum water content, shrinkage will not occur, see Figure 5 for optimum water content. A water content of 17.5% was chosen for preparation of the samples which is less than the optimum water content but high enough to allow bonding to develop. Results for typical tests are shown in Figure 6 for 30% kaolinite content. The samples show greater strength at lower stresses compared to the airfall method and give a better fit to the natural curves. Void ratios are also much closer to natural loess than for the previous method. The void ratio for the artificial sample in Figure 6 was 1.01 compared to the Essex loess, which had an initial void ratio of 0.8. This lower void ratio may have been obtained due to more water present in the system or due to a

greater preconsolidation pressure. The lower void ratio probably accounts for the lower observed settlements.

#### Method 3 - The bonding method

Oedometer results are shown in Figure 7 for method 3. The initial void ratio for this sample was 1.04, which is reasonably close to the void ratios found in natural loess soils. A difference in behaviour is observed between loads of 25 and 200kPa where the artificial soil exhibits less strength than the natural loess. This higher strength in the natural samples could have occurred as a result of higher preconsolidation pressures present in the field or alternatively from enhanced bonding developed with age.

Some important factors for assessing the magnitude of hydrocollapse are initial void ratio, clay and carbonate content, specific gravity and degree of saturation or water content. Additional factors affecting the behaviour of the samples seem to be preparation of the samples and the particle shape. Method 2 appears to give the best results when compared to natural samples, but can suffer from shrinkage during drying.

### Swelling Behaviour

Some specimens show swelling if saturated under low loads, these results are confirmed by Alonso *et al.* (1987). Swelling occurred in one of two samples made with the same proportion of silt and kaolinite (70:30) using the wet method (method 2). This is because one sample was compacted with 5kPa and one with 25kPa resulting in different initial void ratios. The initial void ratios for the two samples are 1.01 and 0.62 respectively. As a result, the sample with the lower void ratio swelled when saturated, because it had been over-consolidated.

Swelling has been shown to occur in natural samples too (Alonso *et al.*, 1987). The reason normally suggested for this is related to swelling in the clay minerals in some samples, however, in these tests kaolinite is used which is not a swelling clay mineral. Alternatively, the soil has been initially lightly over-consolidated and when the soil is saturated it attempts to find its natural equilibrium higher void ratio. The clay bonding in this case has 'locked in' the swelling potential in much the same way as it locks in collapse potential at higher loads. Elastic recovery is observed although plastic deformations obviously cannot be recovered.

### Effect of Clay Content

Methods 2 and 3 have been used to create samples to examine the effect of varying kaolinite content. The same compactive effort is used for each clay content to allow the samples to reach their natural equilibrium. Results for a compactive effort of 5kPa and 50kPa are shown in Figure 8.

Clay content would appear to affect the initial void ratios of the samples and therefore the amount of hydrocollapse observed in the samples. The densest packing is achieved with kaolinite contents of 25% i.e. this is an optimum initial packing arrangement. It seems that 25 percent clay is the optimum amount of clay to fill the voids between the silt particles. Above this clay percentage the clay begins to dominate, the silt particles are pushed apart which creates larger void ratios. Below the optimum 25% clay content, the void ratios may also slightly increase because the clay will not fill as much of the void space between the silt particles

These results explain the hydrocollapse peak observed at 25% clay content (Figure 4), produced using method 1, where a constant mass is used to form each sample. Consider a set of specimens that are forced to pack with a void ratio of 1 for kaolinite contents varying from 0-40%. This void ratio is natural, perhaps for a clay content of 25%, but very dense for clay content higher or lower than this, as shown in Figure 8. The specimens formed with a greater percentage of clay than this optimum will be forced into a denser structure than it would naturally form. Less hydrocollapse will therefore be observed due to the denser initial packing. This paper proposes that the peak hydrocollapse curve observed in Figure 4 is, therefore, merely a function of the preparation of the samples and their initial

void ratios. Samples forced to have the same initial void ratio will only show half the influence of the clay content. The clay content that can be most easily packed will show the greatest hydrocollapse because the effect of the clay on the initial packing was neglected. When the samples are formed at their natural void ratios, increasing the kaolinite percentage results in an increase in hydrocollapse as shown in Figure 8. This shows the true influence of the kaolinite content, as samples have been allowed to form at their natural initial void ratios. Various results from the literature are plotted on the graph and show similar collapse values.

### **Conclusions from Oedometer Tests**

The void ratios, initial stiffness and collapse values produced using method 2 are the most realistic of the three methods when compared to natural loess from Essex see Figure 6. Since these samples were produced by mixing the clay and silt with water, this suggests that perhaps the loess from Essex was deposited in a wet environment. It is proposed that water must have been present to produce the lower void ratios and high stiffness observed.

Method 1 does not take into account the natural void ratios formed at different clay contents. It can therefore not be used to examine the effect of clay content. The peak at 25% clay content is not valid and is not born out by real loess studies as reported in the literature. Method 2 shows similar behaviour to natural loess and provides a good way to make larger specimens, providing the water content is dry of optimum, see Figure 5. It will therefore be used for further testing.

If there is no clay, there will be little potential for hydrocollapse because the contact between the silt grains is stable. As the clay content is increased the potential for collapse will increase due to the tendency for the clay bonds to degrade when saturated. This allows rearrangement of the grains to a denser packing. As clay content is increased further initial void ratios are increased, therefore providing even higher potential collapse settlements in the artificial soil, see Figure 8. Of course, in nature, clay and carbonates will continue to grow, which may reduce the void ratios and potential for hydrocollapse. This further process has not been studied

Preconsolidation pressures also affect the initial void ratio and therefore the potential hydrocollapse, see Figure 9. The preconsolidation pressure appears to have most effect on the stiffness of the dry soil, see Figure 7. The higher the preconsolidation pressure, the stiffer the dry soil. Preconsolidation pressure appears to have less effect on clay content around 25% where denser packing is achieved.

The clay binder appears to provide the strength to maintain the high void ratios which later cause collapse. Water degrades the clay bonds and suctions and allows rearrangement of the particles to a closer packing. Suctions may well participate and degrade in combination with clay bonds. This means models based on suctions only are not fully appropriate for application to loess soils.

Oedometer tests provide results for an element of soil. Different stiffness' can be obtained for different simulated depths of deposit. A finite element model is being developed to make use of the stiffness values to predict deformations, see next section. The new model will simulate the change in stiffness with depth as well as the stiffness changes between dry and saturated conditions.

### **Engineering applications**

Samples representative of real soil are difficult to obtain for a number of reasons. Sampling methods still allow the samples to dry out which makes testing at the natural water content very difficult. Due to the open structure of the loess particles disturbance is likely and collapse results may be affected by any sampling method used. An exact picture of the behaviour of the loess samples will therefore be difficult to obtain due to the above limitations. The model loess has given a better understanding of overall collapsible behaviour. Since the samples are dried in the oven suctions cannot be measured. The clay bonds degrade and facilitate collapse. The model loess has also provided data for calibrating a numerical model, to simulate collapse behaviour. The numerical model predicts the behaviour of the oedometer samples very well, see Figure 10. It will be used in the future for predicting deformations in

a model of a foundation. The results from the model foundation test help to further calibrate the numerical model.

The numerical model uses simple information that can be gathered easily from oedometer data. The initial constrained stiffness,  $E'_0$ , can be obtained directly from oedometer tests and can be subsequently modified for 2-D and 3D applications using Poisson's ratio. Data for a dry sample and a saturated sample are needed and also a prediction of the linear change in stiffness with depth within the deposit. The numerical model uses the data from the dry sample and the saturated sample and predicts collapse assuming the ground conditions change from dry to saturated. Collapse is produced by comparing the behaviour of a saturated sample against a stiffer dry sample, just as in the double oedometer test. The dry and saturated curves are shown in Figure 10. In stark contrast, even the simplest critical state models used in finite element packages need in excess of 9 parameters, from a series of tests that can take weeks or months to prepare. Moreover, difficulties obtaining fully undisturbed samples mean that multiple errors will be introduced in the prediction model. Therefore, the months of testing may still not produce accurate parameters to describe the soil.

The numerical model has been developed to help understand the complex behaviour and mechanisms involved in collapse. Situations such as rising ground water will be examined in detail to assess the deformations that would be observed on the ground. The relative roles of suction and clay bonding do not matter as they are both taken into account by the stiffness values given in the model. Only increasing saturation's can be simulated. This is less significant because the interesting and most devastating part of collapse is when the collapsible soil is wetted for the first time and the foundation fails.

Prediction of the deformation behaviour in this type of soil is important for existing buildings built on the loess ground. Studies can be undertaken to assess the effects of rising ground water levels, ponding at the surface due to leaking gutters, or from a point source within the ground such as a leaking pipe. This may help to decide whether pumping of the ground water is needed or if underground pipes present a hazard and need to be moved, or even if the building is safe.

Further uses for the model include the examination of the effects of burying radioactive waste (see Jefferson et al. 1998) within the layers of loess. The behaviour of the waste and associated displacements could be modelled for increasing saturation. For example, if the layer below the waste collapsed would this present a seepage route for the waste and therefore cause a serious hazard below the ground?

From these simple models it will be easier to get a better understanding of treatment methods. Many sites are flooded and/or compacted in an attempt to reduce the risk of collapse. The model would help to identify how best to treat the ground.

## Conclusions

The main role for the artificial loess has been to create a soil which:

- Behaves sufficiently like a collapsing soil so that its behaviour can be studied,
- Constituents can be controlled and varied to study their effect on collapse behaviour,
- Behaviour under a footing can be examined by using this soil in a model of a foundation.

This paper has discussed three methods for preparing collapsible soil samples that show similar collapse characteristics to natural loess soils. A new technique has been developed to allow the samples to reach their natural void ratios. The samples are compressed with a simulated overburden pressure to produce samples with natural void ratios. As method 1 proves, it is not just void ratio that controls the magnitude of collapse. Even though the void ratios are similar for each of the samples, a peak hydrocollapse is observed for clay contents of 25%. To investigate the influence of clay content on void ratio method 3 has been used to form samples at their natural void ratios for a range of clay contents. Results show that clay content influences both the initial and final void ratios and therefore

affects the magnitude of hydrocollapse. Clay contents of around 25% pack most easily and therefore produce the lowest initial void ratios. The magnitude of hydrocollapse increases with the amount of clay content. Preconsolidation pressures influence the stiffness of the samples when loaded dry and has a small influence on the magnitude of hydrocollapse.

Once saturated, the samples exhibit similar stiffness, producing roughly 0.5mm settlement each time the load is doubled. In preparing samples that model natural loess behaviour it is important to preconsolidate the sample with a representative load, and use the relevant clay content to produce comparable hydrocollapse values.

A numerical model has been successfully employed to predict these oedometer tests and will later be used to predict the settlements below a footing. A small scale laboratory model will be used to assess the accuracy of the prediction of the numerical model. This model could then be used for assessing the safety of structures built on loess and the potential magnitude of collapse. This will enable engineers to assess the hazard of these soils relatively quickly and cheaply.

## References

- ALONSO, E.E., GENS, A. & HIGHT, D.W., (1987). General report. Proc. 9th European Conf. Soil Mech., Dublin 3, 1087-1146.
- ASSALLAY, A.M., (1998). *Structure and Hydrocollapse Behaviour of Loess*. Ph.D. Thesis. Loughborough University, UK
- CULSHAW M.G., HOBBS, P.R.N. & NORTHMORE, K.J., (1992). *Manual Sampling Methods. Engineering Geology of Tropical Red Clay Soils*. British Geological Survey. Technical Report, WN/93/14.
- DENISOV, N. YA. (1951). *The engineering properties of loess and loess loams*. Gosstroizdat, Moscow, 136. (In Russian).
- DIBBEN, S.C., (1998). *The modelling of collapse in silty soils*. Ph.D. thesis. Nottingham Trent University, UK
- DIJKSTRA, T.A., SMALLEY, I.J. & ROGERS, C.D.F., (1995). *Particle packing in loess deposits and the problem of structure collapse and hydroconsolidation*. Engineering Geology, 40, 49-64.
- FOOKES, P.G. & BEST, R., (1969). *Consolidation characteristics of some late Pleistocene periglacial metastable soils of East Kent*. Engineering Geology, 2, 103-128.
- FREDLUND, D.G. & MORGENSTERN, N.R., (1977). *Stress state variables for unsaturated soils*. Journal of Geot. Eng. Division, ASCE, 103, 447-466.
- GENS, A. & NOVA, R., (1993). *Conceptual bases for a constitutive model for bonded soils and rocks*. Proc. Of the International Symposium on Hard Soils - Soft Rocks, Athens, 485-494.
- GIBBS, H.J. & BARA, J.P. (1962). *Stability problems of collapsing soils*. ASCE Journal of Soil Mechanics and Foundation Division, 92, 577-594.
- JEFFERSON, I.F., EVSTATIEV D., ANGELOVA, R., SMALLEY, I.J., (1998). *Improvement of loess soils in north-west Bulgaria for radioactive waste disposal*. Proc 2nd Int Conf On Ground Improvement Techniques, Singapore, 207-212
- LEROUEIL, S. & VAUGHAN, P.R., (1990). *The general and congruent effects of structure in natural soils and weak rocks*. Geotechnique, 40, 467-488.
- LLORET, A. & ALONSO, E.E., (1985). *State surfaces for partially saturated soils*. Proc. 11th ICSMFE, 2, San Francisco, 557-562.
- LUTENEGGER, A.J. & HALLBERG, G.R., (1988). *Stability of loess*. Engineering Geology, 25, 247-261.
- MATYAS, E.L. & RADHAKRISHNA, H.S., (1968). *Volume change characteristics of partially saturated soils*. Geotechnique, 18, 432-448.
- MINKOV, M., (1993). *Liyosovoy Pochvy*. Tsimenttsia na skaliy I dispersniy Pochviy. Publ. House Bulgarian Academy of Science, Sofia, Bulgaria, 8-16 (In Bulgarian)
- NESNAS, K., (1995). *A Finite Element Implementation of a Critical State Model for Unsaturated Soil to simulate Drained Conditions*. PhD Thesis. University of Sheffield, UK

NOLAN, G.T. & KAVANAGH, P.E., (1992). *Computer simulation of random packing of hard spheres*. Powder Technology, **72**, 149-155.  
WHEELER, S.J. & SIVAKUMAR, V., (1995). *An elasto-plastic critical state framework for unsaturated soil*. Geotechnique, **45**, 35-53.



Figure 1. SEM photograph to show crushed sand and clay mixture with clay bridges and coatings.

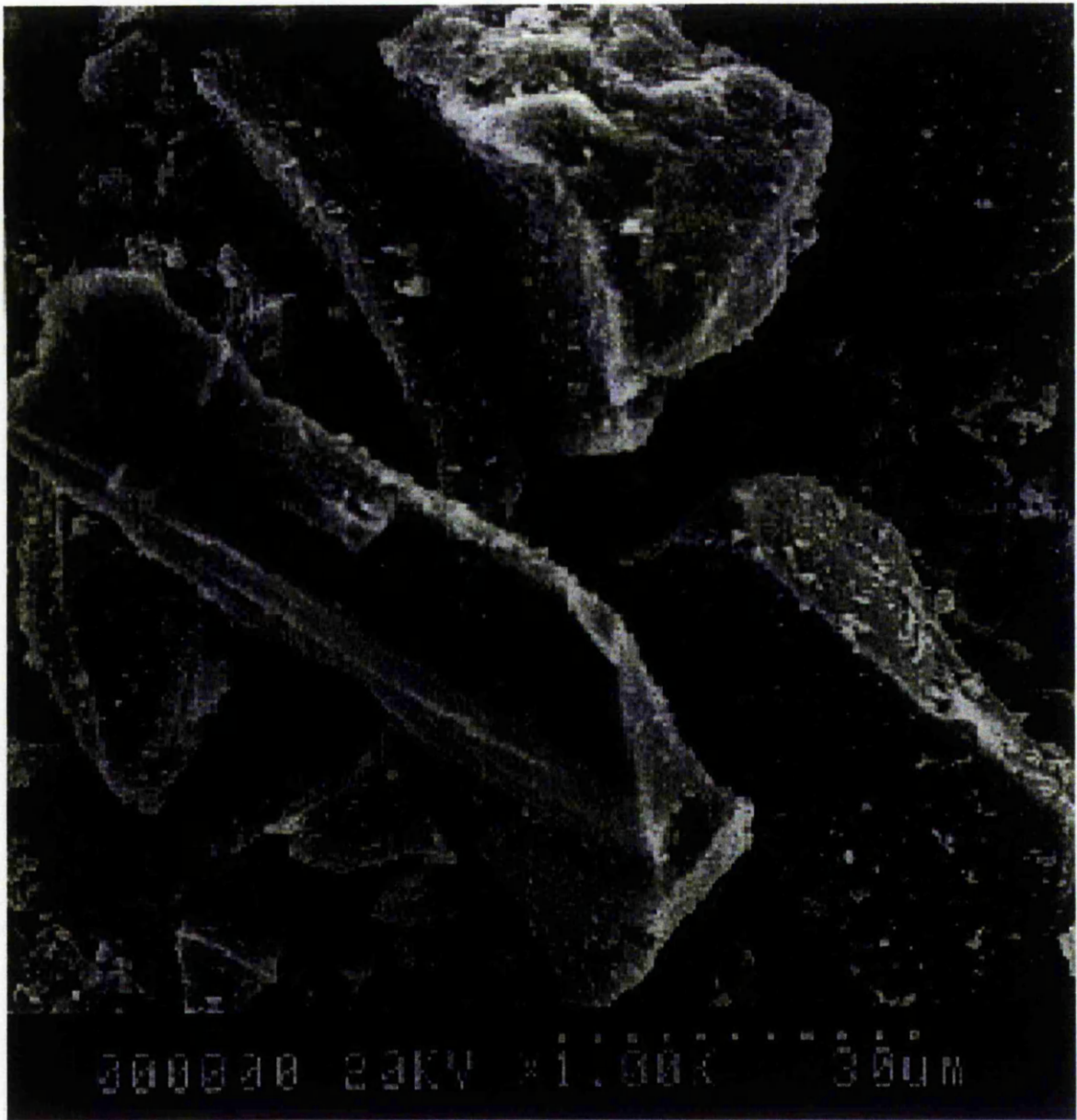


Figure 2. SEM photograph to show the blade shape of the HPF4 particles

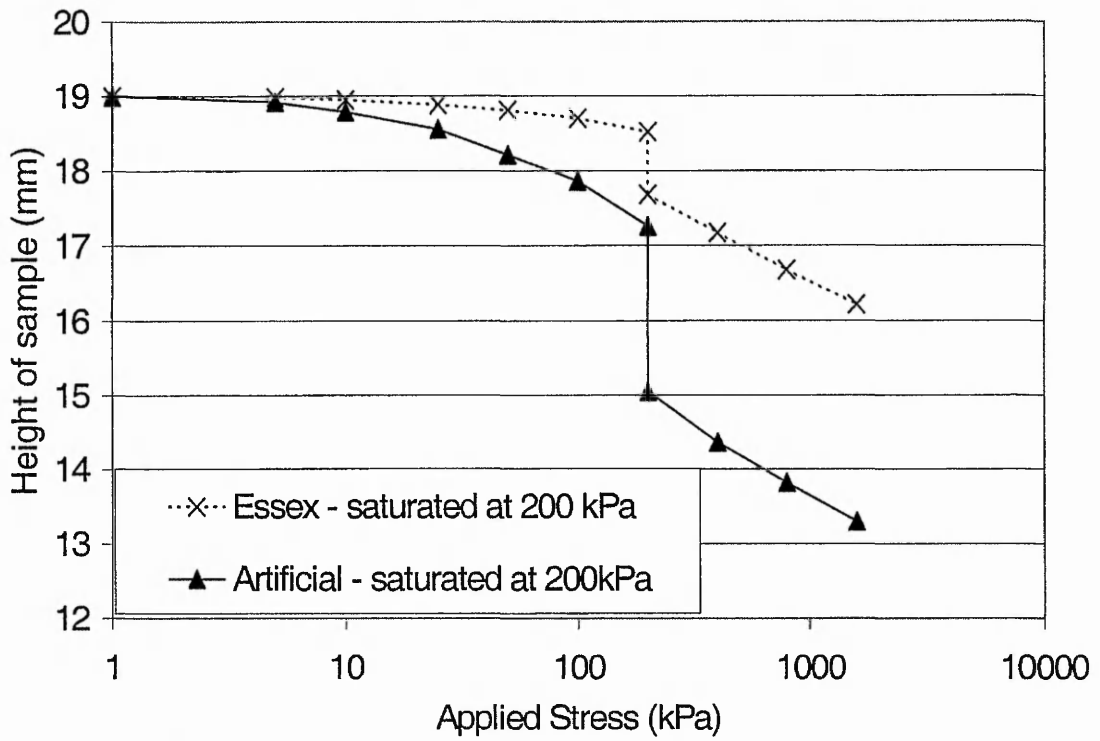


Figure 3. Hydrocollapse data for artificial loess, manufactured from 80% crushed sand and 20% kaolinite using the airfall method (method 1) compared with Essex loess.

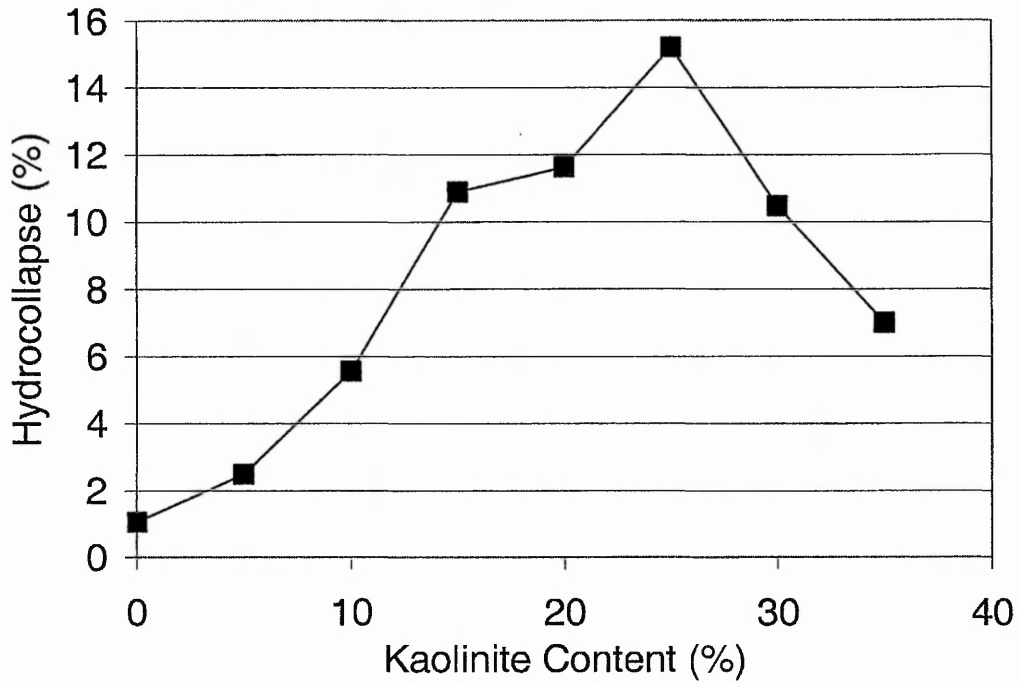


Figure 4. Percentage hydrocollapse for different percentages of kaolinite content in artificial loess made with crushed sand using the airfall method (Method 1).

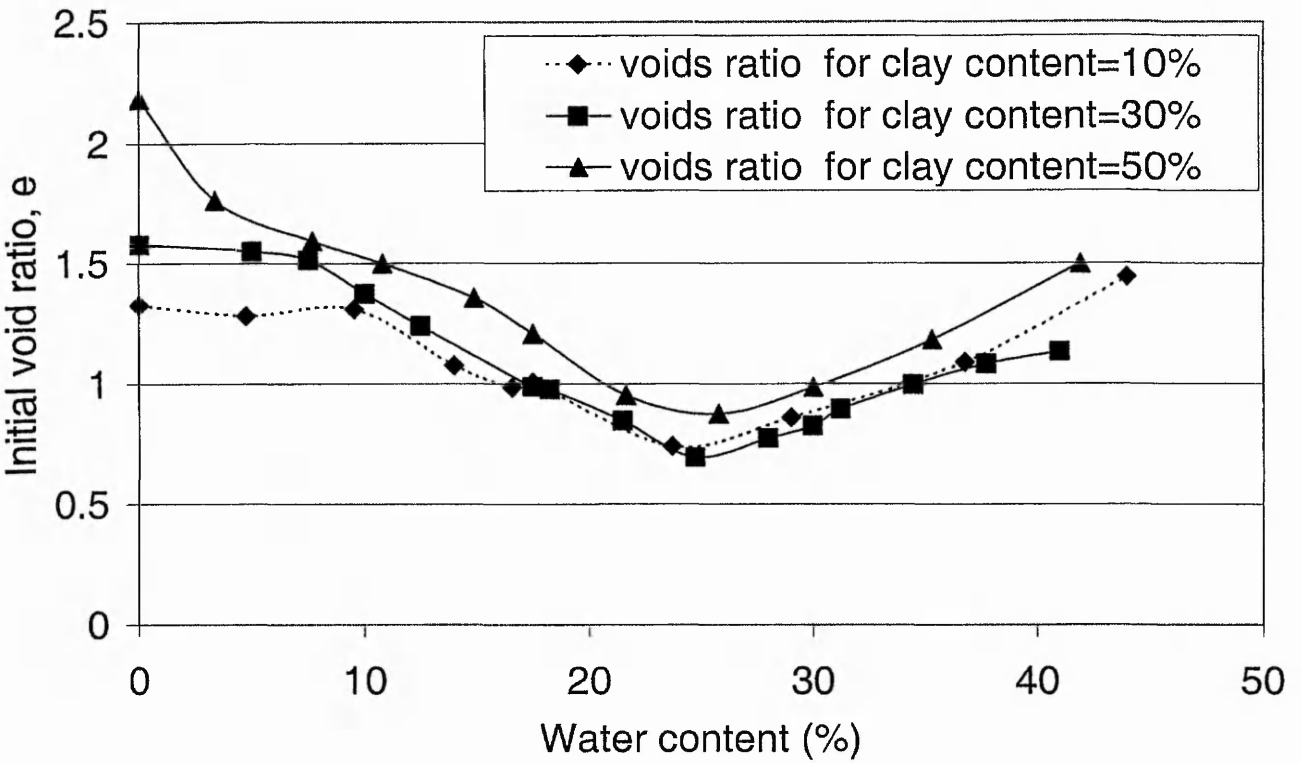


Figure 5. Moisture characteristic curves for kaolinite contents of 10, 30 and 50% in samples made using the wet method (Method 2).

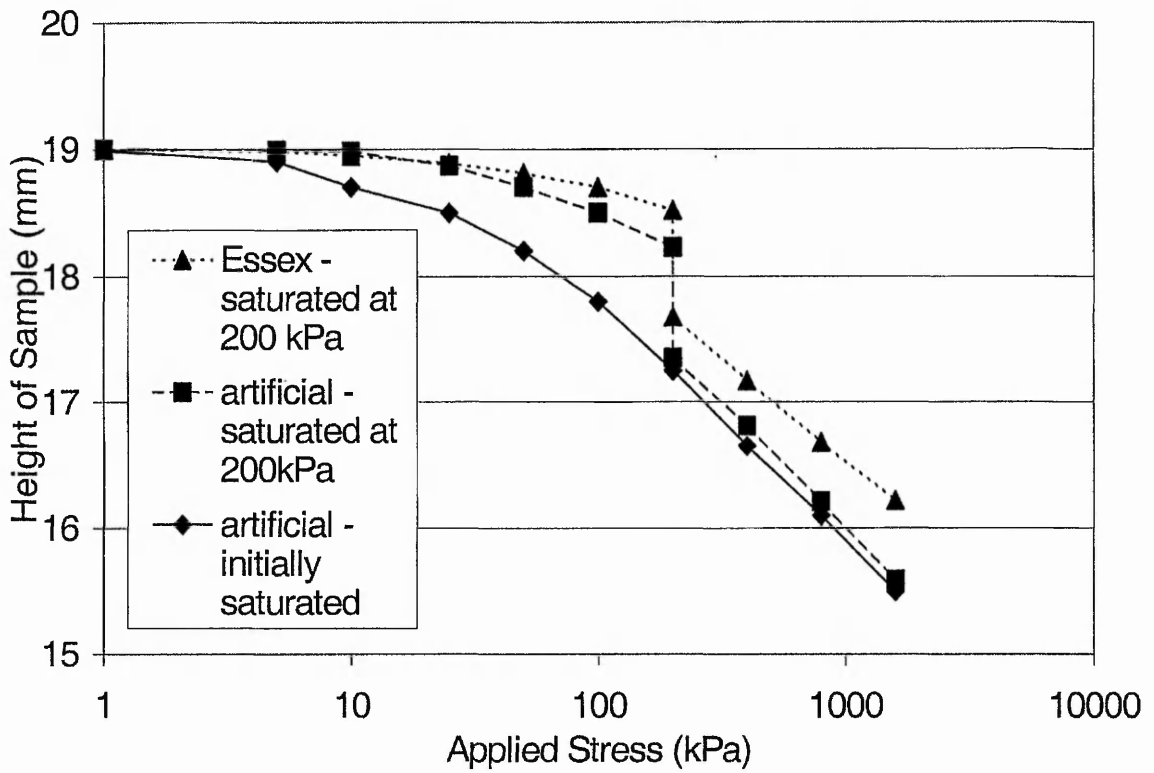


Figure 6. Hydrocollapse of Artificial loess, HPF4 and kaolinite, 70% and 30% respectively, (method 2) compared to loess from Essex.

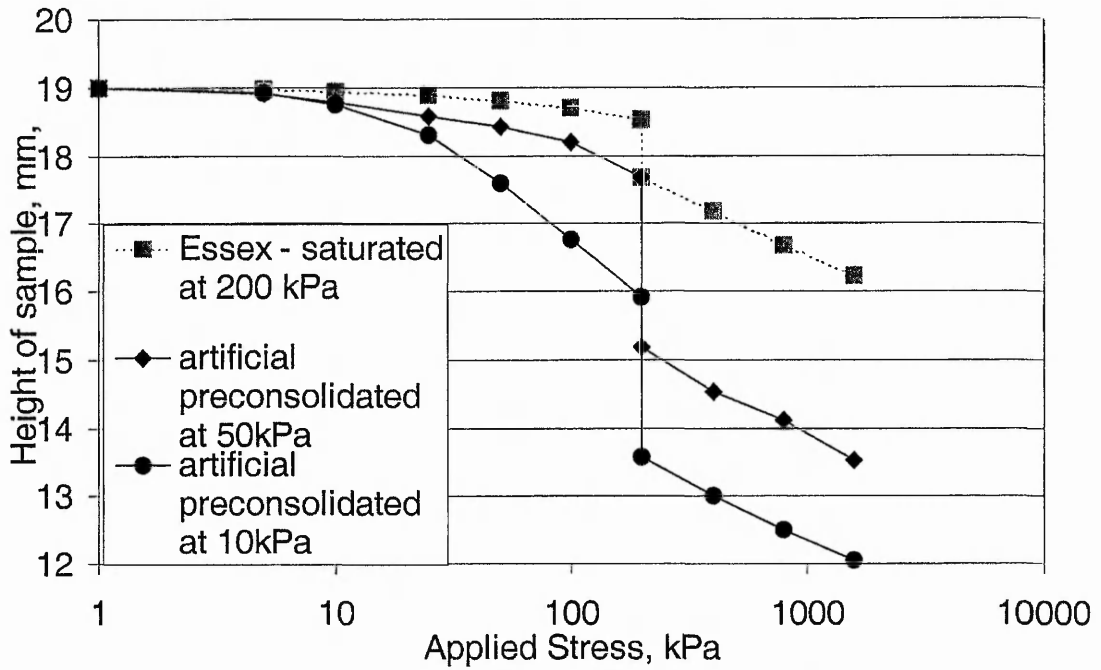


Figure 7. Hydrocollapse of artificial loess, HPF4 / kaolinite, 75% and 25% respectively, consolidated at 10 and 50kPa (method 3) compared to loess from Essex

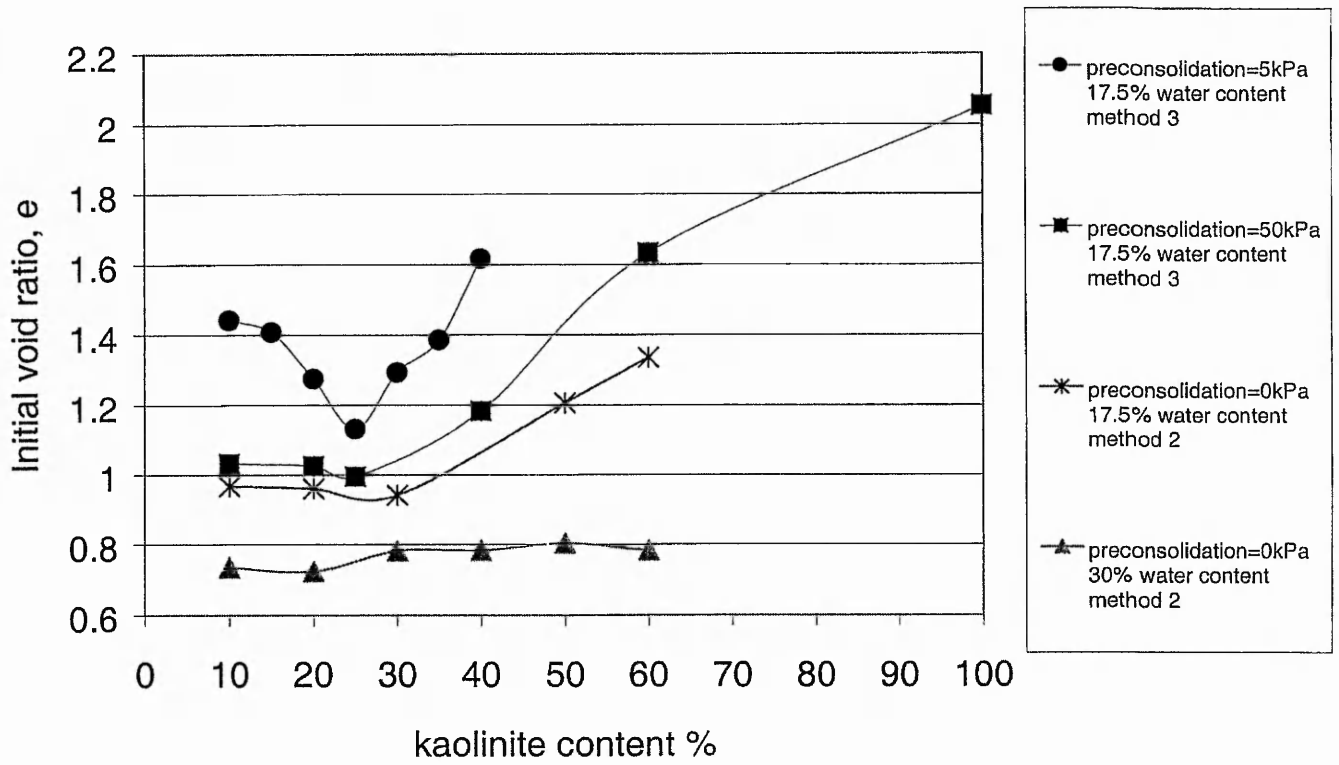


Figure 8. The effect of kaolinite content on initial void ratio. Preparation moisture content = 17.5% for each sample using methods 2 and 3.

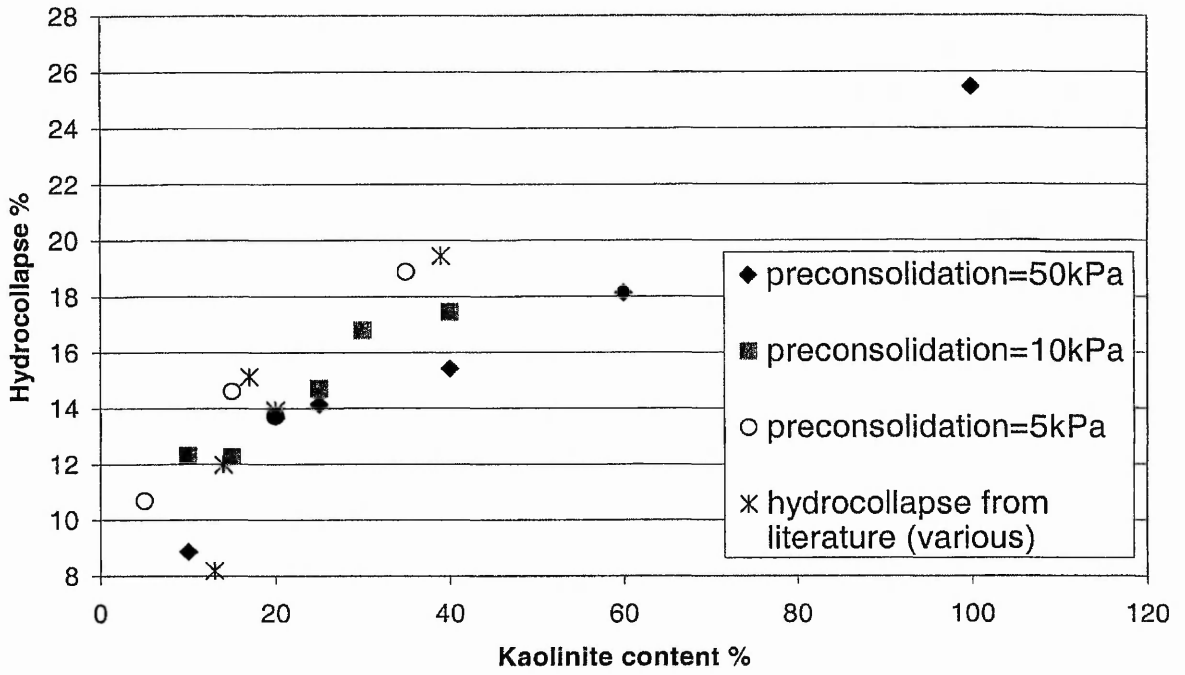


Figure 9. The effect of kaolinite content on hydrocollapse values for oedometer samples

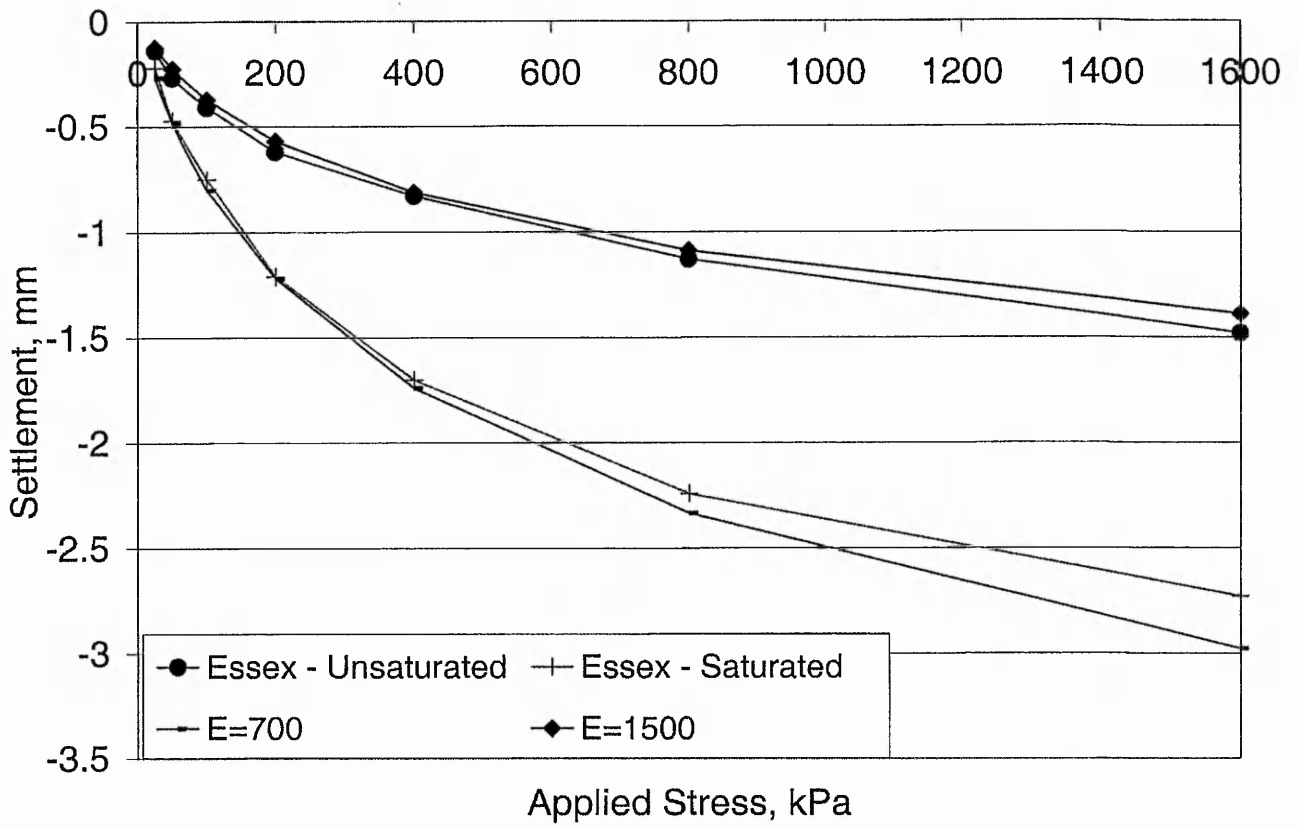


Figure 10. Finite element model results for the oedometer tests (with two stiffness values,  $E=700 \text{ kN/m}^2$  and  $E=1500 \text{ kN/m}^2$ ) compared with oedometer results for samples from Essex.